

UNIVERSITY OF SOUTHAMPTON

FACULTY OF MEDICINE, HEALTH AND LIFE SCIENCES

School of Biological Sciences

**Mechanisms of Action of PPAR γ Ligands and Cellular Role of
PPAR γ in Childhood Neuroblastoma**

By

Verity Claire Emmans BSc (Hons.)

A thesis submitted for the degree of Doctor of Philosophy

September 2006

UNIVERSITY OF SOUTHAMPTON

ABSTRACT

FACULTY OF MEDICINE, HEALTH AND LIFE SCIENCES

SCHOOL OF BIOLOGICAL SCIENCES

Doctor of Philosophy

Mechanisms of Action of PPAR γ Ligands and Cellular Role of PPAR γ in Childhood Neuroblastoma

By Verity Emmans

Neuroblastoma is an embryonal tumour originating from the neural crest and most commonly arises in the adrenal medulla. Between 50 and 60% of patients present with disseminated disease which is highly aggressive. Despite the use of more intensive multi-modal therapies, the overall survival rate of patients with advanced stage neuroblastomas remains poor. In contrast, some neuroblastomas spontaneously regress by either differentiation or apoptosis. These observations have fuelled a search for agents that could cure aggressive neuroblastoma tumours by inducing them to complete differentiation or undergo cell death. Ligands of peroxisome proliferator activated receptor- γ (PPAR γ) attenuated the growth of neuroblastoma cell lines *in vitro* suggesting that they have potential in the treatment of neuroblastoma. The level of PPAR γ activation in neuroblastoma cells correlated with their biological response to the natural PPAR γ ligand 15-deoxy $\Delta^{12,14}$ prostaglandin J₂ (15dPGJ₂). Higher levels of PPRE-mediated transcription were associated with more pronounced growth inhibition of neuroblastoma cells by 15dPGJ₂. The transcriptional activity of PPAR γ in neuroblastoma cells may be regulated by members of the retinoblastoma family, since their ectopic expression in ND-7 neuroblastoma cells *in vitro* repressed induction of PPRE-mediated transcription by 15dPGJ₂ by a mechanism that was dependent on histone deacetylase recruitment. Furthermore, the growth inhibitory effect of 15dPGJ₂ on neuroblastoma cells was enhanced by co-treatment with the HDAC inhibitor Trichostatin A, which suggests that using PPAR γ ligands in combination with agents that enhance their ability to stimulate PPAR γ transactivation might improve their efficacy in neuroblastoma treatment. In IMR-32 neuroblastoma cells, 15dPGJ₂ was dependent on its receptor to mediate its anti-proliferative effect, since stable expression of a PPAR γ dominant negative receptor blocked growth inhibition by 15dPGJ₂. Conversely, growth arrest induced by another PPAR γ ligand ciglitazone was not affected by expression of the receptor mutant, suggesting that PPAR γ ligands can also regulate neuroblastoma growth by PPAR γ -independent pathways. In primary neuroblastoma cells PPAR γ protein levels correlate with the maturational status of the neuroblast, with high expression of PPAR γ observed in cells with a more differentiated phenotype although the function of the receptor remains elusive. To address the cellular role of PPAR γ in neuroblastoma, the factors which control its expression were examined. A transiently transfected PPAR γ 1 promoter reporter was differentially activated in neuroblastoma cell lines with the level of induction mirroring endogenous expression of PPAR γ mRNA in these cell types. Analysis of the PPAR γ 1 promoter sequence revealed a number of putative binding sites that could mediate regulation by Myc family transcription factors. Co-transfection of the PPAR γ 1 promoter reporter with c-Myc or N-Myc expression plasmids attenuated its activity *in vitro*. c-Myc inhibition of the PPAR γ 1 promoter in neuroblastoma cells occurred by a Miz-1 and HDAC independent mechanism. The site of c-Myc repression on the PPAR γ 1 promoter was mapped to a region close to the start site of transcription. This region also mediated transactivation by the Sp1 transcription factor. The finding that PPAR γ 1 promoter activity was negatively by Myc oncogenes involved in the pathogenesis of many human cancers lends supports to the hypothesis that PPAR γ functions as a tumour suppressor.

Acknowledgements

I have many people to thank for helping me complete my PhD. Firstly I wish to express my gratitude to the BBSRC for funding my studentship.

I thank my supervisor Karen for her support and guidance over the past four years, in particular for sharing the art of giving a clear presentation.

I express huge thanks to my advisor Howard for his advice, generation donation of consumables and for always remaining enthusiastic about c-Myc. Many thanks also to Emma for imparting her technical expertise.

I wish to show appreciation to my friends from undergraduate, Nicky, Krysten, Hannah and Andy for their encouragement during my PhD.

I am also very grateful for the companionship of my fellow PhD conquerors, Sarah, Rob, Mich J, Halina and Mich H. Thank you for always lifting my spirit.

Many thanks to my family, Mum, Dad and Brother Leo for their many phone calls, emotional and financial support.

And last, but by no mean least, I express my utmost gratitude to Carl for your selflessness, enduring patience and kindness. I could not have made it without you.

Table of Contents

List of Figures and Tables	5
List of Abbreviations	10
1 INTRODUCTION.....	14
1.1 The nuclear receptor superfamily	14
1.2 PPAR isoforms	15
1.3 PPAR structure	17
1.4 Post-translational modifications of PPARs	22
1.4.1 Phosphorylation	22
1.4.2 Ubiquitination	24
1.4.3 Sumoylation	25
1.5 PPAR ligands	26
1.5.1 PPAR α ligands.....	26
1.5.2 PPAR β/δ ligands.....	27
1.5.3 PPAR γ ligands.....	28
1.6 PPARs heterodimerise with RXR	31
1.7 Sub-cellular localization of PPARs	33
1.7.1 In the cytosol.....	33
1.7.2 PPARs interact with co-repressors in the nucleus	36
1.8 Recruitment of co-activators	39
1.9 Co-activators	40
1.10 Transrepression	42
1.11 The roles of PPARs in normal cell function and disease	44
1.11.1 PPAR α functions	44
1.11.2 PPAR β/δ functions	47
1.12 PPAR γ functions	48
1.12.1 Adipocyte differentiation.....	48
1.12.2 The role of PPAR γ in type II diabetes and the metabolic syndrome	49
1.12.3 PPAR γ and inflammation	51
1.12.4 PPAR γ and cancer	52
1.13 Neuroblastoma.....	59
1.13.1 Etiology and epidemiology.....	59
1.13.2 Pathology and clinical presentation	60
1.13.3 Disease staging	61

1.13.4	Prognostic factors	62
1.13.5	Current treatment for neuroblastoma.....	69
1.13.6	Differentiation therapy.....	71
1.13.7	The cellular role of PPAR γ in neuroblastoma	72
2	MATERIALS AND METHODS	73
2.1	Materials.....	73
2.2	Methods.....	73
2.2.1	Bacterial growth medium	73
2.2.2	Making competent cells.....	73
2.2.3	Glycerol stocks	74
2.2.4	Preparation of Ribonuclease A	74
2.2.5	Small scale isolation of plasmid DNA.....	75
2.2.6	Large scale isolation of plasmid DNA.....	75
2.2.7	Molecular cloning.....	76
2.2.8	Preparation of PPAR γ ligands	81
2.2.9	Preparation of histone deacetylase inhibitor Trichostatin A.....	81
2.2.10	Cell culture.....	81
2.2.11	Freezing cells in liquid nitrogen and resuscitation of frozen cells.....	82
2.2.12	Cell growth	83
2.2.13	Light microscopy	83
2.2.14	DNA transfection of cultured cells	83
2.2.15	Luciferase reporter assay	84
2.2.16	Protein assay	88
2.2.17	Establishment of stable cell lines.....	88
2.2.18	RNA isolation from neuroblastoma cells.....	89
2.2.19	Preparation of cDNA for RT-PCR.....	89
2.2.20	Reverse transcriptase-polymerase chain reaction (RT-PCR)	90
2.2.21	Tritiated thymidine incorporation assay	92
2.2.22	Transient chromatin immunoprecipitation assay	92
3	THE EFFECT AND MECHANISMS OF ACTION OF PPARγ LIGANDS IN NEUROBLASTOMA CELLS <i>IN VITRO</i>	96
3.1	Mechanism of action of the natural PPAR γ ligand, 15-deoxy $\Delta^{12,14}$ prostaglandin J ₂ in neuroblastoma cells	96
3.2	15dPGJ ₂ stimulates PPRE-mediated transcription in the ND-7 murine neuroblastoma cell line.....	97

3.3	15dPGJ ₂ differentially stimulates PPRE-mediated transcription in SK-N-AS, SK-N-SH and IMR-32 human neuroblastoma cell lines	100
3.4	Regulation of PPAR γ transcriptional activity in neuroblastoma cells.....	102
3.5	The effect of the HDAC inhibitor, Trichostatin A on SK-N-AS neuroblastoma cell growth and viability.....	110
3.6	The effect of co-treatment of 15dPGJ ₂ and TSA on SK-N-AS neuroblastoma cell growth and viability.....	117
3.7	The effect of the synthetic PPAR γ ligand ciglitazone on neuroblastoma cell growth <i>in vitro</i>	121
3.8	Ciglitazone stimulates the differentiation of SK-N-AS neuroblastoma cells <i>in vitro</i>	126
3.9	Ciglitazone reduces the viability of neuroblastoma cells <i>in vitro</i>	129
3.10	The effect of ciglitazone on PPAR γ transcriptional activity in neuroblastoma cells <i>in vitro</i>	132
3.11	Discussion	136
4	THE EFFECT OF A PPARγ DOMINANT-NEGATIVE MUTANT ON IMR-32 NEUROBLASTOMA CELLS <i>IN VITRO</i>	148
4.1	Introduction	148
4.2	Establishment of IMR-32 neuroblastoma cells stably expressing a PPAR γ dominant negative receptor	151
4.3	The effect of the natural PPAR γ ligand 15dPGJ ₂ on the growth of IMR-32 neuroblastoma cells stably expressing a PPAR γ dominant negative receptor.....	154
4.4	Stable expression of a PPAR γ dominant negative receptor in IMR-32 neuroblastoma cells blocks stimulation of PPRE-mediated transcription by the natural ligand 15dPGJ ₂	154
4.5	The synthetic PPAR γ ligand ciglitazone inhibits the growth of IMR-32 cells constitutively expressing a PPAR γ dominant negative receptor	156
4.6	The effect of stable expression of a PPAR γ dominant negative receptor on the proliferation and viability of IMR-32 neuroblastoma cells	159
4.7	Discussion	164
5	REGULATION OF PPARγ EXPRESSION IN NEUROBLASTOMA CELLS ...	167
5.1	Introduction	167
5.2	Organisation of the human PPAR γ gene	167
5.3	The PPAR γ 1 promoter is differentially activated in human neuroblastoma cells	168
5.4	Characterisation of the human PPAR γ 1 promoter	169
5.5	Myc regulation of PPAR γ 1 expression in neuroblastoma cells.....	169

5.6	The mechanism of c-Myc transcriptional repression	174
5.7	The Miz-1 transcription factor stimulates PPAR γ 1 promoter activity	181
5.8	Repression of human PPAR γ 1 promoter activity by c-Myc is not dependent on its interaction with Miz-1	181
5.9	The histone deacetylase inhibitor, Trichostatin A stimulates human PPAR γ 1 promoter activity	184
5.10	Determination of the region of c-Myc which mediates its repression of human PPAR γ 1 promoter activity.....	187
5.11	Identification of the site of c-Myc transcriptional repression in the human PPAR γ 1 promoter	196
5.12	c-Myc transcriptional repression of the human PPAR γ 1 promoter occurs by an INR-independent mechanism	201
5.13	The use of a transient chromatin immunoprecipitation assay to evaluate c-Myc binding to the human PPAR γ 1 promoter <i>in vivo</i>	210
5.14	The Sp1 transcription factor stimulates human PPAR γ 1 promoter activity.....	216
5.15	The effect of p53 on human PPAR γ 1 promoter activity in neuroblastoma cells ..	221
5.16	Discussion	229
6	DISCUSSION	239
	Appendix.....	243
	List of References.....	249

List of Figures and Tables

Chapter 1

Figure or Table		Page
Fig. 1.1	Domain structure of PPARs and sites of post-translation modifications.	20
Fig. 1.2	Natural and synthetic PPAR ligands.	29
Fig. 1.3	Translocation of PPARs to the nucleus.	35
Fig. 1.4	Ligand activation of PPARs in the nucleus causes release of co-repressors.	38
Table 1.1	Cofactors recruited by PPARs.	41
Fig. 1.5	Sequential recruitment of co-activators by the PPAR/RXR heterodimer.	43
Fig. 1.6	Sumoylation dependent transrepression by PPAR γ .	45
Fig. 1.7	Cellular responses induced by PPAR γ ligands in cancer cells.	55
Table. 1.2	International Neuroblastoma Staging System	63
Table. 1.3	Prognostic factors in neuroblastoma.	67

Chapter 2

Figure or Table		Page
Table 2.1	Creation of PPAR γ 1 promoter deletion reporters.	78
Table 2.2	Generation of PPAR γ 1 promoter deletion constructs using synthetic oligonucleotides.	80
Table 2.3	List of expression and reporter plasmids used to transiently transfect neuroblastoma and lung cancer cell lines.	85
Table 2.4	Shows the sequences of the forward and reverse primers used to amplify the reverse transcribed cDNA of the cyclophilin gene and PPAR γ 1 dominant negative receptor.	91
Table 2.5	Forward and reverse primers and PCR conditions for ChIP assays.	95

Chapter 3

Figure or Table		Page
Fig. 3.1	The effect of the natural PPAR γ ligand 15dPGJ ₂ on the growth of neuroblastoma cell lines <i>in vitro</i> .	98
Fig. 3.2	The effect of the natural PPAR γ ligand, 15dPGJ ₂ on PPRE-mediated transcription in the murine ND-7 neuroblastoma cell line.	101
Fig. 3.3	The effect of the natural PPAR γ ligand, 15dPGJ ₂ on PPRE-mediated transcription in human neuroblastoma cell lines.	103
Fig. 3.4	The effect of the natural PPAR γ ligand, 15dPGJ ₂ on the reporter activity of a TK- <i>Renilla</i> plasmid which lacks PPREs in neuroblastoma cells.	104
Fig. 3.5	Potential mechanism of pRb transcriptional repression of PPAR γ and factors which modulate the pRb status of tumour cells.	107
Fig. 3.6	The effect of Rb family members on 15dPGJ ₂ -induced PPAR γ activation in neuroblastoma cells.	111
Fig. 3.7	The effect of the histone deacetylase inhibitor, Trichostatin A (TSA) on repression of the transcriptional activity of PPAR γ by the retinoblastoma protein in neuroblastoma cells.	112
Fig. 3.8	The effect of the HDAC inhibitor, Trichostatin A (TSA) on the cell growth of SK-N-AS neuroblastoma cells.	115
Fig. 3.9	The effect of the HDAC inhibitor, Trichostatin A (TSA) on the viability of SK-N-AS neuroblastoma cells.	116
Fig. 3.10	The effect of co-treatment of 15dPGJ ₂ and TSA on the growth of SK-N-AS neuroblastoma cells.	118
Fig. 3.11	The effect of co-treatment of 15dPGJ ₂ and TSA on the viability of SK-N-AS neuroblastoma cells.	119
Table 3.1	The effect of TSA in combination with either 5 or 20 μ M 15dPGJ ₂ on the growth and viability of SK-N-AS neuroblastoma cells.	120
Fig. 3.12	The effect of the synthetic PPAR γ ligand, ciglitazone on neuroblastoma cell growth at concentrations between 0.1 μ M and 20 μ M.	123
Fig. 3.13	The effect of the synthetic PPAR γ ligand, ciglitazone on the growth of ND-7, SK-N-AS, IMR-32 and SK-N-SH neuroblastoma cells.	124
Fig. 3.14	The effect of ciglitazone on the differentiation of neuroblastoma cells.	127
Fig. 3.15	The effect of the synthetic PPAR γ ligand, ciglitazone on the viability of ND-7, SK-N-AS, IMR-32 and SK-N-SH neuroblastoma cells.	130
Fig. 3.16	The effect of the synthetic PPAR γ ligand, ciglitazone on PPRE-mediated transcription in ND-7 neuroblastoma cells.	134

Figure or Table		Page
Fig. 3.17	The effect of the synthetic PPAR γ ligand, ciglitazone on PPRE-mediated transcription in human neuroblastoma cell lines.	135
Table 3.2	Shows how the level of PPAR γ transcriptional activity (2 significant figures) correlates with distinct cellular responses in neuroblastoma cells <i>in vitro</i> .	137
Table 3.3	Comparison of ciglitazone and 15dPGJ ₂ EC ₅₀ values for SK-N-AS, IMR-32, ND-7 and SK-N-SH neuroblastoma cell lines.	144

Chapter 4

Figure or Table		Page
Fig. 4.1	Mechanism of action of the PPAR γ dominant negative receptor.	150
Fig. 4.2	Identification of IMR-32 clones stably expressing the PPAR γ dominant negative receptor.	152
Fig. 4.3	The effect of expression of a PPAR γ dominant negative receptor on the response of IMR-32 neuroblastoma cells to the natural PPAR γ ligand 15dPGJ ₂ .	155
Fig. 4.4	The effect of expression of a PPAR γ dominant negative receptor on induction of PPRE-mediated transcription by 15dPGJ ₂ in IMR-32 cells.	157
Fig. 4.5	The effect of expression of a PPAR γ dominant negative receptor on the response of IMR-32 neuroblastoma cells to the synthetic PPAR γ ligand ciglitazone.	158
Fig. 4.6	The effect of expression of a PPAR γ dominant negative receptor on the growth of IMR-32 neuroblastoma cells.	160
Fig. 4.7	The effect of expression of a PPAR γ dominant negative receptor on [³ H]thymidine incorporation in IMR-32 neuroblastoma cells.	161
Fig. 4.8	The effect of expression of a PPAR γ dominant negative receptor on the viability of IMR-32 neuroblastoma cells.	162
Fig. 4.9	The effect of expression of a PPAR γ dominant negative receptor on basal PPAR γ activity in IMR-32 neuroblastoma cells.	163

Chapter 5

Figure or Table		Page
Fig. 5.1	Organisation of the human PPAR γ gene.	171
Fig. 5.2	The human PPAR γ 1 promoter is differentially activated in neuroblastoma cells.	175
Fig. 5.3	Characterisation of the human PPAR γ 1 promoter.	177
Fig. 5.4.	The effect of Myc family members on human PPAR γ 1 promoter activity in SK-N-AS neuroblastoma cells.	179
Fig. 5.5	The potential mechanisms of c-Myc transcriptional repression.	182
Fig. 5.6	The effect of Miz-1 on PPAR γ 1 promoter activity in SK-N-AS neuroblastoma cells.	185
Fig. 5.7	The effect of the V394D c-Myc mutant on human PPAR γ 1 promoter activity in SK-N-AS neuroblastoma cells.	186
Fig. 5.8	The effect of the HDAC inhibitor, Trichostatin A (TSA) on human PPAR γ 1 promoter activity in SK-N-AS cells.	188
Fig. 5.9.	The effect of the HDAC inhibitor, TSA on c-Myc repression of PPAR γ 1 promoter activity in SK-N-AS neuroblastoma cells.	190
Fig. 5.10	The domain structure of the human c-Myc protein and its binding partners.	192
Fig. 5.11	The effect of c-Myc deletion mutants on human PPAR γ 1 promoter activity in SK-N-AS neuroblastoma cells.	194
Fig. 5.12.	Creation of human PPAR γ 1 promoter reporter deletion constructs.	197
Fig. 5.13	The effect of c-Myc on the activity of PPAR γ 1 promoter deletion constructs.	200
Fig. 5.14	The effect of Miz-1 on the activity of PPAR γ 1 promoter deletion constructs.	202
Fig. 5.15	Creation of human PPAR γ 1 promoter reporter constructs using synthetic oligonucleotides.	203
Fig. 5.16	The effect of c-Myc on the activity of synthetic oligonucleotide PPAR γ 1 promoter reporters.	207
Fig. 5.17	The effect of c-Myc, C/EBP β and the c-Myc V394D mutant on the activity of synthetic oligonucleotide PPAR γ 1 promoter reporters.	208

Figure or Table		Page
Fig. 5.18	The effect of Miz-1 on the activity of synthetic oligonucleotide PPAR γ 1 promoter reporters.	209
Fig. 5.19	Summary of transient chromatin immunoprecipitation (ChIP) assay.	211
Fig. 5.20	Evaluation of the efficiency of transient ChIP primers using either plasmid or input DNA from SK-N-AS cells as the template.	213
Fig. 5.21	Transient ChIP assay PCR results of SK-N-AS cells transfected with either pGL3- γ 1p34oligo or pGL3-Basic or untransfected cells.	214
Fig. 5.22	Optimisation of PCR annealing temperature to reduce non-specific products in transient ChIP assay PCR reactions using DNA recovered from transfected or untransfected SK-N-AS cells.	215
Fig. 5.23	Transient ChIP assay PCR results of SK-N-AS cells transfected with either pGL3- γ 1p34oligo or pGL3-Basic or untransfected cells using new reverse primer.	217
Fig. 5.24	Shows the activity of human PPAR γ 1 promoter constructs relative to pGL3-Basic which lacks a eukaryotic promoter.	219
Fig. 5.25	The effect of Sp1 on human PPAR γ 1 promoter activity in SK-N-AS neuroblastoma cells.	220
Fig. 5.26	The effect of Sp1 on the synthetic oligonucleotide PPAR γ 1 promoter reporter pGL3- γ 1p34oligo.	222
Fig. 5.27	The effect of p53 on human PPAR γ 1 promoter activity in SK-N-AS neuroblastoma cells.	225
Fig. 5.28	The effect of p53 on the activity of PPAR γ 1 promoter deletion constructs.	226
Fig. 5.29	The effect of p53 on human PPAR γ 1 promoter activity in the p53 null H1299 lung cancer cell line.	227
Fig. 5.30	The effect of p53 on Hdm2 promoter reporter activity in the p53 null H1299 lung cancer cell line.	228

List of Abbreviations

Abbreviation	Full name
15dPGJ ₂	15-deoxy Δ - ^{12,14} prostaglandin J ₂
ABC-1	ATP-binding cassette A1
ABMT	autologous bone marrow transplanation
acyl-CoA	acyl coenzyme A
AF-1	activation function 1
AF-2	activation function 2
AMPK	AMP-activated protein kinase
AMY-1	associate of c-Myc-1
AP-1	activator protein-1
Apaf	apoptosis-activating factor
ARA70	activator for the androgen receptor 70
ARF	alternative reading frame protein encoded by the INK4A locus
ATRA	all-trans-retinoic acid
BADGE	bisphenol A diglycidyl ether
BAF60c2	BRG1/Brm-2 associated factor of 60 kDa, subunit c2
BCA	bicinchoninic acid
Bcl-2	B cell lymphoma 2
Bcl-6	B-cell lymphoma 6
BDNF	brain-derived neurotrophic factor
bHLH	basic-helix-loop-helix-leucine zipper
BRCA-1	breast cancer-1
BSA	bovine serum albumin
BTB	broad complex, tram track and Bric-a-brac
C/EBP	CCAATT/enhancer-binding protein
CAP	cbl-associated protein
CARLA	co-activator dependent receptor ligand assay
CBHA	m-carboxycinnamic acid bishydroxamic acid
CBP/p300	creb interacting protein
CDK	cyclin dependent kinase
CDKI	cyclin dependent kinase inhibitor
COX-2	cyclooxygenase 2
CPT	carnitine palmitoyltransferase
DAD	deacetylase activation domain
DEPC	diethyl pyrocarbonate
DMEM	Dulbecco's Modified Eagle's Medium
DMs	double minute chromatin bodies
DMSO	dimethyl sulphoxide
DR	direct repeat
DTT	dithiothreitol

E2F	elongation 2 factor
EDTA	ethylenediaminetetraaceticacid
eIF	elongation factor
ERK	extracellular signal-regulated kinase
FA	fatty acid
FABP	fatty acid binding protein
FAT	fatty acid translocase
FATP-1	fatty acid transport protein-1
FCS	foetal calf serum
FFA	free fatty acids
FISH	fluorescence in situ hybridization
Gadd45	growth arrest and DNA damage 45
GCN5	general control of amino acid biosynthesis protein 5
GFP	green fluorescent protein
GM-CSF	granulocyte-macrophage colony stimulating factor
HAT	histone acetyltransferase
HBS	hepes buffered saline
HDAC	histone deacetylase
HDL	high density lipoprotein
Hdm2	human double minute 2
HETE	hydroxyeicosatetraenoic acid
HODE	hydroxy-octadecadienoic acid
HRE	hormone response element
HRP	horseradish peroxidase
HSP	heat shock protein
HSR	homogenously staining region
HVA	homovanillic acid
INI1	integrase interactor 1
iNOS	nitric oxide synthase
INR	initiator element
INSS	The International Neuroblastoma Staging System
IRS	insulin receptor substrate
JNK	jun NH ₂ -terminal kinase
LAR I	luciferase reagent I
LAR II	luciferase assay reagent II
LB	Lennox broth
LBD	ligand binding domain
LDH	lactate dehydrogenase
LDL	low density lipoprotein
LPL	lipoprotein lipase
MAPK	mitogen-activated protein kinase
MAX	c-Myc associated protein X
MBI	myc box I
MBII	myc box II
MBIII	myc box III

Miz-1	myc interacting zinc finger protein 1
MM-1	c-Myc modulator -1
M-MLV	moloney-murine leukaemia virus
MRP	multidrug resistance protein
NCoR	nuclear receptor co-repressor
NF-Y	nuclear transcription factor-Y
NGF	nerve growth factor
NLS	nuclear localization sequence
NRID	nuclear-receptor-interaction domain
NSE	neuron-specific enolase
OER	oestrogen receptor
PAM	protein associated with Myc
PBS	phosphate buffer saline
PDGF	platelet-derived growth factor
PDGFRB	platelet-derived growth factor receptor beta
PEG	polyethylene glycol
PG	prostaglandin
PGC-1	PPAR γ coactivator protein-1
PGC-2	PPAR γ coactivator protein-2
PIAS1	protein inhibitor of activated STAT1
PKA	protein kinase A
PKC	protein kinase C
PML	promyelocytic leukaemia
PMSF	phenylmethanesulphonyl fluoride
POZ	poxvirus and zinc finger
PPAR	peroxisome proliferator activated receptor
PPRE	peroxisome proliferator response element
PSA	prostate specific antigen
PTEN	phosphatase and tensin homologue 10
PUFA	polyunsaturated fatty acid
RAR	retinoic acid receptor
RB	retinoblastoma protein
RIP140	receptor interacting protein 140
ROS	reactive oxygen species
RXR	retinoid X receptor
SAHA	suberoylanilide hydroxamic acid
SDP-1	SCAN-domain containing protein-1
SDS	sodium dodecyl sulphate
SMRT	silencing mediator of retinoid and thyroid hormone receptors
SNF5	sucrose non-fermenting 5
Sp1	specificity protein-1
SRC-1	steroid receptor co-activator-1
SREBP-1	sterol regulatory element binding protein-1
SUMO-1	small ubiquitin-like modifier-1

SWI/SNF	mating type switching/sucrose non-fermenting
TAF130	TATA-binding protein associated factor-130
TBI	total body irradiation
TBL-1	transducin beta-like protein-1
TBP-48	TATA-binding protein-interacting protein 48
TBP-49	TATA-binding protein-interacting protein 49
TCA	trichloroacetic acid
TFII-I	transcription factor II-I
TIF2	transcriptional intermediary factor-2
TNF- α	tumour necrosis factor- α
TR	thyroid hormone receptor
TRAP220	thyroid hormone receptor associated protein 220
TRRAP	transformation/transcription co-factor-domain-associated protein
TSA	trichostatin A
TZD	thiazolidinedione
VDR	vitamin D receptor
VLDL	very low density lipoprotein
VMA	vanillylmandelic acid
YY-1	ying yang-1
ZIN	zinc finger N-terminal domain

1 INTRODUCTION

1.1 The nuclear receptor superfamily

Peroxisome proliferator activated receptors (PPARs) are members of the nuclear receptor superfamily [1]. Nuclear receptors are unique among transcription factors because they are ligand activated [2]. Members of the nuclear receptor superfamily are thought to have evolved from a common ancestor and have a highly conserved modular structure [2-4]. The human genome encodes at least 48 nuclear receptors, which along with those identified in other species, have been organised into six subfamilies based on sequence alignment and phylogenetic analysis [1,2,4-6]. The largest subdivision, class I, includes PPARs, the thyroid hormone receptor (TR), the vitamin D receptor (VDR) and the retinoic acid receptor (RAR) [2,4-7]. The second subfamily contains the retinoid X receptor (RXR) whereas class III is comprised of steroid receptors like the oestrogen receptor (OER) [2,4-6]. Through their ability to bind a variety of hydrophobic ligands, including steroids, hormones, fatty acids, leukotrienes, prostaglandins, cholesterol derivatives and bile acids, nuclear receptors integrate different intra- and extracellular signals to regulate gene transcription [2,4]. However, some nuclear receptors are termed “orphan” because their respective endogenous ligand has not yet been discovered or may not exist [8-10]. Nuclear receptors interact with hormone response elements (HREs) in target promoters as monomers, homodimers or heterodimers [8,11]. The most common partner identified in heterodimers is RXR which can dimerise with class I and class IV receptors [3,5,12,13]. Whether functioning as a homodimer or a heterodimer, upon binding ligand, nuclear receptors undergo a conformational change which promotes co-activator recruitment and initiates gene transcription. Creation of nuclear receptor knock-out animal models has demonstrated that members of this superfamily have critical roles in development, homeostasis, immune function, cell proliferation, differentiation and cell death *in vivo* [2]. Furthermore, mutations of specific nuclear receptors that inhibit their function are associated with the pathogenesis of certain diseases [14,15].

1.2 PPAR isoforms

The first PPAR was discovered by Issemann and Green in 1990 when they cloned and characterised a receptor from mouse liver cDNA which was activated by a diverse range of peroxisome proliferators, including the hypolipidaemic agents, nafenopin and Wy-14,643 [16]. Subsequently, structural homologues of this receptor were identified in other species including *Xenopus*, rat and human [17,18]. This receptor was later termed PPAR α (NR1C1) when it was demonstrated to be one of a family of PPAR receptors which included PPAR β/δ (NR1C2) and PPAR γ (NR1C3) [17,19-21]. Interestingly sequence comparison of PPARs in *Xenopus* and mammals suggest that the PPAR genes have evolved two to three times faster than other class I nuclear receptors which may account for the PPARs specific ligand binding properties [17].

The human PPAR α gene has been mapped to a region of chromosome 22 (22q12-q13.1) and extends over approximately 131 Kb of genomic DNA [18,22,23]. Characterisation of the human PPAR α gene has revealed that it is composed of twelve exons of which exons, A, 1a, B, 1b, 2a, 2b and part of exon 3 form the 5' untranslated region [23,24]. Use of four different promoters and alternative splicing of exons in the 5' untranslated region generates six PPAR α mRNA variants [23]. Each PPAR α mRNA subtype has different combinations of exons A-2b but they all contain a coding region which consists of the remainder of exon 3 and exons 4-8 and therefore translate in to the same protein of 468 amino acids with a molecular mass of 52 kDa [17,22,23]. Although the structure of the mRNA coding region of mouse PPAR α is comparable with human PPAR α further analysis of the mouse PPAR α gene is necessary to determine if its 5' untranslated region also has a similar genomic organisation to the human isoform [23]. The function of the PPAR α spliced variants remains unclear, however differences in the 5' untranslated region of an mRNA may modulate translational efficiency and tissue specific translational control [25]. PPAR α is expressed in tissues which have a high rate of fatty acid catabolism such as heart, kidney, intestinal mucosa, skeletal muscle and brown fat [21,26-29]. Moreover, PPAR α was detected in lung, placenta and smooth muscle tissue as well as cells of the immune system [26,29].

The human PPAR β/δ gene spans 85 Kb of genomic DNA located on chromosome 6 and is comprised of nine exons and eight introns (6p21.2-p21.1) [30,31]. The 5' untranslated region of PPAR β/δ comprises the first three exons and part of the fourth exon, while the rest of exon 4, exons 5-8 and the start of exon 9 encode a protein of 441 amino acids with a molecular weight of 49.9 kDa [30]. To date, only one transcription start site for human PPAR β/δ has been identified which is located 380 bp upstream from the ATG initiation codon [30]. In contrast, the mouse PPAR β/δ gene contains nine transcription initiation sites found in four promoters [32]. Alternative splicing and promoter usage produces several distinct mRNAs although interestingly the most abundant mouse PPAR β/δ transcript is homologous to the human PPAR β/δ mRNA [32]. Comparison of the human and mouse PPAR β/δ genes shows that there are variations in the number and organisation of exons in the 5' untranslated region which may explain why transcriptional regulation of PPAR β/δ in these two species is different [32]. Alternatively, further examination of the human PPAR β/δ gene structure, like PPAR α could uncover new transcription start sites. PPAR β/δ has a ubiquitous tissue distribution although it is more highly expressed in adipose tissue, small intestine, heart, muscle, skin and brain [33-35].

The human PPAR γ gene has been assigned to chromosome 3 at position 3p25 and spans more than 140 Kb of genomic DNA [17,36,37]. There are four known human PPAR γ mRNAs called γ 1, γ 2, γ 3 and γ 4 which are generated from the use of four different promoters and alternative splicing of nine exons (See also **Fig 5.1**) [36,38,39]. The PPAR γ 1, PPAR γ 3 and PPAR γ 4 transcripts encode an identical protein of 477 amino acids with a molecular mass of 54.2 kDa whereas PPAR γ 2 encodes an additional 28 amino acids N-terminal to the first ATG codon in PPAR γ 1, PPAR γ 3 and PPAR γ 4 resulting in a protein with a molecular mass of 55.6 kDa [38-40]. The organisation of the human and mouse PPAR γ genes are very similar although the mouse gene only gives rise to PPAR γ 1 and PPAR γ 2 transcripts, however the proteins they encode show a high level of sequence identity compared with their human homologues [40,41]. In humans, significant expression of PPAR γ 2 and PPAR γ 4 has only been detected in adipose tissue while PPAR γ 3 expression was also demonstrated in macrophages [36,38,39,42]. Conversely, PPAR γ 1 is widely distributed and is the major isoform expressed in most human tissues [28,36,43-45]. The distinct yet overlapping expression profiles of the three PPAR receptors provided

the first indication that PPARs had both specific and similar biological functions [9,21].

1.3 PPAR structure

PPARs, like other nuclear receptors, have a modular structure comprising of six regions each assigned a letter from A to F (**Fig. 1.1**). The N-terminal A/B region of several nuclear receptors including PPAR α and PPAR γ contains a ligand independent transactivation function (AF-1) although it remains to be determined if PPAR β/δ also has AF-1 activity [46,47]. Among the nuclear receptor superfamily, the AF-1/N-terminal region is the least conserved domain, both in size and amino acid composition, and in all studied examples had a disordered structure [2,4,48]. The AF-1 domain is rich in acidic amino acids and resembles the acidic activation domain of other transcription factors such as NF- κ B [48]. In addition, the AF-1 sequence has the potential to form an amphipathic α -helix and intriguingly mutation of hydrophobic residues within this sequence, that were predicted to disrupt the helix structure, attenuated AF-1 activity more than mutation of individual acidic amino acids [47]. This suggested that α -helix formation could be an essential step in AF-1 mediated gene activation. Indeed recent studies have indicated that interaction between a co-activator and the N-terminal region of the nuclear receptor either induces or stabilises a folded form of the AF-1 domain [48].

Region C contains the DNA binding domain (DBD) of the PPAR, the most conserved motif of nuclear receptors, which consists of two zinc fingers and a C-terminal extension [49-51]. The DBD contains nine cysteine residues and within each zinc finger four of these cysteines form a tetrahedral complex with one zinc ion (**Fig. 1.1**) [4]. Amino acids at the base of the first zinc finger are in a region termed the “P box” which recognises the DNA response element [2,4]. In the second zinc finger amino acid residues between the fifth and sixth cysteine residue are referred to as the “D box” and are involved in receptor dimerisation [49]. The two zinc finger motifs fold to create a single structural domain containing two helices [4,52]. The first helix is formed from residues starting at the third conserved cysteine residue and enters the DNA major groove contacting specific bases, while the second helix which begins at the C-terminus of the second zinc finger is arranged perpendicular to helix 1 [4,52]

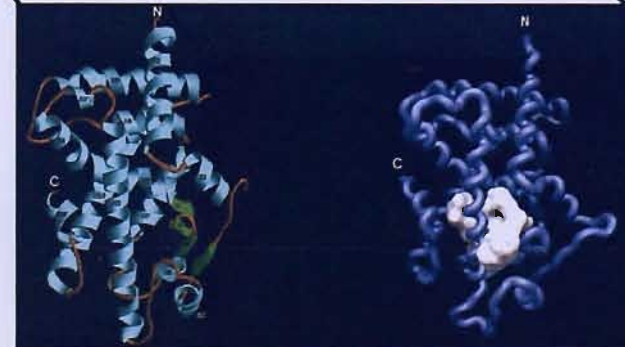
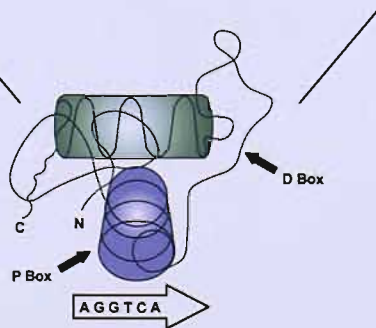
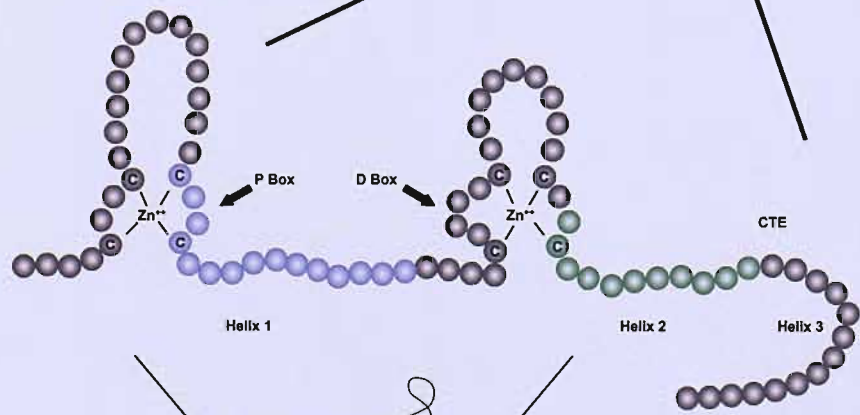
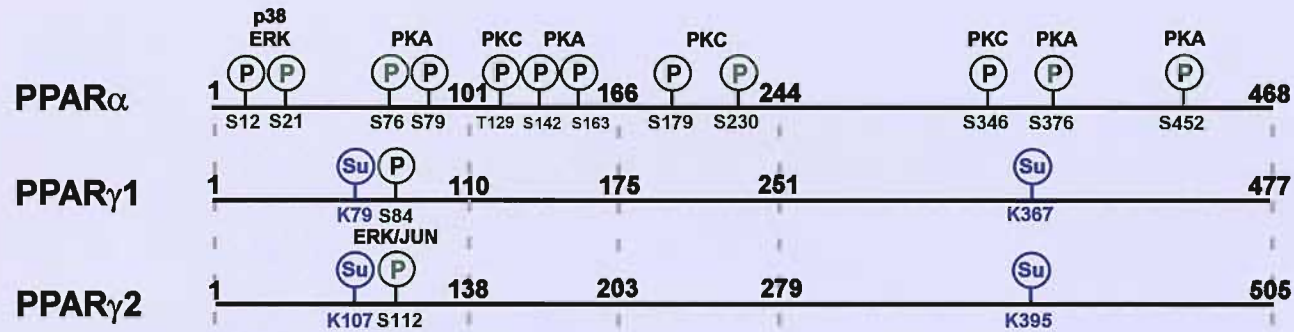
(Fig 1.1). The PPAR C-terminal extension contains T and A boxes which recognise bases in the 5' extended sequence of the PPAR response element and modulates the specificity and polarity of PPAR DNA binding (see section 1.6) [53]. Region D of nuclear receptors is speculated to function as a hinge to allow movement of the DNA and ligand binding domains without creating steric hindrance problems [2]. The D domain may also mediate protein-protein interactions with cofactors [4]. Although the presence of nuclear localisation sequences (NLS) in PPAR receptors have not yet been reported, analysis of PPAR protein sequences using the PredictNLS tool (<http://cubic.bioc.columbia.edu/predictNLS/>) identified a putative NLS in each human PPAR isoform near the border of its C and D domain which is a common location for the NLS of other nuclear receptors [11,54]. A second NLS may be contained in the PPAR ligand binding domain since a naturally occurring truncated human PPAR α receptor which lacks part of the hinge region and the ligand binding domain resided in the cytoplasm whereas wild-type PPAR α was localised in the nucleus [55].

The E/F domain or ligand binding domain (LBD) is multi-functional since it is essential for ligand interaction, co-activator recruitment and dimerisation [56]. The LBD of all three PPAR isoforms consists of thirteen α -helices and a small four stranded β -sheet [57-60]. Helices 4, 5, 8 and 9 are sandwiched between helices 1, 3, 7 and 10 at the top half of the LBD [59]. This arrangement anchors helices 3, 7 and 10 allowing them to form a scaffold for the ligand binding pocket which is located in the bottom half of the protein [57,59]. Helices 7, 9 and 10 are also involved in dimerisation with RXR [61]. Helix 12 which contains the ligand dependent transcriptional activation function-2 (AF-2) domain is exposed on the surface of the LBD. The AF-2 sequence is highly conserved among nuclear receptors and mediates co-activator binding. The overall structure of the PPAR LBD is similar to those of other nuclear receptors although it does have some distinct features [57-60]. Firstly, the PPAR LBD contains a unique helix termed H2' between the first β -strand and H3 that appears to provide a channel through which ligands can enter the pocket [3,57,59]. This entry site may be needed because in the apo-PPAR structure, another potential entrance to the ligand binding pocket, which is created by the displacement of helix 12 in other apo-nuclear receptor LBDs, is obstructed by helix 12 in the PPAR receptor since it is folded back against the LBD, similar to the helix 12 conformation

in the holo-RAR γ LBD [58]. Overall, despite the position of H12, the PPAR ligand binding pocket is still more accessible to the surface because of the presence of helix 2' and the alternative placement of helix 2. Furthermore, the PPAR ligand binding pocket has an approximate volume of 1300 Å³, which is considerably larger than ligand binding pockets found in other class I nuclear receptors, such as the thyroid hormone receptor, and means that the PPAR ligand only occupies around 30-40% of its total capacity [17,19]. The characteristics of the PPAR LBD suggest why PPARs are able to bind a more diverse range of ligands.

Most known PPAR agonists share features including a hydrophilic head group, a central hydrophobic part and a flexible linker to the tail [60]. Although the majority of the interactions between the PPAR ligand and the LBD are hydrophobic, the hydrophilic head of the ligand forms hydrogen bonds with conserved histidine and tyrosine residues in the LBD which result in a fixed conformation of the head group. The ligand binding pockets of the three PPAR isoforms are a comparable size, however variations in their shape and amino acid composition modulates their ligand specificity. The PPAR α and PPAR γ ligand binding site is a T-shaped with a central domain that extends from the c-terminal AF-2 helix (helix 12) to the β -sheet [57,60]. At the level of the β -sheet the central domain divides in to two interconnected cavities along an axis parallel to helix 3 [57,58,60]. In contrast, PPAR β has a Y-shaped ligand binding pocket and each arm of the pocket is approximately 12 Å in length [59]. There is a narrowing of the PPAR β pocket adjacent to helix 12 which indicates why the larger head groups of some PPAR ligands can not fit in to the pocket and therefore restricts the type of ligands PPAR β can bind compared with PPAR α and PPAR γ [62]. As PPAR α and PPAR γ have comparable shaped ligand binding pockets the basis for selectivity between these two isoforms is a substitution of tyrosine-314 in PPAR α for histidine-323 in PPAR γ [62]. These amino acid residues form hydrogen bonds with the hydrophilic head group of the PPAR ligand. However, the larger volume of the tyrosine-314 side chain in the PPAR α ligand binding pocket forces a 1.5 Å shift in the position of its ligand which cannot be accommodated by some PPAR γ specific ligands. For instance, a 1.5 Å shift of the PPAR γ agonist farglitazar in the PPAR α ligand binding pocket would result in a steric interaction between the farglitazar head group and the phenylalanine-273 residue of PPAR α

Fig. 1.1. Domain structure of PPARs and sites of post-translation modifications. PPARs like other nuclear receptors have a modular structure with six regions denoted A-F. Above the domain structure are depicted the sites of post-translation modification of human PPAR α , PPAR γ 1 and PPAR γ 2. For each site the type of modification, either phosphorylation (P) or sumoylation (Su) is indicated. The specific kinases which catalyse phosphorylation of different residues in the PPAR protein are also described. PPARs can be phosphorylated by either ERK (extracellular signal-regulated kinase), JNK (Jun NH₂-terminal kinase), PKA (protein kinase A) or PKC (protein kinase C). The A/B domain has a ligand independent transactivation function (AF-1). The C domain is the DNA binding domain which consists of two conserved zinc fingers. The two zinc finger motifs fold to create a single structural domain containing two helices (left diagram below domain structure). The first helix (shown in purple) is formed from the residues starting at the third conserved cysteine residue and enters the DNA major groove, while the second helix (shown in green) which begins at the c-terminus of the second zinc finger is arranged perpendicular to helix 1. The E/F domain is the ligand binding domain and has a ligand dependent activation function (AF-2). Below the domain structure on the right are two images of the ligand binding domain of PPAR γ (from From R.T.Nolte *et al*, *Nature*, **395**(1998): 187-194). The first image shows the secondary structure of the ligand binding domain, which comprises of 13 α -helices and a small 4 stranded β -sheet (right diagram). The second image is a space filled diagram which shows the peptide backbone of the ligand binding domain in blue and the volume of the ligand binding pocket in white.



which demonstrates why this ligand has a 1,000-fold selectivity for PPAR γ over PPAR α [62]. Additionally, the PPAR α ligand binding pocket is more lipophilic and less solvent exposed, therefore this isoform is better suited to interact with saturated fatty acids [62].

1.4 Post-translational modifications of PPARs

The transcriptional activity and stability of PPARs are regulated by a number of post-translational modifications including phosphorylation, ubiquitination and sumoylation [63,64].

1.4.1 Phosphorylation

The effect of phosphorylation on PPAR receptor activity is dependent on the isotype, the amino acid residue that is modified and the specific kinase which catalyses the reaction [63,65]. PPARs are the substrates of several different kinases, such as the mitogen activated protein kinases (MAPKs), cAMP-dependent kinase (PKA) and protein kinase C (PKC), which are stimulated by a variety of endogenous or exogenous signals [65,66]. Three MAP kinase pathways have been identified in mammalian cells. The extracellular signal-regulated kinase subgroup encompasses ERK1 and ERK2 that can be activated by insulin and growth factor stimulation via a Ras-dependent signal transduction cascade. Conversely, the activity of members of the Jun NH₂-terminal kinases (JNK) or p38 kinases is increased in response to environmental stress of cytokines such as tumour necrosis- α (TNF- α) [67,68]. Treatment of hepatocytes with insulin was demonstrated to induce a time-dependent increase in PPAR α phosphorylation and was correlated with enhanced basal and ligand-dependent PPAR α transcriptional activity [66]. It has subsequently been shown that the stimulatory effect of insulin on PPAR α activity is mediated by ERK1 and ERK2 phosphorylation of two serines (S12 and S21) in the A/B region of human PPAR α [69]. The mechanism by which phosphorylation promotes PPAR α transactivation remains elusive although the effect of insulin on the AF-1 region of PPAR α was mirrored by the addition of triiodothyronine receptor β 1, a strong binder of co-repressors. These findings indicated that the phosphorylation of the AF-1 domain of PPAR α triggers dissociation of co-repressors thereby relieving their partial

silencing of AF-1 transcriptional activity [65,69]. Moreover, phosphorylation of the same serine residues in the PPAR α AF-1 domain by p38 kinases increased coactivation specifically by PPAR γ co-activator-1 (PGC-1), however since neither co-repressors or PGC-1 directly interact with the AF-1 region of PPAR α this suggests that cross-talk occurs between domains [65,70]. The major phosphorylation sites of protein kinase A and protein kinase C have been mapped to the DNA binding domain and the hinge region of PPAR α respectively, although PKA and PKC can also modify serine residues in other domains of PPAR α (**Fig. 1.1**) [71-73].

Phosphorylation of PPAR α by PKA has been shown to stimulate ligand-dependent transactivation through a mechanism that stabilises PPAR α DNA binding [65,66,72]. PKC phosphorylation of PPAR α also increases ligand-dependent gene transcription, an effect which could be mediated by modulation of protein-protein interactions between the PPAR α hinge region and co-factors [73].

In contrast to PPAR α , phosphorylation of PPAR γ can repress its transcriptional activity. Indeed, epidermal growth factor and platelet derived growth factor stimulated phosphorylation of PPAR γ , through the MAPK signalling pathway in adipocyte cell lines, which decreased the basal and ligand-dependent transcriptional activity of PPAR γ [66]. Both ERK and JNK MAP kinases, but not p38 kinases, phosphorylate PPAR γ at a consensus MAP kinase site in its N-terminal A/B region, which is conserved between species, however is unique among the PPAR isoforms [67,74]. In humans, the MAPK site corresponds to serines at position 84 and 112 in PPAR γ 1 and PPAR γ 2 respectively (**Fig. 1.1**) [67]. Mutation of these residues to alanine abolishes MAPK phosphorylation of PPAR γ and ectopic expression of a S112A PPAR γ 2 mutant in NIH3-3T3 fibroblast cells increased their sensitivity to ligand-induced adipogenesis and blocked inhibition of differentiation by mitogens [67,75] (See section 1.12.1). Phosphorylation of PPAR γ by MAPK kinases has no effect on the receptor's nuclear localisation, affinity for RXR α or ability to interact with DNA, although it does impair ligand binding affinity [65]. Shao *et al* demonstrated that interdomain communication between the A/B and E/F domain of PPAR γ alters the conformation of the receptor which favours ligand binding and that phosphorylation of PPAR γ hinders the cross-talk between its domains [76]. Conversely insulin, under certain conditions, appears to promote phosphorylation and activation of PPAR γ via a MAP kinase pathway. However, this effect was not

mediated by the conserved MAP kinase site in the A/B region of PPAR γ , as insulin was equally effective at activating a S112A PPAR γ 2 mutant compared with the wild-type receptor. This suggested that although the insulin-dependent MAP kinase pathway increases phosphorylation of PPAR γ this effect may not be mediated by direct phosphorylation by ERK1/ERK2 [77]. In addition to the MAPK pathway, phosphorylation by AMP-activated protein kinase (AMPK) attenuates the basal and ligand-dependent functions of PPAR γ [66]. Post-translational modification of the PPAR β/δ isoform has been less extensively studied and as yet no sites of phosphorylation on the receptor have been mapped. Nevertheless, both cAMP and PKA activators increase the ligand independent -dependent transcriptional activity of PPAR β/δ indicating a potential role for this kinase in the modulation of PPAR β/δ function [66].

1.4.2 Ubiquitination

Several studies indicate that the turnover of PPARs, like other nuclear receptors, is modulated by the ubiquitin-proteasome pathway [63]. Proteins are targeted for degradation by the proteasome in an ATP-dependent manner, after covalent attachment of multiple 8 kDa polypeptides, called ubiquitin [78]. A single ubiquitin molecule is transferred to the substrate protein in a three step process [63,79]. In the first step, ubiquitin is activated by an ubiquitin-activating enzyme (E1). The activated ubiquitin is subsequently transferred to an ubiquitin carrier protein (E2) which shuttles ubiquitin to the ubiquitin-protein ligase (E3). Finally, ubiquitin-protein ligase (E3) bound to the substrate, catalyses formation of an isopeptide linkage between the terminal carboxyl of ubiquitin and the ϵ -amino group of a lysine residue in the target protein [80]. Once the first ubiquitin molecule is transferred to the protein substrate, the process is repeated to produce a polyubiquitin chain joined by a series of isopeptide linkages [78,81]. Interestingly, ligand activation of PPAR α and PPAR γ appears to have opposing effects on their ubiquitin-mediated degradation [78,79,82]. Ligand binding to PPAR α reduced its ubiquitination and thereby protected the receptor from degradation whereas ligand binding was shown to be essential for proteasomal degradation of PPAR γ [79,82]. However, in these studies PPAR α and PPAR γ turnover was examined after 5 and 20 hours of ligand treatment respectively [79,82]. These findings led Blanquart *et al* to speculate that PPAR

ligands may regulate degradation of their receptor in a time-dependent manner. Initially, the ligand may attenuate PPAR turnover in order to increase transcriptional activity of the receptor, however in the second stage recruitment of a co-factor may promote ubiquitination and degradation which creates a negative feedback loop to balance receptor transactivation [63]. Phosphorylation of nuclear receptors can act as a signal for ubiquitination, although Spiegeleman *et al* demonstrated that both the wild-type and the phosphorylation-deficient form of PPAR γ 2 (S112A mutant) were degraded after ligand activation, therefore it is improbable that serine phosphorylation is the only mechanism to target PPAR proteins to the ubiquitin-proteasome system [78,82].

1.4.3 Sumoylation

More recently SUMO-1 (small ubiquitin-like modifier-1) modification of PPAR γ has been implicated in regulating the function of this receptor [64,83,84]. SUMO-1 is an 11-kDa protein that is structurally homologous to ubiquitin [64]. Like ubiquitin, SUMO-1 is covalently linked to lysine residues in target proteins in a three step process, although the E1, E2 and E3 enzymes that catalyse sumoylation are distinct from those that mediate ubiquitin conjugation [83]. Two sumoylation sites have been identified in murine PPAR γ , one in the AF-1 region (mPPAR γ 1, K77, mPPAR γ 2, K107) and the other in the ligand binding domain (mPPAR γ 1, K365, mPPAR γ 2, K395) [64,83-85]. The corresponding lysine residues in the human PPAR γ sequence are indicated in **Fig. 1.1**. SUMO modification of K107 in mPPAR γ 2 did not affect its nuclear localisation but modestly increased the stability of the receptor, possibly by shielding PPAR γ from ubiquitin-mediated degradation [84]. However, sumoylation of this residue also reduced basal and ligand-dependent PPAR γ transcriptional activity [64,83,84]. SUMO conjugation of K107 was not dependent on DNA binding and was augmented by phosphorylation of serine 112 [83,84]. The mechanism by which sumoylation of the AF-1 region attenuates PPAR γ transcriptional activity is still unclear although it is speculated that it abrogates co-factor recruitment. So far this type of post-translational modification appears to be specific for PPAR γ since putative sumoylation sites in murine PPAR α and PPAR β/δ were not covalently linked to SUMO-1 *in vivo* [83]. In contrast to the lysine in the N-terminal A/B region, sumoylation of K365/K395 in the ligand binding domain of PPAR γ did not alter its

ability to activate gene transcription however was essential for PPAR γ -mediated transrepression (see also section 1.10) [85].

1.5 PPAR ligands

A wide variety of natural and synthetic PPAR ligands have been described (**Fig. 1.2**). Identification of PPAR ligands has relied on several different experimental techniques [17]. Traditionally ligand binding assays using radiolabeled ligands have been employed to discover agonists of other nuclear receptors. However, because radiolabeled ligands for PPARs were unavailable or produced unacceptable levels of non-specific binding alternative approaches were sought to overcome these limitations [86]. Forman *et al* developed a novel assay which relied on ligand binding inducing a conformational change in the PPAR receptor which promoted dimerisation and DNA binding and could be detected by a PPAR-responsive reporter [86]. A second technique that has been used is termed CARLA (co-activator dependent receptor ligand assay) and is based on the hypothesis that ligand binding to a PPAR induces an interaction with a co-activator [87]. These approaches have demonstrated that all three PPAR isoforms bind natural polyunsaturated fatty acids including, linolenic acid and eicosapentaenoic acid [20,86-88]. Controversy remained over whether these fatty acids were the *bona fide* endogenous ligands of PPARs, since they were shown to bind to the receptors with weak micromolar affinities, and therefore it was speculated that fatty acid concentrations were unlikely to reach levels required for the receptor activation *in vivo* [17]. More recently however, a fluorescent-based method devised by Lin *et al* revealed that PPAR α can bind to natural fatty acids with affinities in the nanomolar range, suggesting that the interaction between PPARs and such ligands is potentially much stronger than previously reported [89].

1.5.1 PPAR α ligands

As its name suggests the first described activators of PPAR α were a diverse class of compounds called peroxisome proliferators that included fibrates [16]. Fibrates, such as clofibrate, fenofibrate and bezafibrate are hypolipidemic drugs used in the

treatment of dyslipidemia [27,90]. All fibrates appear to require high micromolar concentrations to activate human PPAR α , which may explain why high doses (300-1200 mg/day) are needed for their clinical activity [20]. Although fibrates were originally classified as PPAR α ligands, it has subsequently been demonstrated that their active metabolites can also interact with PPAR γ and PPAR β/δ [20]. For instance, clofibric acid and fenofibric acid were dual activators of PPAR α and PPAR γ but exhibited 10-fold selectivity for PPAR α , while bezafibrate had a comparable affinity for all three isoforms [91]. This led to a search for more potent and selective PPAR α ligands that could function as hypolipidemic drugs. The compound GW9578 has recently been reported as a potent and sub-type specific PPAR α agonist with improved lipid lowering activity compared to fenofibrate [91]. Shortly afterwards it was shown that PPAR α binds fatty acids with the highest affinity of the three isoforms [17]. Furthermore, eicosanoids derived from arachidonic acid through the lipoxygenase pathway including 15-hydroxeicosatetraenoic (15-HETE) (8-hydroxeicosatetraenoic acid (8-S-HETE) in mice) and leukotriene B₄ (LTB₄) were also found to interact with PPAR α [90]. The first and rate limiting step in eicosanoid synthesis is the release of membrane bound arachidonic acid by phospholipase A₂ in either a one or two step process [92]. The free arachidonic acid is metabolised by several different pathways (**Fig. 1.2**). Metabolism of arachidonic acid by 15-lipoxygenase ultimately generates 15-HETE, whereas LTB₄ is the end-product of 5-lipoxygenase [92]. Interestingly in ligand binding assays LTB₄ binds to the PPAR α ligand-binding domain with a K_d of 90 nM suggesting local concentrations within the cells or *in vivo* may be sufficient to activate the receptor [93].

1.5.2 PPAR β/δ ligands

Apart from polyunsaturated fatty acids, other natural PPAR β/δ ligands include methyl palmitate and the eicosanoids, prostaglandin A₁ and PGD₂ [20,94]. In contrast to the other two isoforms, no drugs have been identified that act through the PPAR β/δ receptor. Thus, part of the challenge in determining the function of PPAR β/δ has been the identification of potent and selective PPAR β/δ ligands to use as chemical tools [9]. Johnson *et al* had described a series of synthetic ligands including L-631,033 as weak activators of PPAR β/δ [95]. The structure of these compounds is similar to some eicosanoids [20]. More recently however, a PPAR β/δ agonist called

GW501516, has been developed that has an unsubstituted phenoxyacetic head group that can be accommodated by the narrow PPAR β/δ ligand binding pocket [62,96]. GW501516 was shown to interact with the ligand binding domain of human PPAR β/δ fused to a GAL4 DNA binding domain with nanomolar affinity *in vitro* (EC₅₀ of 1.2 nM) and was 1,000 more selective for PPAR β/δ over the other two isoforms [97].

1.5.3 PPAR γ ligands

Although natural PPAR γ ligands includes poly-unsaturated fatty acids, such as linolenic acid, they are all relatively weak PPAR γ activators [98]. However, it has been demonstrated that conversion of fatty acids to eicosanoids leads to increased PPAR γ mediated transcription. For instance, the 15-lipoxygenase metabolites of linoleic acid, 9-hydroxy-octadecadienoic acid (HODE) and 13-HODE have been shown to act as PPAR γ agonists [20,93]. The J-series of prostaglandins derived from prostaglandin D₂ (PGD₂) have also been established as PPAR γ ligands. The terminal metabolite of the J₂ series, 15-deoxy- $\Delta^{12,14}$ prostaglandin J₂ (15dPGJ₂), produced by a dehydration reaction, was shown to bind and activate PPAR γ at micromolar concentrations *in vitro* [99]. 15dPGJ₂ also stimulated the differentiation of NIH 3T3 fibroblasts *in vitro*, providing some of the first evidence that PPAR γ played a role in adipogenesis [100].

Since its discovery, 15dPGJ₂ has become one of the most widely used natural PPAR γ ligands *in vitro* studies. Chemical decomposition of PGD₂ to produce 15dPGJ₂ yields one major product and three minor geometric isomers, which are isomeric about the three double bonds not in the cyclopentenone ring of 15dPGJ₂ [101]. The four isomers have different potencies, with the prominent isomer IV being the most potent. 15dPGJ₂ is chemically reactive but thermally stable and can be photo-degraded such that a single day's exposure to ambient light can render it less than 50% pure [101]. Sometimes 15dPGJ₂ is reported as the endogenous ligand of PPAR γ , although recent data suggests that like polyunsaturated fatty acids, *in vivo* concentrations of 15dPGJ₂ may not be sufficient for receptor activation [102]. Further study is warranted however to determine if 15dPGJ₂ actually has a stronger affinity for PPAR γ than has been reported [89]. In addition, an alkyl phospholipid

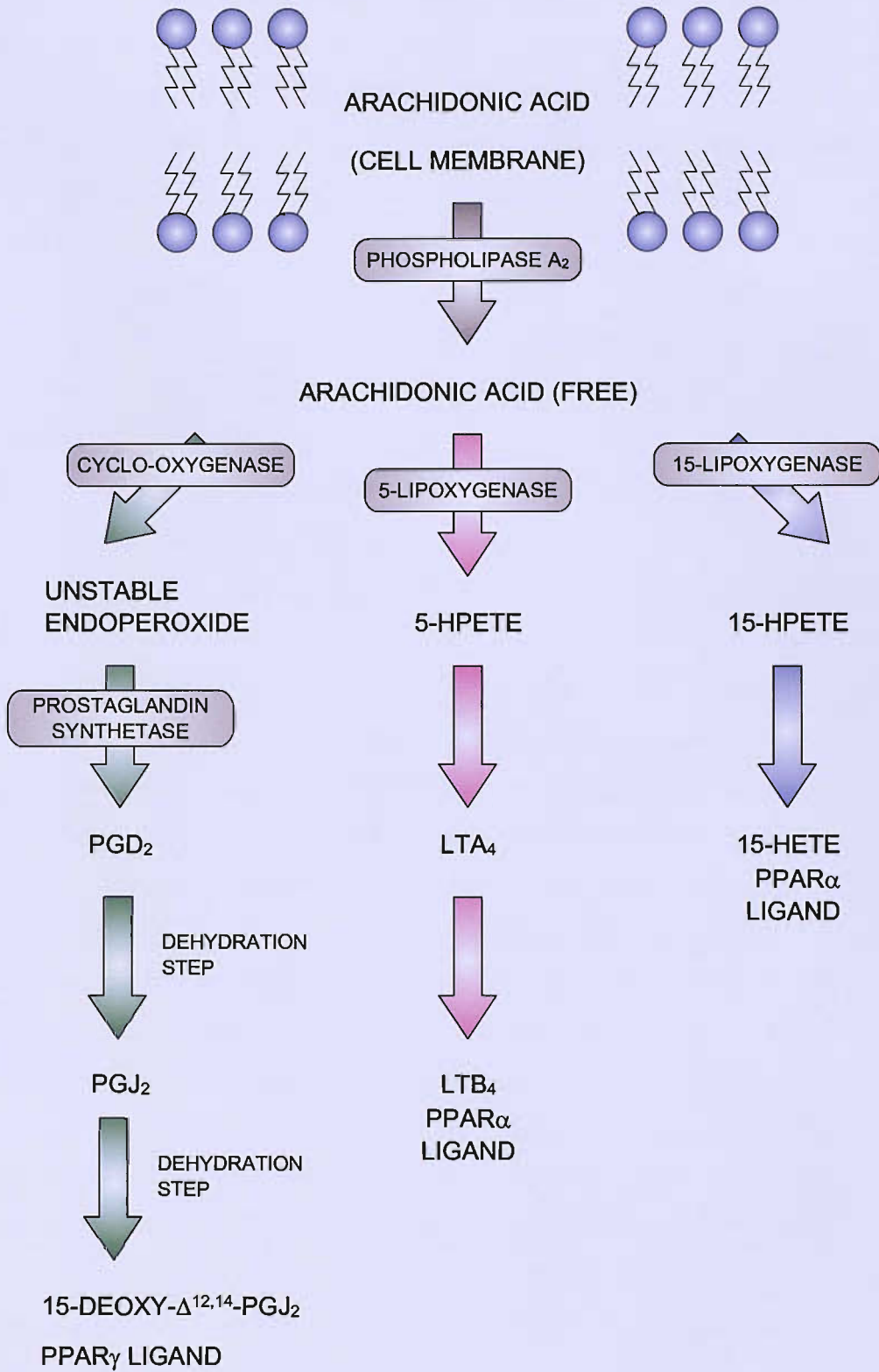
Fig. 1.2. Natural and synthetic PPAR ligands. The table shown in A gives examples of agonists for each PPAR isoform. The scheme in Fig.1.2B shows how metabolism of arachidonic acid can lead to the production of natural PPAR ligands. Once arachidonic acid is liberated from the plasma membrane by phospholipase A₂ in a one or two step process, free arachidonic acid is metabolized by several pathways. The cyclo-oxygenase pathway can lead to the generation of the PPAR γ ligand 15dPGJ₂, whereas arachidonic acid acid metabolized by lipoxygenases initiates the synthesis of leukotriene B₄ and 15-HETE which are PPAR α ligands.

Abbreviations: PGD₂= prostaglandin D₂, PGJ₂= prostaglandin J₂, LTA₄ = leukotriene A₄ LTB₄= leukotriene B₄, HETE = hydroxyeicosatetraenoic acid. HODE = hydroxyotadienoic acid

A.

PPAR ligand	PPAR isoform		
	α	β	γ
Natural	Polyunsaturated fatty acids Leukotrienes and HETEs e.g. 15(S)-HETE, LTB ₄ Saturated fatty acids e.g. palmitic	Polyunsaturated fatty acids e.g. eicosapentaenoic acid Hypolipidemic agents GW501516	Polyunsaturated fatty acids J ₂ prostaglandins e.g. 15dPGJ ₂ Oxidised alky phospholipids 9-HODE 13-HODE Thiazolidinediones e.g. ciglitazone triterpenoids tyrosine-based compounds cyclo-oxygenase inhibitors
Synthetic	Hypolipidemic agents e.g. clofibrac acid	Hypolipidemic agents GW501516	Thiazolidinediones e.g. ciglitazone triterpenoids tyrosine-based compounds cyclo-oxygenase inhibitors

B.



found abundantly in oxidized lipoprotein (oxLDL) was discovered as a high affinity PPAR γ ligand with a K_d of approximately 40 nM [103].

Synthetic PPAR γ agonists have also been identified including thiazolidinediones (TZDs), triterpenoids and tyrosine-based compounds [17,104,105] (**Table 1.2**). TZDs were originally discovered from the screening of clofibric acid analogues to identify compounds which had enhanced anti-lipidemic and anti-hyperglycemic properties in diabetic mice; although at the time the molecular target of TZDs was unknown [20,106]. TZDs were subsequently identified as highly selective PPAR γ ligands, whose rank order of affinity for this receptor *in vitro* mirrored their *in vivo* anti-hyperglycemic activity [104,106]. TZDs such as rosiglitazone and pioglitazone are now used clinically to treat type 2 diabetes. However, the TZDs contain a stereogenic centre at carbon 5 of the heterocyclic headgroup and therefore undergo racemization under physiological conditions [105,107]. Only the (S)-enantiomers of the TZD binds to the PPAR γ receptor with high affinity which has led to a search for PPAR γ agonists with alternative head groups which are less susceptible to racemization [20]. In light of these findings a group of tyrosine-based PPAR γ agonists have been developed which include, GI 262570 (Farglitazar), GW1929 and GW7845 which do not undergo racemization *in vivo* [20,105,107]. This series of compounds were the first anti-diabetic drugs to be optimized based on their activation of the human PPAR γ isoform and contains some of the most potent PPAR γ agonists which activate the receptor at sub-nanomolar concentrations and show a greater than 1000-fold selectivity for PPAR γ over the other PPAR isoforms [62]. Crystallographic studies show that Farglitazar is able to make additional hydrophobic contacts with the PPAR γ ligand binding pocket compared with the TZD rosiglitazone, which provides additional stability to Helix 12 (which contains the AF-2 function) which mediates transcriptional activation [108]. Initial phase II clinical studies with Farglitazar suggest it could act as a highly effective anti-diabetic drug *in vivo* [108].

1.6 PPARs heterodimerise with RXR

Members of the PPAR family form heterodimers with the retinoid X receptor (RXR) [17,19,20,88]. A PPAR/RXR heterodimer binds to a specific hormone response

motif called a peroxisome proliferator response element (PPRE) which was originally identified in the promoter of the acyl coenzyme A (acyl-CoA) oxidase gene [109]. Hormone response elements which bind nuclear receptor dimers are usually composed of two core hexameric motifs called half-sites [2,4]. The half-sites can be arranged as palindromes, inverted palindromes (IPs) or direct repeats (DRs) [2,4]. In a consensus PPRE, the two half-sites are configured as a direct repeat separated by one nucleotide (termed DR1) [8]. The number of bases between the two half-sites in part governs which receptors bind specific DRs. For instance, DRs separated by 3, 4 and 5 base pairs are preferentially regulated by the vitamin D, thyroid hormone and retinoic acid receptor respectively [2]. However, a perfect DR1 can bind several dimers including RXR homodimers, PPAR/RXR and RAR/RXR heterodimers. Therefore, additional features are required for a DR1 to specifically function as a PPRE [110]. For instance, Palmer *et al* demonstrated that the sequence upstream of the DR1 contributes to the selective binding of PPAR α /RXR over the binding of other complexes such as RXR/RXR [110,111].

A subsequent analysis of 16 other natural PPREs confirmed the importance of the 5' flanking region of the DR1 sequences in mediating PPAR/RXR binding and defined a PPRE as a DR1 core flanked by 7 nucleotides at its 5' end that had a consensus sequence of 5' CAAAACT-AGGTCA A AGGTCA-3' [111]. The 5' flanking region is also important in determining the affinity of the individual PPAR isoforms for the PPRE [111]. For example, PPAR α binds with higher affinity to PPREs in which the 5' flanking region and core DR1 strongly match the consensus sequence [111]. The binding efficiency of PPAR α becomes lower with increasing divergence from the consensus sequence for the 5' flanking region, whereas PPAR γ can still bind with relatively high affinity to weak PPRE elements. Interestingly the core DR1 for both strong and weak PPREs is similar and close to the consensus for a perfect DR1 showing that the 5' flanking region is more critical for PPAR α binding compared with PPAR γ [111]. The PPAR interaction with the PPRE is also dependent on the RXR subtype since PPAR γ has an even higher binding strength in the presence of RXR γ compared with RXR α for both strong and weak PPREs [111]. However, the preferred partner for PPAR α and PPAR β is RXR γ for strong PPREs, but RXR α for weak PPREs [111]. The 5' extended direct repeat determines the polarity of the PPAR/RXR heterodimer [53]. The CTE region of PPAR recognizes the 7 nucleotides

in the 5' flanking region and therefore binds to the upstream direct repeat and RXR occupies the downstream motif [53]. This is the reverse polarity compared with other heterodimers which bind direct repeats such as VDR/RXR and TR/RXR [2,4].

PPAR/RXR is an example of a permissive heterodimer, which can be activated by ligands of either of its receptors and is synergistically activated in the presence of both agonists [2,4]. The crystal structure of the PPAR γ /RXR α heterodimer shows that the interface between the two receptors is asymmetric such that the PPAR γ ligand binding domain is rotated approximately 10° from the C2 symmetry axis of the RXR ligand binding domain [61]. The interface consists of both hydrophobic and polar interactions between helix 7, helix 9 and helix 10 and the loop between helix 8 and helix 9 of both receptors. An aspartic acid residue D441 in the first half of helix 10 of PPAR γ forms a critical salt bridge with arginine 393 in helix 9 of RXR α [61]. This salt bridge would be absent in either an RXR or PPAR γ homodimer. The asymmetry of the heterodimer also results in the association of a positively charged region of RXR helix 7 with a negatively charged surface at the end of the PPAR γ AF-2 helix and the 8/9 loop [61]. These findings suggest that PPAR preferentially forms a heterodimer with RXR because it allows the formation of specific interactions, at the interface of the two receptors, which would not occur in a PPAR homodimer, that stabilize the dimer [61,112].

1.7 Sub-cellular localization of PPARs

Upon binding ligand PPARs undergo a conformational change; however there is still controversy over how this mediates receptor activation. Some research suggests that the ligand induced conformational change is a pre-requisite for nuclear localization, whereas other reports show that it is dispensable for this process but is essential for co-activator recruitment. The sub-cellular localization of PPARs in different cell types however indicates that ligand activation of PPARs could involve nuclear translocation and/or recruitment of co-activators.

1.7.1 In the cytosol

Analysis of the intracellular localization of PPARs in certain cell types, indicate that unliganded PPARs like other nuclear receptors, such as the glucocorticoid receptor and the androgen receptor are predominantly cytoplasmic [113]. Furthermore, PPARs may be localized in the cytoplasm because of their interaction with chaperone molecules such as heat shock protein 90 (Hsp90) [114,115] (**Fig. 1.3**). The change in PPAR receptor conformation upon ligand binding could unmask its nuclear localization sequence (NLS) by causing dissociation of the heat shock protein complex [11]. In a simplified model, the NLS is then recognized by a protein called importin- α , which is part of a nuclear import heterotrimeric complex that also contains importin- β [113]. Importin- β mediates the docking interaction on the nuclear membrane/pore. With participation from several other key players in the cytosol and immobile components of the nuclear pore complex, the nuclear translocation event is completed and the PPAR receptor is released from the nuclear import factors [113] (**Fig. 1.3**). It is also speculated that PPAR/RXR heterodimerisation may occur in the cytoplasm to facilitate nuclear entry of the PPAR receptor (**Fig. 1.3, step 4a**) [7]. Ultimately, whether PPAR translocates alone or in complex with RXR, upon reaching the nucleus the PPAR/RXR binds to PPRES in the promoters of target genes. Redistribution of PPAR γ protein from the cytoplasm to the nucleus has been observed in breast, endothelial and lung cell lines after PPAR γ ligand treatment [116,117].

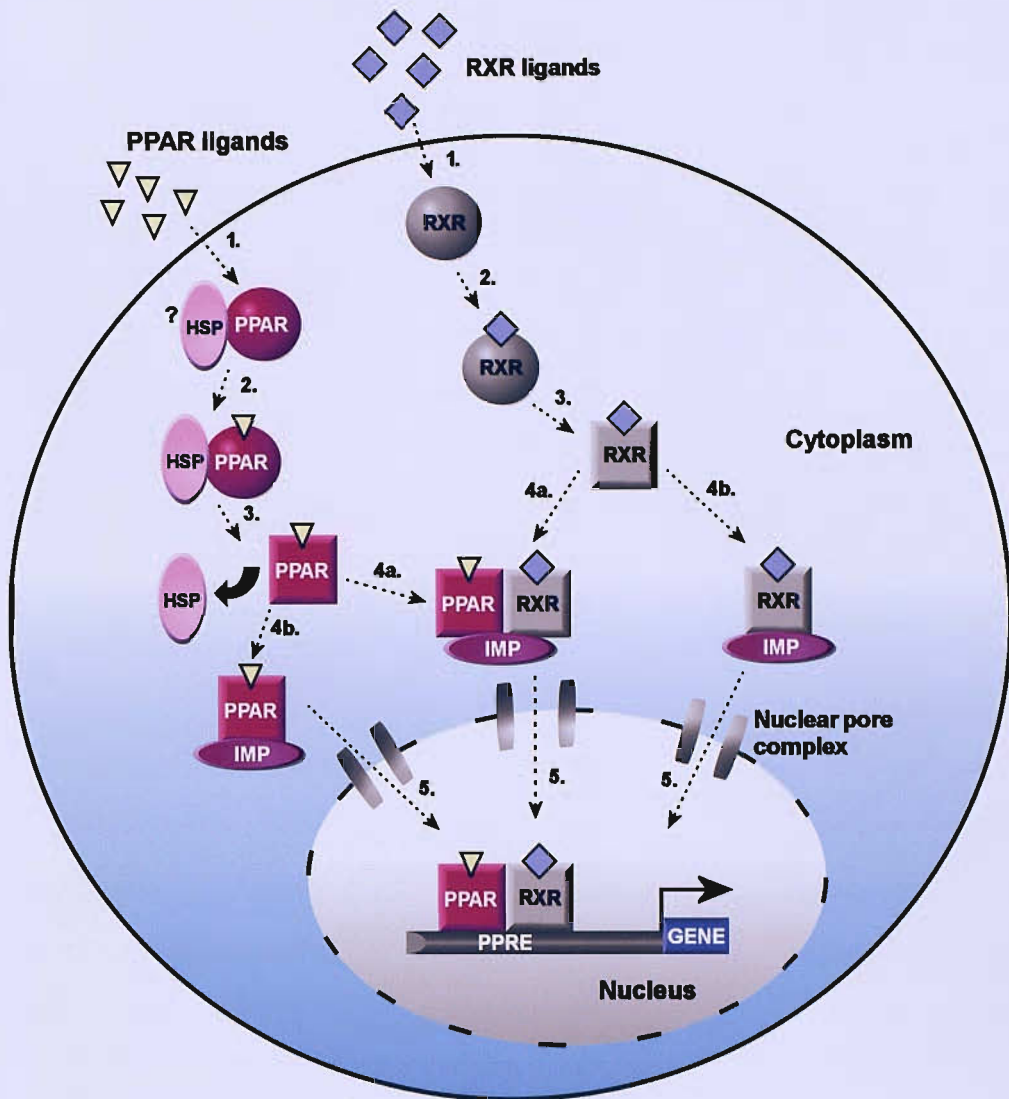


Fig. 1.3. Translocation of PPARs to the nucleus.

1. PPAR and RXR ligands diffuse across the plasma membrane into the cytoplasm of the cell.
2. PPAR and RXR ligands bind to their respective receptors localized in the cytoplasm. There is evidence to suggest that in the absence of ligand PPARs could interact with a chaperone protein such as Hsp90.
3. Ligand binding induces a conformational change in the receptor. In the case of PPAR this may lead to release of the hsp protein and unmask its nuclear localization sequence.
4. PPAR may heterodimerise with RXR in the cytoplasm to promote nuclear entry (A) or translocate alone (B). In either case, the receptors are recognized by importin- α , via their NLS, which mediates nuclear translocation via the nuclear pore complex.
5. Upon release from the nuclear pore factors, PPAR and RXR bind as a heterodimer to peroxisome proliferator response elements (PPREs) in the promoter of target genes.

1.7.2 PPARs interact with co-repressors in the nucleus

Conversely, it has been shown that PPARs chiefly localize in the nucleus. For example, the PPAR α receptor is predominantly nuclear in kidney mouse COS-1 cells and human astrocytes [55,118]. Green fluorescent protein (GFP) chimeras of all 3 PPAR isoforms expressed in a mouse hepatoma cell line (Hepa-1) had a nuclear distribution in both the presence and absence of specific ligands [54]. In addition, a human PPAR γ mutant lacking five carboxyl-terminal amino acids, which could not be activated by a potent TZD, was still able to localize to the nucleus, which suggests that ligand binding in some cell types is not essential for nuclear translocation [118]. Alternatively, nuclear localization of PPARs may be a result of a dynamic equilibrium between nuclear-cytoplasmic and cytoplasmic nuclear shuttling [2].

There is evidence to suggest that in the absence of ligand, nuclear PPARs bound to a PPRE in the promoter of a target gene can interact with co-repressors, termed nuclear co-repressor (NCoR) and silencing mediator of retinoid and thyroid hormone receptors (SMRT). Indeed Yu *et al* detected PPAR γ in anti-SMRT and anti-NCoR immunoprecipitates from whole cell extracts of 3T3-L1 fibroblasts, which had not been treated with exogenous ligand, demonstrating that this PPAR isoform can interact with co-repressors *in vivo* [119]. Furthermore, peptides derived from one of the nuclear receptor interacting motifs of NCoR and SMRT were able to interact with the ligand binding domains of all three isoforms *in vitro* [120]. Interestingly, some studies have suggested that the PPAR β/δ isoform has a higher affinity for co-repressors than PPAR γ or PPAR α . Ectopic expression of PPAR β/δ in 3T3-L1 fibroblasts blocked PPAR γ -mediated adipogenesis suggesting that PPAR β/δ could act as repressor of PPAR γ -dependent gene transcription [33,121]. SMRT and NCoR form the core of a large (>1-2 MDa) protein complex which can also be recruited by other unliganded nuclear receptors such as the thyroid hormone receptor [122]. The repressive activity of the SMRT-NCoR complex is believed to result from the direct or indirect recruitment of histone deacetylases (HDACs) including HDAC3. Removal of acetyl groups on the N-terminal tails of histone lysines by HDACs is associated with the formation of nucleosome-DNA interactions that lead to a more closed chromatin structure [123].

Chromatin structure plays an important role in regulating eukaryotic gene expression [124]. Constitutive heterochromatin which generally has a low gene content and is transcriptionally silent, is found in regions of centromere and telomere DNA and remains tightly compact through out the cell cycle [125,125,126]. In contrast, in euchromatin, where genes are being expressed the DNA is less condensed and more accessible to transcription factors [126]. The repeating unit of chromatin is the nucleosome core particle, which consists of 147 base pairs of DNA wrapped around an octamer of histone proteins [124]. Residues in the amino-terminal tail and at certain exposed sites within the globular domain of the histone protein undergo a variety of post-translational modifications including, acetylation, methylation, phosphorylation, ubiquitylation, sumoylation and ADP-ribosylation [127-129]. The amino group of lysines in the N-terminal tails of histones can be acetylated by histone acetyltransferases (HATs) which is associated with gene activation [128]. Acetylation of the lysines near a gene promoter increases accessibility of the DNA to the basal transcriptional machinery by reducing the affinity of histones for DNA and facilitating the recruitment of other chromatin modifying or remodelling enzymes which recognise the acetylated histone tail via their bromodomain and maintain the transcriptionally active state of the DNA [124,126].

Therefore, recruitment of a HDAC-containing complex by the unliganded DNA bound PPAR receptor prevents gene activation. The interaction between SMRT/NCoR and HDACs is mediated by their N-terminal deacetylase activation domain (DAD) which is essential for co-repressor function [130]. Furthermore, the association of SMRT/NCoR with the PPAR receptor is dependent on CoRNR motifs found in the highly conserved nuclear-receptor-interaction domain (NRID) of co-repressors. A study by Tan *et al* suggests that water insoluble PPAR ligands are transported to PPAR receptors in the nucleus by specific fatty acid binding proteins [131] (**Fig. 1.4**). For instance, the binding of troglitazone to adipocyte fatty acid binding protein (A-FABP) promoted nuclear translocation of A-FABP which allowed the protein to interact with PPAR γ and transfer the agonist directly to the receptor's ligand binding domain [131]. It is proposed that the

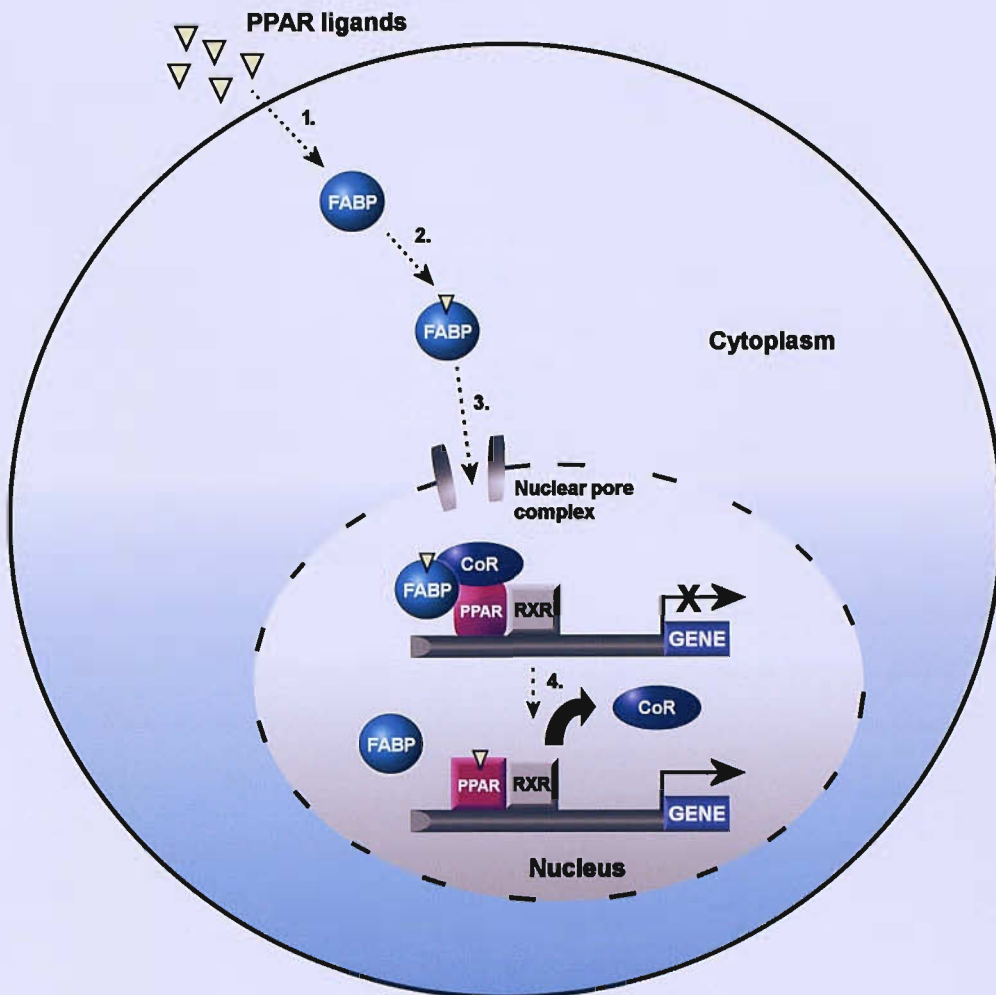


Fig. 1.4. Ligand activation of PPARs in the nucleus causes release of co-repressors.

1. PPAR ligands diffuse across the plasma membrane in to the cytoplasm.
2. In the cytoplasm they interact with a fatty acid binding protein (FABP) (Studies suggest that specific PPAR ligands are recognised by different FABPs.)
3. Upon binding ligand the FABP translocates to the nucleus.
4. In the nucleus FABP interacts with the PPAR (in complex with co-repressors (CoR)) to deliver the ligand straight to the receptor's ligand binding domain. The binding of ligand induces a conformational change in the receptor which releases the co-repressor complex.

change in conformation of the PPAR receptor upon ligand binding releases the co-repressor complex.

1.8 Recruitment of co-activators

Comparison of the apo (unliganded) and holo (liganded) crystal structures of RXR α suggest that upon ligand binding, the RXR α ligand binding domain undergoes a major conformational change which involves the “swinging” of helix 12. In its holo-position helix 12 essentially “seals” the ligand binding pocket and further stabilises ligand binding by contributing to additional ligand-protein interactions [3,132]. However, the extent of movement of helix 12 in response to ligand binding is thought to be dependent on the receptor type [56]. In the case of PPARs, the change in conformation of helix 12 following ligand binding is proposed to be more subtle, since helix 12 in apo-PPAR structures is already closer to its position in the holo receptors [57-60]. Nevertheless, the ligand-binding domain of apo-nuclear receptors in solution is believed to a very dynamic structure with many possible conformations. Furthermore, monitoring of the apo-ligand binding domain of PPAR γ by NMR spectroscopy demonstrated that agonist binding was associated with a pronounced stabilization of the domain conformation [133].

Helix 12 contains the AF-2 domain which consists of a sequence of nine amino acids which are highly conserved among nuclear receptors and form an amphipathic α -helix which is essential for ligand dependent co-activator recruitment [134]. Considerable insight in to the interactions between PPAR ligand binding domains and co-activators, whose nuclear-receptor-interaction domain contain highly conserved LXXLL motifs, has been gained through examination of the human PPAR γ ligand binding domain in complex with 88 amino acids of the co-activator SRC-1 (steroid receptor co-activating factor-1) [57]. The interactions between the PPAR γ AF-2 domain and SRC-1 were predominantly hydrophobic [57]. However, a glutamate in the AF-2 helix (E471) and a lysine in helix 3 (K301) of the LBD form a “charge clamp” in which glutamate E471 forms a hydrogen bond with the backbone amide of Leucine 1 in the LXXLL motif and lysine 301 forms a hydrogen bond with the backbone carbonyl of leucine 4 or 5 in the LXXLL motif [57,135]. There is evidence to suggest that the AF-2 domains of NRs, which share homology with LXXLL

motifs, can interact with the co-activator binding domain of their dimeric partner, thereby allosterically inhibiting the recruitment of co-activators. Therefore, ligand dependent activation of the PPAR may also involve displacement of the RXR AF-2 domain from the PPAR LXXLL-binding pocket. Thiazolidinediones binding to the apo-PPAR γ LBD results in two key hydrogen bonds between H323 and H449 that essentially locks the AF-2 domain in to a charge-clamp configuration, which favours binding to the LXXLL co-activator motif rather than the RXR AF-2 domain [57]. Some PPAR co-activators have been identified which interact with the receptor via their SCAN domains but this association is not dependent on the PPAR AF-2 domain [136].

1.9 Co-activators

An increasing number of co-activators have been identified which interact with PPARs to promote gene transcription (**Table 1.1**). Many co-activators, as described in the previous section, interact directly with the ligand binding domain of PPAR via a highly conserved LXXLL motif. Interestingly amino acids directly adjacent to the LXXLL motif and the specific PPAR agonist used can dictate which co-activators are recruited by the PPAR receptor [137,138]. Members of the p160 co-activators family which includes SRC-1, transcriptional intermediary factor-2 (TIF-2) and activator of the thyroid and retinoic acid receptor (ACTR), contain 3 repeated LXXLL motifs in their nuclear-receptor interaction domain [139]. Other examples of co-activators recruited by PPARs via their LXXLL motif include thyroid hormone receptor associated protein 220 (TRAP220), PPAR γ co-activator-1 (PGC-1), activator for the androgen receptor 70 (ARA-70) and BRG1/Brm-2 associated factor of 60 kDa, subunit c2 (BAF60c2)[140-143]. Members of the LXXLL motif family have different functions which collectively lead to transcriptional activation. For instance, SRC-1 and ACTR have histone acetyltransferase activity, while SRC-1, TIF2 and PGC-1 mediate HAT recruitment [139]. SRC-1 and ACTR both interact with the co-activator CBP/p300 which exhibits HAT activity [139]. Furthermore, BAF60c2 mediates interactions with components of the SWI/SNF (mating type switching/sucrose non-fermenting) chromatin remodeling machinery whereas TRAP220 anchors a multi-

Cofactor	Abbreviation	Interacts with PPAR:	Co-factor motif	Function
Coactivators				
p160 proteins				
Steroid receptor co-activator-1	SRC-1 (NcoA-1)	α β/δ γ	LXXLL	Histone acetyltransferase and recruits CBP
Transcriptional intermediary factor-2	TIF2 (GRIP 1)	α β/δ γ	LXXLL	Interacts with CBP
Activator of the thyroid and retinoic acid receptor	ACTR (RAC3/AIB1/ TRAM1)	α β/δ γ	LXXLL	Histone acetyltransferase
Creb interacting protein	CBP/p300	α γ	LXXLL	Histone acetyltransferase
Thyroid hormone receptor associated protein 220 or PPAR binding protein	TRAP220 (DRIP205)	α γ	LXXLL	Anchors multi-subunit DRIP complex to PPRE that interacts with RNA Pol II
PPAR γ coactivator 1	PGC1	γ	LXXLL	Recruits HATs
Activator for the androgen receptor 70	ARA70	γ	LXXLL	-
BRG1/Brm-associated factor of 60 kDa, subunit 2	BAF60c2	γ	LXXLL	Mediates interaction with chromatin remodeling machinery
PPAR γ coactivator 2	PGC2	γ	SCAN	-
SCAN-domain containing protein-1	SDP-1	γ	SCAN	-
Corepressors				
Nuclear co-repressor	N-CoR	α β/δ γ	CoRNR	Recruits histone deacetylases
Silencing mediator for retinoid and thyroid receptors	SMRT	α β/δ γ	CoRNR	

Table 1.1 Cofactors recruited by PPARs

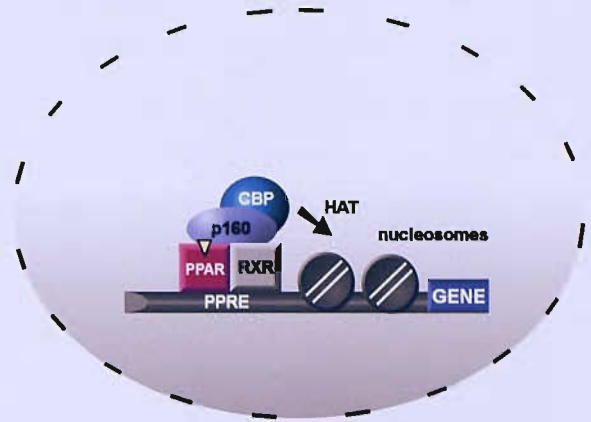
subunit complex of at least 15 DRIP proteins which range in size from 30 to 250 kDa [143,144]. The DRIP complex shares subunits with RNA Pol II holoenzyme suggesting that it may facilitate the recruitment of RNA Pol II to the target promoter by creating a binding surface [141,144]. Other co-activators including PPAR γ coactivator protein-2 (PGC-2) and SDP-1 (SCAN-domain containing protein-1) do not require the charge clamp to interact with PPAR γ , but instead bind through their SCAN domain [136]. Evidence from *in vitro* and *in vivo* studies suggest that gene transactivation by PPAR/RXR heterodimers is mediated by the ordered and sequential recruitment of co-activators [145]. For instance, it has been shown that because p160 co-activators and TRAP-DRIP complexes utilize the same surface on the ligand binding domain they cannot be recruited to the receptor simultaneously because it would result in steric hindrance [144]. Therefore, it is proposed that co-factors that recruit or have HAT activity such as p160 members initially bind to the PPAR/RXR heterodimer in the target promoter and then dissociate. Histone acetylation may promote recruitment of the SWI/SNF complex via BAF60c which leads to nucleosome clearance [145]. This makes the DNA of the target promoter more accessible, facilitating assembly of the large DRIP complex anchored by TRAP220 that targets RNA Pol II and the basal transcriptional machinery to the promoter which ultimately initiates gene transcription [144] (**Fig. 1.5**).

1.10 Transrepression

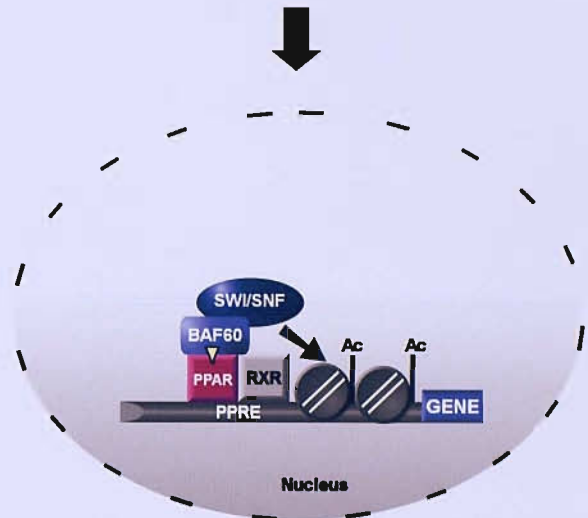
Although PPAR receptors predominantly function as transcriptional activators by directly binding to PPREs, Pascual *et al* have recently shown how ligand dependent sumoylation of PPAR γ can promote transrepression of NF- κ B target genes by the PPAR receptor [85]. Ligand binding is required to induce a conformational change in the ligand binding domain of PPAR γ in order to expose the sumoylation site of the sumo E3 ligase PIAS1 (protein inhibitor of activated STAT1). Following sumoylation of residue K365 (K367 in PPAR γ 1) by PIAS1, PPAR γ is targeted to a co-repressor complex on a specific NF- κ B regulated promoter, such as that of the inducible nitric synthase gene (*iNOS*) [85]. This complex consists of NCoR and SMRT co-repressors, HDAC3 and

Fig. 1.5 Sequential recruitment of co-activators by the PPAR/RXR heterodimer.

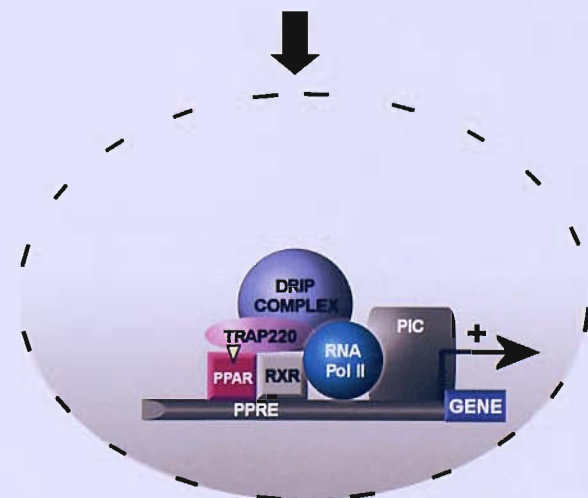
PPAR/RXR is proposed to initial recruit p160 co-activators and CBP which mediate histone acetylation.



Histone acetylation promotes recruitment of chromatin remodelling machinery possible via co-factor BAF60 resulting in nucleosome clearance at the target promoter.



Now that the DNA is more accessible PPAR/RXR can recruit the large multisubunit DRIP complex through TRAP220. This complex makes contact with RNA Pol II which leads to the initiation of gene transcription.



transducin beta-like protein-1 (TBL-1) and TBLR1. In the absence of PPAR γ , lipopolysaccharide treatment stimulates *iNOS* gene transcription by promoting ubiquitin-mediated proteosomal degradation of NCoR/SMRT co-repressors with TBLR1 functioning as the essential E3 ligase [85]. However, PPAR γ prevents recruitment of the ubiquitylation/19S proteasome machinery that facilitates the removal of the co-repressor complex, thus maintaining the promoter in a repressed state [85] (**Fig. 1.6**). This mechanism suggests PPAR γ ligands may mediate their anti-inflammatory effects by stimulating sumoylation dependent PPAR γ transrepression of inflammatory gene promoters (See also section **1.12.3**).

1.11 The roles of PPARs in normal cell function and disease

1.11.1 PPAR α functions

PPAR α is highly expressed in the liver and has been shown to play a critical role in fatty acid catabolism in this tissue [26,90]. In the liver, the fate of the fatty acids is dependent on the energy status of the organism. When fatty acids and carbohydrates are abundant, fatty acids are re-esterified to form triglycerides that are packaged with apoproteins to form VLDL (very low density lipoprotein) which is mainly taken up by adipose tissue for storage [17]. However, when fatty acid levels are higher than carbohydrates, fatty acids are metabolized to provide energy. The initial step required for oxidation of fatty acids, generated by adipose tissue lipolysis, is their uptake up the hepatocyte [26]. This transport of long chain fatty acids and oxidized low-density lipoproteins across the plasma membrane is mediated by fatty acid transport protein-1 (FATP-1) and fatty acid translocase (FAT/CD36) [90]. The fatty acid transport protein-1 gene was identified as a direct PPAR α target gene since it contains a functional PPRE in its promoter [26]. Before fatty acids are metabolized in the liver they must be converted in to their fatty acyl-CoA derivatives, a process which is controlled by fatty acyl-CoA synthetase, which is also a direct target gene of PPAR α [17]. Fatty acyl-CoA derivatives are degraded by either the peroxisomal or mitochondrial fatty acid β -oxidation pathways [19]. The

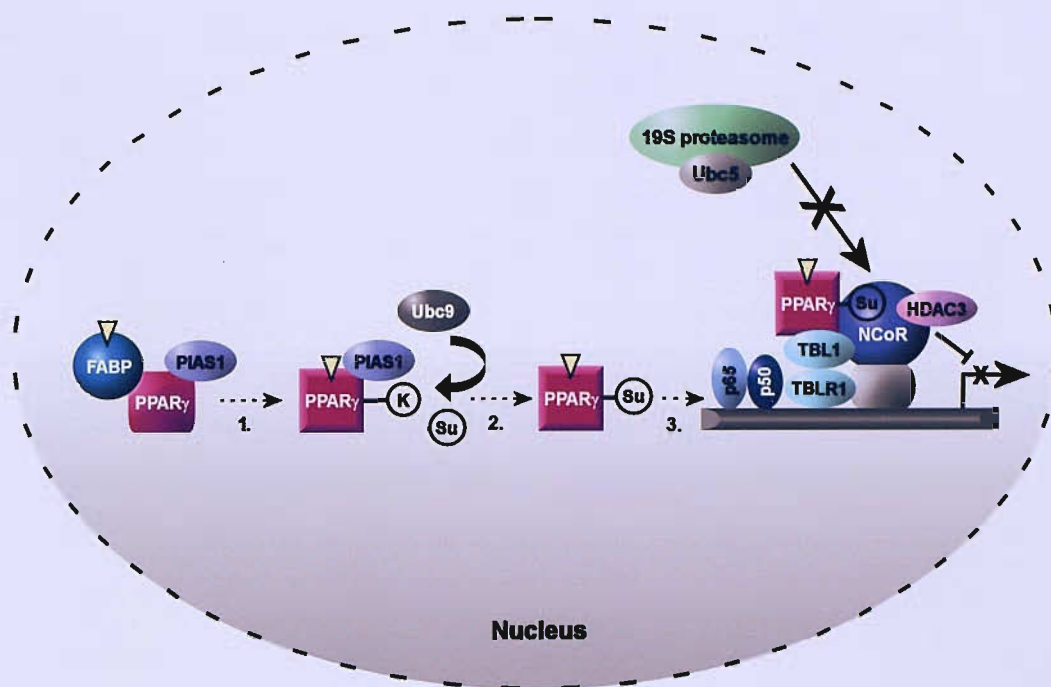


Fig. 1.6 Sumoylation dependent transrepression by PPAR γ .

1. Fatty acid binding protein (FABP) delivers ligand to PPAR ligand binding domain.
2. Ligand binding induces a conformational change in the receptor which exposes the PIAS1 sumoylation site (lysine residue PPAR γ 1 = K367, PPAR γ 2 = K365). Ubc9 serves as the SUMO-1 carrier protein (E2) and delivers the SUMO-1 protein to the E3 ligase PIAS1 which in turn sumoylates the PPAR receptor.
3. Sumoylation of the PPAR receptor targets PPAR to a co-repressor complex on inflammatory gene promoters. The complex consists of transducin beta-like protein-1 (TBL1), TBLR1, NCoR and SMRT co-repressors and HDAC3. Recruitment of PPAR to this complex prevents the ubiquitylation/19S proteasome machinery from removing the co-repressor complex, thus the target promoter is maintained in a repressed state.

oxidation of very long chain fatty acids in peroxisomes is catalysed by acyl-CoA oxidase. One of the main functions of peroxisomal β -oxidation appears to be shortening the length of long chain fatty acids ($>C20$), which predominantly come from the diet, via the removal of two carbons at each round of oxidation in the form of an acetyl-CoA molecule, so they can be further metabolized by the mitochondria [17]. This is because the carnitine-dependent transport system which controls the translocation of fatty acids across the outer and inner mitochondrial membrane excludes very long chain fatty acids ($C>20$). A critical component of the transport system is the carnitine palmitoyltransferase (CPT) enzyme, which catalyses the formation of fatty acyl carnitine which is required for influx of fatty acids into the mitochondria [27]. The promoter of the CPT gene contains a PPRE and is strongly induced by PPAR α . The acetyl-CoA unit produced by each cycle of fatty acid β -oxidation in the mitochondria can either enter the citric acid cycle for complete oxidation to generate ATP or is converted to ketone bodies [17].

The synthetic fibrate class of PPAR α agonists is used clinically to treat dyslipidemia and cause a reduction in triglyceride levels and increase in high density lipoprotein (HDL) cholesterol via PPAR α activation [26,90]. Fibrate induction of PPAR α causes increased expression and activity of lipoprotein lipase (LPL) which catalyses the hydrolysis of triglycerides in circulating chylomicrons, which leads to increased clearance of chylomicron remnants by the liver, which in turn decreases triglyceride levels [90]. Fibrates also attenuate the expression of a natural inhibitor of LPL activity called ApoC-III and induce ApoA-V, a strong reducer of plasma triglyceride levels [90]. High density lipoprotein cholesterol consists of a hydrophobic core containing triglycerides and cholesterol surrounded by a monolayer of phospholipids and apo proteins. The expression of genes encoding the apo proteins found in HDL, apolipoprotein AI and AII are up-regulated by fibrate induced PPAR α activation. Increased HDL cholesterol promotes the transport of lipids from peripheral tissues to the liver which reduces risk of coronary heart disease in patients with obesity or the metabolic syndrome. In addition to its major role in fatty acid metabolism PPAR α has also been implicated in xenobiotic, bile and amino acid metabolism, vascular and glucose homeostasis and inflammation [26,63,146-148].

1.11.2 PPAR β/δ functions

Initially the functions of PPAR β/δ remained more elusive compared with the other two PPAR isoforms [149]. Progress in understanding the physiological role of PPAR β/δ had been impeded by the receptors broad tissue distribution and lack of specific PPAR β/δ ligands [149,150]. However, recent studies using PPAR β/δ null mice have improved informative about some of PPAR β/δ functions[151].

Homozygous loss of PPAR β/δ resulted in embryonic lethality in 90% of mice which was caused by an abnormal gap in the placento-decidual interface, indicating that PPAR β/δ plays a critical role in placentation[151]. PPAR β/δ deficient mice were also smaller and had a decreased adipose mass [35,151]. Furthermore, PPAR β/δ has been implicated in cholesterol transport although there is still controversy over its function in this process. The selective PPAR β/δ agonist GW501516 stimulated expression of the ATP-binding cassette A1 (ABC1) protein, which promoted apolipoprotein A1 specific cholesterol efflux, in macrophage, fibroblast and intestinal cells *in vitro* [97]. In Rhesus monkeys, with comparable symptoms to human metabolic syndrome X, GW501516 increased high density lipoprotein cholesterol (HDLc) which transports cholesterol away from peripheral tissues and decreased fasting triglycerides [97]. In contrast, Palmer *et al* showed that PPAR β/δ expression promoted differentiation of human macrophages *in vitro* [152]. In addition, treatment of primary macrophages with another PPAR β/δ agonist, compound F, overall promoted lipid accumulation, despite increasing expression of ABC1 like GW501516 [152].

PPAR β/δ expression was also up-regulated in the skeletal muscle of mice which had been fasted for 24 hours and could be completely reversed to control levels by re-feeding [34]. The induction of PPAR β/δ was in parallel with increased expression of the fatty acid transporter, CD36 [34]. Stable muscle cell lines over-expressing PPAR β/δ showed enhanced induction of genes involved with fatty acid uptake, transport and metabolism, such as CD36, fatty acid binding protein and lipoprotein lipase. These cell lines also exhibited increased fatty acid oxidation in response to a specific PPAR β/δ agonist, indicating a role for PPAR β/δ in lipid metabolism in skeletal muscle [34]. PPAR β/δ appears to play an essential role in skin wound

healing [149,153]. The immediate response to skin injury is the release of inflammatory cytokines including TNF- α and IFN- γ which stimulate a stress-associated kinase cascade that activates the PPAR β/δ promoter via its AP-1 site [149]. The induction of PPAR β/δ expression stimulates keratinocyte differentiation and increases resistance of keratinocytes to cell death by decreasing PTEN (phosphatase and tensin homologue 10) expression and activating the protein kinase B survival pathway [154]. Further support for the anti-apoptotic role of PPAR β/δ comes from the finding that human PPAR β/δ null human colon cancer cells created by targeted homologous recombination, were defective in establishing tumours in nude mice *in vivo* [155]. Activation of PPAR β/δ stimulates proliferation of intestinal adenomas *in vivo* and human breast, prostate and hepatocellular cancer cell lines *in vitro* [156-158]. Conversely, alternative PPAR β/δ knockout models suggest that PPAR β/δ expression is dispensable for the formation of colonic neoplasms and ligand activation of the receptor may actually inhibit tumour growth [159,160].

1.12 PPAR γ functions

1.12.1 Adipocyte differentiation

The PPAR γ isoform was originally identified as a critical regulator of adipocyte differentiation [159,161-164]. Adipogenesis can be induced in mouse 3T3-L1 fibroblasts *in vitro* by culturing post-confluent cells in a medium containing 3-isobutyl-1-methylxanthine, dexamethasone and insulin (MDI). Immediately after exposure to these agents, the fibroblasts re-enter the cell cycle for a limited period of cell proliferation, termed clonal expansion, which is followed by irreversible growth arrest that is essential for terminal differentiation to occur [165]. The finding that this growth arrest coincides with an induction of PPAR γ expression which continues to be maintained in the mature adipocytes suggested that PPAR γ may be a modulator of this process [165]. This hypothesis is supported by the observation that ectopic expression of PPAR γ in fibroblasts results in their differentiation to lipid-laden adipocytes *in vitro* [162,166]. Similarly, the forced expression of PPAR γ in myoblasts *in vitro*, in the presence of hormonal stimulation causes

transdifferentiation, a process which stimulates lipid accumulation in the myoblasts and expression of tissue-specific fat cell genes which are characteristic of mature adipocytes [167]. Furthermore, PPAR γ ligands including 15dPGJ₂ and TZDs stimulate adipogenesis *in vitro*, which can be blocked by treatment with PPAR γ antagonists or by ectopic expression of a PPAR γ dominant negative receptor [99,100,135,168,169].

The stimulation of PPAR γ expression is a critical step in a cascade of events that regulates adipocyte differentiation and involves co-ordination of several transcription factors [161,170,171]. During the early clonal expansion phase, in response to hormonal stimulation, expression of two members of the CCAAT/enhancer binding protein (C/EBP) family of transcription factors, C/EBP β and C/EBP δ is induced [170]. Together C/EBP β and C/EBP δ activate the transcription of C/EBP α and PPAR γ although PPAR γ expression can also be induced by sterol regulatory element binding protein-1 (SREBP-1)[161]. PPAR γ then triggers cell cycle exit and directly stimulates the expression of several adipocyte-specific genes, including lipoprotein lipase, fatty acid binding protein (aP2), acyl coenzyme A synthase, fatty acid synthase and phosphor-enol pyruvate carboxykinase, which all play a role in fatty acid uptake and storage [161]. Although levels of C/EBP β and C/EBP δ decline during the terminal stages of differentiation it is proposed that C/EBP α co-operates with PPAR γ in the induction of additional target genes and helps to maintain high levels of PPAR γ in the mature adipocyte [171].

1.12.2 The role of PPAR γ in type II diabetes and the metabolic syndrome

Type II diabetes mellitus is a common chronic disease which is characterised by elevated blood glucose levels and increased cardiovascular morbidity and mortality [172,173]. The condition can be caused by decreased sensitivity of tissues to insulin (insulin resistance) and is often associated with hyperinsulinemia, obesity, hypertension and dyslipidemia, which are components of the metabolic syndrome [173-175]. Two drugs from the thiazolidinedione (TZD) family, rosiglitazone and pioglitazone are currently used in the treatment of type II diabetes [173]. TZDs are high affinity PPAR γ ligands (EC₅₀ 20-400 nM) and there is a positive correlation between the potency of TZDs in binding/activation of PPAR γ *in vitro* and decreasing

plasma glucose levels *in vivo*, suggesting that TZDs mediate their anti-diabetic effect through PPAR γ [104]. Furthermore, point mutations in the ligand binding domain of PPAR γ have been discovered in patients which display symptoms characteristic of the metabolic syndrome (or Syndrome X) including insulin resistance, type II diabetes, dyslipidemia, partial lipodystrophy and hypertension [174-179]. For instance, one subject was heterozygous for a single nucleotide substitution at codon 467 in the PPAR γ gene which resulted in a proline to leucine substitution (P467L) [108,176]. This proline residue is located close to helix 12 of the ligand binding domain which in part forms the AF-2 motif that mediates interactions with nuclear cofactors. PPAR γ receptors with substitutions like P467L in this region of the ligand binding domain are transcriptionally inactive and it predicted that such mutations disturb the orientation of helix 12 which favours co-repressor association and impairs ligand binding and co-activator recruitment[176].

Rosiglitazone and pioglitazone treatment alleviates several of the symptoms of type II diabetes by lowering glucose, free fatty acid and triglyceride levels in the blood, reducing plasma insulin concentrations and preserving β -cell function [180]. However, how TZDs regulate these processes is still under investigation. In animal studies, TZDs increased the responsiveness of liver, skeletal muscle and adipose tissue to insulin, which led to improved glucose uptake [181]. One hypothesis proposes that activation of PPAR γ in adipocytes, where PPAR γ expression is highest, indirectly improves the insulin sensitivity of muscle and liver tissue, since adipocytes only take up a relative small proportion of glucose in response to insulin [182]. For instance, through an increase in pre-adipocyte differentiation, adipose tissue sequesters more free fatty acids from the circulation, which could reduce competition between glucose and fatty acids for uptake and oxidation by muscle tissue [181]. TZDs may also block the production of the cytokine tumour necrosis factor- α (TNF- α) which inhibits insulin signalling at the level of tyrosine phosphorylation of the insulin receptor and its major substrate IRS-1 in both muscle and liver [180]. Furthermore, TZDs have been shown to directly increase the expression of proteins involved with insulin signalling, such as CAP (Cbl-associated protein), IRS-2 (insulin receptor substrate-2) and the insulin-responsive glucose transporter GLUT4 in adipocytes [182]. In addition, TZDs can improve insulin signalling by enhancing expression of the hormone adiponectin but suppressing production of the adipocyte

specific protein resistin [182,183]. Although recent contrasting studies suggest that TZDs can also act on other tissues, independent of adipocytes, to decrease serum glucose, triglycerides, free fatty acids and plasma insulin levels [180].

1.12.3 PPAR γ and inflammation

Several studies have suggested that PPAR γ could be involved in the conversion of monocytes to macrophages [184] [185]. *In vitro*, exposure of resting monocytes to granulocyte-macrophage colony stimulating factor (GM-CSF) or oxidised LDL stimulates their differentiation to macrophages and is accompanied by an induction of PPAR γ expression [185]. However, PPAR γ ligands can also exert anti-inflammatory effects by inhibiting the activation of a number of transcription factors which promote the expression of inflammatory response genes [186]. For instance, the PPAR γ agonist 15dPGJ₂ can block NF- κ b dependent transcription which down regulates production of several pro-inflammatory cytokines such as TNF α , IL-1 β and IL-6 [186]. In addition PPAR γ inhibits the expression of inducible nitric oxide synthase (iNOS), gelatinase B, cyclooxygenase 2 (COX-2) and the scavenger A receptor in macrophages [63,186]. Repression of COX-2 levels by liganded PPAR γ occurs because it competes with an activator of COX-2 expression, c-Jun, for binding to the co-activator CBP/p300. Furthermore, activation of PPAR γ can stimulate anti-inflammatory responses by antagonizing the PI3-kinase-mediated signaling cascade via up-regulation of PTEN in macrophages, which induces them to undergo apoptotic cell death [186]. The synthetic ligands troglitazone and rosiglitazone attenuated colonic inflammation in a *vivo* colitis model, suggesting that PPAR γ agonists may have potential in the treatment of inflammatory bowel disease [182].

Atherosclerosis is a pathological disease that ultimately leads to the localised obstruction of an artery due to the progressive build up in the arterial wall of an atheromatous plaque [17]. One of the key processes in the formation of the plaque is the conversion of macrophages to lipid laden foam cells, which is mediated by the internalisation of oxidised LDL through the CD36 scavenger receptor [182]. Two oxidized components of oxLDL particles, 9 and 13 HODE (hydroxyoctadecadienoic acid) are PPAR γ ligands, and therefore uptake of oxLDL causes increased PPAR γ activation. Since CD36 is a target gene of PPAR γ , it is proposed that oxLDL initiates

a positive feedback loop which potentiates uptake of oxLDL by the macrophage. Immunohistochemical analysis of atherosclerotic lesions has demonstrated that PPAR γ is expressed in foam cells *in vivo* [187]. Although these findings suggest that PPAR γ has a pro-atherosclerotic function, clinical data in humans treated with troglitazone demonstrates that PPAR γ does not promote atherogenesis [182]. There is evidence to suggest that PPAR γ can also promote cholesterol efflux. For instance, PPAR γ activation increases LXR α expression, which in turn, leads to stimulation of expression of the ABC1 transporter and cholesterol efflux [19]. PPAR γ agonists have also been shown to raise HDL cholesterol and inhibit inflammatory cytokine production, which may actually help prevent plaque formation.

1.12.4 PPAR γ and cancer

PPAR γ is expressed in at least 22 different human malignancies and evidence from a large number of studies suggest that the receptor may function as a tumour suppressor [188]. For instance, activation of PPAR γ by either natural or synthetic ligands attenuates the growth of cell lines established from breast, hepatocellular, prostate, gastric, pancreatic, salivary gland, lung and bladder carcinomas [117,189-198]. Depending on the cancer cell type, the ligand concentration or the type of PPAR γ agonist, growth inhibition caused by PPAR γ activation can coincide with either cell-cycle arrest or induction of terminal differentiation or programmed cell death. Although the direct *in vivo* target genes of PPAR γ which regulate these cellular processes remain elusive, changes in gene expression in cancer cells in response to PPAR γ ligand treatment have provided insight in to the downstream pathways which might be involved (**Fig. 1.7**) For example, growth arrest promoted by PPAR γ agonists in hepatocellular, renal, colon, non-small lung and breast cancer cell lines *in vitro* was correlated with elevated expression of one or more cyclin dependent kinase (CDK) inhibitors including, p18, p21 and p27 [188,197,199-205]. CDK inhibitors abrogate cell-cycle progression by blocking phosphorylation of the retinoblastoma protein by cyclin/CDK complexes. This promotes cell-cycle withdrawal because in a hypo-phosphorylated state retinoblastoma protein is a negative regulator of cell cycle progression. A consensus PPRE has been identified in the p21 promoter, suggesting that PPAR γ activation may directly increase transcription of this CDK inhibitor [165]. Furthermore, PPAR γ induced growth arrest in cancerous cells has been correlated

with decreased levels of cyclin D1, which is essential for the activity of cyclin dependent kinases CDK2, CDK4 and CDK6 [188,206,207].

Cell cycle exit precedes the terminal differentiation of normal and malignant cells; therefore increased levels of p21 protein are also observed in cancer cells that differentiate in response to PPAR γ ligands [203]. In addition, stimulation of morphological changes and expression of molecular markers which are associated with a more mature, less malignant phenotype have been detected following ligand activation of PPAR γ in certain cancer cell lines, including liposarcoma, glioma, leukaemia, osteosarcoma and pancreatic cancer cell lines *in vitro* [208] [188,190,209-211]. In non-small lung cancer cell lines PPAR γ agonists' up-regulated levels of HTI₅₆ which is a marker of terminally differentiated pneumocytes [203]. Treatment of breast cancer and liposarcoma cells with the synthetic PPAR γ ligand troglitazone *in vitro* caused lipid accumulation and changes in gene expression which were more characteristic of normal breast epithelial cells and mature adipocytes respectively [190,209]. Other alterations in morphology induced by PPAR γ ligands *in vitro*, which are indicative of cellular maturation, include an increase in the cytoplasmic-to-nuclear ratio of colon cancer cells and neurite extension in LAN-5 neuroblastoma cells [212,213].

PPAR γ activation in cancer cells can also induce two types of programmed cell death, apoptosis and type II programmed cell death (autophagy) [214,215]. The cellular hallmark of apoptosis is the internucleosomal fragmentation of nuclear DNA that results in the production of oligonucleosomes of different but distinct lengths [216]. Stimulation of apoptosis triggers a variety of intracellular signalling cascades. However, central to the apoptotic mechanism is the activation of caspases [216] (**Fig. 1.7**). Caspases are cysteine proteases that are synthesised as large inactive precursors from which the enzyme is released by cleavage at aspartic residues [217]. Caspases act in a sequential manner with caspases-8,-9 and -10 functioning as early initiators while caspases-3 and -6 are apoptosis effector molecules [216]. Caspase activation can be stimulated by the tumour suppressor p53 through induction of the pro-apoptotic factor BAX [218]. BAX stimulation is associated with release of cytochrome c from the mitochondria, which in turn activates caspase 9 by binding to Apaf (apoptosis-activating factor) although the exact mechanism of cytochrome c

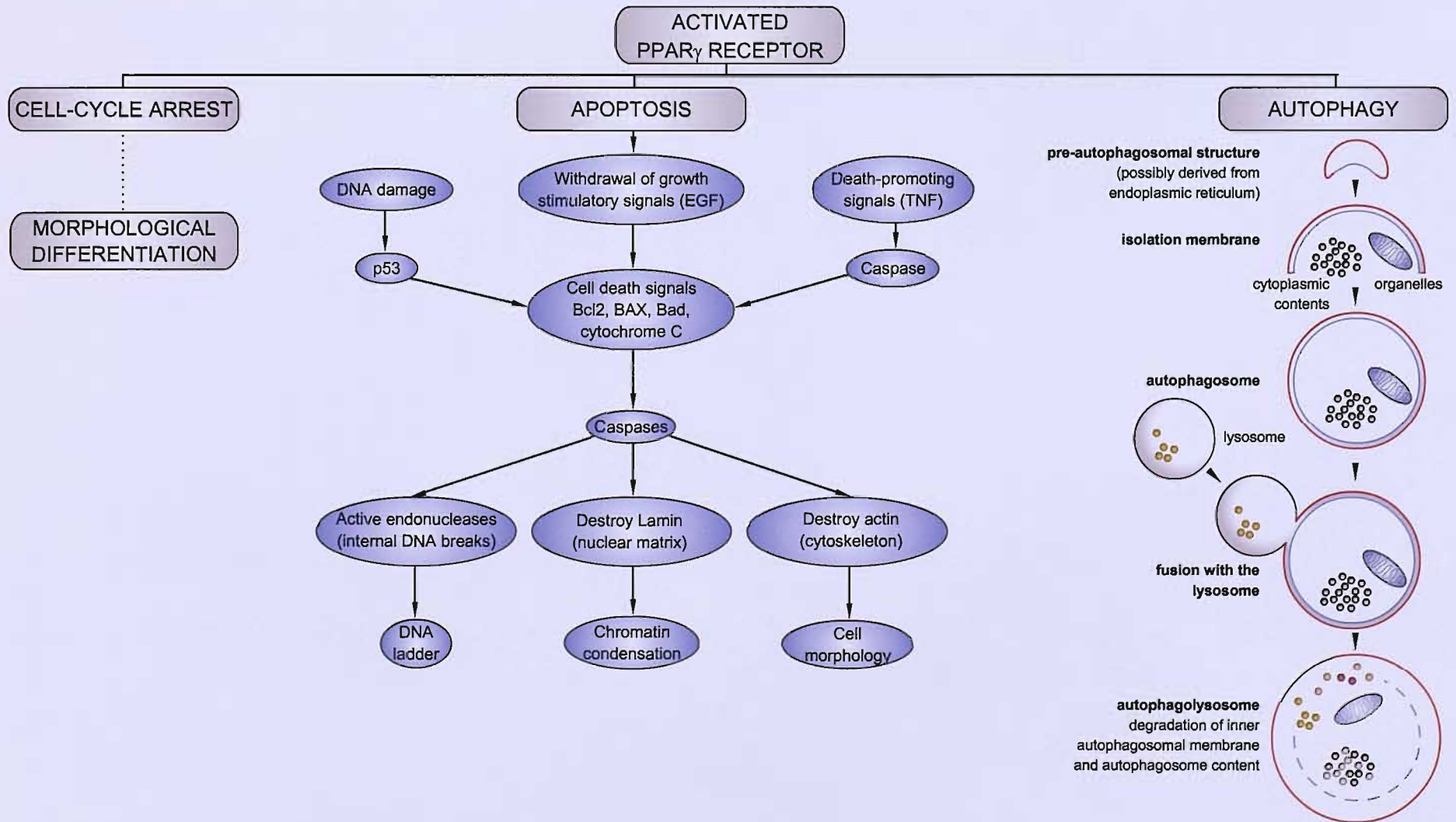
release is still unclear [217]. BAX is antagonised by the anti-apoptotic protein Bcl-2 (B cell lymphoma 2)[217]. Furthermore, induction of p53 and BAX or repression of Bcl-2 levels has been observed in cells treated with PPAR γ ligands suggesting that this pathway might mediate apoptotic cell death by PPAR γ in malignant cells [219,220].

Autophagy in higher eukaryotic organisms has emerged as a multifunctional pathway, which in addition to regulating turnover of cytoplasmic constituents, is also involved in removal of damaged organelles, programmed cell death and development of different tissue specific functions [215,221,222]. Autophagy begins with the formation of a “C” shaped double-membrane pre-autophagosomal structure in the cytoplasm [222]. Several origins for this “wrapping” membrane have been proposed including the ribosome free regions of the endoplasmic reticulum [223]. The structure then grows at each end, enclosing cytoplasmic contents and organelles, to form a double membrane vesicle called an autophagosome [222]. The autophagosome then targets the lysosome, where its outer membrane fuses with the lysosomal membrane [223]. The autophagosome inner membrane, cytoplasmic contents and organelles are then finally degraded by lysosomal hydrolases [215] (**Fig. 1.7**). Induction of autophagy has been observed in prostate cancer and IMR-32 neuroblastoma cell lines *in vitro* following treatment with the natural PPAR γ ligand 15dPGJ₂. PPAR γ may induce autophagy through increased expression of a putative target gene termed PTEN (phosphatase and tensin homologue detected on chromosome 10) [224]. PTEN is proposed to trigger autophagy through inhibition of the phosphatidylinositol (PI) 3-kinase/protein kinase B (Akt/PKB) pathway which promotes cell survival and attenuates programmed cell death [225,226].

A number of studies have demonstrated that PPAR γ ligands can also inhibit the growth of tumours in mice that originated from injections of human breast, lung and prostate cancer cells[219,227,228]. However, investigations of the role PPAR γ in colon cancer *in vitro* and *in vivo* have revealed seemingly opposite findings. For instance, differentiation and reversal of malignant changes were observed upon treatment of colon cancer cell lines with TZD PPAR γ ligands in a study by Sarraf *et*

Fig. 1.7. Cellular responses induced by PPAR γ ligands in cancer cells. The table below gives examples of potential downstream targets of PPAR γ which might mediate cell-cycle arrest, differentiation, apoptosis or autophagy induced by PPAR γ ligands in malignant cells.

Cellular response	Cell cycle arrest	Differentiation	Apoptosis	Autophagy
Potential PPARγ targets	<ul style="list-style-type: none"> • + cyclin dependent kinase inhibitors – p18, p21, p27 • - cyclin D1 	+ CDK p21	<ul style="list-style-type: none"> • +p53 tumour suppressor • + pro-apoptotic BAX • - anti-apoptotic Bcl-2 	+ PTEN phosphatase



al [212]. In addition, they showed that progression of tumours in mice, derived from human colon cancer cells, was attenuated by TZD administration [212].

Heterozygous loss of PPAR γ also caused an increase in β -catenin levels and a greater incidence of colon cancer when mice were treated with the potent carcinogen azoxymethane [229]. β -catenin is normally sequestered in the cytoplasm by the APC protein which promotes its degradation. However, APC gene deficiency, promotes an increase in β -catenin levels and translocation of β -catenin to the nucleus where it enhances the expression of growth-promoting genes, leading to tumour development [188]. For unclear reasons, TZD treatment of colon cancer cells in APC null mice stimulates colon tumour growth by increasing β -catenin levels [188,230,231]. These results suggest that the initiation event in the development of colon cancer can influence the cellular response to PPAR γ ligands [188].

1.12.4.1 PPAR γ mutations in cancer

Several natural mutations of PPAR γ have been described which interfere with the transcriptional activity of the wild type receptor and are implicated in the pathogenesis of cancer. A recent study revealed four different mutations of the PPAR γ gene in sporadic colon cancer cells [232]. One of the mutations involving an exon 3 frameshift resulted in a protein which lacked most of the ligand binding, heterodimerisation and AF-2 activation domains and was therefore assumed to be inactive [232]. The other mutations, one non-sense and two missense mutations occurred in exon 5 which encodes the ligand-binding domain. These PPAR γ receptor mutants exhibited impaired ligand binding and ability to stimulate gene transcription. None of the mutations were found in the corresponding germline DNA which suggested that they were acquired during tumour development [232].

In addition, two variant transcripts of PPAR γ , generated by alternative splicing, have been identified in colon and leukaemia cancer cell lines, that encode dominant negative receptors which inhibited the action of normal PPAR γ [233,234]. Both of these novel PPAR γ isoforms are truncated proteins which lack the entire ligand binding domain [233,234]. Since the PPAR γ variant termed γ ORF4, originally detected in colon cancer cells, retained the ability to heterodimerise with RXR and recognise PPREs, but was transcriptionally inactive, it was proposed that it might

function by sequestering RXR from wild-type PPAR γ or compete for binding to DNA [233]. In contrast, the second PPAR γ mutant (PPAR γ 1_{tr}) interacted weakly with DNA, although its inhibitory effect on PPRE-mediated transcription was relieved by co-transfection with an expression vector encoding p300, suggesting it may act by competing for co-activators despite lacking the AF-2 (activation function-2) domain [234]. Ectopic expression of γ ORF4 and PPAR γ 1_{tr} stimulated cell proliferation *in vitro*. Furthermore, it was demonstrated that γ ORF4 was expressed in primary sporadic colorectal tumour samples and in some cases was found in both the malignant tissue and adjacent mucosa indicating that abrogation of PPAR γ function may play a role in the development of some cancers [233,234]. This hypothesis is further supported by the work of Kroll *et al* who revealed that a translocation in a subset of human follicular carcinomas, which is probably critical in their initiation, resulted in an in-frame fusion of the DNA binding domain of the transcription factor PAX8, with domains A to F of PPAR γ 1, that functioned as a dominant negative suppressor of wild-type PPAR γ 1 transcription [235-238].

1.12.4.2 Clinical trials of PPAR γ ligands in cancer patients

A small number of clinical trials have been conducted in patients with liposarcoma or prostate or colon carcinomas using TZD PPAR γ ligands [209,239-243]. Demetri *et al* reported that administration of troglitazone to three patients with intermediate to high grade liposarcomas induced pronounced histological and biochemical changes in the tumours which indicated that they had undergone differentiation *in vivo* [209]. Tumour biopsies taken from each patient during the course of treatment exhibited extensive cytoplasmic lipid accumulation in the malignant cells [209]. Molecular analysis of the tumour cells also revealed increased expression of adipocyte-specific genes, including aP2, adipsin and PPAR γ [209]. Furthermore, results of a phase II clinical trial of 41 men with advanced prostate cancer using troglitazone showed that 20% of patients had sustained PSA (prostate specific antigen) decline between 1 and 50% and in one patient there was a major decrease in PSA to nearly undetectable levels [239]. PSA is a widely used marker in the diagnosis of prostate cancer since its level correlates with tumour size. Therefore the fall in PSA levels in patients who took part in this study suggest that troglitazone was attenuating tumour progression *in vivo*.

Conversely, clinical trials with another TZD rosiglitazone in liposarcoma and prostate cancer patients have yielded contradictory results, as rosiglitazone treatment did not appear to induce morphological changes or halt tumour progression [240,241]. However, these findings could be based partly on selection of pre-treated refractory cancers which no longer responded to therapeutic interventions [188]. A second criticism is that the PPAR γ concentration required to induce anti-neoplastic effects in humans has not been identified. Therefore, the level of PPAR γ agonist reached in patients by oral treatment may not have been sufficient to inhibit tumour growth [188]. Although more large scale clinical studies are needed the promising findings from some of these preliminary investigations suggest that PPAR γ ligands have potential in the treatment of human malignancies that respond poorly to currently available therapies including advanced staged childhood neuroblastoma.

1.13 Neuroblastoma

1.13.1 Etiology and epidemiology

Neuroblastoma is the most common, extra-cranial solid tumour of childhood which originates from the neural crest [244,245]. With an annual incidence of 8 per million children under the age of 15, neuroblastoma accounts for approximately 6-10% of all paediatric malignancies, however is responsible for more than 15% of cancer fatalities in this age group [244,246-249]. More than 95% of neuroblastoma cases present by 10 years of age with a median age at diagnosis in an unscreened population of 22 months[244,246-248]. Overall neuroblastoma occurs more frequently in boys, giving a male to female ratio of 1.2 to 1, although both sexes have similar incidences of more advanced stage disease [246,247]. Neuroblastomas usually occur sporadically, however in 1-2% of cases there is a family history [245,249]. The etiology of this disease remains unclear although it is speculated to arise during foetal or early postnatal life from immature neural crest cells whose differentiation is aberrantly regulated [246,248,250]. Currently no environmental factors or parental exposures have been identified that consistently influence neuroblastoma occurrence [245,248].

1.13.2 Pathology and clinical presentation

Neuroblastoma is characterised by its diverse pathology, which ranges from localised tumours that have favourable prognosis and can undergo spontaneous regression to disseminated disease which is generally incurable [244,245]. Normally during development, at the stage of neurulation, cells of the neural crest migrate extensively and mature to become cells of the adrenal medulla, the sympathetic nervous system, Schwannian cells, certain types of neuroendocrine cells and mesenchymal-type tissue in the head and neck region[250]. While primary neuroblastoma tumours may occur wherever cells derived from the neural crest are found, they most commonly arise in the adrenal medulla [251]. The location of the primary lesion may be influenced by the patient's age at diagnosis, since children over the age of one exhibit a higher percentage of adrenal and abdominal tumours, but a lower incidence of thoracic and cervical tumours compared with infants [246,247]. However, in one percent of patients no primary tumour is detected.

The gross appearance of neuroblastoma tumours may vary from solid, differentiated lesions with white-pink coloration to highly vascular, diffuse masses with an extremely fragile pseudo-capsule containing haemorrhage, necrosis and calcification[247]. Neuroblastomas are one type of neuroblastic tumour, which also encompasses ganglioneuroblastomas and ganglioneuromas [250]. Neuroblastic tumours have been classified into these three groups based on their degree of cellular differentiation and Schwannian cell content. Neuroblastomas are composed of undifferentiated or poorly differentiated neuroblasts with limited Schwannian cell content [252]. These neuroblasts are classic “small, round, blue” cells with scant cytoplasm and darkly stained nuclei that are similar to those observed in other childhood neoplasms such as rhabdomyosarcoma [253]. Ganglioneuroblastomas contain neuroblasts and regions of mature Schwannian stroma with individually scattered differentiated or differentiating ganglion cells [250]. Conversely, benign ganglioneuromas predominantly consist of mature ganglion cells, Schwannian cells and neuritic processes with little or no neuroblastic component [252].

Between 50 and 60% of neuroblastoma patients are diagnosed with disseminated disease and metastases occur most frequently in bone marrow, bone, liver and skin

[246,253]. The signs and symptoms displayed by the neuroblastoma patient are dependent on the location of the primary lesion and the extent of metastatic disease [245]. Abdominal neuroblastomas can be detected by the presence of a firm fixed abdominal mass; however weight loss, pain and distended abdomen are also frequently observed [247]. In addition, large tumour masses in the lower abdomen and pelvis can result in bladder or bowel dysfunction [247]. Children or infants with paraspinal tumours may present with spinal cord compression which in some instances causes acute paresis or paraplegia, while Horner's syndrome is observed in individuals with cervical or apical thoracic lesions. Patients with disseminated disease often have symptoms of fever and bone pain and if metastases have reached the orbit they can manifest as orbital ecchymoses which resemble facial trauma [245].

1.13.3 Disease staging

In 1988 a multinational, multidisciplinary committee established the International Neuroblastoma Staging System (INSS) which was later revised in 1993 (**Table 1.2**) [254,255]. Accurate disease staging is critical for determining the prognosis and treatment plan of the neuroblastoma patient. Previously, the use of a variety of classification systems made comparison of treatments and results difficult [256]. Furthermore, while it was comparatively simple to define localised and disseminated disease, distinction between intermediate tumour types had proved more challenging [247]. Therefore the INSS incorporated the best features of other staging methods but standardised areas of controversy such as definitions of localised, unresected and regional disease [246]. According to the INSS, patients with stage 1 disease have a completely resectable/excisable tumour with no ipsilateral lymph node involvement, whereas stage 2A-B patients have a localised neoplasm that can be partially or completely excised and ipsilateral lymph nodes are either positive or negative for tumour [254]. In stage 3 neuroblastomas the tumour is usually unresectable and can extend across the midline (vertebral column) and may involve regional lymph nodes [252]. Patients diagnosed with stage 4 neuroblastomas have a primary tumour and metastases in distant lymph nodes, bone, bone marrow, liver, skin and or other organs. The 4S category specifically includes infants less than one year old who present with disseminated disease but which is limited to skin, liver and or bone marrow. Despite having metastatic disease, a high percentage of 4S cases

spontaneously regress without treatment [257]. The INSS is now acknowledged world-wide and used in most neuroblastoma treatment protocols.

1.13.4 Prognostic factors

1.13.4.1 Clinical

Numerous studies of neuroblastoma patients from different countries have consistently demonstrated that age at diagnosis and disease stage are the two most important clinical prognostic factors [251,258-260]. The survival rate of infants under the age of 1 is between 80 and 90% whereas children over the age of 1 have an inferior prognosis with survival rates ranging from 25 to 40% [253]. The diagnosis for patients with INSS stage 1, 2 and 4S tumours is very favourable with survival figures of 75-93% [246,251,258-260]. Overall survival rates for patients with INSS stage 3 and 4 neuroblastomas are poorer compared with lower stage and 4S tumours; however infants less than 1 year old with higher grade tumours have a better prognosis than children over 1 year of age [251]. For instance, infants with INSS stage 3 and 4 tumours have survival rates of 80-90% and 60-75% respectively while children have the worst prognosis with survival figures of only 50% for stage 3 and 15% for disseminated (stage 4) disease[246].

In addition to these clinical features, an increasing number of biological and genetic factors have been identified which can assist in the diagnosis and prediction of outcome of neuroblastoma patients (**Table 1.3**).

1.13.4.2 Biological factors

Neuroblastoma cells synthesise and release the catecholamines, epinephrine, norepinephrine and dopamine or their metabolites vanillylmandelic acid (VMA) and homovanillic acid (HVA) [253,261]. 80-90% of cases of neuroblastoma excrete these substances in to the urine; therefore the detection of increased levels of

Stage	Definition
1	Localised tumour with complete gross excision with or without microscopic residual disease; representative ipsilateral lymph nodes negative for tumour microscopically (nodes attached to and removed with the primary tumour may be positive).
2A	Localised tumour with incomplete gross excision, representative ipsilateral nonadherent lymph nodes negative for tumour microscopically.
2B	Localised tumour with or without complete gross excision, with ipsilateral nonadherent lymph nodes positive for tumour. Enlarged contralateral lymph nodes must be negative microscopically.
3	Unresectable unilateral tumour infiltrating across the midline*, with or without regional lymph node involvement; or localised unilateral tumour with contralateral regional lymph node involvement; or midline tumour with bilateral extension by infiltration (unresectable) or by lymph node involvement.
4	Any primary tumour with dissemination to distant lymph nodes, bone, bone marrow, liver and/or other organs (except as defined by stage 4S).
4S	Localised primary tumour (as defined for stage 1, 2A, or 2B) with dissemination limited to skin, liver and/or bone marrow [†] . Limited to infants <1 year of age.
<p>*The midline is defined as the vertebral column. Tumours originating on one side and crossing the midline must infiltrate to or beyond the opposite side of the vertebral column.</p> <p>[†]Marrow involvement in stage 4S should be minimal, i.e., <10% of total nucleated red blood cells identified as malignant on bone marrow biopsy or on marrow aspirate. More extensive marrow involvement would be considered to be stage 4. The mIBG scan (if performed) should be negative in the marrow.</p>	

Table 1.2. International Neuroblastoma Staging System (INSS)

catecholamines or their metabolites in urine samples is used in the initial diagnosis of neuroblastoma patients [261]. Catecholamine and metabolite levels can be monitored to assess tumour progression, although there is still controversy over which catecholamines/metabolites are associated with different disease stages [262,263]. For instance, Zambrano *et al* demonstrated a correlation between high VMA levels and older patients as well as aggressive tumours [264]. Conversely, Strenger *et al* found high dopamine levels in disseminated neuroblastomas whereas 4S tumours

displayed the greatest VMA levels. They suggested that determining the dopamine/VMA ratio might help to discriminate between stage 4 and 4S neuroblastomas [264].

Neuron-specific enolase (NSE) is one of five isoforms of the glycolytic enzyme, enolase. NSE is released by neuroblastomas into the blood, and its level in serum correlates with disease stage and course [265]. NSE levels greater than 100 ng/ml are indicative of advanced stage disease and associated with poor prognosis [266]. Interestingly, despite their extensive tumour burden, patients with stage 4S disease exhibit significantly lower serum NSE levels compared with those in stage 4 [266]. Furthermore, NSE levels have been shown to decrease following therapy [266]. These findings demonstrate that NSE is a valuable tumour marker for neuroblastoma and quantification of its level in serum can help to assess disease stage, monitor the effect of treatment and detect recurrent disease [262,265]. Two other tumour markers used in the diagnosis of neuroblastoma are ferritin and lactate dehydrogenase (LDH). Serum ferritin released from damaged tissues is in an unglycosylated form whereas glycosylated ferritin is actively secreted by intact cells [267]. A study by Hann *et al* indicated that elevated serum ferritin in neuroblastoma patients was predominantly a consequence of secretion by the tumour and therefore is suggestive of active disease [267]. Like NSE, a decrease in ferritin levels coincides with disease remission following treatment [268]. LDH catalyses the conversion of lactate to pyruvate and its level is elevated in many types of cancer, therefore it is not a specific marker for neuroblastoma, but its detection can help to corroborate findings from other diagnostic techniques [253].

Neurotrophin signalling cascades play a critical role in the normal development of the sympathetic nervous system and in the biology and clinical behaviour of neuroblastomas [269,270]. Neurotrophins that function in neuronal maturation, include nerve growth factor (NGF), brain-derived neurotrophic factor (BDNF), neurotrophin-3 and neurotrophin-4 and they mediate their effect through Trk receptor tyrosine kinases [248,269,270]. So far, three Trk receptors, TrkA, TrkB and TrkC have been implicated in regulating the growth, differentiation and survival of neuroblastoma cells [248,269]. TrkA binds NGF with high affinity whereas TrkB is the receptor for BDNF and neurotrophin-4 and TrkC is the high affinity receptor for neurotrophin-

3[269]. Differential expression of these neurotrophin receptors is strongly correlated with the biological responses and clinical characteristics of neuroblastomas. The TrkA receptor is highly expressed in low stage neuroblastoma tumours and is associated with favourable prognosis [271,272]. Furthermore, NGF treatment of primary neuroblastoma cells with elevated levels of TrkA receptor or neuroblastoma cell lines stably expressing TrkA promotes morphological differentiation and neurite outgrowth [269,271,272]. However, in culture, in the absence of NGF these cells undergo programmed cell death. Like TrkA, TrkC is expressed in neuroblastomas which have a favourable outcome. Conversely, TrkB is predominantly expressed in advanced stage tumours, many of which also express BDNF [248,270]. These findings have led to the hypothesis that the expression profile of Trk receptors, at the time malignant transformation, impacts on neuroblastoma behaviour *in vivo*. In this model, low-stage tumours, especially those in infants, expressing high levels of the TrkA receptor, will terminally differentiate in the presence of NGF or if NGF is limiting enter an apoptotic death pathway. In contrast, in aggressive disease expression of the TrkB receptor and its ligand BDNF establishes an autocrine pathway which promotes cell growth and survival even in the absence of exogenous neurotrophins [248].

CD44 is a cell surface glycoprotein which mediates cell-cell and cell-extracellular matrix interactions and has been implicated in the progression and metastasis of tumours [273,274]. However, in contrast to other human malignancies, lack of CD44 protein expression is associated with shorter progression-free survival periods in neuroblastoma patients [275]. In addition, CD44 protein levels positively correlate with the grade of tumour cell maturation and CD44 expression is induced by differentiation agents such as retinoic acid suggesting that CD44 acts as a differentiation marker in neuroblastoma [273,275]. Often neuroblastoma patients respond well to initial chemotherapy but relapse either during the course of treatment or shortly after it has been completed because they develop drug resistance [248]. The multidrug-resistance-associated protein (*MRP*) gene encodes a 190-Kd membrane-bound glycoprotein that *in vitro* has been shown to mediate resistance to a variety of drugs derived from natural products [276]. Analysis of MRP expression in primary tumour specimens from neuroblastoma patients demonstrated that high MRP

levels *in vivo* were strongly associated with lower survival rates and suggesting that this might be the mechanism by which neuroblastomas acquire drug resistance [276].

Telomeres are structures found at the end of eukaryotic chromosomes and are composed of hundreds of hexameric DNA repeats with the consensus TTAGGG [277,278]. The function of telomeres is to prevent loss of genomic DNA during replication and to stabilise chromosomes [277]. Telomeres are maintained by a multi-subunit ribonucleoprotein enzyme called telomerase, which uses a short RNA template within the enzyme itself to replicate the hexanucleotide repeats [278]. Normally telomerase is expressed in embryonic cells and cells involved in tissue renewal but not in somatic tissues [277]. Therefore, in most somatic cells at each round of cell division telomeres become shortened until they can no longer protect chromosomal ends leading to cell death [278]. Conversely, telomerase expression and maintenance of telomeres has been observed in cells from many types of human cancer including neuroblastoma [278]. Telomere maintenance is speculated to be an essential step in immortalisation of malignant cells. Indeed, increased telomerase activity and telomere length are both predictors of poor outcome in neuroblastoma patients [277,278]. Detection of telomerase activity may also be useful in assessing the success of treatment, since if neuroblastoma tumours remain positive for telomerase activity after chemotherapy the prognosis is unfavourable [277].

1.13.4.3 Genetic abnormalities

Several genetic features, in particular *N-myc* gene copy number, DNA ploidy, deletion or loss of heterozygosity of chromosome 1p and gain of chromosome 17q have been identified as independent prognostic factors in neuroblastoma.

The *N-myc* oncogene was first cloned in 1983 by identifying an amplified DNA sequence, with homology to another oncogene *c-myc*, in neuroblastoma cell lines with double minute chromatin bodies (DMs) or homogeneously staining regions (HSRs) [279,280]. DMs and HSRs are hallmarks of DNA amplification and commonly observed in tumour cells [248,281,282].

Prognostic group	Description	Outcome	
		Favourable	Unfavourable
Clinical factors			
Stage		1,2, 4S	3,4
Age		<365 days	>365 days
Tumour markers			
Ferritin	Increased serum ferritin caused by secretion from tumour.	Low	High
LDH	LDH levels elevated in many tumour types –general tumour marker.	Low	High
NSE	NSE released by tumour and correlates with disease stage.	Low	High
Histology	Tumours with favourable histology are differentiated and Schwannian-stroma rich.	Favourable	Unfavourable
Biologic factors			
TrkA expression	Stable expression of TrkA promotes neuroblastoma differentiation.	High	Low
TrkC expression	TrkC expression also associated with differentiated neuroblastomas	High	Low
TrkB expression	Expression of TrkB promotes cell growth		High/FL
CD44 expression	Cell surface glycoprotein – acts as differentiation marker	High	Low
MRP expression	May mediate resistance to chemotherapeutic agents in neuroblastoma	Low	High
Telomerase	Telomere maintenance proposed to be essential for immortalisation of malignant cells	Low	High
Genetic factors			
N- <i>myc</i> oncogene	Ectopic expression of N-Myc transforms cells <i>in vitro</i> . Proposed to stimulate expression of growth-promoting genes.	Normal Copy number	Amplified
DNA index	Hyperdiploid tumours are associated with whole chromosome gains, rather than less favourable genetic abnormalities	>1.0 (hyperdiploid)	1.0 (diploid)
Chromosome 1p	Region speculated to contain at least two tumour suppressor genes	Normal	Deletion
Chromosome 17q	Region of partner chromosome lost following partial gain of 17q	Normal	Gain
Abbreviations: LDH = lactate dehydrogenase; NSE = neuron-specific enolase; FL = full-length transcript; MRP = multidrug resistance protein			

Table. 1.3. Prognostic factors in neuroblastoma

It is postulated that amplification is initiated when the *N-myc* gene, located on chromosome 2, is transposed to DMs [279]. DMs, which are circular extra-chromosomal DNA fragments, may subsequently be integrated in to other chromosomal sites as HSRs [244,282]. The *N-myc* copy number is usually increased by 50- to 700-fold following amplification which results in high levels of *N-myc* mRNA and protein expression [247,248,279]. Brodeur *et al* subsequently showed that *N-myc* amplification in neuroblastomas was strongly correlated with advanced stage disease and poor prognosis [283]. These initial findings have been verified by multiple independent studies and *N-myc* amplification, which occurs in approximately a third of neuroblastoma cases, has now been established as a highly significant predictor of survival independent of age and disease stage [244,284-286]. Indeed, along with other prognostic factors, routine detection of *N-myc* status, by Southern blotting, genomic PCR or fluorescence in situ hybridization (FISH), is used in the assignment of neuroblastoma patients to low, high or intermediate risk groups [244,247,287]. Ectopic over-expression of *N-myc* has been demonstrated to transform cell lines *in vitro* and transgenic mice, with neuroectodermal cells that constitutively over-express *N-myc*, develop neuroblastoma tumours *in vivo* [248,285]. Although these studies confirm that *N-myc* functions as an oncogene, the mechanism by which N-Myc protein regulates malignant development is only beginning to be elucidated but is thought to involve inappropriate activation or repression of growth-related genes. While amplification of *N-myc* clearly plays a role in neuroblastoma progression, controversy remains over the prognostic significance of N-Myc protein expression in neuroblastomas with single-copy *N-myc* [288]. However, some tumours with out *N-myc* amplification have been shown to express high levels of N-Myc protein which correlated inversely with survival probability [289,290].

Normal human cells have a diploid DNA content; however hyperdiploidy (increased DNA content) is common in cancerous cells. Interestingly, hyperdiploid DNA content mostly in the near-triploid range is observed in 80% of neuroblastoma tumours from infants and is an indicator of favourable outcome in this age group [247,248,291]. In contrast, diploid DNA content is associated with advanced stage disease, poor prognosis and treatment failure [244,291]. It is speculated that the positive prognosis for neuroblastomas with hyperdiploidy is a consequence of whole

chromosome gains compared with the chromosomal rearrangements, including amplifications, deletions and unbalanced translocations which are characteristic of diploid neoplasms [246,248]. Therefore, assessment of DNA content, possibly by flow cytometric analysis of cell nuclei, has potential in the prognosis of neuroblastomas identified in infants [244,248].

Several chromosomal abnormalities that occur with high frequency have been identified in neuroblastoma including chromosome 17q gain and deletion or loss of heterozygosity of chromosome 1p. Fluorescence in situ hybridization analysis has revealed gain of material from chromosome 17 in 63-83 % of neuroblastoma tumours [244,248]. The gain may involve the entire chromosome, as observed in certain triploid tumours, or only a distal segment of the long arm, 17q21-qter [244,292]. The partial gain of 17q is usually a consequence of an unbalanced translocation with a partner chromosome [293]. The most common partner is the short arm of chromosome 1 although remarkably the 17q12-qter segment has also been found at 30 other sites on 20 different chromosomes [244]. The segment on the partner chromosome distal to the breakpoint is lost and a segment of 17q translocates to the site [292]. While whole chromosome 17 gains are observed in tumours exhibiting favourable clinical and genetic features, unbalanced partial gain of 17q is indicative of tumour progression and is strongly correlated with advanced stage disease and with tumours in children over the age of 1 [292,293]. In 1977 Brodeur *et al* first identified deletions of 1p in cytogenetic analysis of primary neuroblastoma tumours and cell lines [248]. This study also revealed that there is a wide range of breakpoints on 1p from 1p22 to 1p36 [248]. Deletions of 1p are correlated with unresectable and metastatic disease and introduction of 1p material in to neuroblastoma cells *in vitro* causes morphological differentiation and suppression of tumour growth [244,294]. This infers that distal 1p could contain a gene or genes important in the development of neuroblastoma. Further studies have shown that there are two regions of distinct allelic loss, suggesting that there may be at least two tumour suppressor genes on 1p, one located distally in 1p36.2-3 and one more proximal in 1p35-36.1 [244].

1.13.5 Current treatment for neuroblastoma

Analysis of clinical, biological and genetic markers allows neuroblastoma patients to be assigned in to low-, intermediate- and high-risk categories, which assists in determining the treatment policy[245,247]. Low risk neuroblastoma patients include infants and children with INSS stage 1 disease, INSS stage 2 patients, with single copy *N-myc* or favourable histology, and INSS stage 4 patients with favourable biology [248]. Patients with stage 1 or stage 2 disease in this group have localised tumours, which can usually be treated with surgery alone. [245,247]. Indeed post-surgery individuals with stage 1 neuroblastomas have a disease free survival rate of 95% [246]. Similarly, stage 2 patients have excellent survival rates following surgery and even in cases where residual disease requires further treatment with chemotherapeutic agents [247]. Infants and children with stage 4S neuroblastomas often only require supportive care which is effective for 90% of cases [247,257].

Intermediate-risk patients consist of patients diagnosed with stage 3 disease at any age and infants less than 1 year of age with stage 4 neuroblastomas [245,247]. Treatment of intermediate-risk patients involves surgery and moderately intensive chemotherapy. Radiotherapy is used in the management of patients with biological unfavourable stage 3 tumours with residual disease. More aggressive chemotherapy regimens are only considered if the patient does not respond to initial therapy or have recurrent disease [253]. Patients in this category have an excellent prognosis post-therapy with reported survival rates of greater than 80% [247]. Neuroblastoma patients in the high-risk category are stage 2 patients, stage 3 children or stage 4 infants all with *N-myc* amplified tumours. This category also includes stage 4 patients older than 1 year [247]. In addition to surgery, “Megatherapy” or intensive consolidation therapy is now often employed in advanced stage neuroblastomas and combines high dose myeloablative chemotherapy and or total body irradiation (TBI) with either autologous bone marrow transplanation (ABMT) or peripheral blood stem cell reinfusion [253,295]. Despite the use of more intensive therapies and better supportive care there has been little improvement in the overall survival rate of high-risk patients over the past 20 years. Indeed the current survival probability for high-risk patients is only 10-20% [246,247]. Since conventional cancer treatments are proving ineffective in the treatment of aggressive neuroblastomas a search for alternative therapeutic strategies is warranted [252].

1.13.6 Differentiation therapy

The normal process of differentiation of tissues usually requires either slowing or complete arrest of cell growth. Furthermore, many tumours in addition to their fast rate of proliferation often fail to express molecular markers or exhibit morphological features characteristic of the terminally differentiated phenotype [190]. Based on these observations Pierce was the first to propose the concept that human malignancies might be treated by forcing cells to complete terminal differentiation [190]. To date one of the most successful clinical examples of “differentiation therapy” has been the use of all-*trans* retinoic acid in the treatment of acute promyelocytic leukemia [296]. The PML/RAR α oncogenic protein of promyelocytic leukaemias which is the result a fusion of the retinoic acid receptor- α (RAR α) gene on chromosome 17 with part of the promyelocytic leukaemia (PML) protein gene on chromosome 15 [296]. The PML/RAR α protein is still able to bind to RAR α response elements but exhibits defective interactions with co-repressors which attenuates RA-target gene expression and blocks haematopoietic differentiation [14,15]. Treatment with all-*trans* retinoic acid is proposed to overcome this transcriptional repression to promote tumour regression. The use of all-*trans*-retinoic acid for the remission induction therapy of acute promyelocytic leukaemia has increased the overall remission rate to greater than 90% [296].

Neuroblastoma is an attractive target for differentiation therapy since it has the highest rate of spontaneous regression of all human malignancies and neuroblastoma tumours that exhibit a more mature histology are associated with favourable prognosis [246,297]. Initially retinoids including all-*trans*-retinoic acid (ATRA) and 13-*cis*-retinoic acid showed potential as a treatment for neuroblastoma since they induced neuroblastoma differentiation *in vitro*, resulting in a downregulation of N-*myc* mRNA expression and sustained arrest of tumour cell proliferation [252]. However, the results of phase I and II clinical trials using 13-*cis* retinoic acid to treat children with high tumour burdens were disappointing [245]. A subsequent phase III clinical trial demonstrated that 13-*cis*-retinoic acid therapy was beneficial for patients without progressive disease when it was administered after chemotherapy or transplantation [295]. Nevertheless, this still suggested that there was the potential to identify more effective differentiating agents for the treatment of neuroblastoma.

1.13.7 The cellular role of PPAR γ in neuroblastoma

Expression of PPAR γ mRNA has been detected in a number of different neuroblastoma cell lines [213,228]. Furthermore, a study by Han *et al* showed that PPAR γ protein levels in primary neuroblastoma tissue correlated with the maturational status of the cell, with high PPAR γ protein expression observed in neuroblasts that exhibited a more differentiated phenotype [213]. Although these findings suggested that the PPAR γ signalling pathway might be involved in neuroblastoma differentiation, the precise function of PPAR γ in this neoplasm is unclear. The growth of neuroblastoma cell lines is attenuated by treatment with PPAR γ ligands *in vitro*. Additionally, the natural PPAR γ ligand 15dPGJ₂ is a stronger inhibitor of neuroblastoma cell growth compared with retinoids *in vitro* suggesting that PPAR γ ligands might be a more efficacious treatment for neuroblastomas (unpublished data). Depending on the cell type and the ligand concentration used, growth inhibition of neuroblastoma cells by 15dPGJ₂ can be accompanied by differentiation, autophagy or apoptosis. Although it has previously been demonstrated that 15dPGJ₂ stimulates PPAR γ transcriptional activity in neuroblastoma cells, it remains unclear how PPAR γ activation regulates distinct cellular responses in this malignant cell type. Therefore, the aim of this project was to identify the mechanisms of action of PPAR γ ligands and provide insight into the cellular role of the PPAR γ receptor in neuroblastoma.

2 MATERIALS AND METHODS

2.1 Materials

Chemicals were obtained from Sigma-Aldrich (Poole, Dorset UK) unless otherwise stated. Tissue culture plastics and cell culture medium were obtained from Invitrogen.

2.2 Methods

2.2.1 Bacterial growth medium

2.2.1.1 Lennox L Broth (LB) medium

20 g of LB medium were dissolved in 1 litre of distilled water and autoclaved under standard conditions. Once cooled, LB medium was made into LB^{amp} medium, by the addition of ampicillin to give a final concentration of 100 µg/ml.

2.2.1.2 LB agar

LB medium was prepared and 1.5% (w/v) agar was added prior to autoclaving. When agar had cooled adequately, ampicillin was added to give a final concentration of 100 µg/ml.

2.2.2 Making competent cells

10 ml of LB was inoculated with a single colony of DH5 α *Escherichia coli* cells and incubated in a shaker incubator at 37°C overnight. 100 μ l of overnight culture was used to inoculate 10 ml of fresh LB. Cells were grown at 37°C for ~ 2-3 hours until their OD₆₀₀ reached 0.400 and they were in the exponential phase of growth. Cells were centrifuged at 3000 rpm for 10 minutes, the supernatant discarded and the pellet placed on ice. The pellet was re-suspended in 5 ml of sterile ice-cold 100 mM CaCl₂ and centrifuged at 3000 rpm for 10 minutes. The pellet was re-suspended in 500 μ l of sterile ice-cold 100 mM CaCl₂ and placed on ice for 30 minutes. Plasmid DNA was mixed with 100 μ l of competent cells, which were left on ice for 30 minutes. Cells were heat shocked at 42°C for 1.5 minutes and returned to ice for a further 30 minutes. Cells were rescued by mixing with 400 μ l of LB and incubating with shaking at 37°C for 30 minutes. Cells were pelleted at 3000 rpm for 5 minutes and re-suspended in 100 μ l LB, before being plated out on LB^{amp} agar and incubated in a warm room overnight at 37°C.

2.2.3 Glycerol stocks

10 ml of LB was inoculated with a colony of DH5 α cells or 10 ml LB^{amp} was inoculated with a colony of DH5 α cells transformed with plasmid DNA. Cultures were incubated in a shaker incubator at 37°C overnight. 500 μ l of overnight culture was mixed 1:1 with sterile glycerol and vortexed gently to mix. Glycerol stocks were initially frozen in liquid nitrogen and subsequently stored at -80°C until use.

2.2.4 Preparation of Ribonuclease A

To prepare Ribonuclease A (RNase A) that was DNase free, pancreatic RNase A was dissolved to a concentration of 10 mg/ml in 0.01 M sodium acetate (pH 5.2) and heated to 100°C for 15 minutes. The solution was subsequently allowed to cool slowly to room temperature before adjusting its pH to 7.4 by adding 0.1 volumes of 1M Tris(hydroxymethyl) aminomethane hydrochloride (Tris-HCl) (pH 7.4). The RNase A solution was finally dispensed in to aliquots and stored at -20°C until use.

2.2.5 Small scale isolation of plasmid DNA

10 ml cultures were inoculated with a single colony of DH5 α s transformed with the required plasmid and grown in LB^{amp} in a shaker incubator at 37°C overnight. Overnight cultures were centrifuged at 3000 rpm for 10 minutes. Pellets were re-suspended in 100 μ l glucose-Tris buffer (1% glucose, 25 mM Tris pH 8.0, 10 mM ethylenediamine tetra-acetic acid (EDTA)) and incubated at room temperature for 5 minutes. 200 μ l of cell lysis solution (0.2 M NaOH, 1% sodium dodecyl sulphate (SDS)) was added to the suspension, which was inverted twice and placed on ice for 5 minutes. 150 μ l of neutralization solution (3 M Potassium acetate, 11.5 % glacial acetic acid) was added to the preparation, which was inverted and placed on ice for a further 15 minutes. The samples were centrifuged at 12000 rpm for 15 minutes. The supernatant (lysate) was collected and was extracted 1:1 with 1:1 phenol:chloroform and centrifuged at 12 000 rpm for 5 minutes. The top layer was transferred to a fresh tube and treated with 10 units of RNase A for 1 hour at 37°C. The solution was extracted once with 1:1 phenol:chloroform. The top layer was then transferred to a clean tube, mixed with sodium acetate (3 M pH 5.2) and a double volume of ethanol and placed in a -40°C freezer for 30 minutes to precipitate the plasmid DNA. The plasmid DNA was then pelleted at 12 000 rpm for 10 minutes, air-dried and re-suspended in 40 μ l of sterile water.

2.2.6 Large scale isolation of plasmid DNA

10 ml cultures were inoculated with a single colony of DH5 α containing the required vector and grown in LB^{amp} in a shaker incubator at 37°C for 6 hours. These pre-cultures were used to inoculate 500 ml volumes of LB which had been pre-warmed in a shaker incubator at 37°C prior to the addition of ampicillin. These 500 ml LB^{amp} cultures were incubated in a shaker incubator at 37°C overnight. Overnight cultures were centrifuged at 4000 rpm for 20 minutes at 4°C in Sorvall RC-3B centrifuge (Kendro Laboratory Products Limited, Bishop's Stortford, Hertfordshire, UK). The pellets were resuspended in 4 ml sucrose-Tris buffer (730 mM sucrose, 50 mM Tris-HCl (pH 8.0)) containing 188, 000 Units of lysozyme. The suspensions were placed on ice for 15 minutes, then 500 mM EDTA pH 8.0 was added to make final

concentration of 10 mM and the suspensions were returned to ice for a further 15 minutes. A 3 ml volume of 3x Triton buffer (150 mM Tris-HCl pH 8, 187.5 mM EDTA, 3% (v/v) Triton X-100) was added and the samples were mixed and incubated on ice for 30 minutes until lysis occurred. Samples were centrifuged at 18000 rpm for 1.5 hours at 4°C in a Beckman J2-21 centrifuge (Beckman Coulter Inc., Fullerton, California) and the supernatant (lysate) was collected. The supernatant was made up to 500 mM NaCl, extracted 1:1 with 1:1 phenol: chloroform and centrifuged at 3000 rpm for 10 minutes. The top layer was decanted to a fresh tube and chloroform was added to make a 1:1 mix. The preparation was mixed vigorously with the chloroform and centrifuged at 3000 rpm for 10 minutes. The top layer was collected, to which 16.7 mM (10%) polyethylene glycol (PEG) was added and dissolved at 37°C. Once the PEG had dissolved the solution was stored at 4°C overnight. Next day the preparation was centrifuged at 12000 rpm for 20 minutes at 4°C to obtain a pellet. The pellet was re-suspended in 500 µl 0.1 M Tris-HCl (pH 8) and treated with 10 units RNase A for 1 hour at 37°C. 500 µl PEG buffer (33.4 mM PEG 6000, 1 M NaCl, 1 mM EDTA, 10 mM Tris pH 8) was added to the preparation, which was placed on ice for 1 hour. A pellet was obtained by centrifugation at 12000 rpm for 15 minutes and resuspended in 400 µl Tris-NaCl (10 mM Tris-HCl (pH 8), 500mM NaCl). This solution was treated with a further 10 units of RNase A for 2 hours at 37°C and extracted twice with 1:1 phenol:chloroform. The DNA was then ethanol precipitated, centrifuged at 12000 rpm for 10 minutes, air-dried in a tissue culture hood and dissolved in 100 µl tissue-culture sterile water. Plasmid DNA was visualised on a 1% agarose gel and its optical density was measured at 260 nm using a spectrophotometer to determine its concentration.

2.2.7 Molecular cloning

2.2.7.1 Generation of human PPAR γ 1 promoter deletion reporter constructs

Originally Fajas *et al* cloned a region of DNA from -2.8 kb to +60 bp, relative to the second transcription start site of PPAR γ 1, in to pGL3-Basic via *Sac* I and *Xho* I sites to create the PPAR γ 1 promoter reporter, pGL3- γ 1p3000[36]. To generate PPAR γ 1 promoter deletion constructs pGL3-PPAR γ 1p216 and pGL3-PPAR γ 1p78, the pGL3-

PPAR γ 1p3000 reporter was digested with *Sac* I and *Sma* I, and *Sac* I and *Sac* II respectively, since the promoter region contains a *Sma* I site starting at 159 bp and *Sac* II site starting at 22 bp upstream from the second start site of PPAR γ 1 transcription (restriction endonucleases from Promega, Chilworth UK). These endonucleases only resulted in truncations of the PPAR γ 1 5' regulatory region since there are no restriction sites for these enzymes in the rest of the pGL3-Basic vector (See **Table 2.1**). Following restriction digest the linearised plasmid was gel purified using a QIAquick Gel Extraction Kit (Qiagen, UK) and 3' overhangs were converted to blunt ends by treatment with T4 DNA polymerase (Promega, Chilworth, UK). 20 μ l of the gel purified DNA was mixed with 5 μ l of 5x T4 DNA Polymerase Buffer, 5 units of T4 DNA Polymerase, 2 μ l of dNTPs (10 mM), 22 μ l of sterilized DNA grade water and incubated at 37°C for 5 minutes and then heated at 75°C for 10 minutes to stop the reaction by denaturing the polymerase. The reaction was carried out in the presence of high concentration of dNTPs to prevent degradation of duplex DNA. The DNA was cleaned using a QIAquick PCR Purification Kit (Qiagen, UK) and set up in a ligation with T4 DNA Ligase (Promega, Chilworth, UK). Approximately 200 ng of vector was mixed with 1 μ l of 10x Rapid Ligation Buffer, 0.5 units of T4 DNA Ligase and 5 μ l of sterilized DNA grade water. The ligation was left at room temperature for at least 4 hours. The ligated vector was then used to transform DH5 α s and transformant colonies were screened by digesting their DNA from mini preparations with *Bgl* I and *Xho* I. The restriction digests were then run on an agarose gel to verify which of the transformants, were actual clones. The integrity of the promoter region in these clones was verified by sequencing (The Sequencing Service, University of Dundee).

2.2.7.2 Creation of human PPAR γ 1 promoter reporters using synthetic oligonucleotides

The human PPAR γ 1 promoter reporters, pGL3- γ 1p78oligo, pGL3- γ 1p58oligo and pGL3- γ 1p34oligo were created using synthetic oligonucleotides. Three pairs of oligonucleotides were synthesized so that when annealed and then ligated together they formed a continuous 78 bp sequence of the PPAR γ 1 5' regulatory region from -18 bp to +60 bp relative to the second transcription initiation site (Biomers.net, The

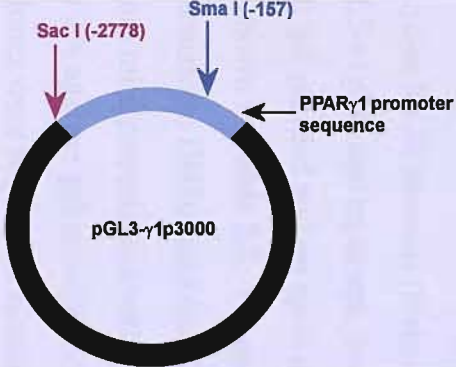
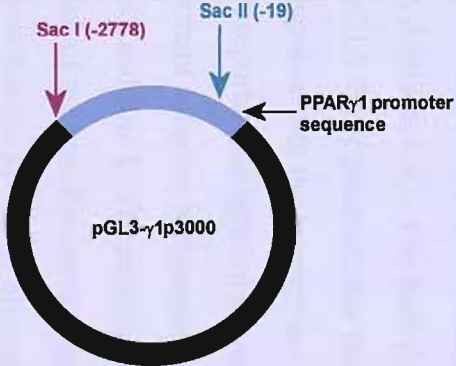
Construct Name	Digested pGL3- γ 1p3000 with:	Size of released promoter fragment (bp)	Truncated promoter sequence in construct (bp)
pGL3- γ 1p216	 <p>The diagram shows a circular plasmid labeled pGL3-γ1p3000. A blue arc represents the PPARγ1 promoter sequence. Two restriction sites are indicated: Sac I at position -2778 (marked with a red arrow) and Sma I at position -157 (marked with a blue arrow). The promoter sequence is highlighted in blue.</p>	2621 (From -2778 to -157)	216 (From -156 to + 60)
pGL3- γ 1p78	 <p>The diagram shows a circular plasmid labeled pGL3-γ1p3000. A blue arc represents the PPARγ1 promoter sequence. Two restriction sites are indicated: Sac I at position -2778 (marked with a red arrow) and Sac II at position -19 (marked with a blue arrow). The promoter sequence is highlighted in blue.</p>	2759 (From -2778 to -19)	78 (From -18 to + 60)

Table 2.1. Creation of PPAR γ 1 promoter deletion reporters. This table shows the restriction enzymes used to digest pGL3- γ 1p3000 to create the PPAR γ 1 promoter deletion reporters, pGL3- γ 1p216 and pGL3- γ 1p78. The positions of the restriction endonuclease sites and start and end positions of the promoter fragments are relative to the second PPAR γ 1 transcription start site in the PPAR γ 1 promoter sequence. For each construct the size of the promoter fragment released following the restriction digest and the truncated promoter fragment which remains in the construct have been calculated.

Biopolymer Factory, Germany). Initially each oligonucleotide was diluted to a final concentration of 100 μ M with sterile DNA-grade water. To anneal each pair, 20 μ l of the required oligonucleotides were mixed and then incubated at 94°C and allowed to cool gradually to room temperature. Different combinations of annealed oligonucleotide pairs were ligated together to create the required insert for each reporter (See **Table 2.2**). For the pGL3- γ 1p78oligo reporter, the plasmid pGL3-Basic was digested with *Acc65* I and *Hind* III, gel purified using a QIAquick Gel Extraction Kit (Qiagen, UK) and then set up in a ligation with the oligonucleotide pairs indicated in **Table 2.2**. To create the pGL3- γ 1p58oligo and pGL3- γ 1p34oligo reporters, pGL3-Basic was first digested with *Acc65* I and *Nhe* I respectively and then the linearised plasmids' 5'overhangs were partially filled using *Pfu* DNA Polymerase (Promega, Chilworth, UK). In brief, 20 μ l of digested plasmid was mixed with 4 μ l of *Pfu* DNA Polymerase 10x Buffer with MgSO₄, 0.75 μ l of each required dNTP (10 mM), 0.75 Units of *Pfu* DNA Polymerase and 12.5 μ l of sterile DNA-grade water to make a total volume of 40 μ l. This mixture was incubated at 74°C in an Omnigene PCR thermocycler for 30 minutes (Hybaid, Ashford, UK). For both the pGL3- γ 1p58oligo and pGL3- γ 1p34oligo reporters, the pGL3-Basic plasmid was then digested with *Hind* III; gel purified and set up in a ligation with the appropriate oligonucleotide pairs as shown in **Table 2.2**. For each reporter, the ligation of vector and insert was used to transform DH5 α s and transformant colonies were screened by digesting their DNA from mini preparations with *Bgl* I and *Xho* I. The restriction digests were then run on a 2% agarose gel to verify which of the transformants, were actual clones. These clones were sequenced to confirm that the synthetic oligonucleotide inserts, exactly matched the endogenous PPAR γ 1 5'regulatory region (The Sequencing Service, University of Dundee).

Oligonucleotide pairs								
Oligo 1	Oligo 2	Oligo 3	Oligo 4	Partial Fill	Oligo 5	Oligo 6	Partial Fill	Hind III
5' - <u>GTAC</u> GGGCAGGCGGGGCCAGCGC-3'		5' <u>ACT</u> CGGAGCCCGAGCCCGAGCCGC-3'			5' - <u>AG</u> CCCGCCGCTGGGGCGCTTGGGTCTGGCCTCGAG-3'			
3' -CCCGTCCGCCCCGGGTCGCGTG-5'		3' -AGCCTCGGGCTCGGGCTCGGCGTC-5'			3' -GGCGGCGGACCCCGCGAACCCAGCCGGAGCTC <u>TCGA</u> -5'			
	Acc 65 I		Partial Fill				Partial Fill	Hind III
			Acc 65 I				Nhe I	

Construct name	Vector	Insert	Cloning details
pGL3- γ 1p78oligo	pGL3-Basic	pGL3-Basic Annealed oligos pairs 1+2, 3+4, 5+6 which have been ligated together	pGL3-Basic digested with <i>Acc65 I</i> and <i>Hind III</i> . Gel purified vector used to set up ligation with oligo pairs 1+2, 3+4, 5+6 which had already been ligated. Oligo pairs 1+2 and 5+6 have complementary overhangs to <i>Acc65 I</i> and <i>Hind III</i> overhangs in cut pGL3-Basic vector.
pGL3- γ 1p58oligo	pGL3-Basic	Annealed oligos pairs 3+4, 5+6 which have been ligated together pGL3-Basic	pGL3-Basic digested with <i>Acc65 I</i> and <i>Acc65 I</i> overhang partially filled with dGTP and dTTP, then cut with <i>Hind III</i> and gel purified. Used to set up ligation with oligo pairs 3+4, 5+6 which have previously been ligated. Oligo pair 3+4 has complementary overhang to partially filled <i>Acc65 I</i> overhang in cut pGL3-basic vector. Oligo pair 5+6 has complementary overhang to <i>Hind III</i> overhang in cut pGL3-basic vector.
pGL3- γ 1p34oligo	pGL3-Basic	Oligo pair 5+6	pGL3-Basic digested with <i>Nhe I</i> and <i>Nhe I</i> overhang partially filled with dCTP and dTTP, then cut with <i>Hind III</i> and gel purified. Used to set up a ligation with oligo pair 5+6 which has complementary overhangs to partially filled <i>Nhe I</i> overhang and <i>Hind III</i> overhang in cut pGL3-Basic vector.

Table 2.2. Generation of PPAR γ 1 promoter deletion constructs using synthetic oligonucleotides. Details of the vector, insert and cloning method for each vector are described.

2.2.8 Preparation of PPAR γ ligands

2.2.8.1 15-deoxy $\Delta^{12,14}$ prostaglandin J₂

15-deoxy $\Delta^{12,14}$ prostaglandin J₂ (11-oxoprostano-5Z, 12E, 14Z-tetraen-1-oic acid) (15dPGJ₂) was obtained from Cayman Chemicals (Alexis Corporation, Bingham, UK) supplied in methyl acetate. Solvent was removed by evaporation under N₂ and 15dPGJ₂ was re-suspended in 100 μ l dimethyl sulphoxide (DMSO) and stored at –20°C. The stock was diluted at 1:10, 1:100 and 1:1000 with DMSO so that the 15dPGJ₂ could be used at concentrations of 0.1, 1, 5, 10 and 20 μ M.

2.2.8.2 Ciglitazone

Ciglitazone (5-[[4-[(Methylcyclohexyl)methoxy]phenyl]methyl-2,4-thiazolidinedione) was obtained from Tocris (Bristol, UK) or Cayman chemicals (Alexis Corporation, Bingham, UK) as a white solid. Ciglitazone was dissolved in DMSO to give a stock solution of 100 mM, which was stored at –20°C. This stock was diluted 1:10 with DMSO so that ciglitazone could be used at concentrations of 25, 50, 100, 150 and 200 μ M.

2.2.9 Preparation of histone deacetylase inhibitor Trichostatin A

Trichostatin A (4, 6 –Dimethyl-7-[p-dimethyl-aminophenyl]-7-oxohepta-2,4-dienohydroxamic acid) was obtained from Upstate signaling solutions (Dundee Technology Park, UK) as a white powder. Trichostatin A was dissolved in DMSO to give stock concentration of 2 mg/ml (6.6 μ M/L). Trichostatin A was used at concentrations between 1 ng/ml and 400 ng/ml.

2.2.10 Cell culture

The human neuroblastoma cell lines SK-N-AS, IMR-32, SK-N-SH and the mouse neuroblastoma cell line, ND-7 were used for cell culture experiments. For some p53 transient transfection experiments the lung cancer cell line H1299 was also used. All neuroblastoma cell lines were maintained in Dulbecco's Modified Eagle's Medium (DMEM) and H1299 cells were maintained in RPMI-1640 (Roswell Park Memorial Institute-1640) medium, both containing 10% (v/v) foetal calf serum (FCS) and 100mM glutamine, supplemented with 0.1mg/ml penicillin-streptomycin. Cells were incubated at 37°C in a humidified atmosphere containing 5% (v/v) CO₂. SK-N-AS, IMR-32, SK-N-SH and H1299 cells were passaged by incubation with 1x Trypsin-EDTA (500 units Trypsin, 0.53 mM EDTA) whereas ND-7 cells were detached by gentle agitation.

SK-N-AS cell line was derived from the bone marrow of a female patient with neuroblastoma and consists of a single polygonal shaped cell [298]. SK-N-SH cells were derived from the bone marrow of a 4-year-old Caucasian female with neuroblastoma and have neuroblast-like or epithelial like morphology. The IMR-32 cell line which is *N-myc* amplified was derived from the abdominal neuroblastic tumour of a 13-month old Caucasian male [299]. The cell line has two morphologically distinct cell types. The predominant cell type is a small, neuroblast-like cell, which grows densely forming focal adhesions. The minor cell type is a fibroblast-like cell, which is relatively large and well spread and occurs in small numbers. ND-7 cells are a hybrid cell line derived from neonatal rat dorsal root ganglia neurons fused with the mouse neuroblastoma cell line N18Tg2 [300].

2.2.11 Freezing cells in liquid nitrogen and resuscitation of frozen cells

Adherent cells were centrifuged at 1000 rpm for 3 minutes and the culture media was carefully removed. Cells were re-suspended in 1 ml of freezing culture media (10% (v/v) DMSO in complete media) and stored on dry ice at -70° and frozen overnight at -80°C before being transferred to liquid nitrogen stores. For resuscitation, cells were rapidly thawed and diluted in 6 ml of complete culture medium. The cells were then pelleted at 1000 rpm for 3 minutes and the culture media was decanted off. Cells were then re-suspended in 6 ml of fresh complete media, transferred to a tissue

culture flask and incubated at 37°C in a humidified atmosphere containing 5% (v/v) CO₂.

2.2.12 Cell growth

Neuroblastoma cells were seeded at 4×10^4 cells per well in to 6 well plates and incubated for 5 hours at 37°C to facilitate attachment before treatment. Treated and untreated cells were counted over 3 days, 24 hours following administration of the ligand. Cells were scraped and harvested in their DMEM media and centrifuged at 3000 rpm for 5 minutes. The cells were re-suspended in 25 µl PBS and 25 µl 0.4% trypan blue, visualized with a Nikon TMS microscope (x10 objective lens) and counted using a haemocytometer (Nikon, Surrey, UK). Viable and non-viable cells were counted separately. Four counts were made per treatment per day, and the average calculated. The average number of cells counted on the haemocytometer grid gave the number of cells $\times 10^4$ per ml and as the volume of cell suspension was known, the total number of cells could be determined.

2.2.13 Light microscopy

SK-N-AS cells were observed using a digital camera linked to a Leica DM IL microscope (x40 objective lens) (Leica Microsystems GmbH, Ernst-Leitz-Strasse 17-37, 35578 Wetzlar). SK-N-AS cells were seeded at 4×10^4 cells per well in complete media and incubated for 5 hours at 37°C to allow the cells to attach before treatment. SK-N-AS cells were administered with a vehicle control (DMSO) or 100 µM ciglitazone and visualized after 72 hours.

2.2.14 DNA transfection of cultured cells

Cells were plated at 2×10^5 cells per well in 6-well dishes in complete media and allowed to attach overnight. Two tubes were set up per sample; tube A contained 2 µg of reporter plasmid DNA and 12.4 µl of CaCl₂ (2 M) made up to a total volume of 100 µl with sterile water and tube B contained 100 µl of 2x Hepes Buffered Saline

(HBS) (280 mM NaCl, 50 mM N-(2-Hydroxyethyl) piperzaine-N'-(2-ethanesulphonic acid)(Hepes free acid), 2.8mM disodium hydrogen phosphate (Na_2HPO_4), pH 7.12). When a reporter construct was co-transfected with different quantities of an expression plasmid, the total amount of DNA for each transfection was normalized with an empty expression vector control (pcDNA3.1) (**Table 2.3**). The contents of tube A were added slowly drop-wise to the contents of tube B to form a translucent precipitate, which after 10 minutes at room temperature was transferred drop-wise to the culture media. The 6-well dish was tilted slightly when adding the precipitate to the media to avoid the precipitate directly contacting the cells and the media was then gently swirled to ensure even distribution of the precipitate. The cells were incubated at 37°C for 4 hours, when the medium containing the precipitate was removed. The cells were washed with serum free media before replacing the cells with fresh complete media. The cells were incubated at 37°C with or without treatment for 24 hours and then harvested.

2.2.15 Luciferase reporter assay

Neuroblastoma or lung cancer cells transfected with a luciferase reporter construct were harvested 24 hours post transfection, washed with PBS (Phosphate Buffer Saline) and assayed for luciferase activity. When cells were co-transfected with a firefly and *Renilla* luciferase reporter, luciferase activity was measured using a dual-luciferase reporter assay kit (Promega, Chilworth, UK). In brief, the cells were lysed in passive lysis buffer and freeze thawed twice. Cell debris was pelleted and the supernatant was transferred to a fresh tube. Some of the supernatant was first mixed with luciferase assay reagent II (LAR II) and the firefly luminescence of the sample measured. Secondly, Stop & Glo reagent was added to the same tube and the *Renilla* luminescence was measured. For each sample the firefly and *Renilla* luminescence was measured three times in a TD-20/20 luminometer (Turner Designs, Sunnyvale, California) and an average luminescence was calculated. When cells were transfected with a firefly luciferase reporter only, luciferase activity was measured using a single luciferase assay kit (Promega, Chilworth, UK). In brief, the cells were lysed in reporter lysis buffer and freeze thawed twice. The cell debris was pelleted and some of the supernatant was mixed with luciferase reagent I (LAR I) and the luminescence was measured three times and an average luminescence was calculated.

Construct name	Vector	Insert	Details of plasmid or construct
Expression plasmids			
pcDNA3.1	Mammalian expression plasmid from Invitrogen.	-	Ampicillin and Neomycin resistance genes for selection in bacteria and mammalian cells respectively. Expression of gene controlled by CMV promoter.
pC53-SN3	pCMV-Neo-Bam mammalian expression vector	Wild-type human p53 cDNA	Kind gift from Dr J.P. Blaydes, Cancer Sciences Division, Southampton General Hospital. Ampicillin and Neomycin resistance genes for selection in bacteria and mammalian cells respectively.
pCMV4-p107	pCMV4	Human p107 cDNA	Kind gift from Dr N.S.B. Stone, Department of Haematological Medicine, Guy's, King's, St Thomas' School of Medicine, Rayne Institute, London. Ampicillin and Neomycin resistance genes for selection in bacteria and mammalian cells respectively.
pCMV-p130	pCMV-Neo-Bam mammalian expression plasmid	Human p130 cDNA	Kind gift of Dr N.S.B. Stone, Department of Haematological Medicine, Guy's, King's, St Thomas' School of Medicine, Rayne Institute, London. Ampicillin and Neomycin resistance genes for selection in bacteria and mammalian cells respectively. p103 cDNA from pBSKHA-p130 (<i>EcoR</i> V/ <i>Sac</i> II-fragment) cloned in to pCMV-Neo-Bam.
pCMV-pRb	pCMV-Neo-Bam mammalian expression plasmid	pRb cDNA	Kind gift of Dr N.S.B. Stone, Department of Haematological Medicine, Guy's, King's, St Thomas' School of Medicine, Rayne Institute, London.
pCMV-pRb Δ PD	pCMV-Neo-Bam mammalian expression plasmid	pRb cDNA lacking sequence encoding pocket domain	Kind gift of Dr N.S.B. Stone, Department of Haematological Medicine, Guy's, King's, St Thomas' School of Medicine, Rayne Institute, London.
pEF c-Myc	pUC 119 mammalian expression	Human c-Myc cDNA	Kind gift of Dr Y. Shang, Department of Adult

	plasmid		Oncology, Dana-Farber Cancer Institute, Harvard Medical School, Boston. Ampicillin resistance gene for selection in bacteria.
pmiw-N-Myc	pMisv mammalian expression plasmid	Human N-Myc cDNA	Kind gift of Dr H. Kondoh, Institute of Molecular and Cellular Biology, Osaka University, Suita, Japan. Ampicillin resistance gene for selection in bacteria
pCMV-Miz-1	pCMV mammalian expression vector	Human Miz-1 cDNA	Kind gift of Dr F.Hanel, Hans Knoll-Institut for Naturstoff-Forschung, Heidelberg, Germany. Ampicillin and Neomycin resistance genes for selection in bacteria and mammalian cells respectively.
V394D c-Myc mutant	pcDNA3.1 expression plasmid	cDNA encodes V394D mutant of c-Myc (Val ³⁹⁴ -Asp) produced by 2 step PCR	Kind gift of Dr A. Lapham, Cancer Sciences Division, Southampton General Hospital. The mutant was cloned in to <i>Bam</i> H I and <i>Eco</i> R I sites in the pcDNA3.1 vector. Ampicillin and Neomycin resistance genes for selection in bacteria and mammalian cells respectively.
c-Myc deletion mutants: Δ7-91 Δ56-103 Δ142-262 Δ265-320 Δ264-368 Δ371-412 Δ414-433	pUC8 vector	Human c-Myc cDNA with the indicated deletions	Kind gift of Dr J. Stone, Jackson Laboratory, Bar Harbor, Maine. The original plasmid contained normal human c-Myc cDNA which was used as a template to create series of deletion mutants.
pcDNAflagγ1L46 8A/E471A	pcDNA3 from Invitrogen	Human PPARγ1 cDNA containing mutations, L468A and E471A in the AF-2 domain	Kind gift of Professor V.K.K. Chatterjee, Department of Medicine, University of Cambridge, Addenbrooke's Hospital, Cambridge. Ampicillin and Neomycin resistance genes for selection in bacteria and mammalian cells respectively.
Reporter plasmids			
pGL3-Basic	Firefly luciferase reporter from	-	Ampicillin resistance gene for selection in bacteria.

	Promega.		The vector lacks eukaryotic promoter and enhancer sequences.
TK-Renilla	pRL-TK <i>Renilla</i> luciferase reporter vector from Promega	-	Ampicillin resistance gene for selection in bacteria. <i>Renilla</i> luciferase reporter gene expression controlled by herpes simplex virus thymidine kinase promoter
pGL3- γ 1p3000	pGL3-Basic	A 2842 bp 5' regulatory region of the human PPAR γ 1 gene	Construct from Dr J. Auwerx, Department d'Athérosclérose, Institut Pasteur, Lille, France. Promoter region inserted in to pGL3-Basic via <i>Sac</i> I and <i>Xho</i> I sites
PPREx3-TK-Luc	Luciferase reporter plasmid	Triple repeat of a consensus PPAR response element (PPRE)	Kind gift from Professor Ronald Evans, The Salk Institute for Biological Studies. Luciferase reporter.
Hdm2luc03	pGL3-Basic	Proximal region of Hdm2 promoter containing two consensus p53 binding sites	Kind gift from Dr J.P. Blaydes, Cancer Sciences Division, Southampton General Hospital. Ampicillin resistance genes for selection in bacteria.
pPAC-Sp1	pPAC expression plasmid	cDNA for Sp1	Kind gift of Dr P.A. Marsden, Renal Division and Department of Medicine, University of Toronto, Canada. Ampicillin resistance genes for selection in bacteria.
pMSV-C/EBP β	pMSV expression plasmid	cDNA for C/EBP β	Kind gift of Dr S. McKnight, University of Texas, Dallas. Ampicillin resistance genes for selection in bacteria.

Table 2.3. List of expression and reporter plasmids used to transiently transfect neuroblastoma and lung cancer cell lines. See table 2.1 and 2.2 for details of PPAR γ 1 promoter deletion reporters also used in transfection assays.

2.2.16 Protein assay

Lysates from neuroblastoma cells transfected with luciferase reporter plasmids were assayed for protein using the bicinchoninic acid (BCATM) protein assay kit (Pierce, Rockford, Illinois). A standard curve was produced from a series of diluted albumin standards which were prepared from a 2 mg/ml stock of bovine serum albumin (BSA) (in 0.09% saline and 0.05% sodium azide) using lysis buffer as the diluent. The working range of the assay was 20-2,000 µg/ml. 25 µl of each standard or unknown sample were pipetted in a microplate well and then mixed thoroughly with 200 µl of the working reagent which comprised of 50 parts BCATM Reagent A and 1 part of BCATM Reagent B (50:1, Reagent A:B). The plate was covered and incubated at 37°C for 30 minutes, cooled to room temperature and then the absorbance of the samples was measured at 570 nm on a plate reader.

2.2.17 Establishment of stable cell lines

IMR-32 cells were seeded at 1×10^6 cells per 96 mm culture dish in 5 ml of complete media and allowed to attach overnight. Cells were transfected with 6 µg of each plasmid using the liposome based transfection reagent, Metafectine (Biontex Laboratories, Germany). In brief, the plasmid (6 µg) and Metafectene (18 µl) were added to separate tubes containing 300 µl of medium that was free of serum and antibiotics. The contents of the tubes were then combined and mixed by gentle pipetting and allowed to incubate at room temperature for 20 minutes to allow the DNA-lipid complex to form. The DNA-lipid complex was then added to the media in the culture dish and mixed gently. The cells were then incubated at 37°C for 5 hours then the transfection mixture was removed and replaced with fresh complete media. For PPAR γ dominant negative experiments, IMR-32 cells were transfected with 6 µg of pcDNAFlag- γ 1 L468A/E471A (Kind gift of Professor V.K.K Chatterjee, Department of Medicine, University of Cambridge, Addenbrooke's hospital) or pcDNA3.1 (Invitrogen) as the vector only control. Transfected cells were cultured for 72 hours then treated with Geneticin disulphate salt (G418) in fresh complete

media (800 µg per ml of media). Cells were selected by treatment with subsequent doses of G418 in fresh medium, until clones were visible with the naked eye. Individual colonies were “picked” using trypsin-EDTA and cultured as separate cell lines.

2.2.18 RNA isolation from neuroblastoma cells

Total RNA was isolated from neuroblastoma cells using TRI REAGENT[®]. The cell pellet was washed with PBS and then lysed by gentle pipetting with 1 ml of TRI REAGENT[®]. The cells were allowed to lyse at room temperature for 5 minutes before addition of 200 µl of chloroform. TRI REAGENT[®]-chloroform mixes of cells suspensions were mixed vigorously and incubated at room temperature for 2-3 minutes and centrifuged at 12000 rpm for 15 minutes at 2-8°C. The aqueous layer was isolated and the RNA was precipitated with isopropyl alcohol and collected by centrifugation at 12000 rpm for 10 minutes. The RNA pellet was air-dried and re-suspended in 22 µl of autoclaved, 0.1% (v/v) diethyl pyrocarbonate (DEPC)-treated water and stored at -80°C. The RNA concentration (µg/µl) was determined by measuring its optical density at 260 nm.

2.2.19 Preparation of cDNA for RT-PCR

Total cell RNA was used to synthesise cDNA. 1 µg of RNA was mixed with 1 µl of 90 OD Units/ml of random hexamers in 0.1% (v/v) DEPC water (Amersham Pharmacia Biotech Limited, Little Chalfort, UK), 1 µl of 10 mM dNTP mix (Promega, Chilworth, UK) and 0.1% (v/v) DEPC water to a total volume of 10 µl. This mixture was incubated at 70°C for 10 minutes and then cooled on ice. To this mix 4 µl of 5 x Reverse transcriptase buffer, 2 µl of 0.1M DTT, 0.5 µl RNAsin, 1 µl of Moloney-Murine Leukaemia Virus (M-MLV) reverse transcriptase and 2.5 µl of 0.1% (v/v) DEPC water were added to make a total volume with RNA of 20 µl. The final mix was incubated at room temperature for 10 minutes to ensure elongation of the random hexamers and subsequently at 37°C for 50 minutes. It was then heated to 80-94°C to denature the M-MLV reverse transcriptase and stored at -80°C before use.

2.2.20 Reverse transcriptase-polymerase chain reaction (RT-PCR)

cDNA was amplified using cyclophilin and PPAR γ dominant negative specific primers created to generate RT-PCR products of the cyclophilin gene and the FLAG epitope-tagged human PPAR γ 1 L468A/E471A double mutant inserted in to the pcDNA3 expression vector (Invitrogen) (Table 2.4). The PPAR γ dominant negative primers were designed to amplify a region which included part of the FLAG epitope and the PPAR γ gene to distinguish between expression of the PPAR γ 1 mutant and endogenous PPAR γ 1. Cyclophilin was used as a control to normalise cDNA levels. Reactions (5 μ l cDNA, 5 μ l 10 x PCR buffer, 20 μ l 25 mM magnesium chloride, 3 μ l 10 mM dNTP mix, 0.5 μ l forward primer, 0.5 μ l reverse primer and 15.5 μ l of 0.1% (v/v) DEPC-treated water) were incubated in Omnigene PCR thermocycler (Hybaid, Ashford, UK) for optimum number of cycles with 2.5 Units of Taq polymerase (Promega, Chilworth, UK). The optimum number of cycles was determined by analysing PCR products on an agarose gel every 5 cycles, after an initial measurement at 25 cycles. 25 cycles was used as an initial measurement because the PCR products needed to be observed in the exponential phase of amplification, where differences in level of expression could be seen. If the amplification reached plateau phase, then lower expressed mRNA would be amplified to a similar level as highly expressed mRNA, since abundant mRNA at plateau phase would have already reached a maximum level of expression due to the limits of the reaction mix. PCR products were run on a 1.5% (w/v) agarose gel and visualized by UV light.

A

cDNA sequence	Forward primer sequence	Reverse primer sequence	PCR Product size (bp)
Cyclophilin	5'-TTG GGT CGC GTC TGC TTC GA-3'	5'-GCC AGG ACC TGT ATG CTT CA-3'	250
PPAR γ dominant negative	5'-CAA GAT GAC CAT GGG TG-3'	5'-GAG CTG AGT CTT CTC AG-3'	350

B

Primers	Denature (°C)	Time (seconds)	Anneal (°C)	Time (seconds)	Extension (°C)	Time (seconds)	No. of cycles
Cyclophilin	94	30	54	30	72	30	25
PPAR γ dom neg	94	40	50	40	72	45	35

Table 2.4 A. Shows the sequences of the forward and reverse primers used to amplify the reverse transcribed cDNA of the cyclophilin gene and PPAR γ 1 dominant negative receptor and the size of the RT-PCR product. **Table 2.4 B** shows the denaturing, annealing and extension temperatures and times for the RT-PCR of cyclophilin and PPAR γ 1 dominant negative receptor and the optimum number of cycles to distinguish differences in mRNA expression. The optimum number of cycles was determined by analysis of PCR products on a 1.5% agarose gel every 5 cycles after an initial measurement at 25 cycles.

2.2.21 Tritiated thymidine incorporation assay

IMR-32 cells stably expressing a PPAR γ 1 dominant negative receptor or empty expression vector IMR-32 control cells were plated out at 4×10^4 cells per well in 6-well plates in duplicate and allowed to attach overnight. Each day 1 μ Ci of [3 H]Thymidine was added per well to a total of two wells per cell line and the cells were incubated at 37°C for 18 hours. The cells were then washed rapidly two times with ice cold PBS. The cells were extracted by scraping in to 500 μ l of 62.5 mM Tris-HCl pH 7.5 containing 0.1% SDS. Duplicate aliquots (i.e. 250 μ l) were precipitated with 750 μ l of ice cold 10% trichloroacetic acid (TCA) and incubated on ice for 30 minutes. After this time the precipitates were diluted to 5 ml with ice cold 10% TCA and collected on GF/C Glass Microfibre Filters (Whatman, UK). The filters were washed three times, with 1 ml each of ice cold 10% TCA and methanol and then dried. The filters were counted in opti-phase Hi-safe scintillant (Fisher Scientific, UK) using a Beckman scintillation counter.

2.2.22 Transient chromatin immunoprecipitation assay

SK-N-AS cells were seeded at 5×10^5 cells per 96 mm culture dish in 5 ml of complete media and allowed to attach overnight. On day 2 separate dishes of SK-N-AS cells were transfected with 5 μ g of the PPAR γ 1 promoter reporter, pGL3- γ 1p34oligo or pGL3-Basic using calcium phosphate, while a third dish served as the un-transfected control. The cells were incubated for 4 hours at 37°C, after which the media containing the precipitate was removed. The cells were washed twice with serum free media and the replaced with fresh complete media. After 24 hours to link protein to DNA, formaldehyde was added directly to the culture medium to a final concentration of 1% and incubated at 37°C for 10 minutes. Following this incubation as much medium as possible was removed and the cells were washed twice with ice cold PBS before the cells were harvested by scrapping in PBS. The cells were pelleted for 4 minutes at 2000 rpm at 4°C. If required, SDS lysis buffer (1% SDS, 10mM EDTA, 50 mM Tris-HCl, pH 8) was warmed to room temperature to dissolve

precipitated SDS before adding protease inhibitors (10 μ l of 10mM PMSF (Phenylmethylsulphonylfluoride) and 1 μ l of 1 μ g/ μ l aprotinin added per 1 ml of SDS lysis buffer). Cell pellets were re-suspended in 200 μ l of the prepared SDS lysis buffer and incubated on ice for 10 minutes. The lysate was then sonicated to shear DNA to lengths between 200 and 1000 basepairs using an XL-2020 sonicator (Heat Systems (now known as Misonix Inc, New York). Sonication conditions for SK-N-AS cells had previously been optimized and showed that DNA was sheared to the appropriate length using the sonicator equipped with a 2 mm tip set to power level 1 and a process time of 60 seconds, with 10-seconds “off” between each 10-second pulse. The samples were centrifuged for 10 minutes at 13,000 rpm at 4°C and the sonicated cell supernatant transferred to a fresh micro-centrifuge tube. Duplicate aliquots (i.e. 100 μ l) of the sonicated cell supernatant were diluted 10-fold in Chip dilution buffer (0.01% SDS, 1.1% Triton X-100, 1.2 mM EDTA, 16.7 mM Tris-HCl, pH 8.0, 167 mM NaCl) which had previously been mixed with protease inhibitors as described above for SDS lysis buffer. 20 μ l of the diluted cell supernatant was kept and served as the input for the PCR reaction in the later part of the experiment. To reduce non-specific background the cell supernatant was pre-cleared with 30 μ l of Salmon Sperm DNA/Protein A Agarose-50% Slurry (Upstate cell signaling solutions, New York) at 4°C for 4 hours with agitation. The agarose was pelleted by centrifugation at 1000 rpm for 60 seconds and the supernatant fraction was collected. 2 μ l of the immunoprecipitating antibody (Anti-c-Myc mouse monoclonal antibody, Calbiochem, San Diego, United States) was added to the 1ml supernatant fraction and incubated overnight at 4°C with rotation. For each sample, the second 1ml supernatant fraction collected served as the no-antibody control. The next day, 30 μ l of Salmon Sperm DNA/Protein A Agarose Slurry was added to both the antibody and no-antibody 1 ml supernatant fractions for 1 hour at 4°C with rotation. The agarose was pelleted by gentle centrifugation at 1000 rpm for 60 seconds and the supernatant containing unbound, non-specific DNA was removed. The protein A agarose/antibody/protein-DNA complex (and no-antibody control protein A agarose) was then washed twice for 2-5 minutes with 1 ml of each of the following buffers on a rotating platform in the order given; Low Salt Immune complex wash buffer (0.1% SDS, 1 % Triton X-100, 2 mM EDTA, Tris-HCl pH 8.0, 150 mM NaCl), High Salt Immune complex wash (0.1% SDS, 1 % Triton X-100, 2 mM EDTA, Tris-HCl pH 8.0, 500 mM NaCl), LiCl Immune complex wash buffer (0.25M LiCl, 1% NP40, 1%

deoxycholate, 1 mM EDTA, 10mM Tris-HCl, pH 8.0) and TE Buffer (10 mM Tris-HCl pH 8.0, 1 mM EDTA pH 8.0). To elute the protein-DNA complex from the antibody, 250 μ l of freshly prepared elution buffer (1% SDS, 0.1 M NaHCO₃) was added to the pelleted protein A agarose/antibody/protein-DNA complex. The elution buffer and agarose were vortexed briefly and incubated at room temperature for 15 minutes with rotation. The agarose was centrifuged at 1000 rpm for 60 seconds and the supernatant fraction (eluate) was transferred to a fresh tube. The elution step was repeated and the two eluate fractions were combined. 20 μ l of 5 M NaCl was added to the combined eluates (500 μ l) and the protein-DNA cross-links were reversed by heating at 65°C for 4 hours. The protein-DNA cross-links of the input samples were also reversed at the same time. The DNA was recovered by phenol-chloroform extraction and ethanol precipitation. The precipitated DNA was pelleted by centrifugation at 12,000 rpm for 10 minutes, air dried and re-suspended in 22 μ l of DNA-grade sterile water. These samples were analysed by PCR using the primers and conditions shown in **Table 2.5**.

A

DNA sequence	Forward primer sequence	Reverse primer sequence	PCR Product size (bp)
1. pGL3- γ 1p34oligo	5'-AGCCGCCGCCTGGGGCGCTTGGGTCGGCCTCGAG -3'	5'-AAC CAG GGC GTA TCT CTT-3'	192
2. pGL3- γ 1p34oligo	5'-AGCCGCCGCCTGGGGCGCTTGGGTCGGCCTCGAG -3'	5'-CTT CTG CCA ACC GAA CGG AC-3'	280

B

Primers	Denature (°C)	Time (seconds)	Anneal (°C)	Time (seconds)	Extension (°C)	Time (seconds)	Analysed after (cycle no):
pGL3- γ 1p34oligo primer pair one	94	30	50	30	72	30	25
	94	30	64.1	30	72	30	25
pGL3- γ 1p34oligo primer pair two	94	30	60	40	72	30	25

Table 2.5 A. Shows the sequences of the forward and reverse primers used to amplify the region of the pGL3- γ 1p34oligo reporter in the transient chip assay and the size of the RT-PCR products. Two different reverse primers were used with the same forward primer in separate PCR reactions. The second reverse primer was designed to try to reduce amplification of non-specific PCR products. **Table 2.5 B** shows the denaturing, annealing and extension temperatures and times for the PCR of the pGL3- γ 1p34oligo reporter for each primer set. PCR products were analysed on a 1.5% agarose gel every 5 cycles after an initial measurement at 25 cycles.

3 THE EFFECT AND MECHANISMS OF ACTION OF PPAR γ LIGANDS IN NEUROBLASTOMA CELLS *IN VITRO*

3.1 Mechanism of action of the natural PPAR γ ligand, 15-deoxy $\Delta^{12,14}$ prostaglandin J₂ in neuroblastoma cells

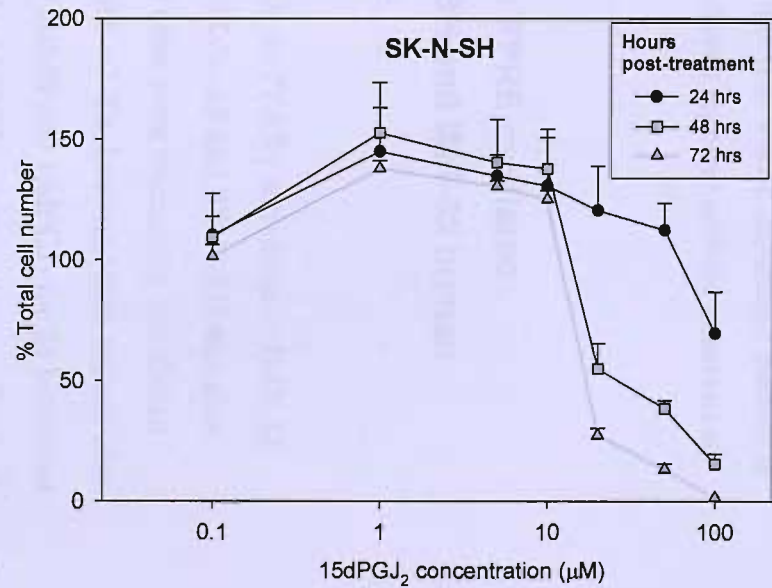
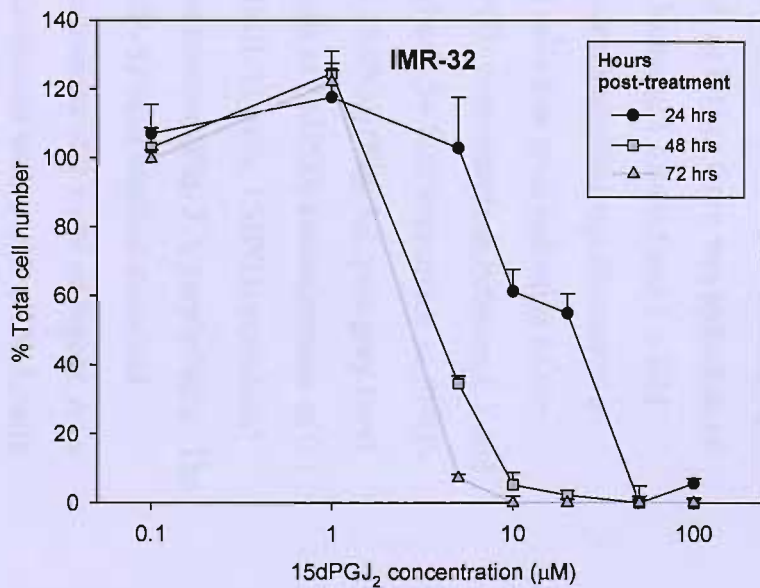
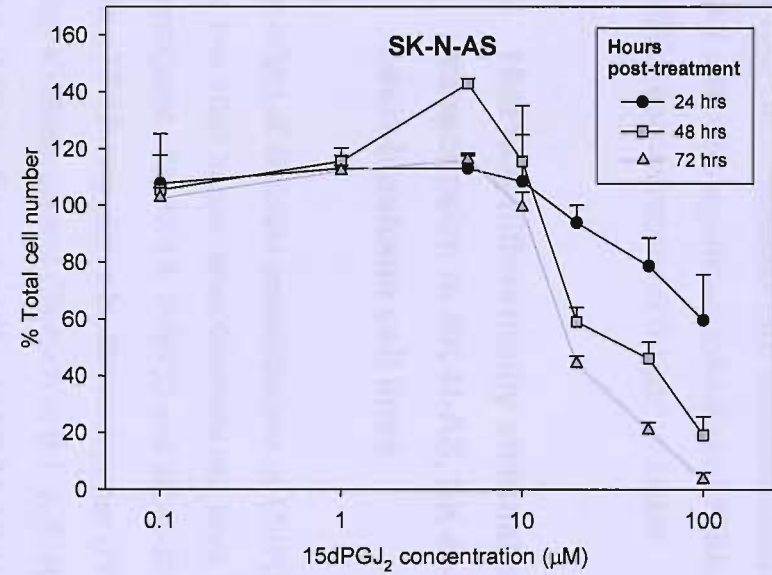
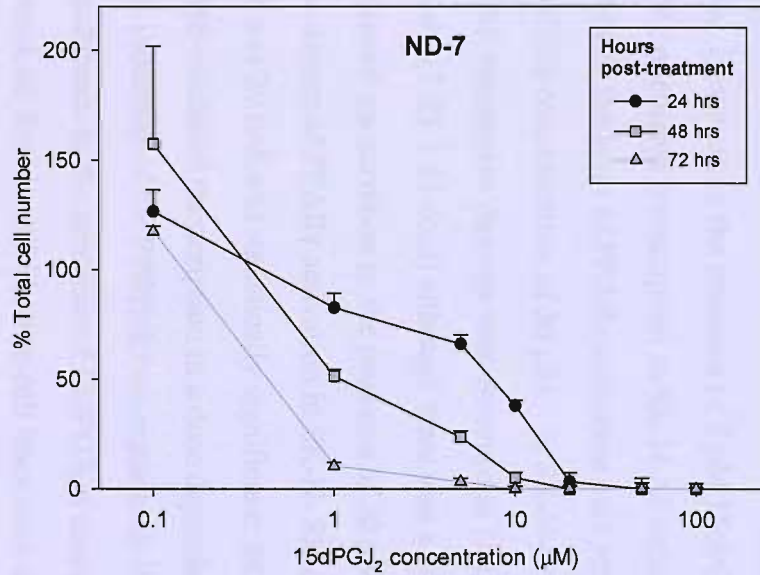
Expression of PPAR γ has been detected in primary tissues and established cell lines originating from a variety of human malignancies[188]. Treatment of breast, prostate, colon, gastric, pancreatic, salivary gland, lung and bladder cancer cell lines with the natural PPAR γ ligand, 15-deoxy $\Delta^{12,14}$ prostaglandin J₂ (15dPGJ₂) has been shown to inhibit their growth *in vitro* [117,189,190,193,196,198,203,205,212,227] [239,301-304]. Similarly, we have tested the effect of this ligand on neuroblastoma cells in culture and have also demonstrated that 15dPGJ₂ can attenuate their rate of proliferation although the concentration of 15dPGJ₂ required to induce this response varied between the neuroblastoma cell lines (**Fig. 3.1**) [228] [305] (and unpublished data). Furthermore, growth inhibition mediated by 15dPGJ₂ in neuroblastoma cells, as in other cancer cell lines, was accompanied by either differentiation or cell death although the cellular response observed appeared to be dependent on the both the ligand concentration and the neuroblastoma cell line. For instance, IMR-32 neuroblastoma cells incubated with 5 μ M 15dPGJ₂ underwent growth arrest accompanied by type II programmed cell death (or autophagy), whereas 20 μ M 15dPGJ₂ stimulated apoptosis. In SK-N-AS and ND-7 neuroblastoma cells treatment with 5 μ M 15dPGJ₂, however, induced differentiation and apoptosis respectively. Although 15dPGJ₂ has been identified as a high affinity ligand for PPAR γ it can also elicit its biological actions by mechanisms independent of its nuclear receptor [20,100,306-311]. It has been previously shown however, by Rodway *et al* in our group that 15dPGJ₂ induced cell death in IMR-32 cells is dependent on PPAR γ transcriptional activity, since transient transfection of PPRE decoy DNA, which competes with endogenous PPRE elements in the promoters of PPAR γ target genes for the activated receptor, inhibited the decrease in cell viability caused by 15dPGJ₂ [228]. This finding is supported by the work of Kim *et al* who demonstrated that 15dPGJ₂ inhibition of growth in SK-N-SH cells was attenuated by the PPAR γ

specific antagonist GW9662[312]. Tumourgenesis is associated with dysfunction of differentiation and apoptosis, therefore, activation of PPAR γ which stimulates these processes could lead to reversal of the malignant phenotype and is a potentially attractive approach to cancer therapy [190,203,209]. Conversely, low concentrations of 15dPGJ₂ can cause cellular proliferation as demonstrated in neuroblastoma, colon cancer, breast cancer and glioma cell lines *in vitro* [189,208,313]. If PPAR γ agonists such as 15dPGJ₂ are to be developed as a treatment for neuroblastoma and other cancers it is critical to understand how PPAR γ can regulate such disparate biological processes. A study by Clay *et al* indicated that the level of PPAR γ activation could influence the biological response to 15dPGJ₂ in breast cancer cells *in vitro* [189]. For example, a 15dPGJ₂ concentration of 1 μ M caused cellular proliferation of the MDA-MB 251 breast cancer cell line and was correlated with low level PPAR γ activation (<5 fold) whereas treatment with 2.5 μ M 15dPGJ₂ caused moderate PPAR γ induction (5-10 fold) and the cell line to undergo growth arrest and differentiation. Incubation of the breast cancer cell line with 10 μ M 15dPGJ₂ stimulated apoptosis and resulted in a high level of PPAR γ activation (>10 fold). Therefore, experiments were carried out to investigate if the degree of PPAR γ activation could also modulate the response of neuroblastoma cells to 15dPGJ₂.

3.2 15dPGJ₂ stimulates PPRE-mediated transcription in the ND-7 murine neuroblastoma cell line

A PPRE driven reporter gene assay was previously used to show stimulation of PPAR γ transcriptional activity in IMR-32 neuroblastoma cells treated with 5 μ M 15dPGJ₂ [228]. Therefore, this approach was extended to evaluate the effect of different concentrations of 15dPGJ₂ on PPRE-mediated transcription in IMR-32 and other neuroblastoma cell lines and to establish whether there is a correlation between the level of PPAR γ activation and the cellular response to this ligand. Firstly, the murine neuroblastoma cell line ND-7 was transiently transfected with a luciferase reporter construct regulated by 3 PPREs upstream of thymidine kinase promoter (PPREx3-TK-Luc).

Fig. 3.1. The effect of the natural PPAR γ ligand 15dPGJ $_2$ on the growth of neuroblastoma cell lines *in vitro*. The neuroblastoma cell lines, ND-7, SK-N-AS, IMR-32 and SK-N-AS were plated out in complete media in 6-well dishes at 4×10^4 cells per well and treated with either a vehicle control (DMSO) or 0.1, 1, 5, 10, 20, 50 and 100 μ M 15dPGJ $_2$ and growth profiles were measured over 72 hours. Two samples were counted in duplicate per treatment per day using a haemocytometer. Data represents the mean percentage of the total cell number, relative to the number of cells in the presence of the vehicle control (DMSO) \pm S.D. These experiments were completed by Dr Karen Lillycrop and Emma Phillips.



The cells were then treated with either a vehicle control (DMSO) or 0.1, 1, 5, 10 and 20 μM 15dPGJ₂ for 24 hours and assayed for luciferase activity. As shown in **Fig. 3.2** 15dPGJ₂ stimulated PPRE-mediated transcription in a dose dependent manner in ND-7 cells with significant induction of PPRE-driven reporter activity observed at 15dPGJ₂ concentrations of 0.1 μM or higher.

3.3 15dPGJ₂ differentially stimulates PPRE-mediated transcription in SK-N-AS, SK-N-SH and IMR-32 human neuroblastoma cell lines

The effect of different concentrations of 15dPGJ₂ on PPAR γ activation in IMR-32 and two other human neuroblastoma cell lines, SK-N-AS and SK-N-SH was also investigated. SK-N-AS, IMR-32 and SK-N-SH cells were transiently transfected with a PPAR responsive luciferase reporter (PPRE-x3-TK-Luc) and then treated with either a vehicle control (DMSO) or 0.1, 1, 5, 10 and 20 μM 15dPGJ₂ for 24 hours and assayed for luciferase activity. In SK-N-AS cells, 15dPGJ₂ at concentrations between 0.1 and 1 μM did not stimulate the PPAR responsive reporter (**Fig. 3.3**, dark grey bars). However, in the presence of 5 μM 15dPGJ₂ or higher there was induction of PPRE-mediated transcription in SK-N-AS cells between 1.47-fold and 3.6-fold although the level of PPAR γ activation only reached statistical significance at a 15dPGJ₂ concentration of 20 μM . In SK-N-SH cells low level induction of the PPAR responsive reporter was observed at 15dPGJ₂ concentrations between 0.1 and 10 μM (1.33-1.61-fold) although there was a higher 3.54-fold stimulation of PPRE-mediated transcription in the presence of 20 μM 15dPGJ₂ (**Fig. 3.3**, pale grey bars). The degree of PPAR γ activation in SK-N-SH cells at 15dPGJ₂ concentrations of 0.1 μM and 20 μM was statistically significant. In IMR-32 cells, 15dPGJ₂ stimulated PPRE-mediated transcription in a dose dependent manner (**Fig. 3.3**, purple bars). The fold induction of the PPRE-driven reporter in IMR-32 cells reached statistical significance in the presence of 15dPGJ₂ at concentrations of 0.1 μM or higher. As a control, all four neuroblastoma cell lines were transfected with a with a TK-*Renilla* reporter plasmid (pRL-TK Vector) which lacks the three upstream PPREs and subsequently treated with the same concentrations of 15dPGJ₂ (0.1-20 μM)

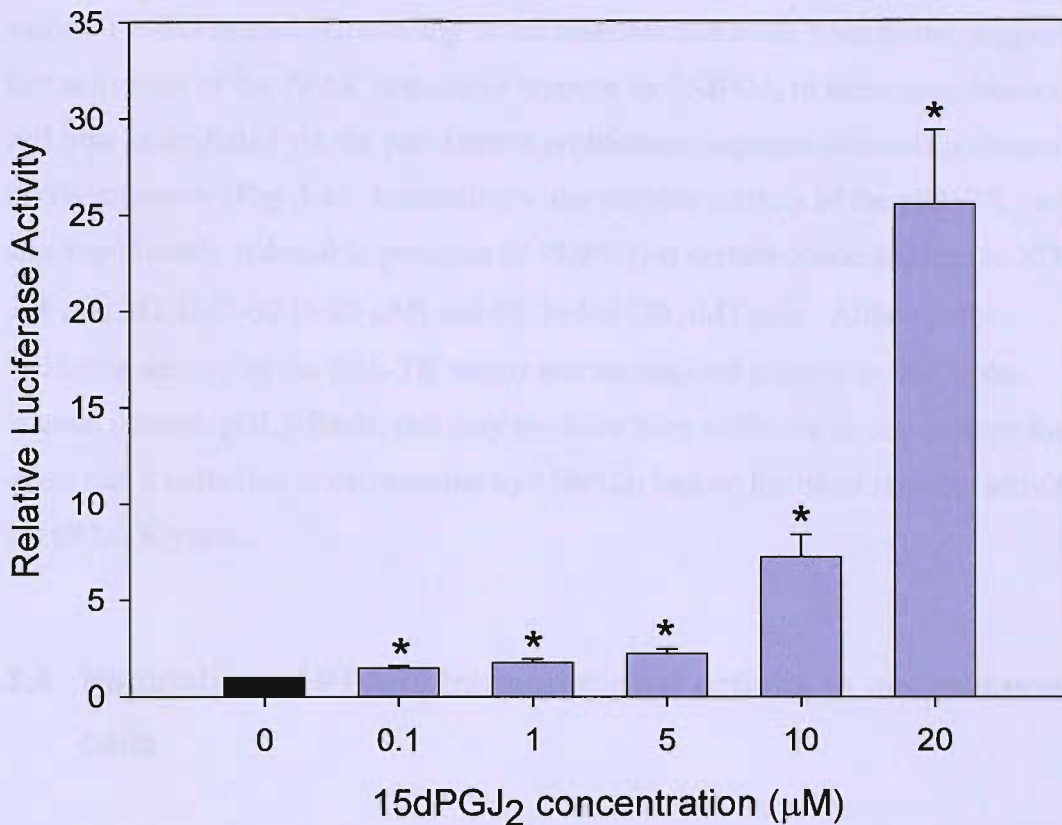


Fig. 3.2. The effect of the natural PPAR γ ligand, 15dPGJ₂ on PPRE-mediated transcription in the murine ND-7 neuroblastoma cell line. ND-7 cells were transiently transfected with 2 μ g of a *Renilla* luciferase reporter construct under the control of three peroxisome proliferator response elements (PPREs) upstream of a thymidine kinase promoter (PPREx3-TK-Luc). Cells were treated with either DMSO (vehicle control) or 0.1, 1, 5, 10 and 20 μ M 15dPGJ₂ for 24 hours then harvested and luciferase activity measured. Data shows the mean relative luciferase activity of the PPREx3-TK-Luc reporter compared with its activity in vehicle DMSO treated ND-7 cells, and represents three independent experiments \pm S.D. The activity of the PPREx3-TK-Luc construct was normalized for transfection efficiency and differences in cell number by co-transfecting ND-7 cells with the firefly luciferase reporter, pGL3-Basic. Statistics were calculated using a Student's *t*-test and showed that compared with DMSO treated ND-7 cells, 15dPGJ₂ caused significant activation of the *Renilla* luciferase reporter driven by a PPRE-regulated promoter at concentrations of 0.1 μ M or higher ($p < 0.05$) (*).

for 24 hours and then assayed for luciferase activity (**Fig. 3.4**). The pRL-TK reporter was not activated in the presence 15dPGJ₂ compared with its luciferase activity in vehicle DMSO treated cells, in any of the neuroblastoma cell lines tested, suggesting that activation of the PPAR responsive reporter by 15dPGJ₂ in these neuroblastoma cell lines is mediated via the peroxisome proliferator response elements upstream of its TK promoter (**Fig. 3.4**). Interestingly, the reporter activity of the pRL-TK vector was significantly reduced in presence of 15dPGJ₂ at certain concentrations in ND-7 (1 μM-20 μM), IMR-32 (5-20 μM) and SK-N-SH (20 μM) cells. Although the luciferase activity of the pRL-TK vector was normalized relative to that of the internal control, pGL3-Basic, this may not have been sufficient to compensate for the effect that a reduction in cell number by 15dPGJ₂ had on the basal reporter activity of the pRL-TK vector.

3.4 Regulation of PPAR γ transcriptional activity in neuroblastoma cells

Since the level of PPAR γ transactivation appeared to influence the biological response of neuroblastoma cells to 15dPGJ₂ further study was warranted to elucidate how PPAR γ transcriptional activity is modulated in neuroblastoma and other human malignancies, although evidence for several different potential mechanisms is emerging. For instance, the A/B domain of PPAR γ contains a consensus mitogen activated protein kinase (MAPK) site, which when phosphorylated by either ERK2 (extracellular-signal regulated kinase 2) or JNK (c-Jun NH₂-terminal kinase) attenuated both basal and ligand dependent gene transcription [67,74]. Indeed, induction of PPRE-mediated transcription by 15dPGJ₂ in IMR-32 neuroblastoma cells was enhanced by co-incubation with the MAPK inhibitor PD98059, suggesting that the responsiveness of neuroblastoma cells to PPAR γ ligands could in part correlate with MAPK activity in the cell [228]. PPAR γ -mediated transcription may also be affected by a mutation in the PPAR γ receptor or variation in the expression of RXR α , a critical PPAR γ co-activator or PPAR β/δ [33,232,314,315]. To date the direct targets of PPAR γ which mediate the effect PPAR γ ligands in cancer cells *in vivo* are unknown.

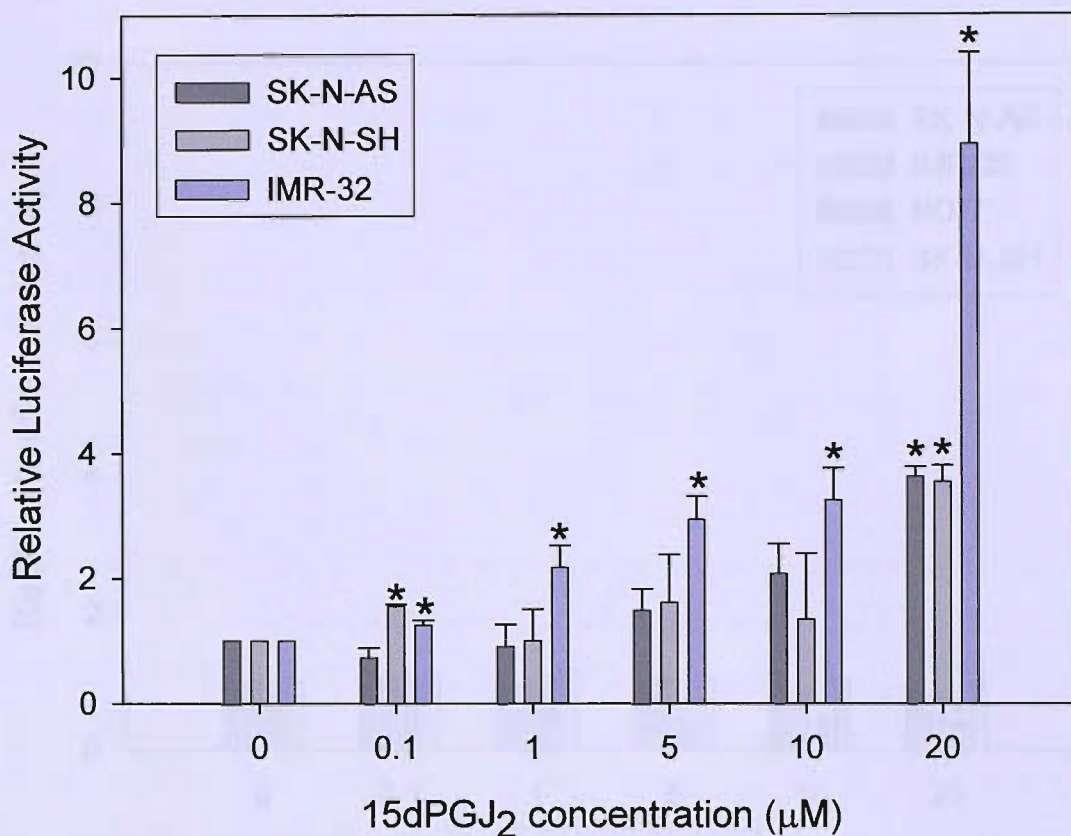


Fig. 3.3. The effect of the natural PPAR γ ligand, 15dPGJ₂ on PPRE-mediated transcription in human neuroblastoma cell lines. SK-N-AS, SK-N-SH and IMR-32 cells were transiently transfected with 2 μ g of a *Renilla* luciferase reporter construct under the control of three peroxisome proliferator response elements (PPREs) upstream of a thymidine kinase promoter (PPREx3-TK-Luc). Cells were treated with either DMSO (vehicle control) or 0.1, 1, 5, 10 and 20 μ M 15dPGJ₂ for 24 hours then harvested and luciferase activity measured. Data shows the mean relative luciferase activity of the PPREx3-TK-Luc reporter compared with its activity in vehicle DMSO treated cells, and represents three independent experiments \pm S.D. The activity of the PPRE-x3-TK-Luc construct was normalized for transfection efficiency and differences in cell number by co-transfecting the cell lines with the firefly luciferase reporter, pGL3-Basic. Statistics were calculated using a Student's *t*-test and showed that compared with DMSO treated cells, 15dPGJ₂ caused significant induction of *Renilla* luciferase reporter activity driven by a PPRE-regulated promoter, at a concentration of 20 μ M in SK-N-AS cells, at concentrations of 0.1 and 20 μ M in SK-N-SH cells and at concentrations of 0.1 μ M or higher in IMR-32 cells ($p < 0.05$) (*).

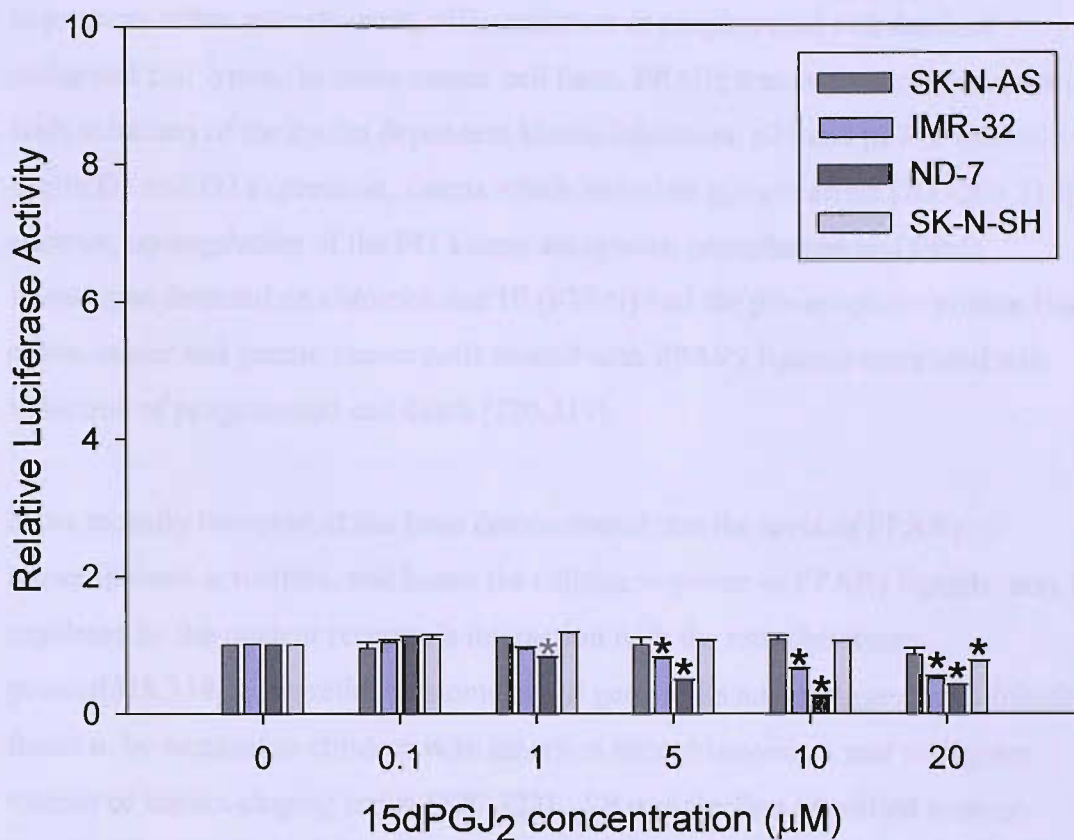


Fig. 3.4. The effect of the natural PPAR γ ligand, 15dPGJ₂ on the reporter activity of a TK-*Renilla* plasmid which lacks PPRES in neuroblastoma cells. SK-N-AS, IMR-32, ND-7 and SK-N-SH cells were transiently transfected with 2 μ g of a *Renilla* luciferase reporter construct under the control of a thymidine kinase promoter but which lacks 3 upstream PPRES (pRL-TK vector). Cells were treated with either DMSO (vehicle control) or 0.1, 1, 5, 10 and 20 μ M 15dPGJ₂ for 24 hours then harvested and luciferase activity measured. Data shows mean relative luciferase activity of the pRL-TK reporter, compared with its activity in DMSO treated cells, of three independent luminescence readings \pm S.D. The activity of the pRL-TK construct was normalized for transfection efficiency and differences in cell number by co-transfecting the cell lines with the firefly luciferase reporter, pGL3-Basic. Statistics were calculated using a Student's *t*-test and showed that compared with DMSO treated cells, the luciferase activity of the pRL-TK reporter was significantly reduced in the presence of 15dPGJ₂ at concentrations of 1 μ M or higher in ND-7 cells, at concentrations of 5 μ M or higher in IMR-32 cells and at a concentration of 20 μ M in SK-N-SH cells ($p < 0.05$) (*).

Detection of changes in gene expression in response to PPAR γ ligands *in vitro* however, has provided insight in to some of the pathways that PPAR γ might regulate to promote either growth arrest, differentiation or programmed cell death of malignant cell types. In some cancer cell lines, PPAR γ transactivation was associated with induction of the cyclin dependent kinase inhibitors, p21 and p27 or inhibition of cyclin D1 and D2 expression, events which stimulate growth arrest [200-203,316]. In contrast, up-regulation of the PI3 kinase antagonist, phosphatase and tensin homologue detected on chromosome 10 (PTEN) and the pro-apoptotic protein Bad in colon cancer and gastric cancer cells treated with PPAR γ ligands correlated with induction of programmed cell death [220,317].

More recently however, it has been demonstrated that the level of PPAR γ transcriptional activation, and hence the cellular response to PPAR γ ligands, may be regulated by the nuclear receptor's interaction with the retinoblastoma protein[318,319]. The retinoblastoma or *RB* gene as its name suggests was initially found to be mutated in children with inherited retinoblastoma, a rare malignant tumour of the developing retina [320-322]. *RB* was the first identified tumour suppressor gene and the pRb protein it encodes is now known to be a critical regulator of the cell cycle, differentiation and apoptosis [321,323-326]. Two other pRb family members have since been discovered called p107 and p130 which were named after their apparent molecular weights [327-332]. p107 and p130 are structurally homologous to pRb and studies with mice deficient in one or more pRb family members have shown that they have both distinct and redundant cellular functions *in vivo* [327,328,330].

pRb is a large 928-amino acid residue nuclear protein, which like other members of the pRb family, is regulated by cell cycle dependent phosphorylation[333]. pRb has three domains, the N- terminus, an A/B box domain and the C-terminus or C-domain [320,333-335]. The crystal structure of pRb shows that there is an extensive interface between the A box and B box which acts as a scaffold to ensure stable folding of the B box, which together the A box forms a "pocket" which can interact with a number of proteins including E2F transcription factors [320,333,334]. For instance, active un-phosphorylated pRb forms a complex with E2F1, 2 or 3 at the cyclin E promoter *in vivo* which attenuates cyclin E transcription and therefore inhibits S phase entry

and cell cycle progression [321,329,336,337]. In response to mitogenic signals, cyclin D acting with cyclin dependent kinase 6 (CDK6) phosphorylates pRb which disrupts its interaction with E2F transcription factors allowing transversal from G₁ to S-phase [321,324,333]. Induction of the cyclin D/CDK6 complex is however antagonized by the cyclin dependent kinase inhibitor p16^{INK4} [329]. Several mechanisms of transcriptional repression by pRb family members have been proposed including the recruitment of group I histone deacetylases, HDAC1, 2 and 3 to the promoters of target genes which mediate deacetylation of histones resulting in chromatin condensation and inhibition of transcription [321,329,333,336,338,339].

For example, PPAR γ , pRb and HDAC3 were shown to bind *in vivo* to a region of the lipoprotein lipase gene promoter which contained the consensus PPRE [319].

Formation of the PPAR γ -pRb-HDAC3 complex was dependent on ligand binding by PPAR γ and an interaction between the pRb A/B pocket and C-domain and the E/F domain of PPAR γ [319]. In addition, incubation of pRb expressing mouse embryo fibroblasts (MEFs) (Rb^{+/+}) with the HDAC inhibitor, trichostatin A (TSA) increased PPRE-mediated transcription in the presence of rosiglitazone, indicating that pRb does mediate repression of PPAR γ transactivation by HDAC recruitment [318,319]. Furthermore, rosiglitazone mediated adipogenesis was more pronounced in pRb null MEFs (Rb^{-/-}) compared with Rb^{+/+} MEFs [319]. Therefore, while hypophosphorylated pRb does participate in the cell cycle exit required for the terminal differentiation of adipocytes, it is postulated that pRb is phosphorylated and thus inactive when PPAR γ needs to stimulate the expression of target genes, such as lipoprotein lipase required for adipogenesis [319].

pRb was also demonstrated to regulate the cellular response of osteosarcoma cells to the PPAR γ ligand rosiglitazone [318]. Treatment of Rb expressing osteosarcoma cells (U2OS) with rosiglitazone stimulated growth arrest, whereas in Rb null osteosarcoma cells (SaOS) cells apoptosis was observed [318]. The growth arrest and apoptosis induced by rosiglitazone was abrogated in cells in which PPAR γ was inactivated by siRNA indicating that the effects of rosiglitazone were mediated by PPAR γ in these cell lines [318]. The pRb status of a cancer cell is influenced by several factors (**Fig. 3.5**). Loss of pRb due to deletion or mutation of both *RB* alleles

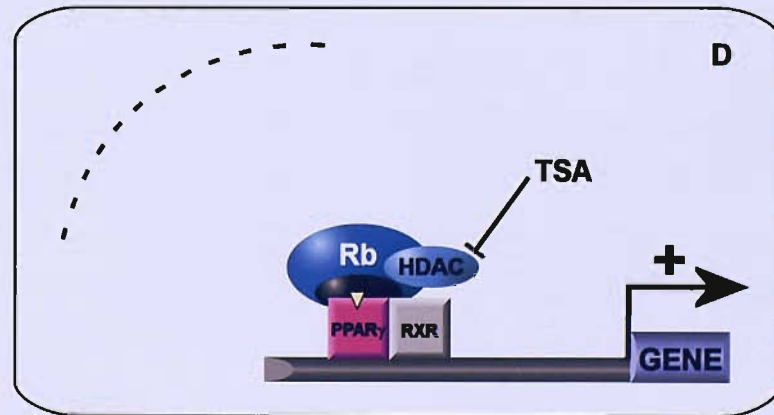
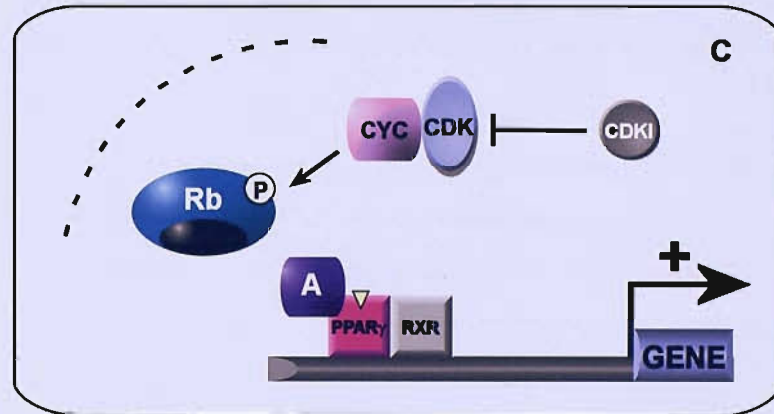
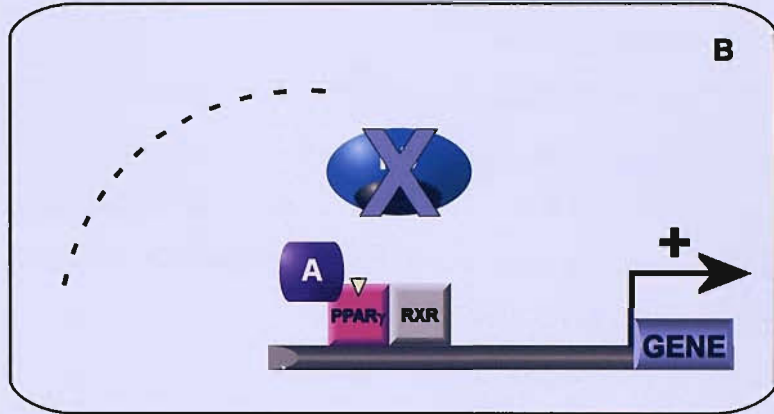
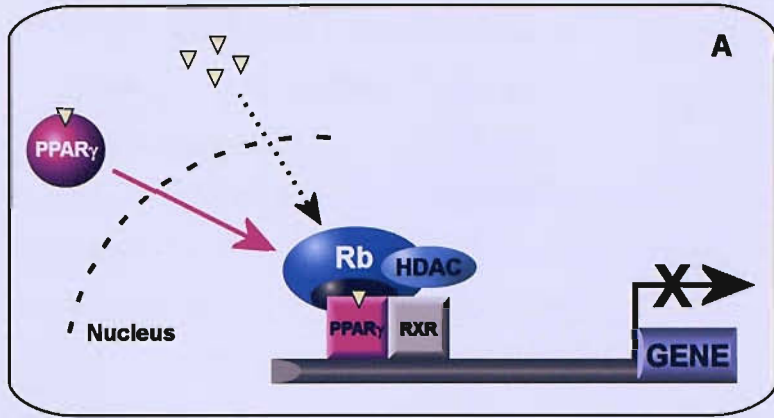
Fig. 3.5. Potential mechanism of pRb transcriptional repression of PPAR γ and factors which modulate the pRb status of tumour cells.

A. pRb has been shown to interact with PPAR γ via its pocket domain (represented by the black circle) and inhibit PPRE-mediated transcription through recruitment of a HDAC or HDAC containing complex. Formation of the PPAR γ -pRb-HDAC complex appears to be dependent on ligand binding by PPAR γ . This may be because ligand binding promotes a conformational change required for PPAR γ nuclear localization. Alternatively if PPAR γ is constitutively localized in the nucleus ligand binding may induce a more subtle change in receptor conformation which allows pRb association.

B. Some specific cancers, such as retinoblastoma or osteosarcoma are initiated by deletion or mutation of both *RB* alleles which leads to loss of pRb expression. In the absence of pRb, if PPAR γ is functional it can recruit a complex of co-activators (labeled A) which promotes gene transcription. PPAR γ activation in the absence of pRb could stimulate apoptosis potentially abrogating propagation of cells in which pRb is deregulated. However, if the PPAR γ pathway is also mutated or compromised this may lead to tumourgenesis.

C. Phosphorylated pRb can not interact with transcription factors such as PPAR γ . pRb is phosphorylated by cyclin dependent kinases (CDK) which are inhibited by cyclin dependent kinase inhibitors (CDKI). Over-expression of cyclins (CYC) and CDKs or mutation of CDKIs would lead to an increase in hyperphosphorylated pRb and hence promote PPRE-mediated transcription. For instance, the level of cyclin D1 may indirectly modulate the level of PPAR γ transcriptional activity in neuroblastoma through pRb phosphorylation.

D. The inhibitory effect of pRb on PPAR γ -mediated transcription is relieved by treatment of cells with the HDAC inhibitor, TSA. If pRb does modulate PPAR γ in neuroblastoma, co-treatment of these tumour cells with a HDAC inhibitor might augment the growth inhibitory effects of PPAR γ ligands by stimulating PPRE-mediated transcription.



is observed in some human carcinomas; however pRb can also be inactivated by specific mutations of the pocket domain, disruption of *p16^{INK4}* or over expression of D type cyclins or CDK6 [329,340]. Elevated cyclin D1 expression has been detected in both primary neuroblastoma and cell lines [341]. It is therefore plausible that the degree of cyclin D1 expression could in part govern the amount of hyperphosphorylated pRb which in turn modulates the level PPAR γ activation and hence the cellular response in neuroblastoma cells to PPAR γ ligands. In some instances loss of Rb function which leads to release of free E2F activates ARF (the alternative reading frame protein encoded by the INK4A locus) which then triggers the p53 apoptotic pathway. This may act as a mechanism to prevent propagation of cells in which the pRb pathway is deregulated [320,323]. It could therefore be speculated that induction of apoptosis by PPAR γ ligands in cancer cells with inactivated pRb might serve a similar function. Unlike, pRb, p107 and p130 are not classified as tumour suppressors although p130 in particular has been found to be mutated in a number of cancers [331]. However, since p130 and p107 can actively repress E2F target gene transcription by similar mechanisms to pRb, p107 and p130 could also potentially modulate PPAR γ activity in neuroblastoma cells. Therefore the effect of retinoblastoma family members of PPAR γ mediated transcription in neuroblastoma cells was investigated.

ND-7 cells were co-transfected with a PPAR responsive reporter (PPRE-TK-Luc) and 2 μ g of an expression plasmid encoding either pRb, p107, p130 or an Rb mutant which lacks the pocket domain or an empty expression plasmid (pcDNA3.1). The cells were then treated with 5 μ M 15dPGJ₂ or a vehicle control (DMSO) for 24 hours and assayed for luciferase activity. In the presence of the empty expression plasmid, 15dPGJ₂ induced a 2-fold activation of the PPAR responsive reporter construct relative to cells treated with the vehicle control (DMSO) (**Fig. 3.6**). In the presence of transfected Rb, p107 or p130 however, the ability of 15dPGJ₂ to stimulate PPAR reporter activity was attenuated (**Fig. 3.6**). Furthermore, in ND-7 cells transfected with pRb, PPRE-mediated transcription in the presence of 15dPGJ₂ was significantly repressed below the basal level observed in vehicle treated cells. Conversely, expression of the Rb mutant which lacks the pocket domain did not have any effect on 15dPGJ₂ induced PPAR γ activation, suggesting that this motif is required for Rb transcriptional inhibition of PPAR γ in this cell type. To examine whether the ability

of pRb to attenuate PPAR γ transactivation in neuroblastoma cells was dependent upon HDAC recruitment, ND-7 cells were again co-transfected with a PPAR responsive reporter and an expression plasmid encoding pRb or an empty expression plasmid. Cells were then treated with 5 μ M 15dPGJ₂ or a vehicle control (DMSO) in the presence or absence of the potent HDAC inhibitor TSA for 24 hours and then harvested and assayed for luciferase activity. As observed before, in the presence of transfected pRb, 5 μ M 15dPGJ₂ did not activate the PPAR responsive reporter. In TSA treated cells however, 15dPGJ₂ in the presence of pRb stimulated PPRE-mediated transcription (3.2-fold) (Fig. 3.7). This result suggests that TSA blocked the repressive effect of Rb on PPAR γ -mediated transcription, which implies that regulation of PPAR γ activity by pRb in this cell line could be dependent on an interaction with a HDAC.

3.5 The effect of the HDAC inhibitor, Trichostatin A on SK-N-AS neuroblastoma cell growth and viability

These initial pRb transfection experiments in ND-7 cells, support the model proposed by Fajas *et al* in which active hypophosphorylated pRb, in the presence of either an endogenous or exogenous PPAR γ ligand, forms a repressive complex with PPAR γ and a HDAC which attenuates PPRE-mediated transcription [318,319]. As in osteosarcoma cells, depending on the pRb status of the neuroblastoma cell, the level PPAR γ activation mediated by 15dPGJ₂ may be lower as a result of inhibition by pRb leading to growth arrest but not apoptosis. Co-treatment of neuroblastoma cells with a HDAC inhibitor however, could augment the growth inhibitory effect of a PPAR γ agonist by relieving the repressive effect of pRb on PPAR γ , enhancing PPRE-mediated transcription and directly stimulating the expression of pro-apoptotic genes such as Bax [200,318]. Numerous studies have demonstrated that HDAC inhibitors promote growth arrest, differentiation and programmed cell death of cancer cells *in vitro* [342-345]. *In vivo* as well as inhibiting tumour growth, HDAC inhibitors also act to prevent invasion, angiogenesis and metastasis [343]. These cellular processes are abrogated by increased HDAC activity that is frequently observed in human carcinomas [342]. Originally acetylation was believed to stimulate gene transcription by disrupting the interaction of histones with DNA leading to a less condensed

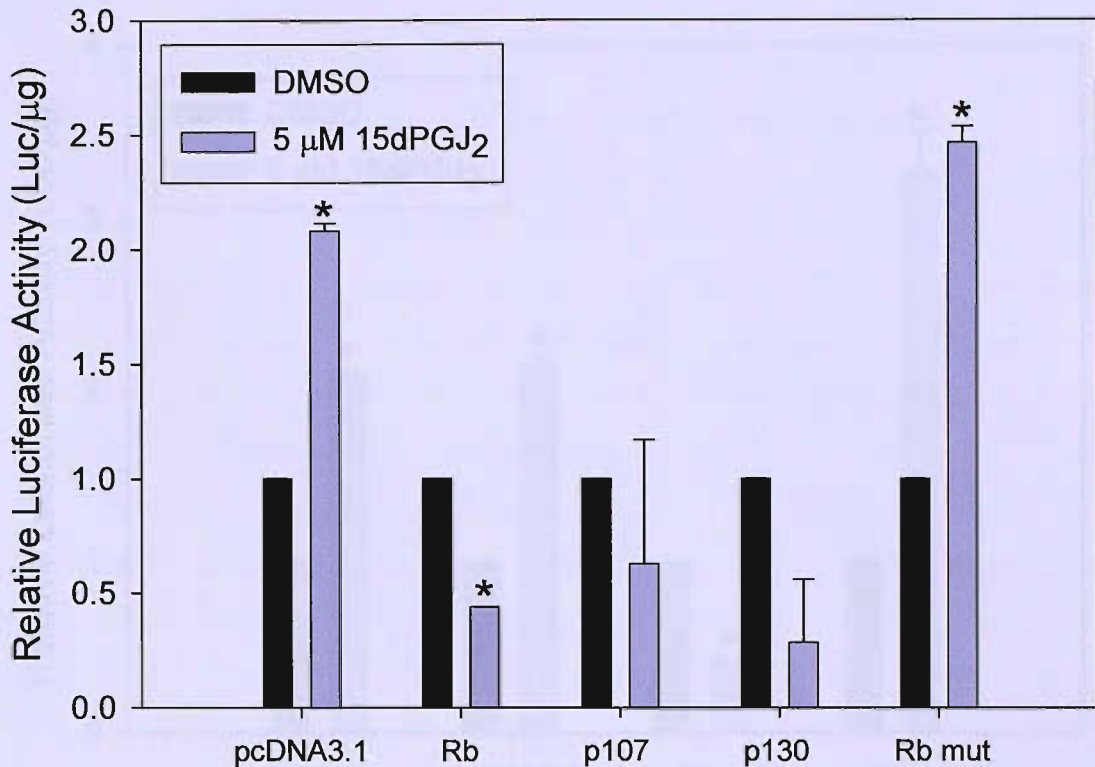


Fig. 3.6. The effect of Rb family members on 15dPGJ₂ induced PPAR γ activation in neuroblastoma cells. ND-7 cells were co-transfected with 2 μ g of a PPAR responsive reporter (PPREx3-tk-Luc) and an expression plasmid encoding either pRb, p107, p130 or an Rb mutant which lacks the pocket domain, or an empty expression vector control (pcDNA 3.1) (2 μ g). The cells were subsequently treated with either a vehicle control (DMSO) or 5 μ M 15dPGJ₂ for 24 hours then harvested and luciferase activity measured. Data shows the relative mean luciferase activity (per μ g of protein) of the PPRE-regulated *Renilla* reporter relative to its activity in vehicle DMSO treated cells and represents two independent experiments \pm S.D. Statistics were calculated using a Student's *t*-test and showed that compared with vehicle DMSO treated cells 15dPGJ₂ caused a significant induction of PPRE-mediated transcription in the presence of the empty expression vector control and the expression plasmid encoding the pRb mutant ($p < 0.05$) (*). In contrast, reporter activity of the PPREx3-TK-Luc construct in 15dPGJ₂ treated cells in the presence of the pRb expression plasmid was significantly attenuated ($p < 0.05$) (*).

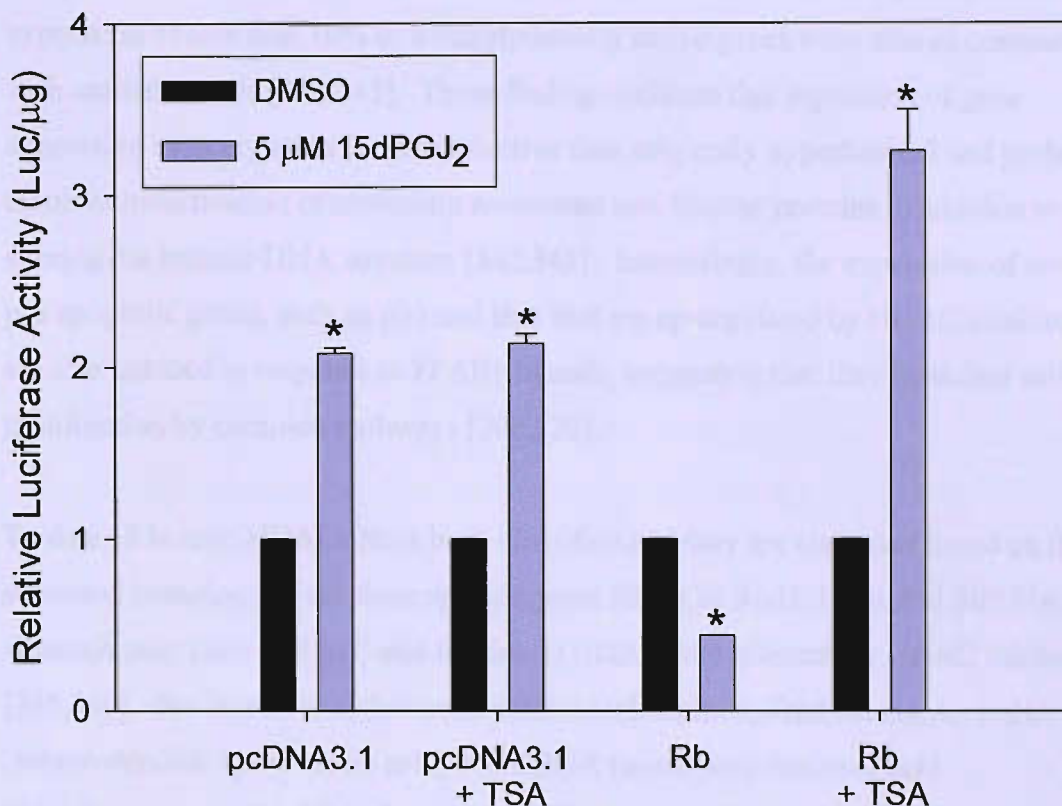


Fig. 3.7. The effect of the histone deacetylase inhibitor, Trichostatin A (TSA) on repression of the transcriptional activity of PPAR γ by the retinoblastoma protein in neuroblastoma cells. ND-7 cells were co-transfected with 2 μ g of a PPAR responsive reporter construct (PPRE-TK-Luc) and an expression plasmid containing Rb or an empty expression vector control (2 μ g). The cells were treated with DMSO (vehicle control) or 5 μ M 15dPGJ₂ either alone in combination with TSA (50 ng per ml = 1.65×10^{-7} M) for 24 hours and then harvested and luciferase activity measured. Data shows the relative mean luciferase activity (per μ g of protein) of the PPRE-regulated *Renilla* reporter relative to its activity in vehicle DMSO treated cells either in the presence or absence of TSA and represents two independent experiments \pm S.D. Statistics were calculated using a Student's *t*-test and showed that compared with vehicle DMSO treated cells 15dPGJ₂ either alone or in the presence of TSA, caused a significant induction of PPRE-mediated transcription in the presence of the empty expression vector control ($p < 0.05$) (*). As observed previously, reporter activity of the PPREx3-TK-Luc construct in 15dPGJ₂ treated cells in the presence of the pRb expression plasmid was significantly attenuated ($p < 0.05$) (*). The luciferase activity of PPREx3-TL-Luc construct in ND-7 cells co-transfected with pRb was however significantly stimulated in the presence of TSA ($p < 0.05$) (*).

chromatin which was more accessible to transcription factors. However, microarray analysis of cell lines following treatment with HDAC inhibitors has shown that the expression of less than 10% of transcriptionally active genes were altered compared with untreated cells [342,345]. These findings indicate that regulation of gene expression by acetylation is more selective than originally hypothesized and probably involves modification of chromatin associated non-histone proteins in addition to altering the histone-DNA structure [342,345]. Interestingly, the expression of several pro-apoptotic genes, such as p53 and Bax that are up-regulated by HDAC inhibitors are also induced in response to PPAR γ ligands, suggesting that they modulate cell proliferation by common pathways [200,220].

To date 18 human HDACs have been identified and they are classified based on their structural homology to the three specific yeast HDACs; Rpd3, Hda1 and Sir2/Hst, although only class I (Rpd3) and II (Hda 1) HDACs are affected by HDAC inhibitors [345,346]. For instance, hydroxamic acids which include, Trichostatin A, SAHA (suberoylanilide hydroxamic acid) and CBHA (m-carboxycinnamic acid bishydroxamic acid) inhibit class I and II HDACs by chelating the active site zinc which is essential for their enzymatic activity [342,345-347]. Several phase I and II clinical trials of HDAC inhibitors, including those of the TSA class, are in progress or have been completed in patients with advanced cancer [348-350]. For instance, either intravenous or oral administration of SAHA lead to clinical improvement in renal cell carcinoma, thyroid carcinoma and B and T cell lymphoma patients with responses ranging from complete regression to prolonged disease stabilization [348-350]. These encouraging results have prompted the development of second generation HDAC inhibitors based on SAHA, such as NVP-LAQ824 with enhanced stability and improved methods of HDAC inhibitor delivery to tumours [342,351,352].

Although HDAC inhibitors are well tolerated by patients and show promise as anti-cancer therapy, it is predicted that their efficacy will be maximized by combining them with other therapeutic agents [342,353,354]. For example the pretreatment or co-administration of HDAC inhibitors with nuclear receptor ligands, heat shock protein

antagonists, proteasome inhibitors and DNA methylating agents has been shown to either additively or synergistically enhance the apoptosis of cancer cells *in vitro* and in mouse tumour models [342]. Several types of HDAC inhibitor including the short-chain fatty acid, sodium butyrate, the benzamide derivative MS-27-275, the TSA/4-phenylbutyrate hybrid BL1521 and the hydroxamic acid CBHA have been shown to attenuate the growth of neuroblastoma cells *in vitro* [354-361]. However, the reduction in tumour volume, caused by treatment with a low dose of CBHA (50mg/kg of mouse) and the retinoic acid receptor ligand, all trans-retinoic acid, in mice implanted with human neuroblastoma xenographs, was synergistic compared with the sum of the effects of the two agents administered separately [362]. Furthermore the growth inhibition observed when lower doses of CBHA were combined with all trans-retinoic acid was similar to that achieved with the maximum dose of CBHA, but with out the side effects of mild weight loss and skin toxicity [362]. Since the retinoic acid receptor (RAR) has been found in complex with a HDAC, it is plausible that the synergistic effect of CBHA and all trans-retinoic acid is the result of HDAC inhibition enhancing the expression of RAR target genes in the presence of ligand [354,362].

Therefore, to determine if HDAC inhibitors might similarly potentiate the growth inhibitory action of 15dPGJ₂, the effect of Trichostatin A on SK-N-AS neuroblastoma cell growth was investigated. This cell line was chosen because it was previously shown to be less responsive to 15dPGJ₂, requiring higher concentrations of ligand to induce growth inhibition compared with IMR-32 and ND-7 cells. SK-N-AS cells were plated out at 4×10^4 cells per well in 6-well dishes and treated with either vehicle control (DMSO) or 10, 50, 100, 200 or 400 ng of TSA per ml of complete media and the growth and viability of the cells was then monitored over 72 hours. These TSA concentrations were initially tested since it had already been demonstrated that they inhibited histone acetylase activity and promoted histone acetylation in a mouse mammary gland tumour cell line *in vitro* [363]. As shown in **Fig. 3.8**, TSA at concentrations of 50 ng/ml or higher caused significant growth inhibition of SK-N-AS cells 24 hours post-treatment.

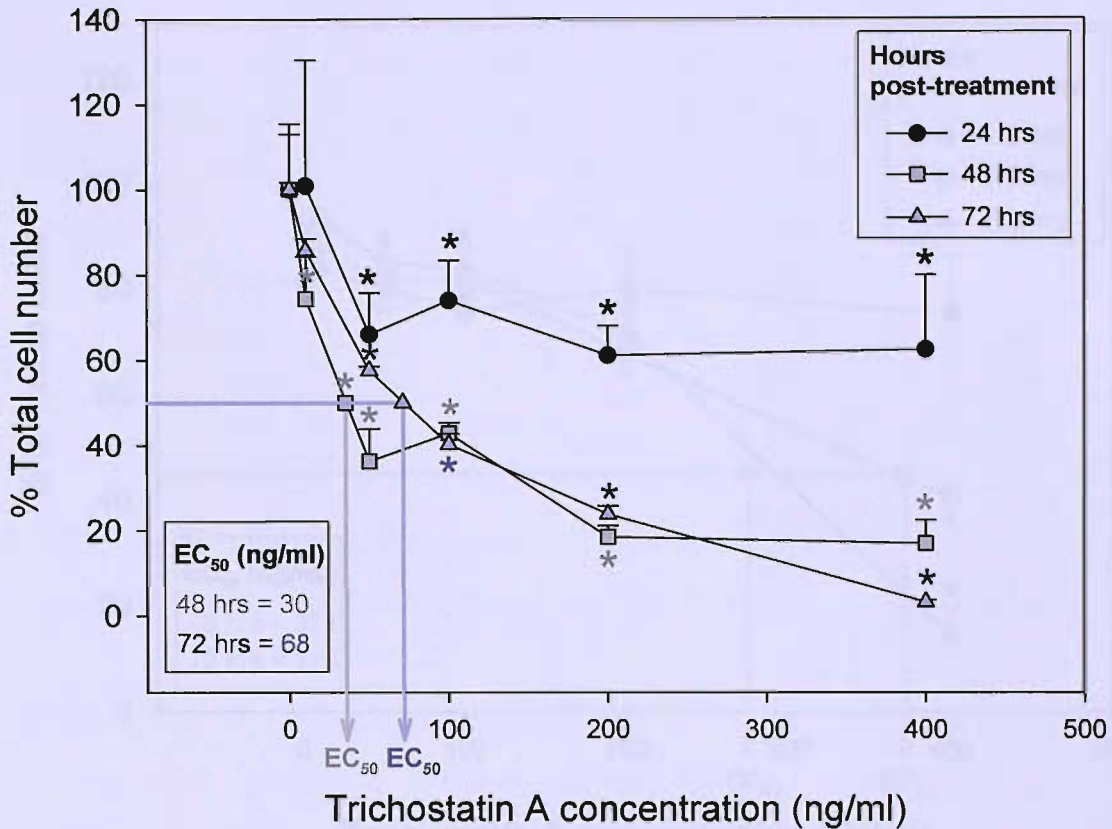


Fig. 3.8. The effect of the HDAC inhibitor, Trichostatin A (TSA) on the cell growth of SK-N-AS neuroblastoma cells. SK-N-AS were plated out in 6-well dishes at 4×10^4 cells per well and treated with either a vehicle control (DMSO) or increasing concentrations of TSA (10-400 ng/ml of complete media) and the effect on cell growth was measured over 72 hours. Two samples were counted in duplicate per treatment using a haemocytometer. Data represents the mean percentage of the total cell number, relative to the number of cells in the presence of the vehicle control (DMSO) \pm S.D. of four separate counts. Statistics were calculated using a Student's *t*-test and showed that compared with DMSO treated cells, TSA at concentrations of 50 ng/ml or higher caused significant inhibition of SK-N-AS cells growth 24 hours post-treatment ($p < 0.05$) (*), whereas the decrease in cell number observed at a TSA concentration of 10 ng/ml only reached statistical significance at 48 hours ($p < 0.05$)(*) but not at 24 or 72 hours ($p < 0.05$)(*). The TSA concentration required to induce 50% growth inhibition of SK-N-AS cells (EC_{50}) 48 and 72 hours following treatment is indicated on the graph.

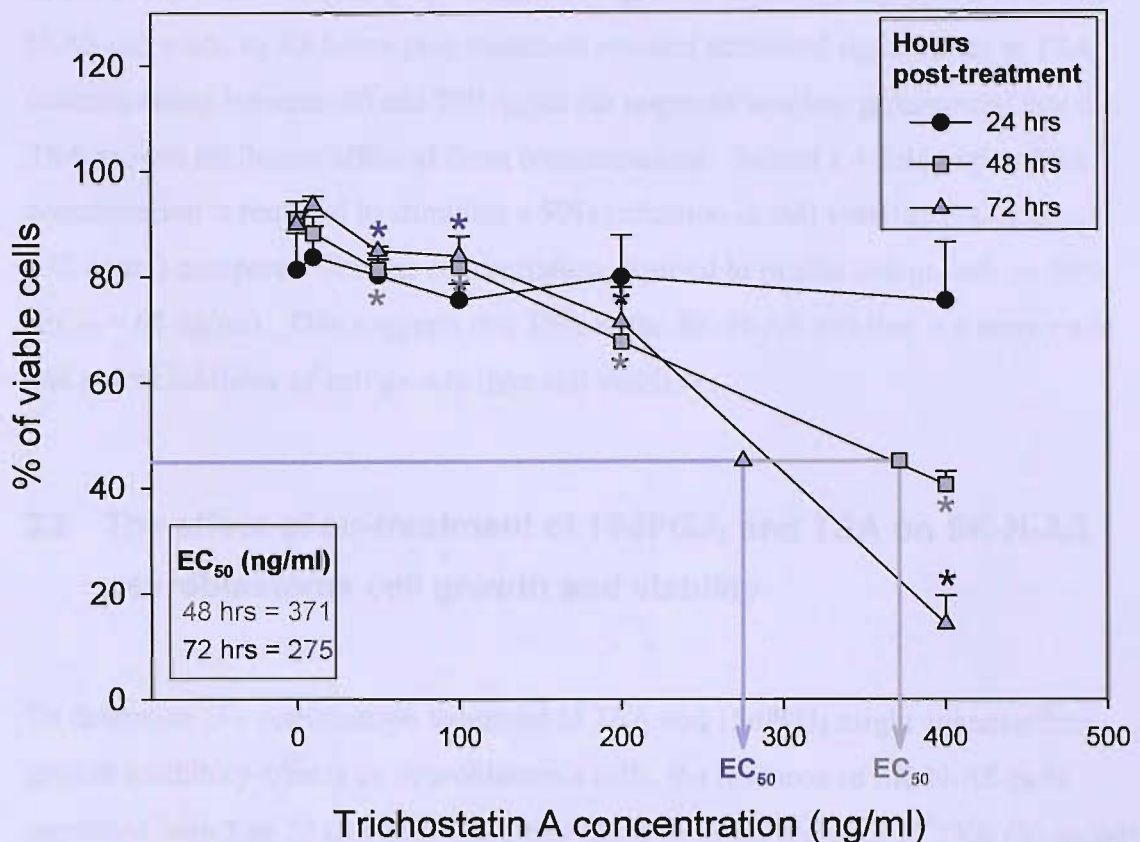


Fig. 3.9. The effect of the HDAC inhibitor, Trichostatin A (TSA) on the viability of SK-N-AS neuroblastoma cells. SK-N-AS neuroblastoma cells were plated out in complete media in 6-well dishes at 4×10^4 cells per well and treated with a vehicle control (DMSO) or increasing concentrations of TSA (10-400 ng/ml of complete media) and cell viability was monitored over 72 hours. The proportion of viable cells was determined by trypan blue staining. Two samples were counted in duplicate per treatment per day using a haemocytometer. Data are expressed as the mean % of viable cells (trypan blue negative) relative to the total number of cells counted per well and represents the mean of four separate counts \pm S.D. Statistics were calculated using a Student's *t*-test and showed that TSA at concentrations of 50 ng/ml or higher caused a significant decrease in SK-N-AS cell viability 48 hours ($p < 0.05$) (*) and 72 hours ($p < 0.05$) (*) post-treatment. The TSA concentration required to cause a 50% reduction in the number of viable SK-N-AS cells (EC_{50} viability) 48 and 72 hours following treatment is indicated on the graph.

In contrast, the same concentrations of TSA only significantly attenuated the viability of SK-N-AS cells 48 hours post-treatment (**Fig. 3.9**). Although the decrease in SK-N-AS cell viability 48 hours post-treatment reached statistical significance at TSA concentrations between 50 and 200 ng/ml the response was less pronounced than the TSA growth inhibitory effect at these concentrations. Indeed a 4-fold higher TSA concentration is required to stimulate a 50% reduction in cell viability ($EC_{50\text{viability}} = 275$ ng/ml) compared with the concentration required to inhibit cell growth by 50% ($EC_{50} = 68$ ng/ml). This suggests that TSA in the SK-N-AS cell line is a more rapid and potent inhibitor of cell growth than cell viability.

3.6 The effect of co-treatment of 15dPGJ₂ and TSA on SK-N-AS neuroblastoma cell growth and viability

To determine if a combination treatment of TSA and 15dPGJ₂ might enhance their growth inhibitory effects on neuroblastoma cells, the response of SK-N-AS cells incubated with 5 or 20 μ M 15dPGJ₂ either alone or in the presence of TSA (50 ng/ml) was examined over 72 hours (**Fig. 3.10** and **Fig. 3.11**). This TSA concentration was chosen since its effect on cell growth and viability was at least 50% less than the maximum response. It would therefore be possible to observe if the combination of TSA and 5 or 20 μ M 15dPGJ₂ had an additive or synergistic effect on the growth and viability of SK-N-AS cells respectively. SK-N-AS cells were administered with a low (5 μ M) and high (20 μ M) dose of 15dPGJ₂, to investigate if a low concentration of 15dPGJ₂ when combined with a HDAC inhibitor could result in growth inhibition comparable to that achieved at the higher dose of 15dPGJ₂ in this cell line. The interaction of these two agents was assessed statistically using the same method as Rashid *et al* [364]. The mean observed combined effect of 15dPGJ₂ and TSA was compared to the sum of the individual effects (predicted effect) using a Student's *t*-test. The effect of co-treatment of 15dPGJ₂ and TSA was classified as synergistic when the observed experimental value was significantly greater than the predicted value (**Table 3.1**). Interestingly, although the growth inhibition of SK-N-AS cells achieved by combined treatment of TSA with either 5 or 20 μ M 15dPGJ₂ was greater than the response of either agent alone the effect was only additive since the observed

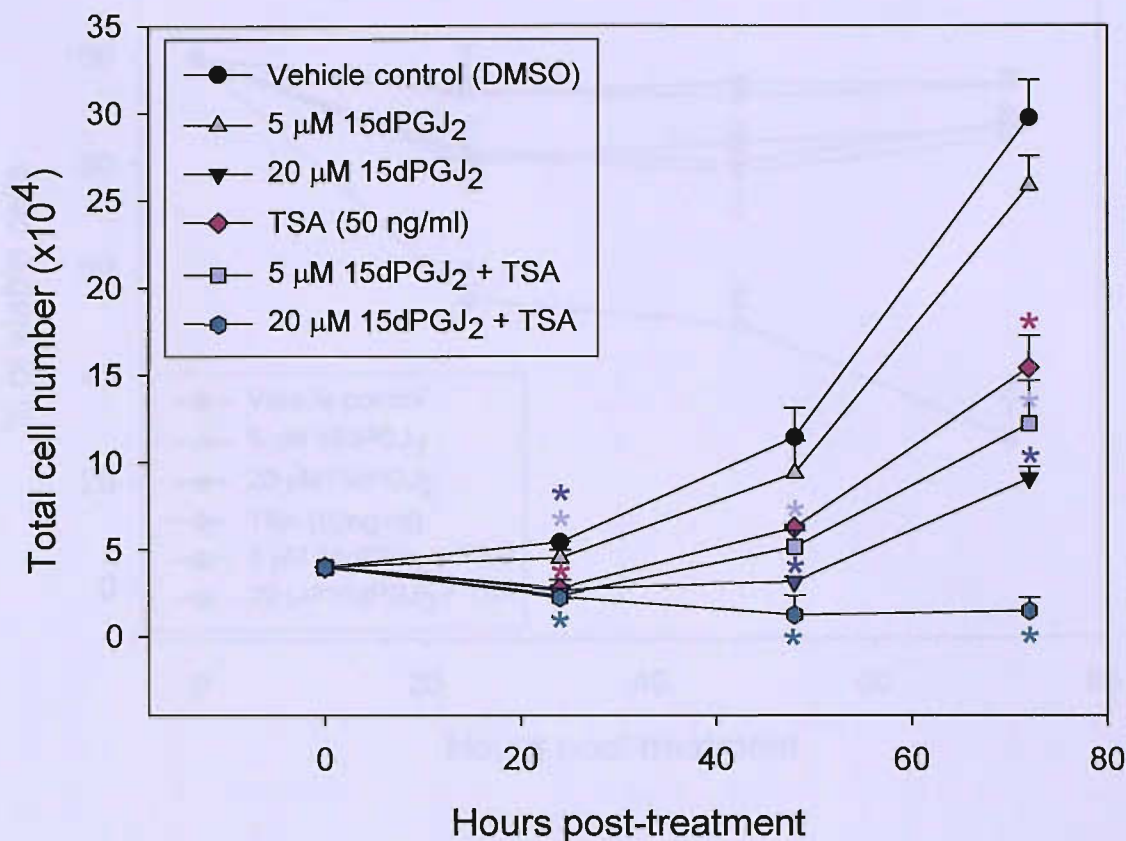


Fig. 3.10. The effect of co-treatment of 15dPGJ₂ and TSA on the growth of SK-N-AS neuroblastoma cells. SK-N-AS cells were plated out in complete media in 6-well dishes at 4×10^4 cells per well and treated with either a vehicle control (DMSO) or 5 or 20 μM 15dPGJ₂ either alone or in combination with TSA (50 ng/ml of complete media) and growth profiles were measured over 72 hours. Two samples were counted in duplicate per treatment per day using a haemocytometer. Data represents the mean total cell number ($\times 10^4$) of two independent experiments \pm S.D. Statistics were calculated using a Student's *t*-test and showed that 20 μM 15dPGJ₂ ($p < 0.05$) (*) or TSA ($P < 0.05$) (*) alone or in combination (*) caused significant inhibition of SK-N-AS cell growth 24 hours post-treatment ($p < 0.05$). While treatment of SK-N-AS cells with 5 μM 15dPGJ₂ alone (grey triangles) did not significantly attenuate cell growth over the 72 hour time course, when 5 μM 15dPGJ₂ was used in combination with TSA the total cell number was significantly reduced 24 hours after treatment ($p < 0.05$) (*).

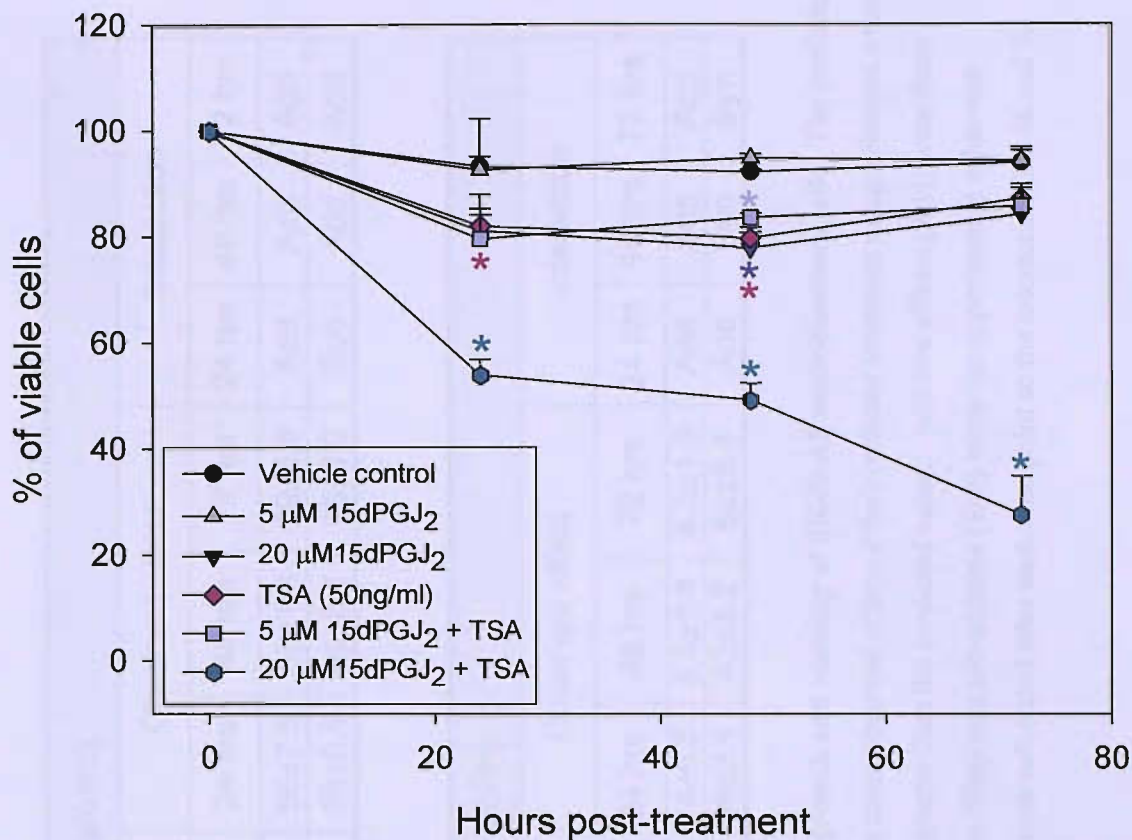


Fig. 3.11. The effect of co-treatment of 15dPGJ₂ and TSA on the viability of SK-N-AS neuroblastoma cells. SK-N-AS cells were plated out in complete media in 6-well dishes at 4×10^4 cells per well and treated with either a vehicle control (DMSO) or 5 or 20 μ M 15dPGJ₂ either alone or in combination with TSA (50 ng/ml of complete media) and cell viability was monitored over 72 hours. The proportion of viable cells was determined by trypan blue staining. Two samples were counted in duplicate per treatment per day using a haemocytometer. Data are expressed as the mean % of viable cells (trypan blue negative) relative to the total number of cells counted per well and represents two independent experiments \pm S.D. Statistics were calculated using a Student's *t*-test and showed that 20 μ M 15dPGJ₂ alone significantly reduced SK-N-AS cell viability 48 hours post-treatment but not at 24 or 72 hours ($p < 0.05$) (*). TSA treatment alone significantly reduced the number of viable SK-N-AS cells 24 and 48 hours post-treatment although the decrease in viability observed 72 hours after treatment did not reach statistical significance ($p < 0.05$) (*). While treatment of SK-N-AS cells with 5 μ M 15dPGJ₂ alone (grey triangles) did not significantly attenuate cell viability, when 5 μ M 15dPGJ₂ was used in combination with TSA (purple square) cell viability was significantly reduced but only at the 48 hour time point ($p < 0.05$) (*). In contrast, co-treatment of 20 μ M 15dPGJ₂ and TSA significantly reduced the number of viable cells throughout the 72 hour time course ($p < 0.05$) (*).

% inhibition of cell growth										
Cell line	Treatment	Predicted effect			Observed effect			Interaction		
		24 hrs	48 hrs	72 hrs	24 hrs	48 hrs	72 hrs	24 hrs	48 hrs	72 hrs
SK-N-AS	5 μ M 15dPGJ ₂ + TSA	65 \pm 11	63 \pm 5.3	60 \pm 22	56 \pm 7.5	55 \pm 1.6	59 \pm 5.3	Add	Add	Add
	20 μ M 15dPGJ ₂ + TSA	98 \pm 8.1	120 \pm 16	110 \pm 4.5	58 \pm 0.6	89 \pm 8.4	95 \pm 3.0	Sub	Add	Add

% inhibition of cell viability										
Cell line	Treatment	Predicted effect			Observed effect			Interaction		
		24 hrs	48 hrs	72 hrs	24 hrs	48 hrs	72 hrs	24 hrs	48 hrs	72 hrs
SK-N-AS	5 μ M 15dPGJ ₂ + TSA	12 \pm 4.0	9.9 \pm 3.7	6.5 \pm 2.0	14 \pm 6.5	8.6 \pm 0.4	8.3 \pm 1.3	Add	Add	Add
	20 μ M 15dPGJ ₂ + TSA	23 \pm 10	27 \pm 4.2	17 \pm 2.9	39 \pm 2.9	43\pm3.2	62\pm6.4	Add	Syn	Syn

Table 3.1. The effect of TSA in combination with either 5 or 20 μ M 15dPGJ₂ on the growth and viability of SK-N-AS neuroblastoma cells. The predicted value represents the sum of the individual effects of the agents and was compared with the mean observed effect of the combined treatment using a Student *t*-test. The effect was classified as synergistic (Syn) if the experimental value was significantly greater than the predicted value. Additive effects (Add) were those where the experimental value was not significantly different from the predicted value. The effect was sub-additive (Sub) when the experimental value was significantly less than the predicted value. The predicted and observed combined effects were calculated after each time point so the interaction, 24, 48 and 72 hours post-treatment could be determined.

values were not significantly different from the predicted values (**Fig. 3.10** and **Table 3.1**). Conversely, while co-administration of 5 μM 15dPGJ₂ and TSA also had an additive effect on cell viability, the combination of 20 μM 15dPGJ₂ and TSA did result in a synergistic decrease in cell viability, 48 and 72 hours post-treatment, compared the effect of either agent alone (**Fig. 3.11** and **Table 3.1**). These results suggest that growth inhibition caused by TSA in SK-N-AS cells is in part controlled by a mechanism that is distinct from the PPAR γ pathway. It is possible however, that TSA could induce cell death in SK-N-AS cells, in part through stimulating PPAR γ activation in the presence of its ligand by releasing this nuclear receptor from the inhibitory effect of a HDAC-containing complex.

3.7 The effect of the synthetic PPAR γ ligand ciglitazone on neuroblastoma cell growth *in vitro*

Previously only the response of neuroblastoma cells to the natural PPAR γ ligand 15dPGJ₂ had been investigated. PPAR γ however binds a range of synthetic agonists, which includes a group of drugs called thiazolidinediones (TZDs) [20]. The TZDs rosiglitazone and pioglitazone are used clinically in the treatment of type 2 diabetes. In addition to their anti-diabetic properties, TZDs, like the natural PPAR γ ligand 15dPGJ₂, have also been shown to attenuate the growth of cancer cell lines and tumour progression in mice [219]. For example, it was demonstrated that the first known TZD, ciglitazone, inhibited the growth of prostate cancer, pancreatic cancer, B-cell lymphoma, GH-secreting adenoma, osteosarcoma and lung cancer cells *in vitro* [192,193,203,211,365-367]. Since TZDs have a relatively low toxicity and were well tolerated by prostate and liposarcoma patients in small scale clinical trials, TZDs have therapeutic potential in children with advanced staged neuroblastomas who currently have limited treatment options [209,239].

Therefore, the effect of the TZD ciglitazone on neuroblastoma cell growth *in vitro* was studied. Ciglitazone has a comparable binding affinity to 15dPGJ₂ for PPAR γ (3 μM and 2.5 μM respectively) and attenuated the growth of prostate cancer cells at similar doses to 15dPGJ₂ [99,100,106,192]. Therefore, SK-N-AS and IMR-32 cells were treated with a vehicle control (DMSO) or ciglitazone at concentrations in the

same range that had been used earlier for 15dPGJ₂ (0.1 -20µM) and their growth profiles monitored over 72 hours. Ciglitazone however, at these concentrations, 72 hours post-treatment did not significantly inhibit the growth of any of the neuroblastoma cell lines tested (**Fig. 3.12**).

In some cancer cell lines such as those derived from breast and lung tumours, the anti-proliferative effects of TZDs were less potent compared with 15dPGJ₂ [203,301]. In view of these findings the effect of higher concentrations of ciglitazone on neuroblastoma cell growth was investigated. Murine ND-7 neuroblastoma cells and human SK-N-AS, IMR-32 and SK-N-SH cells were plated out in complete media in 6-well dishes at 4×10^4 cells per well and incubated at 37°C for 5 hours to facilitate attachment. The cells were then treated with a vehicle control (DMSO) or 25, 50, 100, 150 and 200 µM ciglitazone for 72 hours and the effect on cell growth measured. Ciglitazone repressed the growth of all four neuroblastoma cell lines *in vitro* (**Fig. 3.13**).

Determination of the ligand concentration required to induce 50% growth inhibition (EC₅₀), at each time point, demonstrated that in ND-7, SK-N-AS and SK-N-SH cells attenuation of growth by ciglitazone occurred gradually and was more pronounced at the end of the 72 hour time course. Of the neuroblastoma cell lines investigated, IMR-32 cells were the most resistant to the anti-proliferative effects ciglitazone and 72 hours post-treatment the ciglitazone EC₅₀ concentration for IMR-32 cells was 52 µM compared with EC₅₀ values of 13 µM , 36 µM and 30 µM for ND-7, SK-N-AS and SK-N-SH cells respectively (**Fig. 3.13**, table). After 72 hours, ciglitazone was a more potent inhibitor of murine (ND-7) neuroblastoma cell growth at concentrations between 0 and 25 µM. Cell growth was attenuated by 71% in the presence of 25 µM ciglitazone in ND-7 cells while cell growth at the same concentration of ciglitazone in the human cell lines was only inhibited by between 23 and 35 % (**Fig. 3.13**). Ciglitazone, however at concentrations of 50 µM or higher caused a similar level of growth inhibition of both murine and human neuroblastoma cell lines.

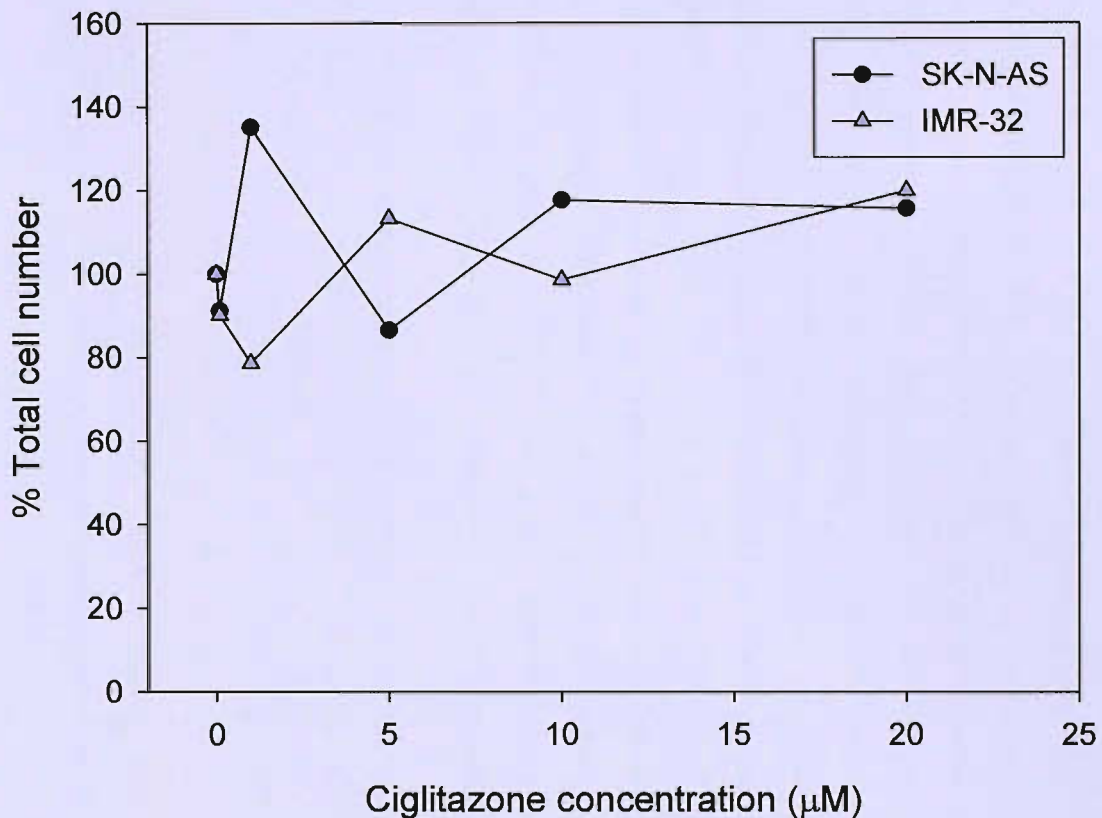
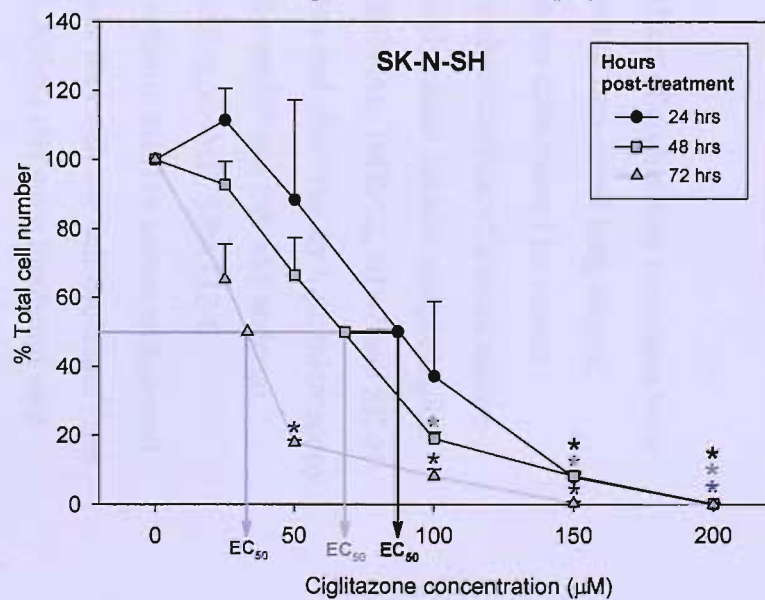
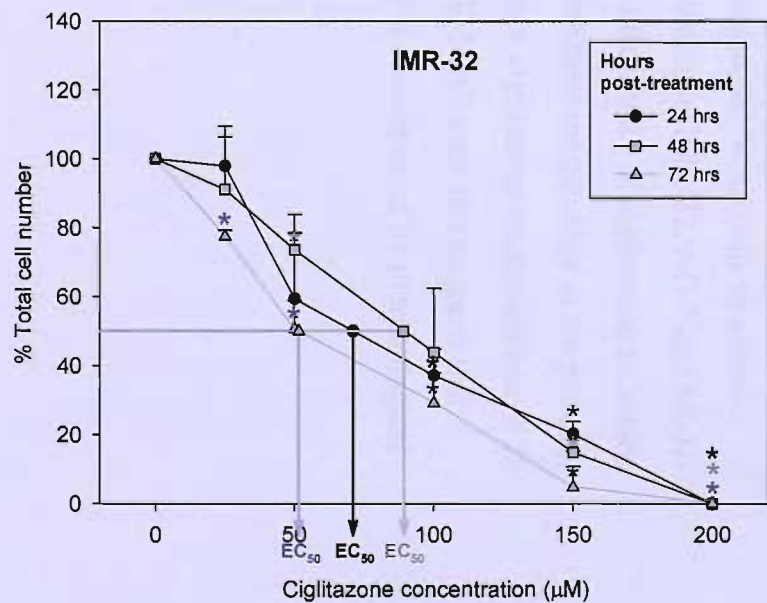
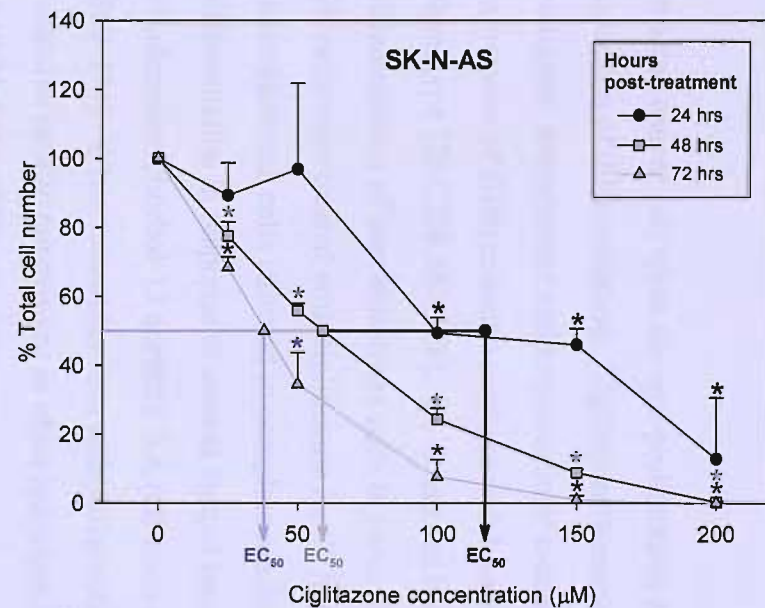
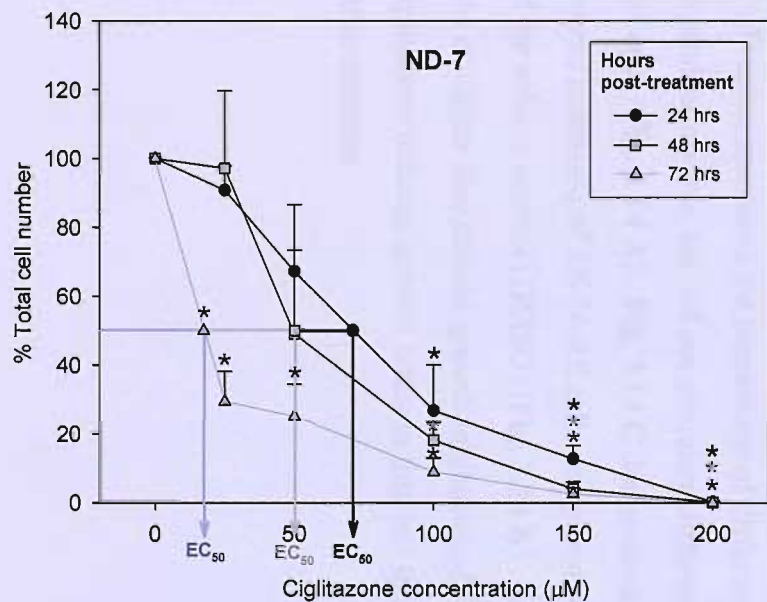


Fig. 3.12. The effect of the synthetic PPAR γ ligand, ciglitazone on neuroblastoma cell growth at concentrations between 0.1 μ M and 20 μ M. SK-N-AS and IMR-32 cells were plated out in 6-well dishes at 4×10^4 cells per well and treated with either DMSO (vehicle control) or 0.1, 1, 5, 10 and 20 μ M ciglitazone and the effect on cell growth was measured over 72 hours. Two samples were counted in duplicate per treatment using a haemocytometer. Data shows the mean of four separate counts and is presented as the % total cell number relative to the number of cells in the presence of the vehicle control (DMSO) 72 hours post-treatment. Statistics were calculated using a Student's *t*-test and showed that 72 hours after treatment there was no significant difference in total cell number between vehicle and ciglitazone treated cells ($p < 0.05$).

Fig. 3.13. The effect of the synthetic PPAR γ ligand, ciglitazone on the growth of ND-7, SK-N-AS, IMR-32 and SK-N-SH neuroblastoma cells. To determine the effect of ciglitazone on cell growth, the neuroblastoma cells were plated out in complete media in 6-well dishes at 4×10^4 cells per well and treated with either a vehicle control (DMSO) or 25, 50, 100, 150 and 200 μM ciglitazone and growth profiles were measured over 72 hours. Two samples were counted in duplicate per treatment per day using a haemocytometer. Data represents the mean percentage of the total cell number, relative to the number of cells in the presence of the vehicle control (DMSO) \pm S.D. of two independent experiments. Statistics were calculated using a Student's *t*-test and showed that ciglitazone at concentrations of 25 μM (or higher) caused significant inhibition of ND-7 cell growth 72 hours post-treatment ($p < 0.05$) (*) whereas ciglitazone concentrations of 100 μM or higher caused significant growth inhibition after only 24 hours ($p < 0.05$) (*). Ciglitazone at a concentration of 25 μM (or higher) caused significant inhibition of SK-N-AS cell growth 48 hours post-treatment ($p < 0.05$) (*) whereas ciglitazone concentrations of 100 μM or higher caused significant growth inhibition after only 24 hours ($p < 0.05$) (*). In IMR-32 cells, ciglitazone at concentrations of 50, 150 and 200 μM but not 100 μM caused significant inhibition of cell growth 48 hours post-treatment ($p < 0.05$) (*) whereas ciglitazone concentrations of 150 μM or higher caused significant growth inhibition after only 24 hours ($p < 0.05$) (*). In SK-N-SH cells, ciglitazone at 50 μM (or higher) caused significant inhibition of cell growth 72 hours post-treatment ($p < 0.05$) (*) whereas ciglitazone concentrations of 150 μM or higher caused significant growth inhibition after only 24 hours ($p < 0.05$) (*). The ciglitazone concentration required to induce 50% growth inhibition (EC_{50}) for each cell line 24, 48 and 72 hours following treatment is indicated on the graphs and summarized in the table below:

Hours post treatment	EC_{50} (μM)			
	ND-7	SK-N-AS	IMR-32	SK-N-SH
24	67	117	67	83
48	50	54	84	63
72	13	36	52	30



3.8 Ciglitazone stimulates the differentiation of SK-N-AS neuroblastoma cells *in vitro*

In some cancer cell types the anti-proliferative effect of ciglitazone correlates with induction of differentiation. Ciglitazone treatment of non-small lung cancer, malignant astrocytoma and hepatocellular carcinoma cells caused increased expression of differentiation markers which were characteristic of a more mature phenotype [203,208,367,368]. To determine if ciglitazone induces morphological differentiation of neuroblastoma cells *in vitro*, SK-N-AS, IMR-32, ND-7 and SK-N-SH cells were treated with ciglitazone for 72 hours and observed by light microscopy. Neuroblastoma cells cultured in complete medium proliferate but will undergo differentiation in response to several factors including, cAMP, TPA (12-0-tetradecanoylphorbol-13 acetate), RA (all-trans-retinoic acid) or serum withdrawal [369-373]. When neuroblastoma cells differentiate they exit the cell cycle and form extensive neurite outgrowths as observed when LAN-5 cells were incubated with 15dPGJ₂ [213,373]. For this experiment a neuroblastoma cell was classified as differentiated if the length of its neurite outgrowth was greater than one cell body. Ciglitazone increased the percentage of differentiated SK-N-AS cells in a dose-dependent manner but did not stimulate differentiation of IMR-32, ND-7 and SK-N-SH cells (**Fig. 3.14 A**). **Fig. 3.14 C** demonstrates the ability of ciglitazone to induce neurite extension of SK-N-AS cells compared with their morphology in the presence of the vehicle control (DMSO) (**Fig. 3.14 B**). Since ciglitazone concentrations of 25 μ M or higher also caused growth inhibition of SK-N-AS cells this suggests that ciglitazone induced growth arrest in this cell line is accompanied by morphological differentiation.

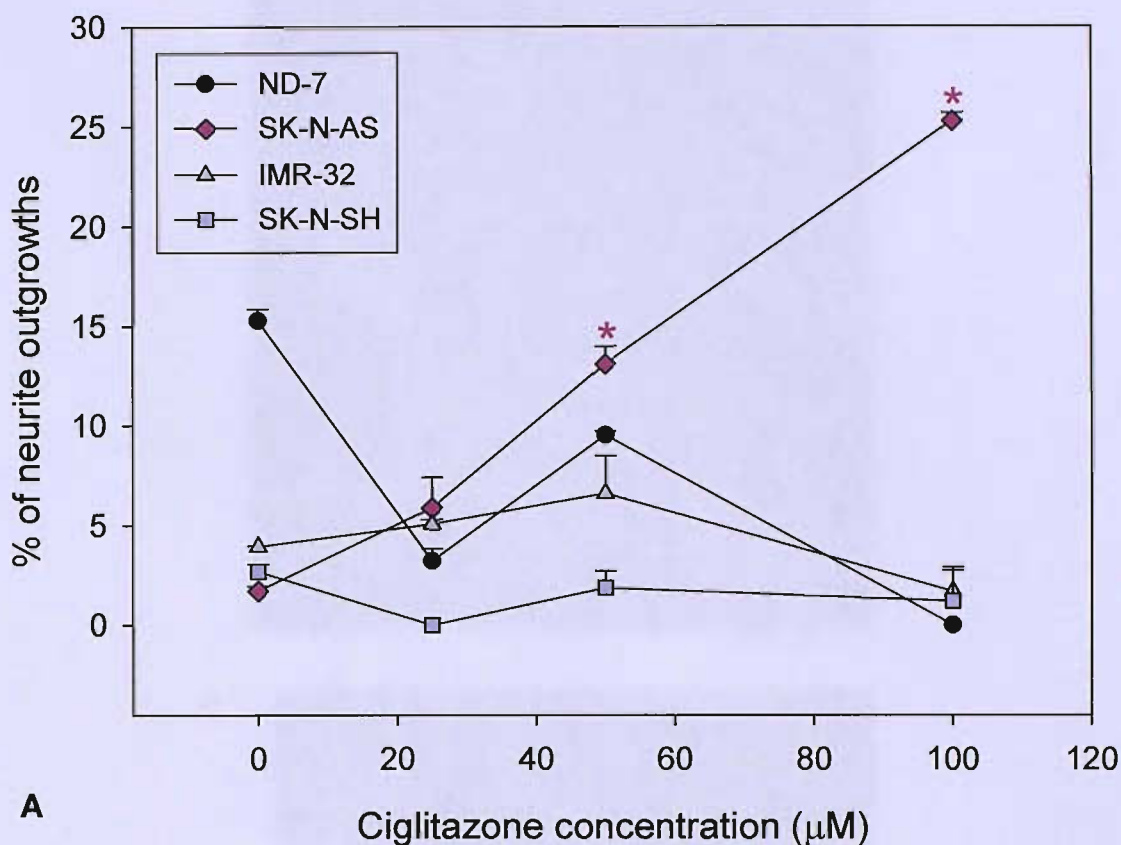
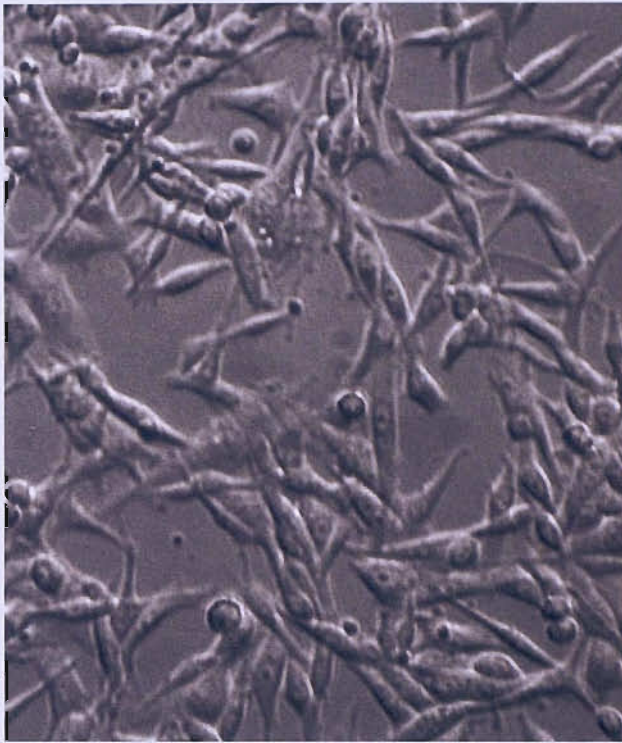


Fig. 3.14. The effect of ciglitazone on the differentiation of neuroblastoma cells. ND-7, SK-N-AS, IMR-32 and SK-N-SH cells were plated out in complete media in 6-well dishes at 4×10^4 cells per well and treated with either vehicle control (DMSO) or 25, 50 and 100 μM ciglitazone for 72 hours. To determine if ciglitazone induced differentiation, neuroblastoma cells with neurite outgrowths greater than one cell body were counted and expressed as the percentage of the total number of cells in the field of view. Cells were counted in triplicate per treatment after 72 hours and the data represents the mean % of cells with neurite outgrowths \pm S.D. (A). Statistics were calculated using a Student's *t*-test and showed that ciglitazone at concentrations of 50 μM or higher caused a significant increase in the percentage of SK-N-AS cells with neurite outgrowths (*) ($p < 0.05$). The morphology of SK-N-AS cells in the absence (B) and presence of 100 μM ciglitazone (C) was assessed by light microscopy 72 hours post-treatment. In addition to SK-N-AS cells with neurite outgrowths, some of the cells have rounded up. This may be accounted for by the decreased cell viability also observed at this ciglitazone concentration (Fig. 3.15).

B



C



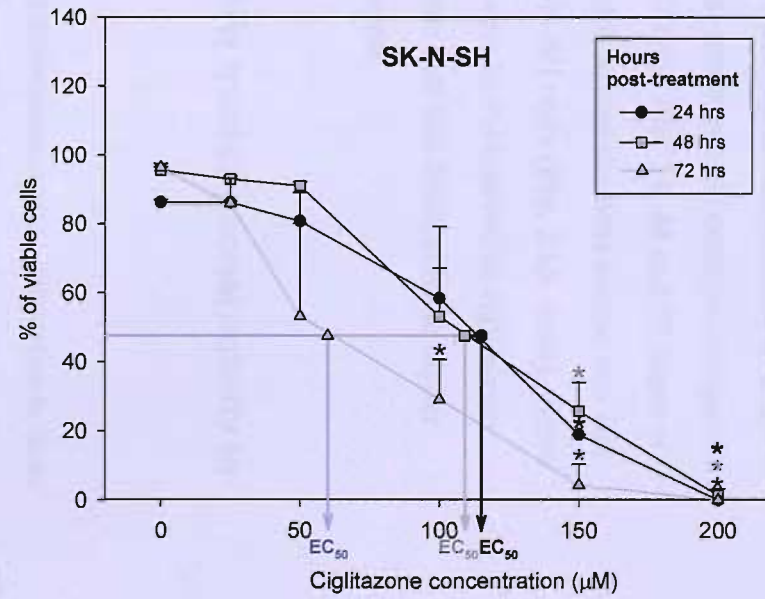
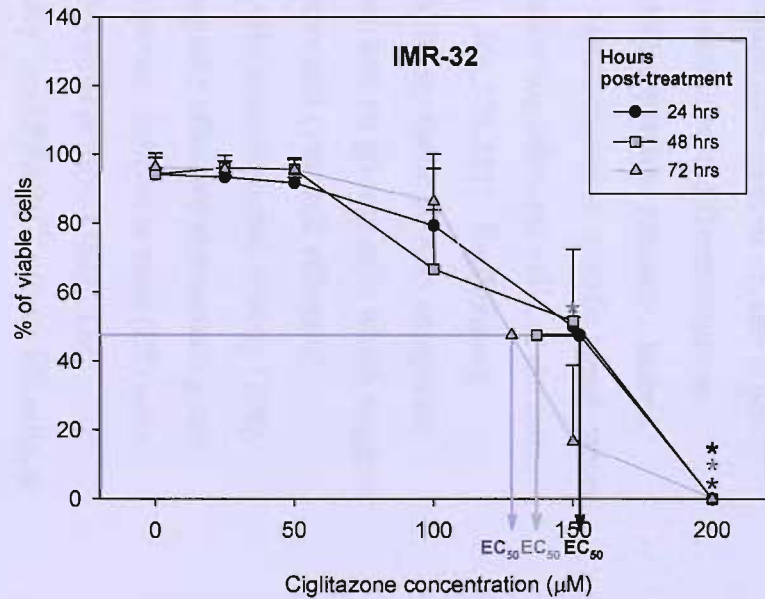
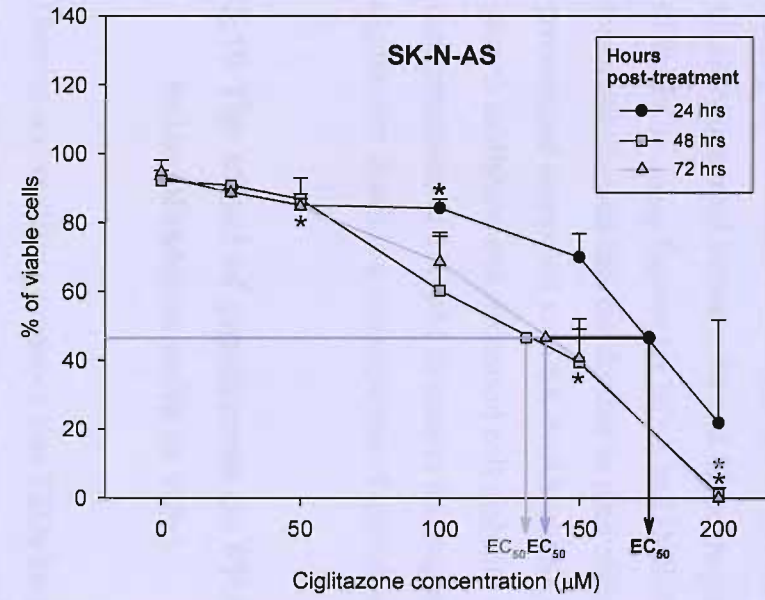
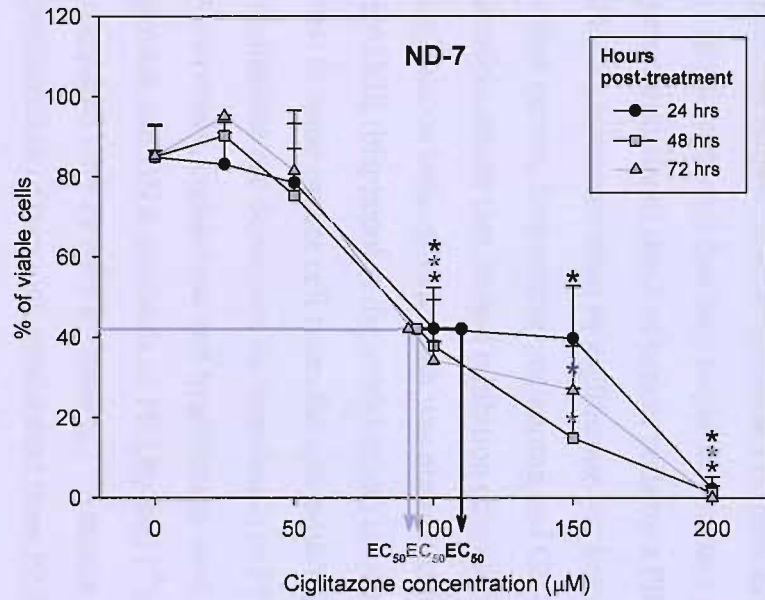
3.9 Ciglitazone reduces the viability of neuroblastoma cells *in vitro*

Ciglitazone can decrease cell viability in cancer cells by inducing programmed cell death. Apoptosis following ciglitazone treatment has been observed in pancreatic, lung, osteosarcoma, malignant astrocytoma, melanoma, GH-secreting adenoma and B-cell lymphoma cell lines *in vitro* [193,203,208,211,366,374]. Cell viability can be measured using a trypan blue exclusion assay. Trypan blue is a negatively charged chromophore which is excluded from viable cells with an intact plasma membrane. Dying cells which have loss of membrane integrity take up the dye and are termed trypan blue positive [192]. For instance, cells undergoing necrosis or type II programmed cell death (autophagy) show increased plasma membrane permeability [192]. Although early on in apoptosis the membrane of the cell remains intact, during the later stages of apoptosis the integrity of the membrane does become compromised and the cells are referred to as late apoptotic (Type III) or secondary necrotic cells [214,375-378]. The trypan blue exclusion assay alone cannot distinguish between these different types of cell death, however it has previously been shown that the decrease in the percentage of viable cells, determined using this technique, negatively correlated with induction of apoptosis or autophagy detected by TUNEL (terminal deoxynucleotidyl transferase mediated X-UTP nick-end labeling) assay and MDC (monodansylcadaverine) staining respectively [228,379,380]. Therefore, initially the trypan blue exclusion assay was used to study the effect of ciglitazone on the viability of neuroblastoma cells *in vitro*.

ND-7, SK-N-AS, IMR-32 and SK-N-SH were plated out in complete media in 6-well dishes at 4×10^4 cells per well were treated with either a vehicle control (DMSO) or 25, 50, 100, 150 and 200 μM ciglitazone and the number of viable and non-viable cells were counted over 72 hours. Ciglitazone treatment decreased the viability of all four neuroblastoma cells, although only at concentrations of 100 μM or higher (**Fig. 3.15**).

Fig. 3.15. The effect of the synthetic PPAR γ ligand, ciglitazone on the viability of ND-7, SK-N-AS, IMR-32 and SK-N-SH neuroblastoma cells. The neuroblastoma cell lines were plated out in complete media in 6-well dishes at 4×10^4 cells per well and treated with a vehicle control (DMSO) or 25, 50, 100, 150 and 200 μM ciglitazone and cell viability was monitored over 72 hours. The proportion of viable cells was determined by trypan blue staining. Two samples were counted in duplicate per treatment per day using a haemocytometer. Data are expressed as the mean % of viable cells (trypan blue negative) relative to the total number of cells counted per well and represent two independent experiments \pm S.D. Statistics were calculated using a Student's *t*-test and showed that ciglitazone at concentrations of 100 μM or higher caused a significant decrease in ND-7 cell viability 24 hours post-treatment (*) ($p < 0.05$). In SK-N-AS cells, ciglitazone at a concentration of 100 μM caused a significant decrease in the number of viable cells 24 hrs post-treatment (*) ($p < 0.05$) but the decrease in cell viability observed after 48 and 72 hours at this ciglitazone concentration did not reach statistical significance. In SK-N-AS cells a significant decrease in cell viability was seen 72 hrs post-treatment in the presence of 50, 150 and 200 μM ciglitazone (*) ($p < 0.05$). In IMR-32 cells a ciglitazone concentration of 200 μM caused a significant decrease in the number of viable cells 24 hours post-treatment (*) ($p < 0.05$) whereas the decrease in cell viability observed at a ciglitazone concentration of 150 μM reached significance after 48 hours but not at 72 hours. In SK-N-SH cells there was a significant decrease in cell viability 72 hours post-treatment at ciglitazone concentrations of 100 μM (*) whereas ciglitazone concentrations of 150 μM or higher caused a significant decrease in cell viability after 24 hours (*) ($p < 0.05$). The ciglitazone concentration required to cause a 50% reduction in the number of viable cells ($\text{EC}_{50 \text{ viability}}$) for each cell line 24, 48 and 72 hours following treatment is indicated on the graphs and summarized in the table below:

Hours post treatment	EC_{50} (μM) (Viability)			
	ND-7	SK-N-AS	IMR-32	SK-N-SH
24	108	175	152	116
48	91.0	125	137	109
72	92.0	136	127	58.0



Calculation of the ligand concentration required to induce a 50% decrease in the percentage of viable neuroblastoma cells (EC_{50} viability) at each time point indicated the largest increase in trypan blue uptake in SK-N-AS cells occurred between 24 and 48 hours post-treatment whereas in SK-N-SH the most significant decrease in cell viability occurred between 48 and 72 hours post-treatment. In contrast, comparison of the EC_{50} viability figures for ND-7 and IMR-32 cells after 24, 48 and 72 hours of treatment showed that the decline in their viability across the time course was less pronounced compared with SK-N-AS and SK-N-SH cells (Fig. 3.15, table). Since growth inhibition and decreased cell viability were both observed at ciglitazone concentrations of 100 μ M or greater this suggests that cell death at these higher ciglitazone doses is a consequence of growth arrest.

3.10 The effect of ciglitazone on PPAR γ transcriptional activity in neuroblastoma cells *in vitro*

Despite accumulating evidence that TZDs have anti-tumourigenic properties both *in vitro* and *in vivo* there is still controversy over how these drugs mediate their effect on cancer cell proliferation. As TZDs are known to improve sensitivity to insulin and promote adipocyte differentiation via transcriptional activation of PPAR γ it was originally proposed that they might also induce growth arrest, differentiation or programmed cell death of cancer cells by a PPAR γ dependent pathway. Indeed, PPAR γ transactivation by ciglitazone has been demonstrated in specific breast cancer, colon cancer, lung cancer, melanoma and GH-secreting adenoma cells, at the same concentrations that caused inhibition of growth [366,374,381]. Furthermore ciglitazone induced cell death was abrogated by the synthetic PPAR γ antagonist BADGE (bisphenol A diglycidyl ether) in human and rat glioma cells which suggests that in some cancer cell types the anti-proliferative and cytotoxic effects of ciglitazone are dependent on stimulation of PPAR γ transcriptional activity [208]. Conversely, ciglitazone and troglitazone were equally effective at attenuating cell growth and DNA synthesis of PPAR γ null ($^{-/-}$) mouse embryonic stem (ES) cells compared with PPAR γ expressing ($^{+/+}$) mouse ES cells *in vitro* [382]. The proliferation of tumours, established from PPAR γ $^{-/-}$ and PPAR γ $^{+/+}$ mouse ES cells, in mice were also almost completely suppressed by troglitazone treatment [382]. The

findings of this study were corroborated by the work of Shiau *et al* which showed that close structural analogues of troglitazone and ciglitazone, that were deficient in PPAR γ ligand binding activity, retained the ability to induce apoptosis of prostate cancer cells *in vitro* [383]. Recent publications indicate that the PPAR γ independent growth inhibitory effects of TZDs could be mediated by a variety of mechanisms which include, production of reactive oxygen species (ROS), modulation of the MAP kinase pathway or attenuation of translation initiation [382,384,385].

Thus to establish if ciglitazone stimulates PPAR γ -mediated transcription in neuroblastoma cells, ND-7, SK-N-AS, IMR-32 and SK-N-SH cell lines were transiently transfected with a PPAR responsive reporter (PPRE-TK-Luc) and then treated with either a vehicle control (DMSO) or 25, 50, 100, 150 and 200 μ M ciglitazone for 24 hours. The cells were then harvested and luciferase activity measured. In ND-7 cells, ciglitazone stimulated PPRE-mediated transcription in a dose-dependent manner with statistically significant induction of PPRE-driven reporter activity observed at concentrations of 25 μ M or higher (**Fig. 3.16**). In human SK-N-SH cells significant activation of the PPAR responsive reporter was observed at a ciglitazone concentration of 25 μ M (1.7-fold) but no stimulation of PPRE-mediated transcription was observed at ciglitazone concentrations of 50 and 100 μ M (**Fig. 3.17**). Although ciglitazone induced PPAR γ transcriptional activity at a concentration near its EC₅₀ for this cell line, these results indicate that at higher doses ciglitazone may activate PPAR γ independent pathways in SK-N-SH cells. In contrast, in SK-N-AS and IMR-32 cells ciglitazone did not significantly induce the luciferase activity of the PPAR responsive reporter at any of the concentrations investigated (**Fig. 3.17**). As no induction of PPRE-mediated transcription was observed at concentrations near the EC₅₀ for these two cell lines this suggests that in SK-N-AS and IMR-32 cells ciglitazone mediates its anti-proliferative effect in part by a PPAR γ independent mechanism.

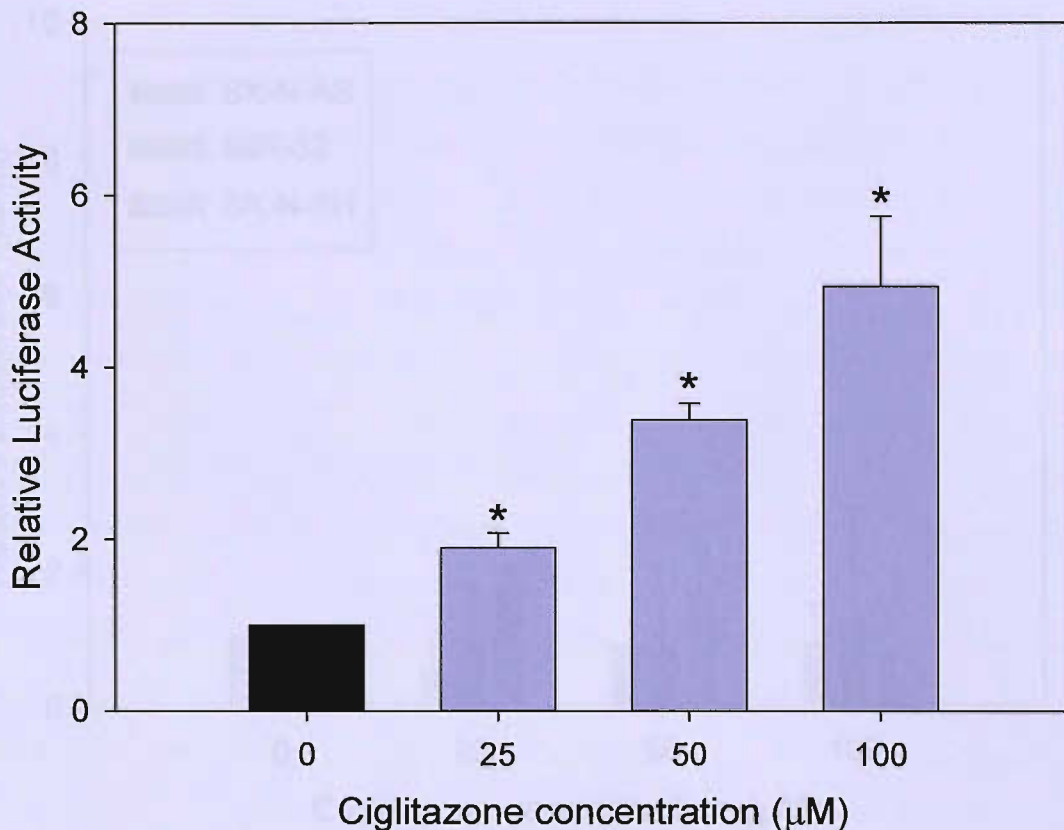


Fig. 3.16. The effect of the synthetic PPAR γ ligand, ciglitazone on PPRE-mediated transcription in ND-7 neuroblastoma cells. ND-7 cells were transiently transfected with 2 μ g of a *Renilla* luciferase reporter construct under the control of three peroxisome proliferator response elements (PPREs) upstream of a thymidine kinase promoter (PPREx3-TK-Luc). Cells were treated with either a vehicle control (DMSO) or 25, 50 and 100 μ M ciglitazone for 24 hours then harvested and luciferase activity measured. Data shows the mean relative luciferase activity of the PPREx3-TK-Luc reporter compared with its activity in vehicle DMSO treated ND-7 cells, and represents two independent experiments \pm S.D. The activity of the PPREx3-TK-Luc construct was normalized for transfection efficiency and differences in cell number by co-transfecting ND-7 cells with the firefly luciferase reporter, pGL3-Basic. Statistics were calculated using a Student's *t*-test and showed that compared with DMSO treated ND-7 cells, ciglitazone at concentrations of 25 μ M or higher caused significant activation of the *Renilla* luciferase reporter driven by a PPRE-regulated promoter ($p < 0.05$) (*).

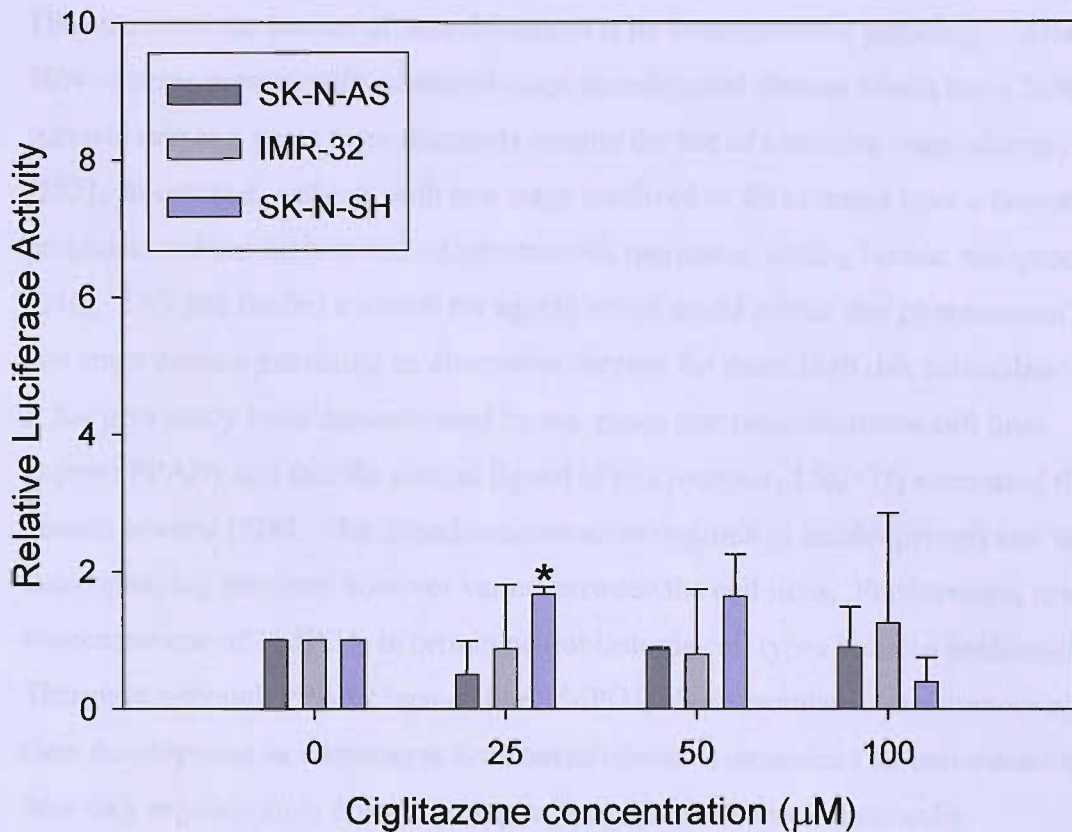


Fig. 3.17. The effect of the synthetic PPAR γ ligand, ciglitazone on PPRE-mediated transcription in human neuroblastoma cell lines. SK-N-AS, SK-N-SH and IMR-32 cells were transiently transfected with 2 μ g of a *Renilla* luciferase reporter construct under the control of three peroxisome proliferator response elements (PPREs) upstream of a thymidine kinase promoter (PPREx3-TK-Luc). Cells were treated with DMSO (vehicle control) or 25, 50 and 100 μ M ciglitazone for 24 hours then harvested and luciferase activity measured. Data shows the mean relative luciferase activity of the PPREx3-TK-Luc reporter compared with its activity in vehicle DMSO treated cells, and represents two independent experiments \pm S.D. The activity of the PPRE-x3-TK-Luc construct was normalized for transfection efficiency and differences in cell number by co-transfecting the cell lines with the firefly luciferase reporter, pGL3-Basic. Statistics were calculated using a Student's *t*-test and showed that compared with DMSO treated cells, ciglitazone caused significant induction of *Renilla* luciferase reporter activity driven by a PPRE-regulated promoter, at a concentration of 25 μ M in SK-N-SH cells (*) ($p < 0.05$), however ciglitazone at other concentrations and in other neuroblastoma cell lines did not have a significant effect on the reporter activity of the PPREx3-TK-Luc construct.

3.11 Discussion

The characteristic feature of neuroblastoma is its heterogeneous pathology. Around 50% of cases present with advanced stage disseminated disease which has a 20% survival rate at 5 years from diagnosis despite the use of intensive chemotherapy [252]. In contrast, patients with low stage localized or 4S tumours have a favourable prognosis and the highest rate of spontaneous regression among human malignancies [246]. This has fuelled a search for agents which could mimic this phenomenon in late stage disease providing an alternative therapy for these high risk neuroblastomas. It has previously been demonstrated by our group that neuroblastoma cell lines express PPAR γ and that the natural ligand of this receptor, 15dPGJ₂ attenuated their growth *in vitro* [228]. The ligand concentration required to inhibit growth and the accompanying response however varied between the cell lines. Furthermore, low concentrations of 15dPGJ₂ in certain neuroblastoma cell types induced proliferation. Therefore although PPAR γ ligands like 15dPGJ₂ show promise as anti-tumour agents, their development as a treatment for neuroblastoma is dependent on understanding how they regulate such diverse biological responses in these cancer cells.

Use of a PPAR responsive reporter assay showed that 15dPGJ₂ stimulated PPRE-mediated transcription in all four neuroblastoma cell lines examined and the level of PPAR γ transcriptional activity correlated with the degree of growth inhibition (**Fig. 3.1** and **Table 3.2**). Low level PPAR γ transactivation was associated with either proliferation or a certain degree of growth inhibition, whereas greater stimulation of PPRE-mediated transcription was observed at 15dPGJ₂ concentrations which resulted in more pronounced attenuation of cell growth. Furthermore, the degree of PPAR γ transcriptional activity at each 15dPGJ₂ concentration correlated with distinct biological responses in each neuroblastoma cell line. For instance, in the murine ND-7 cell line, treatment with 0.1 μ M 15dPGJ₂ stimulated PPAR γ transcriptional activity by 1.49-fold which was associated with cell proliferation, whereas in the presence of 1 μ M 15dPGJ₂ a 1.75-fold induction of PPAR γ transcriptional activity was observed and correlated with growth inhibition and differentiation. In the presence of 2 μ M 15dPGJ₂ PPRE-mediated

15dPGJ ₂ (μ M)	SK-N-AS		IMR-32		ND-7		SK-N-SH	
	Level of PPAR γ activation	Cellular response	Level of PPAR γ activation	Cellular response	Level of PPAR γ activation	Cellular response	Level of PPAR γ activation	Cellular response
0	1.0	Typical growth	1.0	Typical growth	1.0	Typical growth	1.0	Typical growth
0.1	0.7	Typical growth	1.3	Typical growth	1.5	proliferation	1.6	proliferation
1	0.9	proliferation	2.2	proliferation	1.8	Growth inhibition differentiation	1.0	proliferation
5	1.5	Differentiation	2.9	Growth arrest autophagy	2.2	Growth inhibition apoptosis	1.6	proliferation
10	2.1	Differentiation	3.3	Growth inhibition apoptosis	7.2	Growth inhibition apoptosis	1.3	proliferation
20	3.6	Growth inhibition differentiation	8.9	Growth inhibition apoptosis	25	Growth inhibition apoptosis	3.5	Growth inhibition

Table 3.2. Shows how the level of PPAR γ transcriptional activity (2 significant figures) correlates with distinct cellular responses in neuroblastoma cells *in vitro*.

transcription was stimulated by 2-fold which appears to attenuate cell growth and induce apoptosis (**Table 3.2**). A given concentration of 15dPGJ₂, however did not induce the same level of PPRE-mediated transcription in the different neuroblastoma cell lines studied. For example, 10 μM 15dPGJ₂ stimulated PPAR γ transcriptional activity by 2-, 3.25-, 7.23- and 1.61 fold in SK-N-AS, IMR-32, ND-7 and SK-N-SH neuroblastoma cells respectively (**Table 3.2**). The differential PPAR γ transactivation observed appears to relate to the sensitivity of the neuroblastoma cell lines to 15dPGJ₂. For instance, in SK-N-AS and SK-N-SH cells, which were more resistant to the growth inhibitory effects of 15dPGJ₂ relative to ND-7 and IMR-32 cells, the level of PPAR γ -mediated transcription at any concentration of this natural ligand was generally lower compared with the stimulation of PPAR γ transcriptional activity in IMR-32 and ND-7 cells.

Interestingly, the same level of PPAR γ activation in the four neuroblastoma cell lines was associated with different cellular responses. For example, a 2-3-fold stimulation of PPRE-mediated transcription in the four neuroblastoma cell lines correlated with differentiation, autophagy and apoptosis in SK-N-AS, IMR-32 and ND-7 cells respectively. These specific cellular processes are probably mediated by the activation of different target genes in each of the neuroblastoma cell lines, which suggests that the response of the neuroblastoma cells to 15dPGJ₂ is in part modulated by their genotype. There must also be a mechanism which determines how low level PPAR γ -mediated transcription stimulates proliferation in certain neuroblastoma cell types whereas higher levels of PPAR γ transactivation cause inhibition of cell growth.

Several putative PPAR γ target genes have been identified which suggest how PPAR γ may modulate differentiation, autophagy and apoptosis. Recent publications have demonstrated that the expression of cyclin dependent kinase inhibitors (CDKIs), including p21, are up-regulated during growth arrest and cell differentiation *in vitro* and *in vivo* [165]. Ectopic expression of PPAR γ in non-precursor fibroblasts resulted in their differentiation to adipocytes and was correlated with an increase in the expression of the cyclin dependent kinase inhibitors (CKIs) p21 and p18 [165]. Growth arrest and differentiation in response to PPAR γ ligands was also accompanied by induction of p21 expression in hepatocellular, renal, colon, non-small lung and breast cancer cell lines *in vitro* [199-204]. The p21 promoter contains

a consensus PPRE, which suggests that PPAR γ could promote differentiation of adipocytes and cancer cells by directly activating p21 transcription [165]. Another potential target gene of PPAR γ is the tumour suppressor PTEN (phosphatase and tensin homologue detected on chromosome 10). PTEN inhibits the phosphatidylinositol (PI) 3-kinase/protein kinase B (Akt/PKB) pathway which promotes cell survival and attenuates programmed cell death [225,226]. Activation of PPAR γ by the synthetic ligand rosiglitazone stimulated PTEN expression in breast and colon cancer cell lines and was correlated with a reduced proliferation rate [317]. Like the p21 promoter, the sequence upstream of the PTEN transcription start site contains two putative PPREs both of which were shown to bind PPAR γ in a gel retardation assay *in vitro* [317]. PTEN is a plausible candidate target gene for PPAR γ in neuroblastoma cells since it has been implicated in the initiation of autophagy and apoptosis, types of cell death which have both been detected in response to different concentrations of 15dPGJ₂ in IMR-32 cells [224,386-388]. Treatment with PPAR γ ligands has also been associated with the induction of other pro-apoptotic genes such as BAX, Bad and the tumour suppressor p53 [200,220].

Despite these findings the direct *in vivo* targets of PPAR γ in human malignancies including neuroblastoma are unknown. To begin to address this question in neuroblastoma cells it would be beneficial to evaluate which genes show altered expression following treatment with 15dPGJ₂ using a cDNA microarray. Having identified genes whose expression was significantly up-regulated by administration of 15dPGJ₂; directing binding by PPAR γ to the promoters of these genes *in vivo* could be assessed by chromatin immunoprecipitation assay. It would also be interesting to compare the gene expression profile of the four neuroblastoma cell lines in response to 15dPGJ₂ to determine whether there is a variation in the genes that are regulated by 15dPGJ₂ as this might in part explain the cell lines differential biological response to this ligand.

Since the degree of PPAR γ transactivation appeared to be important in governing the biological response of neuroblastoma cells to 15dPGJ₂ this prompted us to investigate how PPAR γ transcriptional activity is regulated in neuroblastoma cells. We demonstrate that expression of the critical cell cycle regulator retinoblastoma protein (pRb) or one of its family members (p107 or p130) could modulate the level of

PPAR γ activity in neuroblastoma cells. Co-transfection of ND-7 cells with an expression plasmid encoding pRb, p107 or p130 blocked induction of a PPRE-driven reporter by 15dPGJ₂. In addition, transfected pRb, in the presence of 15dPGJ₂ significantly repressed PPRE-mediated transcription below the level observed in ND-7 cells treated with the vehicle control. A similar response was observed in the presence of transfected p107 and p130 although inhibition of PPRE-mediated transcription did not reach statistical significance however this may be achieved with more experimental repeats. This suggests that as in adipocytes, pRb inhibition of PPAR γ activity is dependent on ligand binding in neuroblastoma cells. The A/B pocket of pRb also appears to be critical for transcriptional repression of PPAR γ as expression of a pRb mutant lacking the pocket domain failed to attenuate activation of the PPAR γ responsive reporter by 15dPGJ₂. Furthermore, treatment of ND-7 cells with the HDAC inhibitor trichostatin A blocked the repressive effect of pRb on stimulation of PPAR γ activity by 15dPGJ₂ indicating that the mechanism of pRb transcriptional inhibition involved HDAC recruitment.

Since it had previously been shown that higher levels of PPRE-mediated transcription in neuroblastoma cells were associated with increased growth inhibition, these results implied that treatment of neuroblastoma cells with a HDAC inhibitor and a PPAR γ ligand might enhance growth inhibition relative to the observed effect in the presence of only the PPAR γ ligand. Indeed, it was demonstrated that growth inhibition in SK-N-AS neuroblastoma cells co-administered with TSA and 15dPGJ₂ was augmented compared with the response of SK-N-AS cells treated with either agent alone, however the effect was only additive. Conversely the combined treatment of TSA and 20 μ M 15dPGJ₂ caused a synergistic decrease of SK-N-AS cell viability. These different effects on SK-N-AS cell proliferation and viability may have been influenced by the concentration of TSA used in these experiments. In SK-N-AS cells treated with TSA alone at a concentration of 50 ng/ml cell growth and viability were attenuated by approximately 50 and 10 % respectively. Therefore it is plausible that a lower concentration of TSA, which abrogates cell proliferation by between 10 and 30 %, is also required to observe whether the enhanced inhibition of growth by 15dPGJ₂ in combination with TSA can reach statistical synergy. Alternatively, HDAC inhibition may specifically affect the activation of PPAR γ target genes that modulate cell viability but not cell growth. Further investigation is necessary to determine if a

HDAC-pRb-PPAR γ complex forms *in vivo* in neuroblastoma cells and whether it is a target of HDAC inhibitors such as TSA since it is possible that PPAR γ could interact with other protein factors that recruit HDACs. To date six structurally distinct class of HDAC inhibitor have been identified which act by binding to different regions of the catalytic domains within class I and II HDACs, however none of these compounds show selectivity for different HDAC isozymes [342]. The development of inhibitors which target specific class I and II HDACs will help to uncover the distinct functions they have in tumourgenesis. For example, pRb has been shown to only recruit HDAC3 to PPAR γ . Therefore if a HDAC3 selective inhibitor could also augment the growth inhibitory effect of 15dPGJ₂ in neuroblastoma cells, this would lend support to the hypothesis that HDAC inhibition was specifically relieving the repressive effect of pRb.

Only specific human malignancies, such as retinoblastoma and osteosarcoma, are initiated by loss of pRb; although it is predicted that the pRb pathway is deregulated by alternative mechanisms in many other tumours. However, the outcome of pRb inactivation will depend on whether the downstream pathways regulated by pRb remain intact in the cancer cell [320]. For instance, in tumour cells expressing wild-type p53, deregulation of pRb triggers apoptosis. In the absence of pRb, free E2F stimulates expression of ARF (the alternative reading frame protein encoded by the INK4A locus) which in turn sequesters MDM2, a protein which targets p53 for degradation by the proteasome [323]. It is speculated that this induction of ARF serves as a protective mechanism that eliminates cells in which pRb is inactivated, hence why p53 is frequently mutated in cancer [323]. Enhanced PPAR γ transcriptional activity due to loss of pRb may similarly prevent development of the malignant phenotype. Recent studies suggest that the pRb status of neuroblastoma cells could in part be regulated by increased expression of cyclin D1 [341]. Cyclin D1 activates its cyclin-dependent kinase partner CDK4 or CDK6 which leads to phosphorylation of pRb disrupting its interaction with, and therefore repression of, transcription factors such as E2F and PPAR γ . Therefore, it would be interesting to correlate the level of PPAR γ -mediated transcription in neuroblastoma cell lines and primary tissues with the amount of hypo-phosphorylated pRb and expression of cyclin D1, pRb and pRb family members. In the absence of pRb, if the function of increased PPAR γ transactivation is to prevent tumour development by, for example,

stimulating the expression of pro-apoptotic genes it is probable that other mechanisms exist to inactivate PPAR γ in human malignancies.

Indeed PPAR γ transcriptional activity is attenuated by MAP kinase phosphorylation and the expression of this enzyme has been shown to be elevated in several human cancers including breast carcinomas [389]. In addition, we have previously shown that activation of a PPAR responsive reporter by 15dPGJ₂ in IMR-32 neuroblastoma cells was increased in the presence of the MAPK inhibitor PD98059 indicating that MAPK expression could also influence the response neuroblastoma cells to PPAR γ ligands [228]. A study of 55 primary sporadic colon carcinoma samples demonstrated that during the development of this cancer PPAR γ mutations are acquired which either block or impair the ability of the receptor to bind ligand and hence stimulate gene transcription, suggesting that reduced PPAR γ transactivation may play a role in cancer pathogenesis [232]. The level of RXR α or a critical co-activator could also limit PPAR γ -mediated transcription in malignant cells [314,315]. Two independent investigations have shown that that expression of PPAR γ -coactivator 1 (PGC-1) was significantly reduced in breast and colon tumours and in breast cancer patients low levels of the co-activator were correlated with poor clinical outcome [314,315]. PPAR β/δ expression may also contribute to transcriptional inactivation of PPAR γ since it has been demonstrated that PPAR β/δ has a higher affinity for co-repressors than PPAR γ or PPAR α and could attenuate PPAR γ target gene activation by competing for binding to PPREs [33,121]. Further study is warranted to discover if mutations of PPAR γ or differential MAPK, PPAR γ co-activator or PPAR β/δ expression also impact on PPAR γ transactivation and hence the cellular response of neuroblastoma cells to 15dPGJ₂ or other PPAR γ ligands.

Other high affinity PPAR γ ligands include a class of drugs called thiazolidinediones (TZDs) which are used clinically in the treatment of type II diabetes [20]. These compounds, like natural PPAR γ ligands, have also been shown to inhibit the growth of cell lines and primary tissues derived from a variety of human malignancies [192,193,203,211,365-367]. In addition, TZDs attenuated tumour progression in mice models *in vivo* [219]. Since these drugs have minimal side effects in diabetics and were well tolerated by cancer patients who took part in small scale clinical trials, this led us to investigate if TZDs have potential as an alternative therapy for the

treatment of advanced staged neuroblastomas [209,239]. The TZD ciglitazone repressed the growth of all four neuroblastoma cell lines examined although comparison of ciglitazone EC_{50} values with those for 15dPGJ₂ demonstrated that it was a less potent inhibitor of cell proliferation relative to this natural ligand (**Table 3.3**). Indeed ciglitazone concentrations between 1.6-18-fold higher than 15dPGJ₂ were required to attenuate neuroblastoma cell growth by 50 %. The ciglitazone EC_{50} value for the murine ND-7 cell line was considerably lower compared with the human neuroblastoma cell lines, however the growth inhibitory effect of ciglitazone at concentrations of 50 μ M or higher was similar in all the neuroblastoma cell lines examined. Calculation of the EC_{50} at each time point demonstrated that IMR-32 cells were the most resistant to ciglitazone treatment since the decrease in the IMR-32 EC_{50} value during the 72 hour time course was 3 to 5 times less compared with the reduction in the EC_{50} values for ND-7, SK-N-AS and SK-N-SH cell lines.

Ciglitazone induced neurite outgrowths from SK-N-AS cells in a dose-dependent manner, but had no effect on ND-7, IMR-32 or SK-N-SH cell morphology. Since the percentage of SK-N-AS cells with extended neurites was statistically significant at ciglitazone concentrations near the EC_{50} for this cell line this suggests that ciglitazone induced growth arrest of SK-N-AS cells was accompanied by differentiation. Furthermore, ciglitazone significantly decreased the viability of all neuroblastoma cell lines tested but only at concentrations of more than 100 μ M suggesting that growth arrest at these doses can lead to cell death. Although the trypan blue exclusion assay used in these experiments is an effective technique for detecting decreased membrane integrity it can not distinguish between necrosis, autophagy or apoptosis. However, the protein synthesis inhibitor cycloheximide could be used to distinguish if the mode of cell death induced by ciglitazone is necrosis or programmed cell death since necrosis does not require protein synthesis whereas apoptosis and autophagy are dependent on *de novo* protein expression [390]. If ciglitazone does stimulate programmed cell death of neuroblastoma cells there are a variety of methods which might be employed to determine if the cells have undergone apoptosis including detection of DNA strand nicks, DNA fragmentation, caspase activation or PARP cleavage [391-393]. Alternatively to assess whether ciglitazone induced cell death occurs

PPAR γ ligand	EC ₅₀ (μ M)			
	SK-N-AS	IMR-32	ND-7	SK-N-SH
15dPGJ ₂	17	5	0.7	19
ciglitazone	36	52	13	30

Table 3.3. Comparison of ciglitazone and 15dPGJ₂ EC₅₀ values for SK-N-AS, IMR-32, ND-7 and SK-N-SH neuroblastoma cell lines. The EC₅₀ value presented here was the concentration of ligand required to inhibit cell growth by 50% 72 hours post-treatment (2 significant figures). The EC₅₀ values for 15dPGJ₂ were calculated from previous cell counting data by Dr Karen Lillycrop, Dr Helen Rodway and Emma Phillips.

through an autophagic mechanism cells could be stained with MDC, a fluorescent dye which selectively stains autophagic vesicles [228]. The ciglitazone EC_{50} values for the four neuroblastoma cell lines are comparable with the concentrations of ciglitazone and two other TZDs, troglitazone and rosiglitazone that were required to inhibit the growth of certain breast, hepatocellular, salivary gland, pancreatic, leukemia and lung cancer cell lines *in vitro*. Since *in vitro* similar concentrations of ciglitazone and 15dPGJ₂ are required to activate PPAR γ (EC_{50} of 3 and 2 μ M respectively) this leads one to question why higher concentrations of ciglitazone are required to inhibit the growth of certain cancer cell types, if like 15dPGJ₂, ciglitazone exerts its effect through its receptor [99,100,106,192]. Indeed, recent publications indicate that TZDs, including ciglitazone may modulate tumour cell proliferation by both PPAR γ dependent and PPAR γ independent mechanisms.

To investigate if ciglitazone induced growth arrest in neuroblastoma cells was associated with stimulation of PPRE-mediated transcription, the activity of a transfected PPAR responsive reporter was assayed following treatment of neuroblastoma cell lines with increasing concentrations of ciglitazone. Interestingly, the effect of ciglitazone on PPAR γ transcriptional activity appeared to be dependent on the neuroblastoma cell type. In ND-7 cells, ciglitazone induced PPRE-mediated transcription in a dose-dependent manner and the level of PPAR γ activation correlated with the degree of growth inhibition. This is in agreement with the results of a study investigating the effect of ciglitazone and rosiglitazone on the growth of pituitary GH-secreting adenomas, which also demonstrated that ciglitazone stimulated PPAR γ transcriptional activity at concentrations which caused growth arrest and apoptosis [366]. Conversely, in human SK-N-SH cells significant low level activation (1.7-fold) was observed in the presence of 25 μ M ciglitazone but not at higher concentrations examined. In SK-N-AS and IMR-32 cells ciglitazone did not significantly stimulate the PPAR responsive reporter at any of the concentrations investigated. Rumi *et al* have similarly shown that in some gastrointestinal tumour cell lines, which expressed PPAR γ , that the TZD troglitazone did not induce PPRE-mediated transcription however still attenuated their growth *in vitro* [394]. Pre-treatment of the cell lines with the PPAR γ antagonist, GW9662 or transfection with a PPAR γ dominant negative did not protect these cells from troglitazone mediated growth arrest indicating that this TZD was acting through a PPAR γ independent

mechanism [394]. Furthermore, ciglitazone and troglitazone inhibited the growth of PPAR γ null mouse embryonic stem (ES) cells to the same extent as PPAR γ expressing ES cells [382].

Despite these findings, further investigation is needed, firstly to explain why ciglitazone only stimulated PPAR γ transcriptional activity in specific neuroblastoma cell lines and secondly to establish the mechanism of PPAR γ independent growth repression. One hypothesis is that IMR-32 and SK-N-AS cells have acquired a mutation in the PPAR γ receptor which impairs binding of ciglitazone but which allows ligand interaction and promotion of gene transcription when exposed to 15dPGJ₂. In support of this idea, examination of colorectal carcinoma samples identified a PPAR γ receptor, with a missense somatic mutation in the ligand binding domain (R288H), which could effectively bind synthetic PPAR γ ligands but demonstrated decreased binding and transcription when incubated with natural ligands [232].

Although still not conclusive, evidence for a variety of mechanisms by which TZDs could attenuate cancer cell growth independent of PPAR γ is emerging. For instance, in PPAR γ ^{-/-} and PPAR γ ^{+/+} mouse embryonic stem cells, ciglitazone and troglitazone induced growth arrest in G₁ via inhibition of translation initiation. This mechanism involved partial depletion of intracellular calcium stores and inactivation of elongation factor eIF α through protein kinase R phosphorylation [382]. Shiau *et al* demonstrated that troglitazone and ciglitazone structural analogues that failed to activate PPAR γ still retained the ability to promote caspase dependent apoptosis in prostate cancer cells by disrupting the association of Bcl-2 and Bcl-XL with Bak[383]. The Bcl2 family consists of members which either block or induce apoptosis. Anti-apoptotic Bcl-2 and Bcl-XL form heterodimers with pro-apoptotic members such as Bak that are inactive, whereas release of Bak from Bcl-2 or Bcl-XL leads to caspase activation and programmed cell death [383]. Ciglitazone also stimulated apoptosis of malignant glioma cells, however in these cell lines the pathway involved production of reactive oxygen species probably by depolarization of the mitochondrial membrane [385]. Furthermore, troglitazone induced growth inhibition of colon cancer cells has been linked to activation of the MAP kinase ERK1/2 which in turn induced expression of the cyclin dependent kinase inhibitor

p21 [394]. The MAPK pathway may in part act as the downstream effector of ROS production, since the MAP kinase cascade in astrocytes was triggered by ciglitazone via a mechanism involving generation of ROS [384]. In addition Chen *et al* have shown that induction of ERK1/2 by ciglitazone can lead to apoptosis by inhibition of NF- κ B transcriptional activity [395]. Intriguingly in this model, ciglitazone required PPAR γ expression to mediate its effect on HT29 colon cancer cells but repressed PPRE-mediated transcription [395]. Instead ciglitazone stimulated phosphorylation of PPAR γ by ERK1/2 which promoted its interaction with the p65 subunit of NF- κ B [395]. Chen *et al* proposed that formation of this complex sequestered both proteins preventing binding to their respective DNA response elements [395]. Since NF- κ B is known to be a key regulator of cell survival, direct antagonism of this pathway by ciglitazone could explain how this TZD triggered programmed cell death. Conversely Allred *et al* demonstrated that the same concentration of ciglitazone used by Chen *et al* induced PPRE-mediated transcription in HT29 cells [381]. The reason for this discrepancy is unclear, indicating that further confirmation of the role of PPAR γ in attenuation of NF- κ B transcriptional activity in this cell type is required.

Several studies have shown that the effective concentrations of rosiglitazone and pioglitazone required to reduce tumour progression in animal models are higher than those that would be used in of type II diabetes patients [396]. Nevertheless, similar doses of troglitazone were used to treat prostate and liposarcoma patients in small scale clinical trials but still had minimal side effects [366]. This indicates that TZDs even at higher doses have potential as an anti-cancer therapy. However, these findings do suggest two other approaches for future studies. Firstly, we need to discover how to maximize PPAR γ transactivation in tumour cells [394]. Secondly, identification of the TZD PPAR γ independent mechanism could lead to the development of PPAR γ ligands, which also target this pathway, without compromising PPRE-mediated transcription, and thus augment growth inhibition of cancers such as neuroblastoma.

4 THE EFFECT OF A PPAR γ DOMINANT-NEGATIVE MUTANT ON IMR-32 NEUROBLASTOMA CELLS *IN VITRO*

4.1 Introduction

Various approaches have been used to investigate if the cellular responses induced by PPAR γ ligands are mediated through their receptor, including PPAR γ antagonists, PPAR γ null cell lines, PPAR γ specific siRNA and PPAR γ dominant negative receptors [318,382,394]. Since in some cell types pharmacological PPAR γ antagonists have been shown to act as partial agonists, or exhibit cytotoxic effects which are distinct from their ability to abrogate PPAR γ transactivation, we decided to inhibit PPAR γ receptor activity in neuroblastoma cells by constitutive expression of a PPAR γ dominant negative receptor [397,398].

The PPAR γ dominant negative receptor used in our experiments was created by Gurnell *et al* by mutating leucine⁴⁶⁸ and glutamic acid⁴⁷¹ in the PPAR γ 1 AF-2 helix to alanine (L468A/E471A PPAR γ 1) [135]. The crystal structure of the PPAR γ ligand binding domain in complex with the co-activator SRC-1 demonstrates that leucine⁴⁶⁸ and glutamic acid⁴⁷¹ are both positioned at the co-activator interface [135]. The side chain of glutamic acid⁴⁷¹ forms hydrogen bonds with backbone amides of residues in the co-activator helix whereas leucine⁴⁶⁸ mediates interactions with the hydrophobic face of the co-activator [57] (**Fig. 4.2**). Therefore, although this PPAR γ receptor mutant is still effective at ligand and DNA binding, its transcriptional activity in the presence of the PPAR γ agonist rosiglitazone is negligible due to impaired co-activator recruitment [135]. Furthermore, the mutant receptor is an inhibitor of basal PPRE-mediated transcription and attenuates ligand dependent transactivation by wild-type PPAR γ [135]. In parallel with natural PPAR γ and other nuclear receptor variants, the artificial PPAR γ mutant, in the absence of ligand, had increased affinity for co-repressors such as SMRT compared with wild type PPAR γ and upon ligand binding exhibited delayed co-repressor release (**Fig. 4.1**) [176,399-402]. It is speculated that formation of interactions between co-activators and wild type PPAR γ

introduces steric constraints in the hydrophobic ligand binding domain which prevents accommodation of co-repressors that have longer helical binding domains [403]. Successive publications have demonstrated that the L468A/E471A PPAR γ 1 dominant negative receptor is a selective and potent inhibitor of PPAR γ signalling both *in vitro* and *in vivo* [135,394,404,405].

There were at least three aims of antagonising the PPAR γ pathway in neuroblastoma cells. Firstly, while a correlation between the level of PPARE-mediated transcription and the degree of growth inhibition caused by the natural PPAR γ ligand 15dPGJ₂ in neuroblastoma cells had been established it was necessary to determine if the anti-proliferative effect and accompanying cellular responses of 15dPGJ₂ were direct consequences of PPAR γ receptor activation. Secondly, although the synthetic PPAR γ ligand ciglitazone also attenuated the proliferation of neuroblastoma cells *in vitro*, ciglitazone concentrations that caused a growth inhibitory effect did not stimulate a PPAR responsive reporter in certain neuroblastoma cell lines. This suggested that ciglitazone could act through a PPAR γ -independent pathway. To test this hypothesis the effect of expression of a PPAR γ dominant negative receptor on ciglitazone action in neuroblastoma cells was studied. Thirdly, introduction of a PPAR γ dominant negative receptor in to colon cancer and smooth muscle cells was demonstrated to stimulate cell proliferation indicating that PPAR γ may function as a tumour suppressor *in vivo* [406,407]. This is in agreement with the finding that ectopic over-expression of PPAR γ in salivary gland, lung and pancreatic cancer cell lines attenuated their growth *in vitro* [304,408-410]. Therefore, the effect of constitutive expression of a PPAR γ dominant negative receptor on the proliferation of neuroblastoma cells was also investigated with the aim of providing insight in to its cellular role in this cancer.

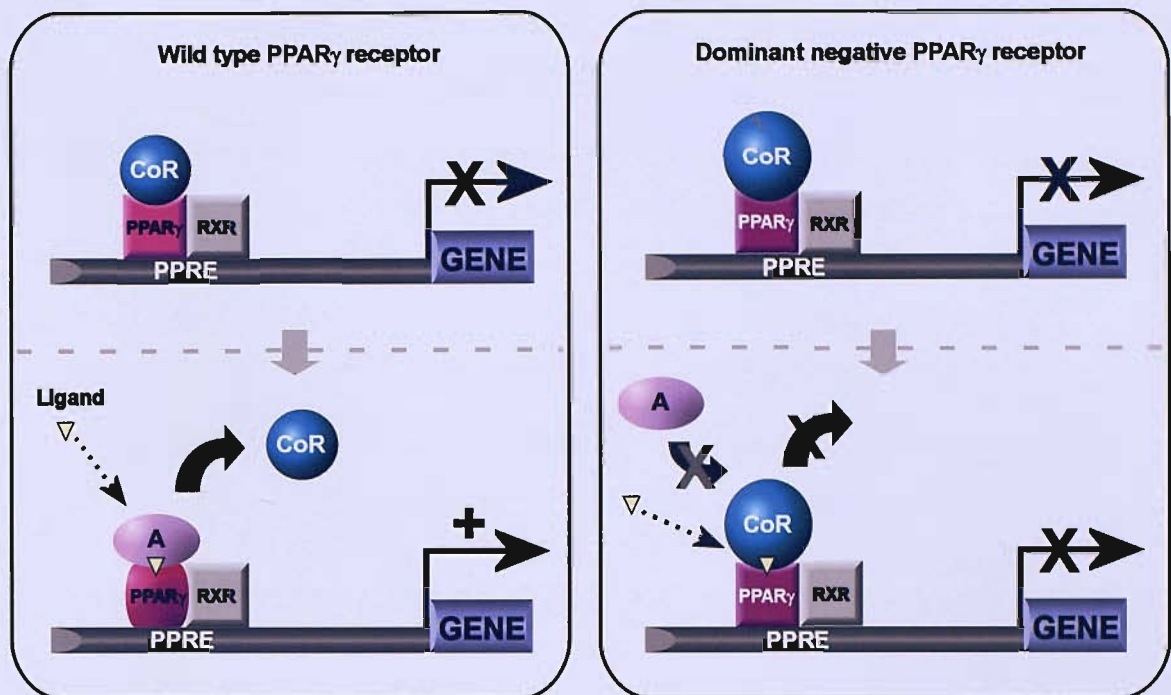


Fig. 4.1. Mechanism of action of the PPAR_γ dominant negative receptor.

In the absence of ligand, wild-type PPAR_γ, bound to a peroxisome proliferator response element (PPRE) in the promoter of a target gene, interacts with a co-repressor complex (CoR). Upon ligand binding (represented by the yellow triangle) the receptor undergoes a conformational change which leads to release of the co-repressor complex and promotes interaction with co-activators (A) stimulating gene transcription. The artificial PPAR_γ mutant receptor (L468A/E471A PPAR_γ1) retains the ability to recognise PPREs however, it has increased affinity for co-repressors in the absence of ligand so is a more potent inhibitor of ligand independent transcription. Although the PPAR_γ dominant negative receptor can efficiently bind ligand it displays delayed co-repressor release and impaired association with co-activators which attenuates ligand dependent transcription. Therefore, this mutant receptor is a dominant negative inhibitor of wild-type PPAR_γ because it can compete for ligand and DNA binding but exhibits aberrant interactions with co-repressors.

4.2 Establishment of IMR-32 neuroblastoma cells stably expressing a PPAR γ dominant negative receptor

To generate a neuroblastoma cell line stably expressing a PPAR γ dominant negative receptor IMR-32 cells were transfected with a pcDNA3 expression vector containing the DNA sequence encoding a FLAG epitope tag, in frame, upstream of full length human PPAR γ 1 cDNA with the substitutions L468A and E471A (pcDNAFlag- γ 1L468A/E471A). Control IMR-32 cells were transfected with an empty expression plasmid (pcDNA3.1). The pcDNA3 plasmid contains a neomycin resistance gene driven by the SV40 promoter for selection in mammalian cells with the antibiotic Geneticin (G418). Following the transfection IMR-32 cells were cultured for 72 hours and then incubated with G418 in fresh complete media. Transfected IMR-32 cells were selected by treatment with successive doses of G418 until clones, that were visible with the naked eye, were picked and cultured as separate cell lines. To verify which cell lines were stably expressing the mutant PPAR γ receptor, RNA was extracted from cells of each potential clone, reverse transcribed and then analysed by PCR. The forward primer used in the PCR was complementary to part of the DNA sequence of the FLAG epitope tag so expression of the dominant negative receptor could be distinguished from endogenous PPAR γ (Fig. 4.2). Expression of the PPAR γ mutant receptor was detected in two of the selected clones (3 and 8) which were cultured and used in subsequent experiments (Fig. 4.2). We decided to express the PPAR γ dominant negative receptor in the IMR-32 cell line, because of the human neuroblastoma cells, they exhibited the largest fold difference in EC₅₀ concentrations for 15dPGJ₂ and ciglitazone (EC₅₀ of 5 and 52 μ M respectively) and 15dPGJ₂ but not ciglitazone stimulated a PPAR responsive reporter in IMR-32 cells suggesting that these two PPAR γ ligands might be inducing their growth inhibitory effect by distinct mechanisms in this cell line.

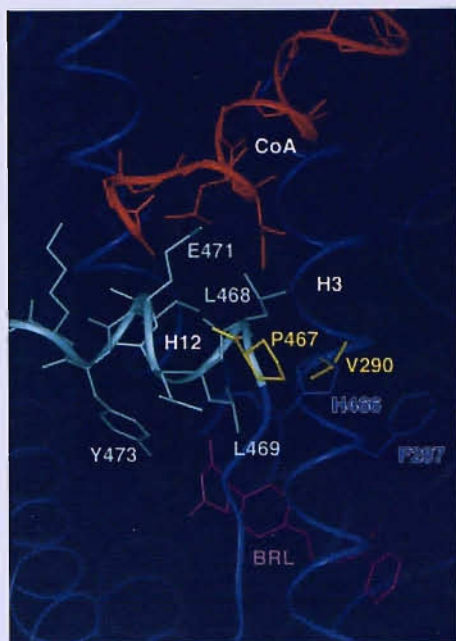
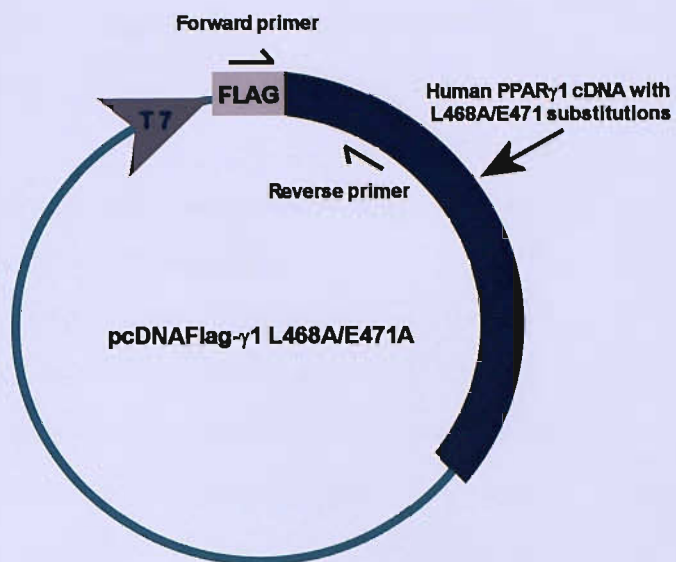
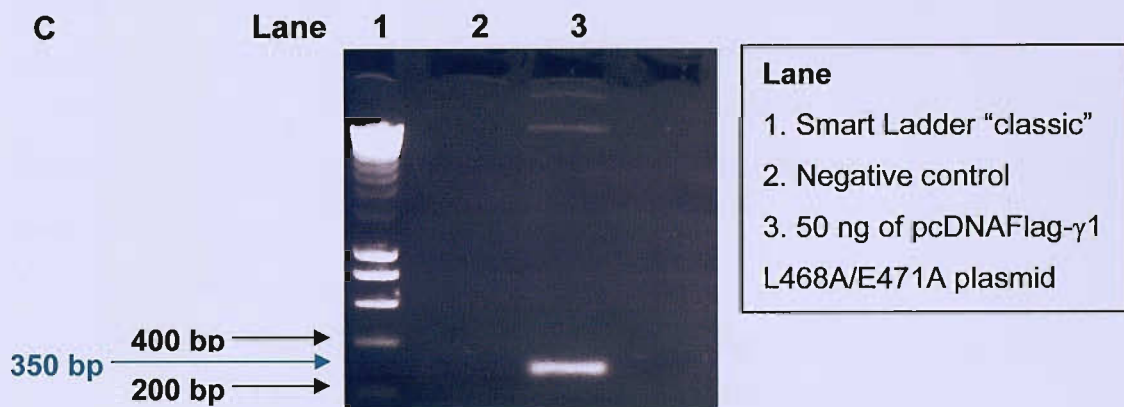
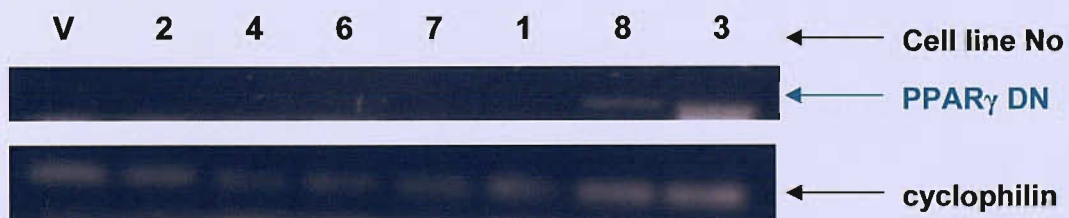
Fig. 4.2. Identification of IMR-32 clones stably expressing the PPAR γ dominant negative receptor.

A. View of the human PPAR γ ligand binding domain in complex with ligand (rosiglitazone shown in magenta) and the receptor interaction domain from the co-activator SRC-1 (CoA, in red). Note Leucine⁴⁶⁸ and glutamic acid⁴⁷¹ of helix 12 (shown in green) are both positioned at the co-activator interface [176]. Their mutation to alanine in the PPAR γ dominant receptor prevents co-activator binding.

B. Diagram showing the expression plasmid encoding the PPAR γ dominant negative receptor. The cDNA of the mutant receptor was cloned in frame downstream of a FLAG epitope tag. For RT-PCR a forward primer was designed so that it was complementary to part of the DNA sequence of the FLAG tag so expression of the dominant negative receptor could be distinguished from endogenous PPAR γ .

C. Results of PCR using 50 ng of the expression plasmid as the template to verify efficiency of primers. As predicted a PCR product of 350 bp was generated (**Lane 3**).

D. RNA was extracted from IMR-32 neuroblastoma cells of each potential clone, reverse transcribed and analysed by PCR. Clones 3 and 8 were shown to express the PPAR γ dominant negative receptor. A control PCR was carried out with cyclophilin specific primers to normalise cDNA levels. RNA extraction and RT-PCR reactions of potential IMR-32 stable cell lines was carried out by Dr Karen Lillycrop.

A**B****C****D**

4.3 The effect of the natural PPAR γ ligand 15dPGJ₂ on the growth of IMR-32 neuroblastoma cells stably expressing a PPAR γ dominant negative receptor

To determine if stable expression of a PPAR γ dominant negative receptor in IMR-32 cells would block growth inhibition by a PPAR γ ligand that is proposed to mediate this effect through its receptor, PPAR γ dominant negative clones 3 and 8 and vector only cells were plated out at 4×10^4 cells per well and treated with either a vehicle control (DMSO) or 5 μ M 15dPGJ₂ (EC₅₀ for this cell line). After 72 hours the total number of vehicle and 15dPGJ₂ treated cells for each independent cell line were measured. As shown in **Fig. 4.3** compared with vehicle treated cells, 15dPGJ₂ at a concentration of 5 μ M significantly attenuated the growth of IMR-32 vector only cells but not IMR-32 cells stably expressing the PPAR γ dominant negative receptor. Interestingly, proliferation of PPAR γ dominant negative clone 8 cells was significantly stimulated in the presence of 15dPGJ₂. These results corroborate the findings of Rodway *et al* in our group who demonstrated that 15dPGJ₂ induced growth arrest in IMR-32 cells was dependent on PPAR γ transcriptional activity, since transient transfection of PPRE decoy DNA, which competes with endogenous PPRE elements in the promoters of PPAR γ target genes for the activated receptor, blocked the decrease in cell number induced by 15dPGJ₂ (unpublished results).

4.4 Stable expression of a PPAR γ dominant negative receptor in IMR-32 neuroblastoma cells blocks stimulation of PPRE-mediated transcription by the natural ligand 15dPGJ₂

Gurnell *et al* have shown that in the presence of the L468A/E471A PPAR γ mutant, induction of endogenous wild-type PPAR γ -mediated transcription by the synthetic PPAR γ ligand rosiglitazone was clearly attenuated *in vitro* [135]. To

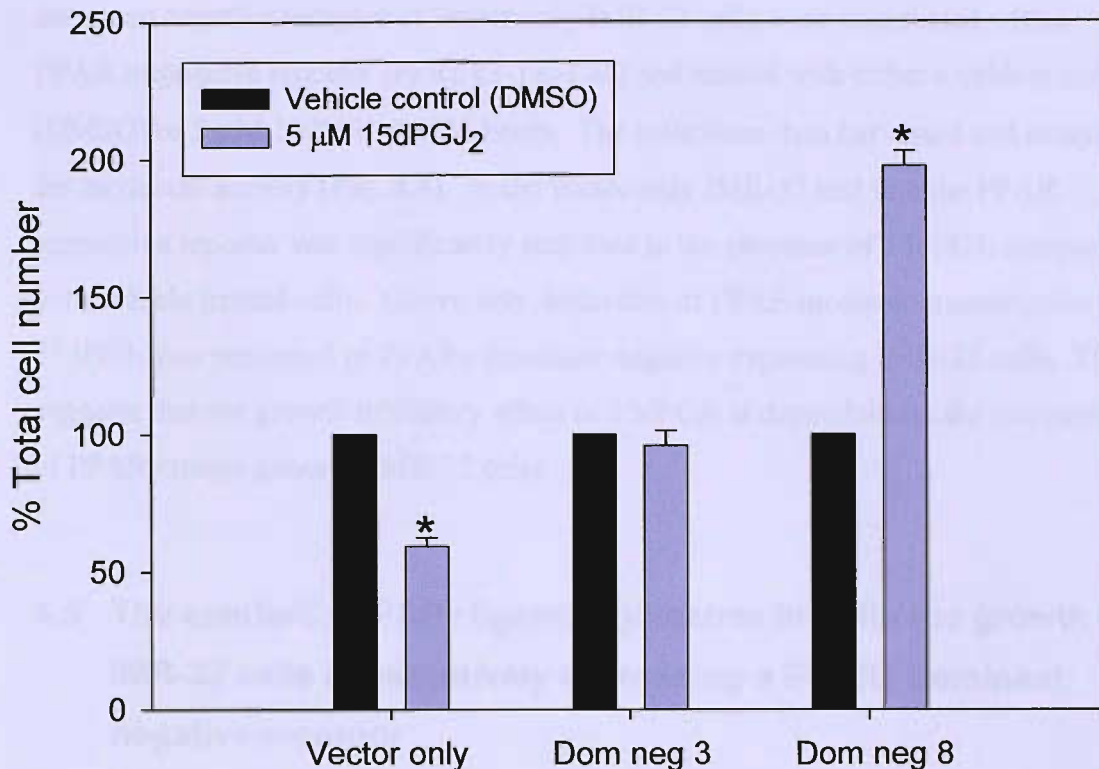


Fig. 4.3. The effect of expression of a PPAR γ dominant negative receptor on the response of IMR-32 neuroblastoma cells to the natural PPAR γ ligand 15dPGJ₂.

IMR-32 cells containing an empty expression vector or IMR-32 clones 3 and 8 stably expressing the PPAR γ dominant negative receptor were plated out in complete media in 6-well dishes at 4×10^4 cells per well and treated with either a vehicle control (DMSO) or 5 μ M 15dPGJ₂ (EC₅₀ concentration for this cell line). 72 hours post-treatment the total number of cells was determined by cell counting using a haemocytometer. Two samples were counted in duplicate per treatment. Data represents the mean percentage of the total cell number relative to the number of cells in the presence of the vehicle control (DMSO) \pm S.D. of two independent experiments. Statistics were calculated using a Student's *t*-test and demonstrated that the growth of IMR-32 vector only cells was significantly repressed by treatment with 5 μ M 15dPGJ₂ ($p < 0.05$) (*). In contrast, 15dPGJ₂ treatment of the PPAR γ dominant negative IMR-32 stable cell lines did not attenuate their growth. Indeed the total number of PPAR γ dominant negative clone 8 cells was significantly increased in the presence of 15dPGJ₂ ($p < 0.05$) (*).

confirm that this PPAR γ mutant also abrogated stimulation of PPRE-mediated transcription by 15dPGJ₂, IMR-32 cells constitutively expressing the PPAR γ dominant negative receptor or vector only IMR-32 cells were transfected with a PPAR responsive reporter (PPREx3-TK-Luc) and treated with either a vehicle control (DMSO) or 5 μ M 15dPGJ₂ for 24 hours. The cells were then harvested and assayed for luciferase activity (**Fig. 4.4**). In the vector only IMR-32 cell line the PPAR responsive reporter was significantly activated in the presence of 15dPGJ₂ compared with vehicle treated cells. Conversely, induction of PPRE-mediated transcription by 15dPGJ₂ was repressed in PPAR γ dominant negative expressing IMR-32 cells. This suggests that the growth inhibitory effect of 15dPGJ₂ is dependent on the activation of PPAR γ target genes in IMR-32 cells.

4.5 The synthetic PPAR γ ligand ciglitazone inhibits the growth of IMR-32 cells constitutively expressing a PPAR γ dominant negative receptor

We next sought further proof that the synthetic ligand ciglitazone regulates IMR-32 cell growth by PPAR γ independent mechanisms, by examining the effect of ciglitazone on the proliferation of IMR-32 cells constitutively expressing a PPAR γ dominant negative receptor. PPAR γ dominant negative clones 3 and 8 and vector only cells were plated out at 4×10^4 cells per well and treated with either a vehicle control (DMSO) or 52 μ M ciglitazone (EC₅₀ for this cell line). After 72 hours the total number of vehicle and ciglitazone treated cells for each independent cell line were counted (**Fig. 4.5**). The level of growth inhibition of the PPAR γ dominant negative stable cell lines achieved by ciglitazone was comparable with its effect on vector only cells (IMR-32 PPAR γ dominant negative cells = 44% inhibition; IMR-32 vector only cells = 48% inhibition). This indicates that induction of PPAR γ transcriptional activity is dispensable for ciglitazone to attenuate the proliferation of IMR-32 neuroblastoma cells.

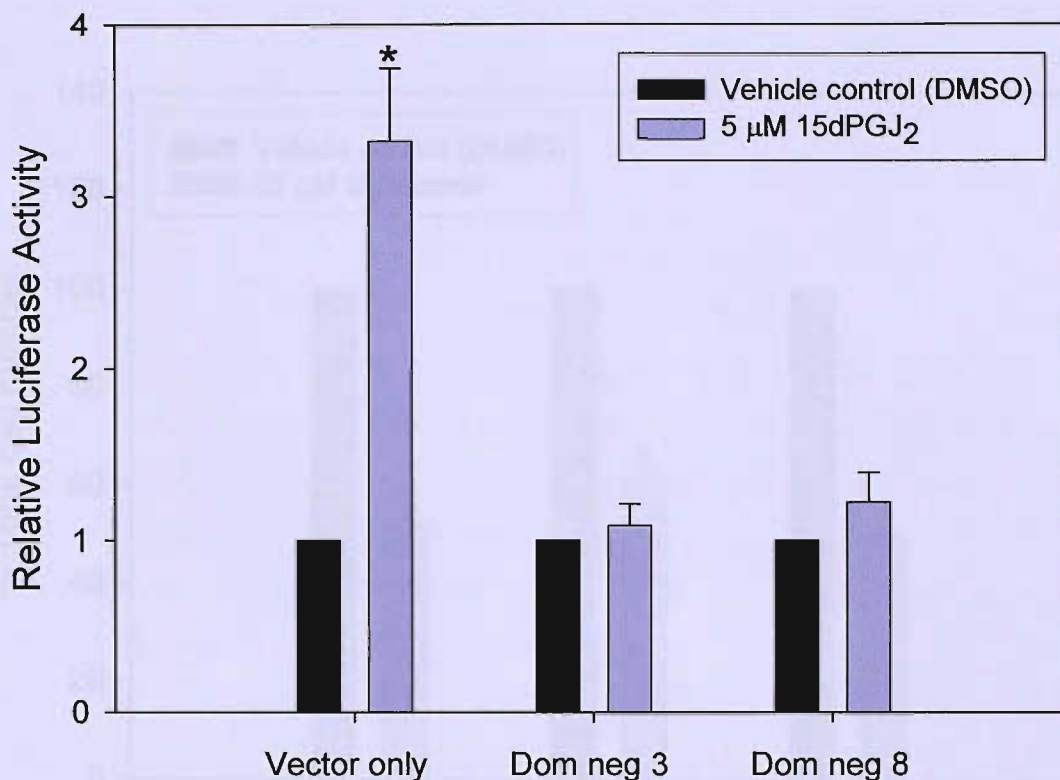


Fig. 4.4. The effect of expression of a PPAR γ dominant negative receptor on induction of PPRE-mediated transcription by 15dPGJ₂ in IMR-32 cells. IMR-32 cells containing an empty expression vector or IMR-32 clones 3 and 8 stably expressing the PPAR γ dominant negative receptor were transiently transfected with 2 μ g of a *Renilla* luciferase reporter construct under the control of three peroxisome proliferator response elements (PPREs) upstream of a thymidine kinase promoter (PPREx3-TK-Luc). Cells were treated with either DMSO (vehicle control) or 5 μ M 15dPGJ₂ (EC₅₀ concentration for this cell line) for 24 hours then harvested and luciferase activity measured. Data shows the mean relative luciferase activity of the PPREx3-TK-Luc reporter compared with its activity in vehicle DMSO treated IMR-32 cells, and represents two independent experiments \pm S.D. The activity of the PPREx3-TK-Luc construct was normalized for transfection efficiency and differences in cell number by co-transfecting IMR-32 cells with the firefly luciferase reporter, pGL3-Basic. Statistics were calculated using a Student's *t*-test and showed that compared with DMSO treated IMR-32 vector only cells, 15dPGJ₂ caused significant activation of the *Renilla* luciferase reporter driven by a PPRE-regulated promoter ($p < 0.05$)(*). In contrast, the PPAR responsive reporter was not significantly induced by 15dPGJ₂ in IMR-32 cells stably expressing the PPAR γ dominant negative receptor.

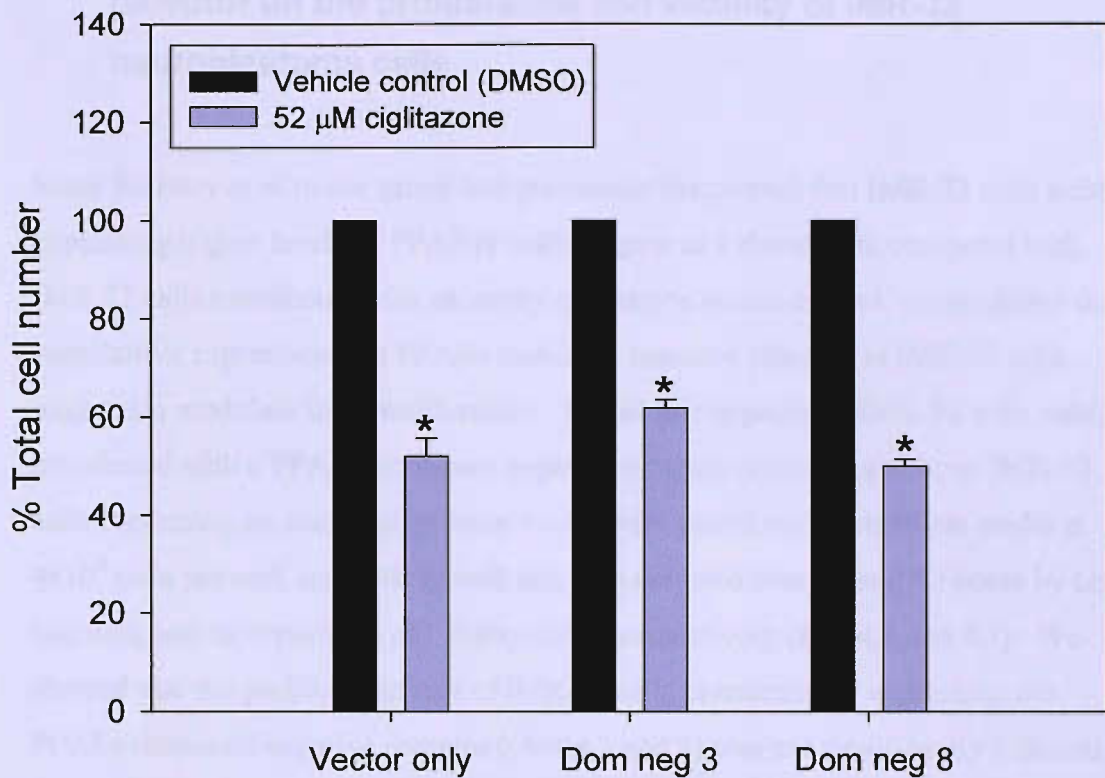


Fig. 4.5. The effect of expression of a PPAR γ dominant negative receptor on the response of IMR-32 neuroblastoma cells to the synthetic PPAR γ ligand ciglitazone.

IMR-32 cells containing an empty expression vector or IMR-32 clones 3 and 8 stably expressing the PPAR γ dominant negative receptor were plated out in complete media in 6-well dishes at 4×10^4 cells per well and treated with either a vehicle control (DMSO) or 52 μ M ciglitazone (EC_{50} concentration for this cell line). 72 hours post-treatment the total number of cells was determined by cell counting using a haemocytometer. Two samples were counted in duplicate per treatment. Data represents the mean percentage of the total cell number relative to the number of cells in the presence of the vehicle control (DMSO) \pm S.D. of two independent experiments. Statistics were calculated using a Student's *t*-test and demonstrated that the growth of IMR-32 vector only cells and IMR-32 cells expressing the PPAR γ dominant negative (clones 3 and 8) was significantly repressed by treatment with 52 μ M ciglitazone ($p < 0.05$) (*).

4.6 The effect of stable expression of a PPAR γ dominant negative receptor on the proliferation and viability of IMR-32 neuroblastoma cells

Since Rodway *et al* in our group had previously discovered that IMR-32 cells stably expressing higher levels of PPAR γ 1 mRNA grew at a slower rate compared with IMR-32 cells transfected with an empty expression vector control, we predicted that constitutive expression of a PPAR γ dominant negative receptor in IMR-32 cells might also modulate their proliferation. To test this hypothesis IMR-32 cells stably transfected with a PPAR γ dominant negative receptor (clones 3 and 8) or IMR-32 cells containing an empty expression vector were plated out in complete media at 4×10^4 cells per well and their growth rate was assessed over 96 and 72 hours by cell counting and incorporation of [3 H]thymidine respectively (**Fig. 4.6** and **4.7**). We showed that the proliferation rate of IMR-32 cells constitutively expressing the PPAR γ dominant negative receptor (clones 3 and 8) was not significantly different from the growth rate of vector only cells when measured by cell counting or [3 H]thymidine incorporation. Furthermore, examination of the three independent cell lines by trypan blue exclusion assay indicated that there was also no difference in the viability of PPAR γ dominant negative expressing IMR-32 cells compared to vector only cells (**Fig. 4.8**). We speculated that expression of the PPAR γ dominant negative receptor failed to alter IMR-32 cell growth because it did not have a significant effect on basal PPRE-mediated transcription. Therefore, to examine this possibility we compared basal PPAR γ activity in IMR-32 cells stably expressing the PPAR γ dominant negative receptor (clones 3 and 8) and vector only cells by transfecting them with a PPAR responsive reporter. We demonstrated that the level of basal PPRE-mediated transcription in IMR-32 cells constitutively expressing the PPAR γ dominant negative receptor and vector only cells was similar, which may account for why the PPAR γ mutant receptor did not affect the proliferation of IMR-32 cells (**Fig. 4.9**).

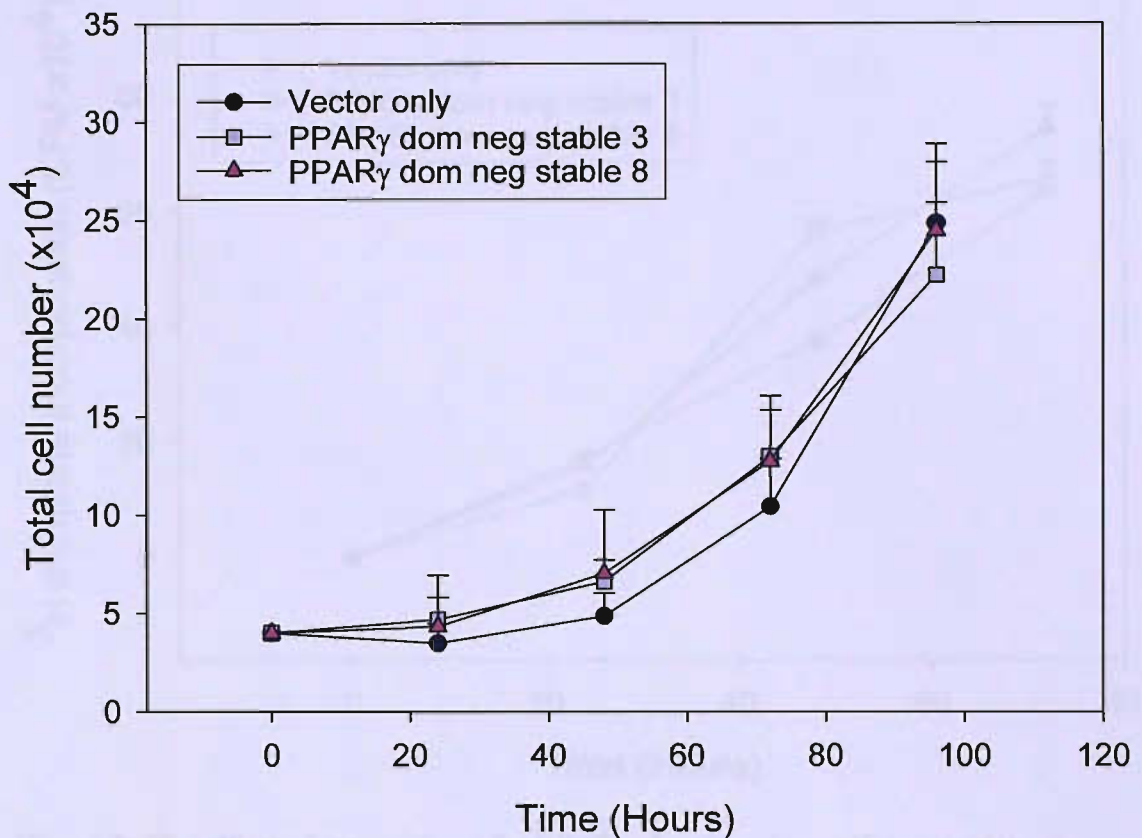


Fig. 4.6. The effect of expression of a PPAR γ dominant negative receptor on the growth of IMR-32 neuroblastoma cells. IMR-32 cells containing an empty expression vector or IMR-32 clones 3 and 8 stably expressing the PPAR γ dominant negative receptor were plated out in complete media in 6-well dishes at 4×10^4 cells per well and their growth was measured over 96 hours by cell counting using a haemocytometer. Two samples were counted in duplicate per treatment per day. Data represents the mean total cell number of 2 independent experiments \pm S.D. Statistics were calculated using a Student's *t*-test and showed that there was no significant difference in the proliferation of IMR-32 cells constitutively expressing the PPAR γ dominant negative receptor compared with IMR-32 vector only cells, as assessed by cell counting (significance level $p < 0.05$).

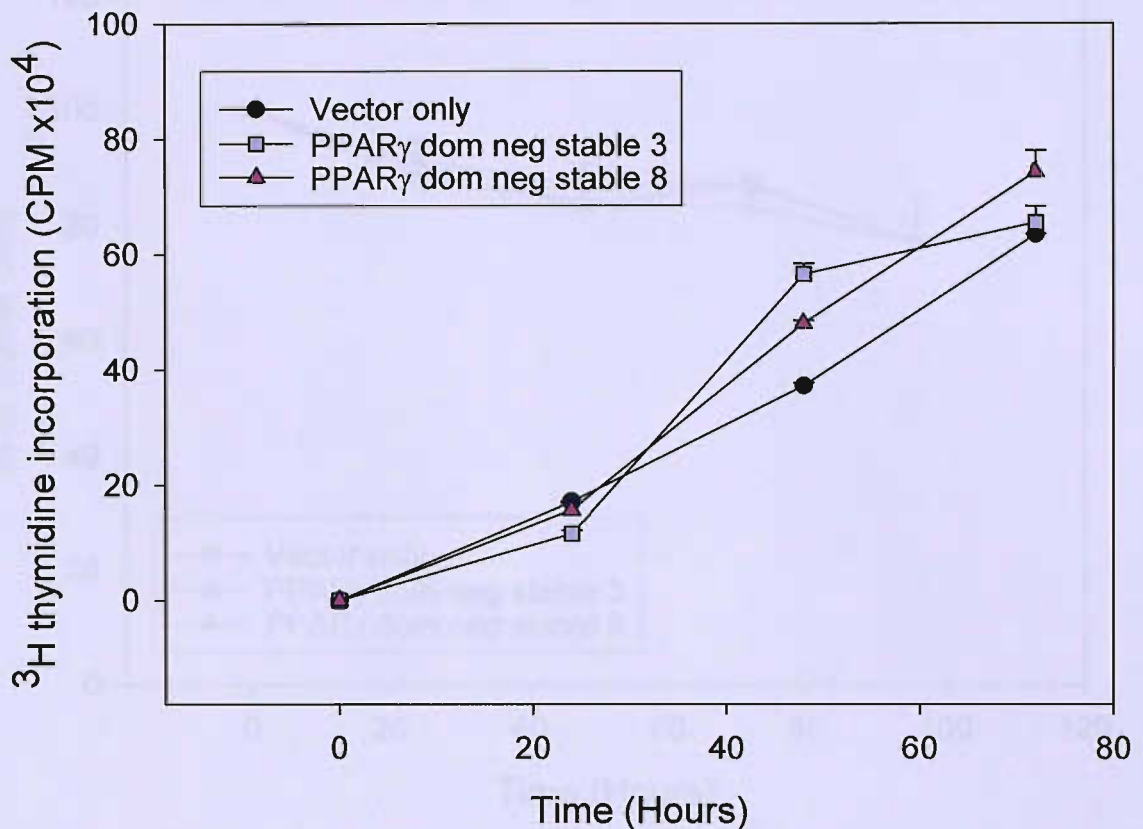


Fig. 4.7. The effect of expression of a PPAR_γ dominant negative receptor on [³H]thymidine incorporation in IMR-32 neuroblastoma cells over a 72-hour period. IMR-32 cells containing an empty expression vector or IMR-32 clones 3 (purple squares) and 8 (pink triangles) stably expressing the PPAR_γ dominant negative receptor were plated out in complete media in 6-well dishes at 4×10^4 cells per well and their growth was measured by detecting incorporation of [³H]thymidine over 72 hours. At each time point [³H]thymidine was added to two wells per cell line and after 18 hours the cells were lysed and duplicate aliquots per well were precipitated with TCA, collected to GF/C glass microfibre filters and counted using a scintillation counter. The data represents the mean of two independent experiments \pm S.D. Statistics were calculated using a Student's *t*-test and showed there was no significant difference in the growth of PPAR_γ dominant negative stable cell lines compared with IMR-32 vector only cells assessed by [³H]thymidine incorporation (significance level $p < 0.05$).

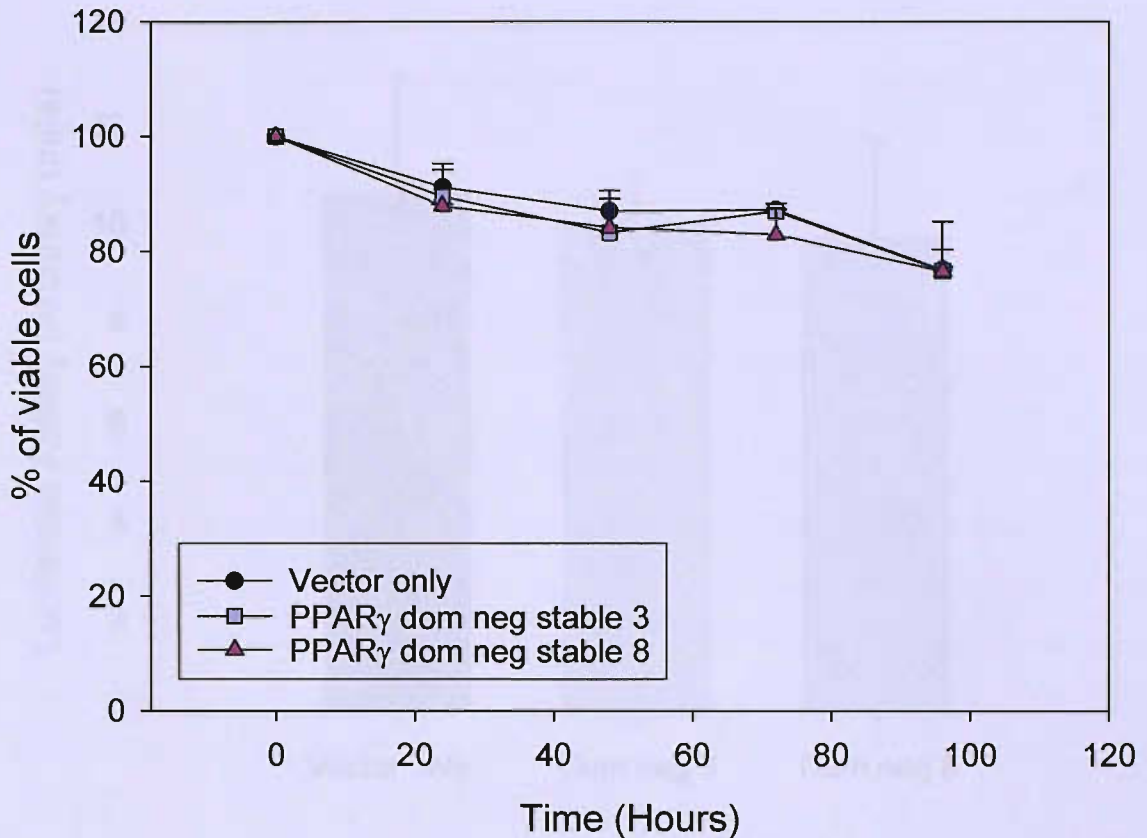


Fig. 4.8. The effect of expression of a PPAR γ dominant negative receptor on the viability of IMR-32 neuroblastoma cells. IMR-32 cells containing an empty expression vector or IMR-32 clones 3 (purple squares) and 8 (pink triangles) stably expressing the PPAR γ dominant negative receptor were plated out in complete media in 6-well dishes at 4×10^4 cells per well and cell viability was monitored over 96 hours by trypan blue exclusion assay. Two samples were counted in duplicate per treatment per day using a haemocytometer. Data are expressed as the mean % of viable cells (trypan blue negative) relative to the total number of cells counted per well and represent two independent experiments \pm S.D. Statistics were calculated using a Student's *t*-test and showed that there was no significant difference in the viability of PPAR γ dominant negative stable cell lines (clones 3 and 8) compared with IMR-32 vector only cells during the 96 hour time course (significance level $p < 0.05$).

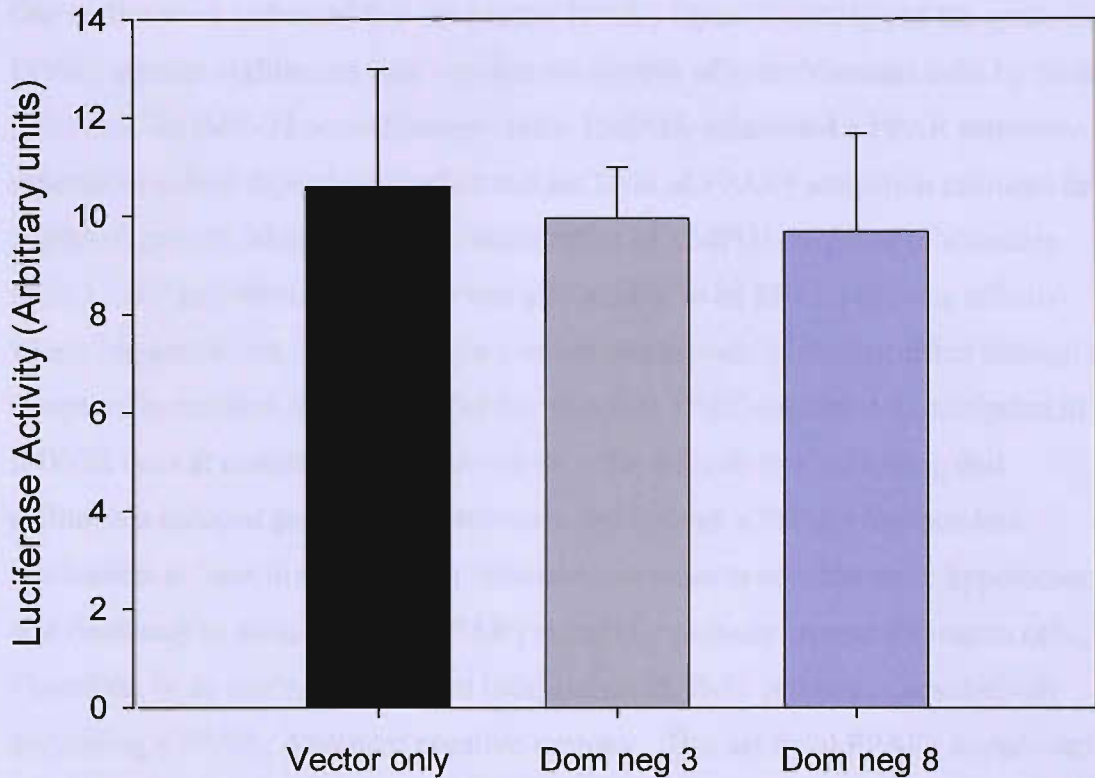


Fig. 4.9. The effect of expression of a PPAR γ dominant negative receptor on basal PPAR γ activity in IMR-32 neuroblastoma cells. IMR-32 cells containing an empty expression vector or IMR-32 clones 3 and 8 stably expressing the PPAR γ dominant negative receptor were transiently transfected with 2 μ g of a *Renilla* luciferase reporter construct under the control of three peroxisome proliferator response elements (PPREs) upstream of a thymidine kinase promoter (PPREx3-TK-Luc). Cells were harvested after 24 hours and luciferase activity measured. Data shows the mean luciferase activity of the PPREx3-TK-Luc reporter (arbitrary units) for each cell line after normalizing its activity (relative to that of the control plasmid pGL3-Basic) for differences in transfection efficiency and cell number and represents two independent experiments \pm S.D. Statistics were calculated using a Student's *t*-test and showed that there was no significant difference in the level of luciferase activity of the PPAR responsive reporter in IMR-32 cells stably expressing the PPAR γ dominant negative receptor (clones 3 and 8) compared the activity of the reporter in IMR-32 vector only cells (significance level $p < 0.05$).

4.7 Discussion

Our earlier work indicated that the natural PPAR γ ligand 15dPGJ₂ and the synthetic PPAR γ agonist ciglitazone may regulate the growth of neuroblastoma cells by distinct pathways. In IMR-32 neuroblastoma cells, 15dPGJ₂ stimulated a PPAR responsive reporter in a dose dependent manner and the level of PPAR γ activation mirrored the degree of growth inhibition. The concentration of 15dPGJ₂ required to attenuate IMR-32 cell proliferation by 50 % was also similar to its PPAR γ binding affinity which suggested that 15dPGJ₂ might mediate this growth inhibitory effect through its receptor. In contrast, ciglitazone did not stimulate PPRE-mediated transcription in IMR-32 cells at concentrations near its EC₅₀ for this cell line indicating that ciglitazone induced growth inhibition occurred through a PPAR γ independent mechanism at least in this cell type. However, in order to confirm these hypotheses it was necessary to antagonise the PPAR γ signalling pathway in neuroblastoma cells. Therefore, to do this we established independent IMR-32 cell lines constitutively expressing a PPAR γ dominant negative receptor. This artificial PPAR γ mutant can efficiently bind DNA and ligand but abrogates transcription by wild-type PPAR γ by showing delayed co-repressor release and inability to recruit co-activators upon ligand binding (**Fig. 4.1**) [135].

IMR-32 cells stably expressing the PPAR γ dominant negative receptor were resistant to growth inhibition by 15dPGJ₂. Furthermore, activation of a PPAR responsive reporter by 15dPGJ₂ was inhibited in the presence of the PPAR γ dominant negative receptor. Conversely, attenuation of growth by ciglitazone was not alleviated in PPAR γ dominant negative stable cell lines compared with vector only cells. In summary, it can be concluded that PPAR γ transactivation is critical for growth arrest by 15dPGJ₂ in IMR-32 cells although is not essential for ciglitazone induced growth inhibition. These results are consistent with findings of separate studies which showed that the anti-proliferative, cytotoxic or anti-inflammatory properties of other TZDs such as troglitazone or rosiglitazone, in certain cell types, were not blocked by transfection with a PPAR γ dominant negative receptor [394,405,411,412]. Therefore, in the future this approach could be used to investigate the dependence of 15dPGJ₂ and ciglitazone on their receptor to mediate growth inhibition of other neuroblastoma cell lines.

Although constitutive expression of a PPAR γ dominant negative receptor attenuated induction of PPRE-mediated transcription and growth inhibition by an exogenous ligand (15dPGJ₂) it did not have a significant effect on basal PPAR γ receptor activity or the proliferation rate of IMR-32 cells. It is possible that the PPAR γ dominant negative receptor was not expressed at a sufficient level to influence the growth of IMR-32 cells. The expression of the PPAR γ dominant negative receptor in IMR-32 cells might be increased by placing the DNA encoding the L468A/E471A PPAR γ 1 under the control of a stronger promoter. It is however unlikely that the expression level of the PPAR γ dominant negative receptor alone can account for its inability to modulate IMR-32 cell growth.

An alternative hypothesis is that the PPAR γ dominant negative receptor is less effective at inhibiting endogenous ligand dependent transcription. *In vitro*, the PPAR γ mutant receptor was shown to efficiently bind the synthetic PPAR γ agonist rosiglitazone, therefore it was predicted that it would also compete with the wild-type receptor for endogenous ligands [135]. Furthermore, adenoviral transfer of a PPAR γ dominant negative receptor inhibited rosiglitazone induced adipogenesis in murine 3T3-L1 fibroblasts and primary human preadipocytes [135,169]. Nevertheless the PPAR γ dominant negative may be less able to interact with endogenous ligands in neuroblastoma cells, so that although the mutant receptor still recognises PPAR response elements and competes with normal PPAR γ for DNA binding, its dominant negative action might be impaired by its failure to sequester endogenous ligands. The identity of genuine endogenous ligands of PPAR γ is uncertain, therefore until they are discovered it will not be possible to compare their affinity for the PPAR γ dominant receptor with synthetic PPAR γ agonists [102,413].

In addition, if PPAR γ does function as a tumour suppressor, its transcriptional activity in neuroblastoma cells may already be abrogated to facilitate development of the malignant phenotype. Therefore, the effect of an artificial PPAR γ dominant negative receptor on endogenous PPAR γ -mediated transcription and proliferation in neuroblastoma cells would be less discernible or negligible because the endogenous receptor is already inactivated. PPAR γ transcriptional activity in neuroblastoma cells could be compromised by a variety of mechanisms including post-translational

modifications like phosphorylation or sumoylation or expression of a natural PPAR γ variant such as γ ORF4 or PPAR γ 1_{tr} [67,74,83,233,234,389] (see also section 1.12.4.1). Further study is warranted to determine if neuroblastoma cells express a natural PPAR γ variant that has dominant negative action over wild-type PPAR γ . It is plausible that treatment of neuroblastoma cells with exogenous PPAR γ ligands might overcome transcriptional repression mediated by a natural PPAR γ dominant negative receptor thus promoting growth arrest by wild-type PPAR γ . This reasoning is supported by functional studies which have shown that *in vitro* higher concentrations of ligand can alleviate dominant-negative inhibition by thyroid hormone β -receptor mutants found in the syndrome of resistance to thyroid hormone (RTH) and that administration of thyroid hormone at doses above its physiological level can restore target tissue sensitivity *in vivo* [108]. If neuroblastoma cells are shown to express a PPAR γ variant it would be interesting to develop an inducible RNA interference system or anti-sense approach to specifically repress expression of the mutant to examine its effect on the action of the wild-type receptor[414,415].

More insight in to cellular role of PPAR γ in neuroblastoma may also be gained through further studies on neuroblastoma cells constitutively over-expressing PPAR γ . To date only the effect of increased PPAR γ expression on the growth rate of neuroblastoma cells has been investigated. However, in addition to proliferating at a faster rate, transformed cells also have the ability to grow in the absence of solid support and invade adjacent tissues [416,417]. Therefore, the effect of modifying the expression of PPAR γ on the capacity of neuroblastoma cells to grow in an anchorage independent manner could be investigated by comparing formation of colonies in soft agar derived from PPAR γ -over-expressing neuroblastoma cells with cells containing the empty vector control[417]. The effect of increased PPAR γ expression on the invasiveness of neuroblastoma cells could be observed *in vitro* by testing their ability to invade through a filter coated with basement membrane Matrigel[416]. If these studies demonstrate that PPAR γ can negatively regulate the growth and behaviour of neuroblastoma cells *in vitro*, then ultimately the effect of constitutive over-expression of PPAR γ on cancer progression *in vivo* must be demonstrated to lend to support the hypothesis that PPAR γ functions as a tumour suppressor.

5 REGULATION OF PPAR γ EXPRESSION IN NEUROBLASTOMA CELLS

5.1 Introduction

Following the discovery that PPAR γ was a major regulator of adipogenesis, expression of the PPAR γ receptor was also implicated in modulating the differentiation of colon epithelium cells, monocytes and trophoblasts [159,184,185,212,418-420]. In all three cell types, higher PPAR γ levels were associated with a more mature phenotype. Furthermore, PPAR γ expression has been correlated with the differentiation status of cells from several human malignancies including colon carcinoma, liver carcinoma and neuroblastoma [197,212,213]. Immunohistochemistry performed on paraffin sections of primary human neuroblastoma tissues revealed that PPAR γ protein was high in neuroblasts with ganglionic differentiation but low or undetectable in primitive neuroblasts [213]. Although these findings suggest a potential role for PPAR γ in neuroblastoma differentiation, the precise function of the receptor in this cancer is unclear. Therefore, we investigated the factors which regulate PPAR γ expression in order to further our understanding of the cellular role of PPAR γ in neuroblastoma.

5.2 Organisation of the human PPAR γ gene

Characterisation of the human PPAR γ gene structure has revealed that it contains nine exons and extends over more than 140 Kb of genomic DNA [36]. Four mRNAs of PPAR γ have been identified, termed γ 1, γ 2, γ 3 and γ 4. The mRNA of the PPAR γ 1 isoform is encoded by eight exons, two exons called A1 and A2 which contain its 5' untranslated region and 6 coding exons (exons 1-6) which are common to all four isoforms [17]. The PPAR γ 1 promoter and initiation start sites for the PPAR γ 1 mRNA are located more than 90 Kb upstream from the PPAR γ 1 start codon in exon 1 (**Fig. 5.1**). This is because of three large introns greater than 20 Kb in size between exons A1, A2, B and 1[36]. The PPAR γ 2 mRNA comprises seven exons, including

exon B, (located between exons A2 and 1) which encodes its 5' untranslated region, start codon and the additional 28 N-terminal amino acids found in the PPAR γ 2 protein. The PPAR γ 3 and PPAR γ 4 mRNA translates in to the same protein as PPAR γ 1 but their transcription is regulated by alternative promoters located in the 5' flanking regions of exon A2 and exon 1 respectively [38] [39]. The PPAR γ 2, PPAR γ 3 and PPAR γ 4 transcripts have a restricted tissue distribution. Significant expression of PPAR γ 2 and PPAR γ 4 only occurs in adipocytes although PPAR γ 3 has also been detected in colon epithelium and macrophages [38]. Conversely, PPAR γ 1 mRNA is widely expressed in human tissues [28,36,43,44]. Elevated expression of PPAR γ protein during the differentiation of specific cell types is a consequence of increased PPAR γ transcription. For instance, expression of PPAR γ 1 and PPAR γ 2 transcripts is stimulated during adipogenesis whereas PPAR γ 1 mRNA but not PPAR γ 2 mRNA is induced in colon epithelium and macrophage differentiation [38,40,42,45,418,421-425]. Furthermore, PPAR γ transcription is regulated by promoter activation rather than modulation of mRNA stability [36,42,422,426]. Therefore, since PPAR γ 1 mRNA is the major isoform found in normal and malignant human tissues, our first objective was to investigate if PPAR γ expression in neuroblastoma cells is modulated by the level of PPAR γ 1 promoter activity.

5.3 The PPAR γ 1 promoter is differentially activated in human neuroblastoma cells

The findings by Han *et al* which showed that PPAR γ protein expression correlated with the differentiation stage of primary neuroblastoma cells are supported by the observation that neuroblastoma cell lines have very different levels of PPAR γ mRNA. For instance, SK-N-AS neuroblastoma cells express more PPAR γ mRNA than IMR-32 neuroblastoma cells (unpublished data by Emma Phillips). To evaluate if the differences detected in PPAR γ transcription in neuroblastoma cell lines are governed by the level of promoter activation, IMR-32 and SK-N-AS neuroblastoma cells were transiently transfected with a PPAR γ 1 promoter reporter (pGL3- γ 1p3000) using calcium phosphate. To account for differences in transfection efficiency between the neuroblastoma cell lines, the PPAR γ 1 promoter reporter luciferase expression was determined relative to the activity of the pGL3-Basic vector, which lacks a eukaryotic

promoter and enhancer sequence. As shown in **Fig. 5.2**, the luciferase activity of the pGL3- γ 1p3000 construct was 4-fold and 10-fold higher compared to pGL3-Basic in IMR-32 and SK-N-AS cells, respectively. The variation in the activity of the PPAR γ 1 promoter reporter mirrored the difference observed in the endogenous levels of PPAR γ mRNA in these two cell lines, demonstrating that PPAR γ transcription is modulated by the level PPAR γ 1 promoter stimulation in neuroblastoma cells. Therefore we wanted to determine the factors responsible for differential PPAR γ 1 promoter activity in neuroblastoma cells *in vitro* since this might provide insight in to the cellular role and regulation of PPAR γ expression in neuroblastoma *in vivo*.

5.4 Characterisation of the human PPAR γ 1 promoter

To identify transcription factors, which could be important in controlling the level of PPAR γ 1 expression in neuroblastoma cells, the DNA sequence from -2.8 kb to +20 relative to the second transcription start site of PPAR γ 1 was analysed using MatInspector to identify putative regulatory elements (www.genomatrix.de/) [427,428] (See also **Appendix**). **Fig. 5.3** highlights potential binding sites in this 5'regulatory region of PPAR γ 1 which could modulate its activity in neuroblastoma cells. These sites, and more listed in the appendix, were initially considered because of the known function and tissue distribution of the transcription factors which bind to them. Among these regulatory binding motifs, were two putative E-boxes (-2780 and -720) which are directly bound by Myc-Max heterodimers and stimulates gene transcription. However, there were also several sites which are proposed to mediate c-Myc transcriptional repression by indirectly recruiting c-Myc, including nuclear transcription factor-Y (NF-Y), elongation 2 factor (E2F) and specificity factor 1 (Sp1) sites and two potential initiator (INR) elements. As the MatInspector tool does not search for potential INR elements we compared the PPAR γ 1 5'regulatory region with the INR consensus sequence which revealed two putative INR close to the second PPAR γ 1 transcription start site.

5.5 Myc regulation of PPAR γ 1 expression in neuroblastoma cells

The Myc family of proto-oncogenes, includes *c-myc*, *N-myc* and *L-myc* which encode basic-helix-loop-helix leucine zipper (bHLHZ) transcription factors [429]. *c-Myc* has been established as a key regulator of normal cell proliferation, cell cycle progression and differentiation [430]. Normally *c-Myc* expression is tightly controlled and correlates with the proliferative status of the cell [431]. *c-myc* is an early growth response gene whose expression is induced in response to mitogens which in turn stimulates cell growth prior to cell division [432-434]. Associated with, but distinct from *c-Myc*'s role in cell growth, is *c-Myc*'s ability to promote the transition from G₁ to S phase of the cell cycle [432]. In contrast, down-regulation of *c-Myc* levels is commonly observed in cells that undergo differentiation [435-437]. Interestingly, ectopic expression of *c-Myc* prevents the terminal differentiation of several cell types including adipocytes *in vitro* suggesting that *c-Myc* may actively repress differentiation programs [438,439].

Our understanding of how *c-Myc* regulates these cellular processes was considerably advanced when it was demonstrated that Myc family members interact, via their helix-loop-helix and leucine zipper motifs, with another bHLHZ protein called MAX (*c-Myc* associated protein X) [429,433,435,440,441]. Formation of this heterodimer is essential for Myc DNA binding and recognition of a sequence termed an E-box with the consensus CAC GTG found in the promoters of some Myc target genes [442]. Each basic region in the Myc-Max heterodimer makes four specific DNA base contacts with the E box as well as numerous phosphate backbone contacts [442]. It had earlier been established that the N-terminal region of *c-Myc* contained a transactivation domain and when *c-Myc* was in complex with Max it could induce expression from a reporter gene under the control of a promoter containing multiple E-box sites [429,435]. Although many putative *c-Myc* target genes were identified it initially proved difficult to verify those that were directly regulated by *c-Myc*. However, the recent development of chromatin immunoprecipitation assays and CpG island arrays have helped to validate if *c-Myc* does indeed bind to the endogenous 5' regulatory regions of these genes *in vivo* [443]. These approaches have shown that *c-Myc* directly activates the expression of genes which drive transition from G₁ to S phase of the cell cycle such as the phosphotyrosine phosphatase *cdc25*, in addition to numerous genes which encode metabolic enzymes and protein factors involved in protein synthesis which would stimulate cell growth [433,443].

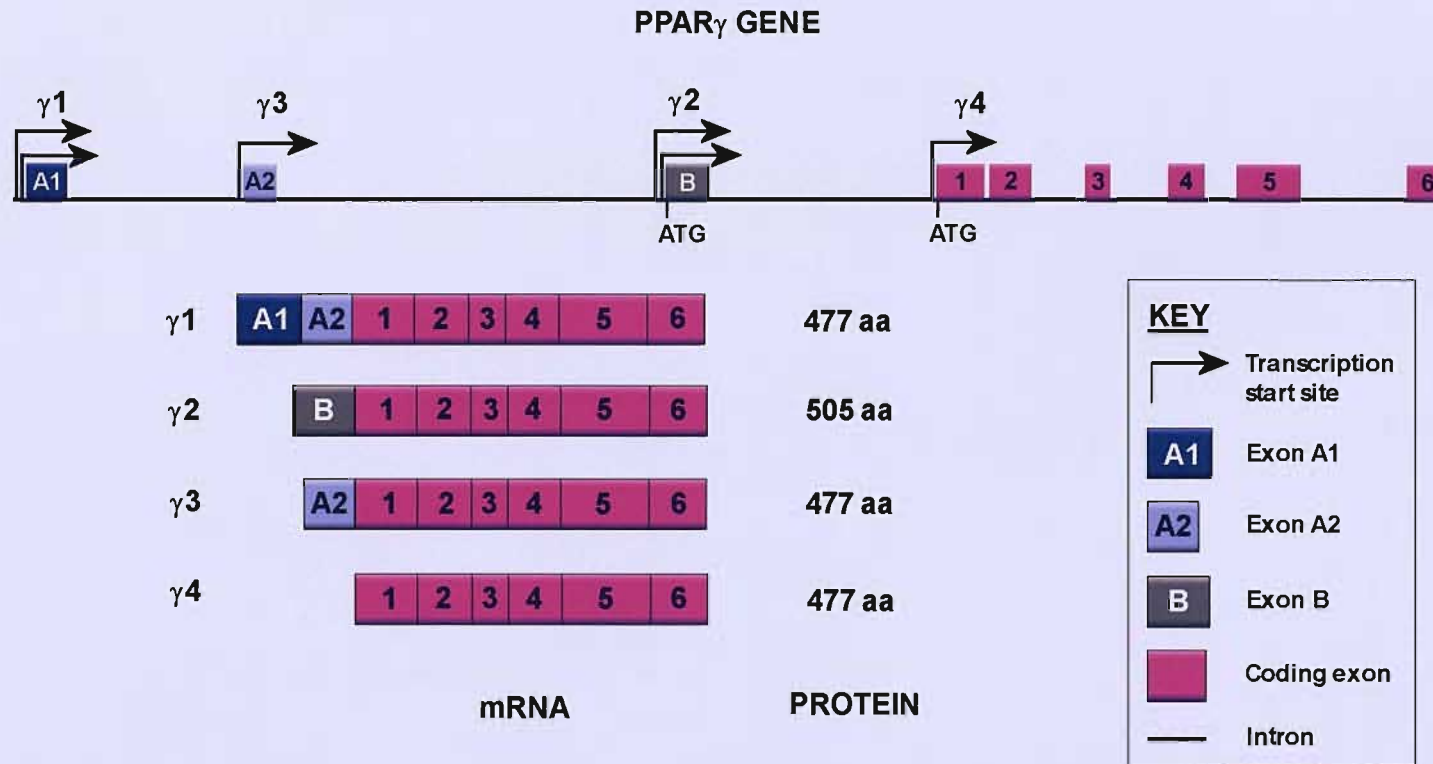


Fig. 5.1. Organisation of the human PPAR γ gene. Four PPAR γ mRNAs have been discovered termed $\gamma 1$, $\gamma 2$, $\gamma 3$ and $\gamma 4$. Common to all 4 transcripts are six coding exons (pink boxes). Exons A1 and A2 are specific to PPAR $\gamma 1$ and encode its 5'untranslated region. The PPAR $\gamma 1$ promoter and transcription start sites (black arrows) of the PPAR $\gamma 1$ mRNA are located more than 90 kb upstream of its start codon in exon 1 due to 3 large introns (solid black lines), between exons A1, A2, B and 1. The PPAR $\gamma 2$ mRNA contains Exon B which encodes its start codon and the extra 28 N-terminal amino acids found in the PPAR $\gamma 2$ protein. The PPAR $\gamma 3$ and PPAR $\gamma 4$ mRNAs encode the same protein as PPAR $\gamma 1$ but their expression is controlled by alternative promoters located in the 5'flanking regions of exon A2 and 1 respectively. The four PPAR γ transcripts are depicted and the size of the protein they encode is indicated.

Increasing evidence suggests that c-Myc stimulates gene transcription by recruiting a co-activator complex which modifies the chromatin structure of the target gene's promoter making it more accessible to the RNA Pol II pre-initiation complex [429,432,444]. For instance, the N-terminus of c-Myc through its association with the 434 kDa cofactor TRRAP (Transformation/transcription co-factor-domain-Associated Protein) recruits GCN5 (general control of amino acid biosynthesis protein 5) which has histone acetyltransferase (HAT) activity [445-447]. c-Myc binding of a TRRAP containing complex was detected at the promoters of several of its target genes, including cyclin D2 *in vivo* and was specifically correlated with acetylation of histone H4, which is often found at genes which are being actively transcribed [448,449]. In addition, the c-Myc bHLHZ motif interacts with INI1 (integrase interactor 1) a human homologue of the yeast protein SNF5 (sucrose non-fermenting 5) which is a subunit of the SWI/SNF ATP-dependent remodelling complex that induces nucleosomes to slide along DNA [450] [429,432]. Other protein partners of c-Myc that have been implicated in chromatin remodelling include TIP48 and TIP49 (TATA-binding protein-interacting proteins 48 and 49) which have the ability to hydrolyse ATP and are predicted to have helicase activity [429,432]. However, microarray analysis of fibroblasts and endothelial cells following ectopic expression of c-Myc has revealed that the mRNA levels of several genes encoding proteins involved in cell cycle control, adhesion, signalling and differentiation are down-regulated [451,452] [453] and it is now known that c-Myc can also function as a repressor of gene transcription [454].

c-myc, *N-myc* and *L-myc* have all been identified as proto-oncogenes and their deregulated expression is associated with the genesis of a wide variety of human malignancies [285]. For example, c-Myc over-expression is frequently observed in human breast, colon, gynaecological and hepatocellular carcinomas [455]. Current figures suggest that in total Myc activation occurs in around 70% of human cancers and occurs through diverse mechanisms including chromosomal translocations, gene amplifications, enhanced translation or stabilisation of the Myc protein [442,456]. Amplification of *N-myc* is reported in around a third of cases neuroblastoma and predominantly occurs in patients with advanced staged disseminated disease, where it correlates with poor prognosis [244,288]. Interestingly several studies have detected expression of both *N-Myc* and *c-Myc* mRNA and protein in primary neuroblastoma

tissue and differentiation of neuroblastoma cells *in vitro* is accompanied by decreased levels of N-Myc and c-Myc [457-460]. Furthermore, in partially differentiated heterogeneous neuroblastomas with N-Myc gene amplification, elevated N-Myc levels only occurred in primitive neuroblasts and not in differentiated ganglionic cells [287].

Therefore, PPAR γ levels appear to be inverse to Myc expression in primary neuroblastoma tissues, since PPAR γ expression was higher in neuroblastoma cells with a more differentiated phenotype, suggesting that Myc family members could negatively regulate PPAR γ expression in neuroblastoma cells [213]. This is supported by the initial finding that human PPAR γ 1 promoter reporter activity was higher in SK-N-AS neuroblastoma cells which have a single N-Myc copy number compared with promoter reporter activity in IMR-32 cells which originated from an N-Myc amplified tumour. However, since the human PPAR γ 1 promoter has potential sites through which c-Myc could either activate or repress PPAR γ 1 transcription it was first necessary to investigate what effect Myc family members have on the activity of the PPAR γ 1 promoter in neuroblastoma cells *in vitro*. Therefore, SK-N-AS neuroblastoma cells were co-transfected with a PPAR γ 1 promoter reporter (pGL3- γ 1p3000) and increasing concentrations of human c-Myc or N-myc expression plasmids, as indicated in **Fig. 5.4**, with the amount of DNA for each transfection normalised with an empty expression vector (pcDNA3.1).

The effect of different Myc concentrations was studied, as previous investigations have shown that Myc can cause biphasic regulation of promoters which contain both E-box and INR elements, where low c-Myc levels stimulated expression, whereas higher levels of c-Myc caused transcriptional repression which was INR-dependent [461]. The cells were harvested 24 hours after transfection and luciferase activity measured. **Fig. 5.4** shows the luciferase activity of the PPAR γ 1 promoter reporter was significantly attenuated in the presence of 0.1 and 2 μ g of c-Myc or N-Myc expression plasmids relative to the luciferase activity of the reporter in the presence of the empty expression vector control. This suggests repression of the human PPAR γ 1 promoter by Myc family members dominates any activation that may occur through the E-boxes at positions -2780 and -725 or that these putative E-boxes are non-functional. Since c-Myc and N-Myc are structurally homologous and are

proposed to regulate gene transcription by similar mechanisms it was decided to initially focus on how c-Myc represses PPAR γ 1 transcription in neuroblastoma cells [285,462].

5.6 The mechanism of c-Myc transcriptional repression

In contrast to the current model of c-Myc transactivation, the mechanism of repression of gene transcription by c-Myc has remained elusive [454]. Early studies suggested that transcriptional inhibition of specific genes in c-Myc transformed cells was not an indirect consequence of activation by the Myc-Max heterodimer, but could be mediated through an initiator element (INR) in the proximal promoter of certain c-Myc target genes, like those which encode cyclin D1 and C/EBP α [463,464]. For instance, c-Myc repression of the core promoter of C/EBP α , a gene whose expression is induced during adipocyte differentiation, was attenuated when its INR was mutated [461]. INR elements are pyrimidine rich with the weak consensus sequence YYYANYYY (where Y = pyrimidine and N = any nucleotide) and bind several transcription factors including TFII-I (transcription factorII-I) and the zinc finger protein ying yang 1 (YY1) which can recruit the pre-initiation complex [461,465]. c-Myc was shown to interact with both TFII-I and YY1 *in vitro*, which suggested that c-Myc might inhibit INR-dependent transcription by blocking the ability of these factors to interact with the basal transcription machinery or other activators [440,466,467]. Indeed, complex formation between c-Myc and TFII-I at an INR appears to preclude TFII-I interaction with TATA binding protein (TBP) which would lead to inhibition of transcription initiation if this association with c-Myc does occur *in vivo* [466]. Although a TBP-c-Myc promoter complex has not been detected, c-Myc can interact with TBP off DNA *in vitro*, which could abrogate transcription by sequestering TBP from TFII-I bound to an INR [466,468].

More recently, the search for protein partners which mediate c-Myc transcriptional repression has led to the discovery of another INR binding transcription factor called Myc-interacting zinc finger protein-1 (Miz-1). Miz-1 was first identified in a two-hybrid screen using the DNA fragment encoding the basic HLH/LZ domain of human Myc fused to the DNA-binding domain of GAL4 as bait [464].

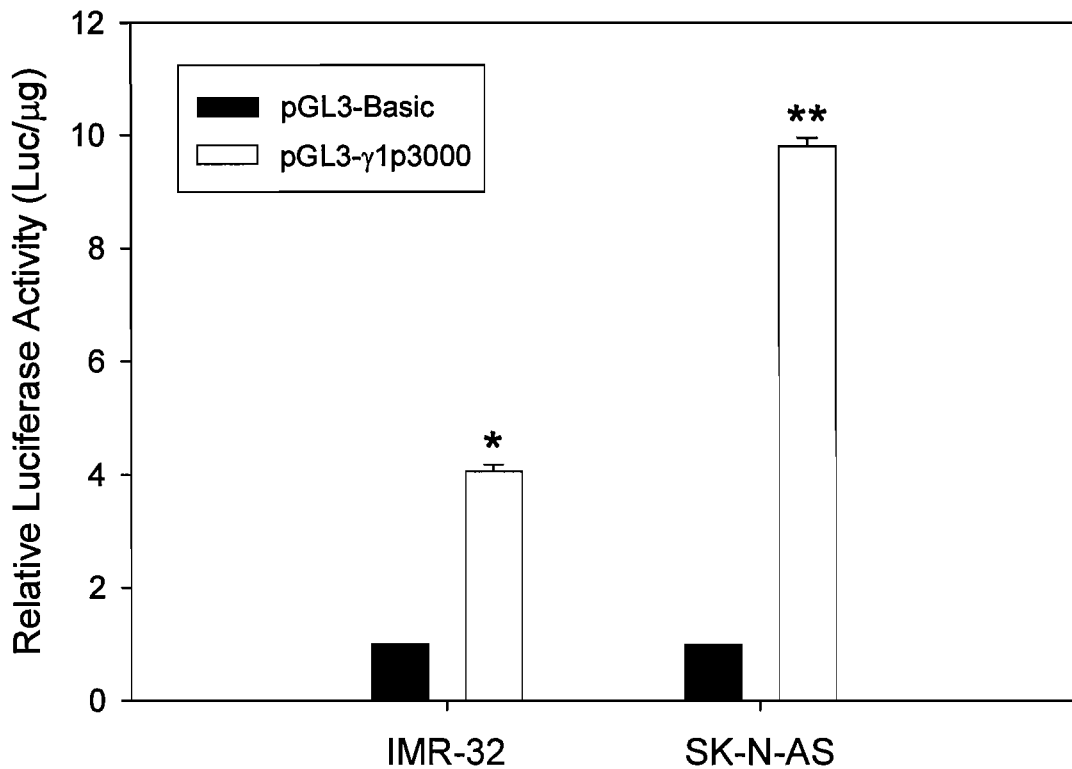


Fig. 5.2. The human PPAR γ 1 promoter is differentially activated in neuroblastoma cells. IMR-32 and SK-N-AS neuroblastoma cells were transiently transfected with 2 μ g of a PPAR γ 1 promoter reporter (pGL3- γ 1p3000) and then harvested after 24 hours and luciferase activity measured. The neuroblastoma cells were also transfected with pGL3-Basic, which lacks a eukaryotic promoter and enhancer sequence, to normalise for transfection efficiency between the different cell lines. Data represents the mean luciferase activity (white bar) of the PPAR γ 1 promoter reporter relative to pGL3-Basic (black bar), of 2 independent experiments \pm S.E. Statistics were calculated using a Student's *t*-test and showed that level of luciferase activity of pGL3- γ 1p3000 was significantly higher compared with the luciferase activity of pGL3-Basic, in IMR-32 (*) ($p < 0.01$) and SK-N-AS (**)($p < 0.005$) neuroblastoma cells.

The cDNA of human Miz-1 encodes a protein of 803 amino acids, with 13 zinc fingers, 12 of which are located in the carboxy-terminal half of the protein and a N-terminal POZ/BTB/ZIN (poxvirus and zinc finger/broad complex, tram track and Bric-a-brac/zinc finger N-terminal domain) domain [464,469]. The POZ domain is conserved motif of 120 amino acids that has been identified in a number of zinc finger proteins and facilitates oligomerisation via homomeric or heteromeric POZ-POZ interactions [469-471]. Originally it was proposed that the POZ domain of some zinc finger proteins such as ZID (zinc finger protein with interaction domain), by promoting the formation of dimeric or multimeric complexes, inhibited their ability to bind DNA *in vitro*. Conversely, oligomerization mediated by the POZ domain of the GAGA transcription factor actually facilitates its binding to multiple GAGA sites in natural promoters *in vivo* stimulating gene transcription [472]. Transcriptional inhibition of target genes by BCL-6 (B-cell lymphoma 6) and PLZF zinc finger proteins is also dependent on their POZ domain since it is critical for interactions with co-repressors such as N-CoR and SMRT [471-473].

Miz-1 is soluble protein that binds via its 12 carboxyl zinc fingers to the INR elements of several promoters and activate gene transcription [464,474,475]. The POZ domain of Miz-1 appears to be indispensable for Miz-1 transactivation and could also mediate recruitment of an essential cofactor [476]. Ectopic expression of human Miz-1 in HeLa cells blocked cell proliferation and induced growth arrest *in vitro* which could be partially reversed in the presence of c-Myc[464]. Since several Miz-1 target genes such as the cyclin dependent kinase inhibitors, *p21^{CIP1/WAF1}* and *p15^{INK4b}* encode proteins which have known functions in cell cycle control this suggested that c-Myc may promote cell growth by inhibiting Miz-1 transactivation. Indeed, it has been established that c-Myc transcriptional repression of the Miz-1 activated genes *p15^{INK4b}*, *p21^{CIP1/WAF1}*, *Mad4* and murine *Nramp1*, is dependent on its interaction with Miz-1[474-483]. In HeLa cells, association between c-Myc and Miz-1 was hypothesised to stimulate a suppressed function of the Miz-1 POZ

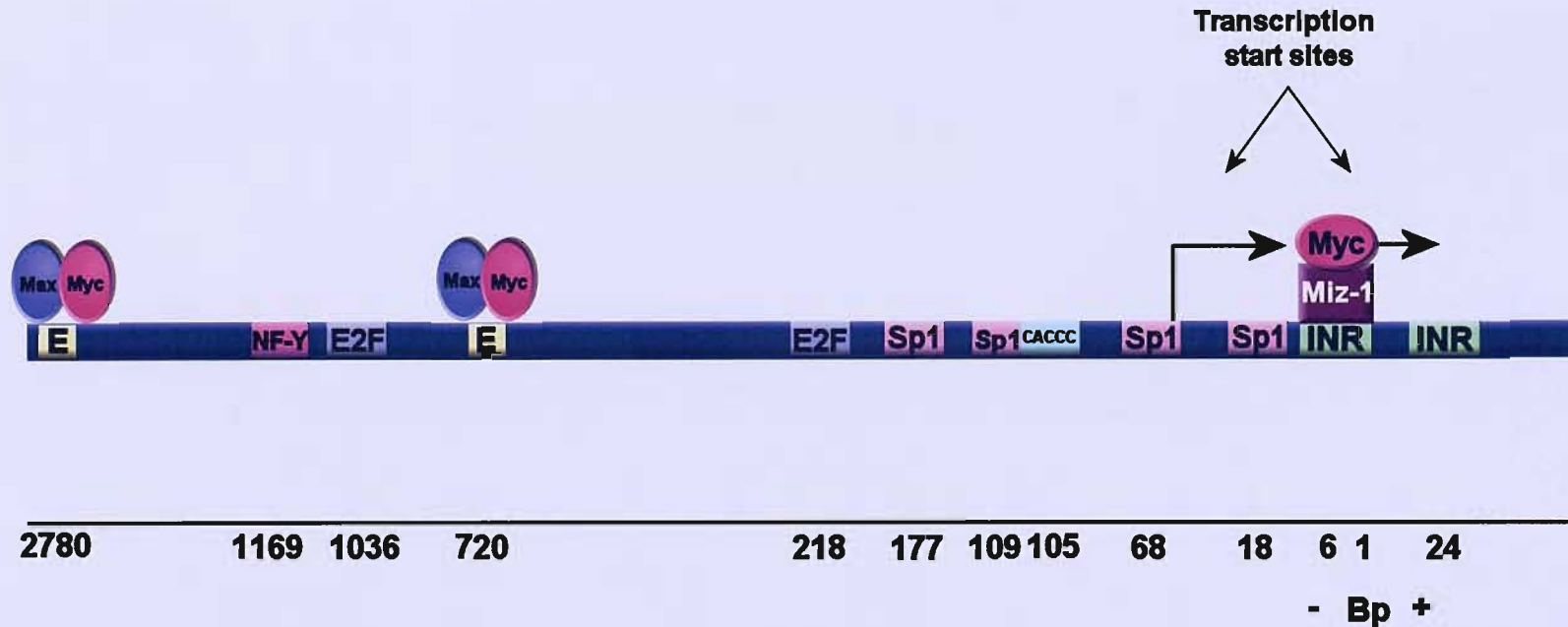


Fig. 5.3. Characterisation of the human PPAR γ 1 promoter. The 2842 bp PPAR γ 1 promoter sequence in the reporter, pGL3- γ 1p3000 was analysed using the MatInspector tool (part of the Genomatix suite which can be found at www.genomatix.de/). The out-put produced by MatInspector highlights regions within the promoter sequence which show homology to the consensus of know transcription factor binding sites. The potential binding sites shown in this figure may be involved in regulation of PPAR γ 1 transcription by Myc family transcription factors and include two E-boxes which directly interact with Myc-Max heterodimers. c-Myc can also be recruited to promoters via protein-protein interactions with factors bound to: NF-Y (nuclear transcription factor-Y) sites, E2F (elongation 2 factor) sites, Sp1 (specificity protein 1) sites, CACCC boxes (also binding site for Sp1) and initiator (INR) elements (binding site for factors including, Miz-1 (Myc interacting zinc finger protein-1)). The indicated positions of the binding sites are relative to the second start site of transcription. Other putative transcription factor binding sites that could modulate PPAR γ 1 promoter activity in neuroblastoma cells are displayed in the Appendix.

domain, which as for some other transcription factors like ZID, prevented it from binding DNA and sequestered Miz-1 to a number of discrete sub-nuclear foci which do not contain DNA [464]. In contrast to these findings, it has also been demonstrated in other cell line systems, that c-Myc can form a complex with INR-bound Miz-1, which may in fact increase its affinity for DNA, but inhibit Miz-1 transactivation by prevent recruitment of the co-activator CBP/p300 [474,479,481,483]. The CBP/p300 and c-Myc interaction domains of Miz-1 overlap suggesting that c-Myc and p300 compete for binding to Miz-1 [474]. In addition, attenuation of $p21^{CIP1/WAF1}$ expression by c-Myc may involve recruitment of the DNA methyltransferase co-repressor, Dnmt3a, which stimulates *de novo* methylation that can silence gene transcription. Dnmt3a was shown to bind to the p21 promoter *in vivo* in the presence of c-Myc; although this association was dependent on c-Myc's interaction with DNA bound Miz-1 [484].

There is however, evidence to suggest that c-Myc can inhibit gene transcription via Miz-1 and INR independent mechanisms (**Fig. 5.5**). For instance, c-Myc interacts with other enhancers of transcription such as Sp1, Smads, NF-Y and AP-1 (activator protein-1) which have binding sites in the proximal promoters of known c-Myc repressed genes [485] [486-488]. Indeed, the $p21^{CIP1/WAF1}$ and $p15^{INK4b}$ promoters, proposed targets of Miz-1 mediated c-Myc repression, could also be inhibited by c-Myc through its complex formation with Sp1 and Smad transcription factors [485,486,489]. Although still unclear, c-Myc may inhibit the transactivation function of these factors by several mechanisms including disrupting co-operation with another transcription factor, sequestration from DNA, co-activator displacement, or recruitment of a histone deacetylase (HDAC) [490-493].

c-Myc, at concentrations that can occur in a normal cell, also negatively regulates its own expression, with the degree of suppression proportional to the level of c-Myc protein [494,495]. Auto-regulation has been mapped to the second (P2) c-Myc promoter, from which the majority of c-Myc transcription is initiated [496]. Repression of the P2 promoter was dependent on c-Myc interaction's with the retinoblastoma family member, p107 and required either a functional E2F or INR element since inhibition was only lost when both E2F sites and INR elements in the

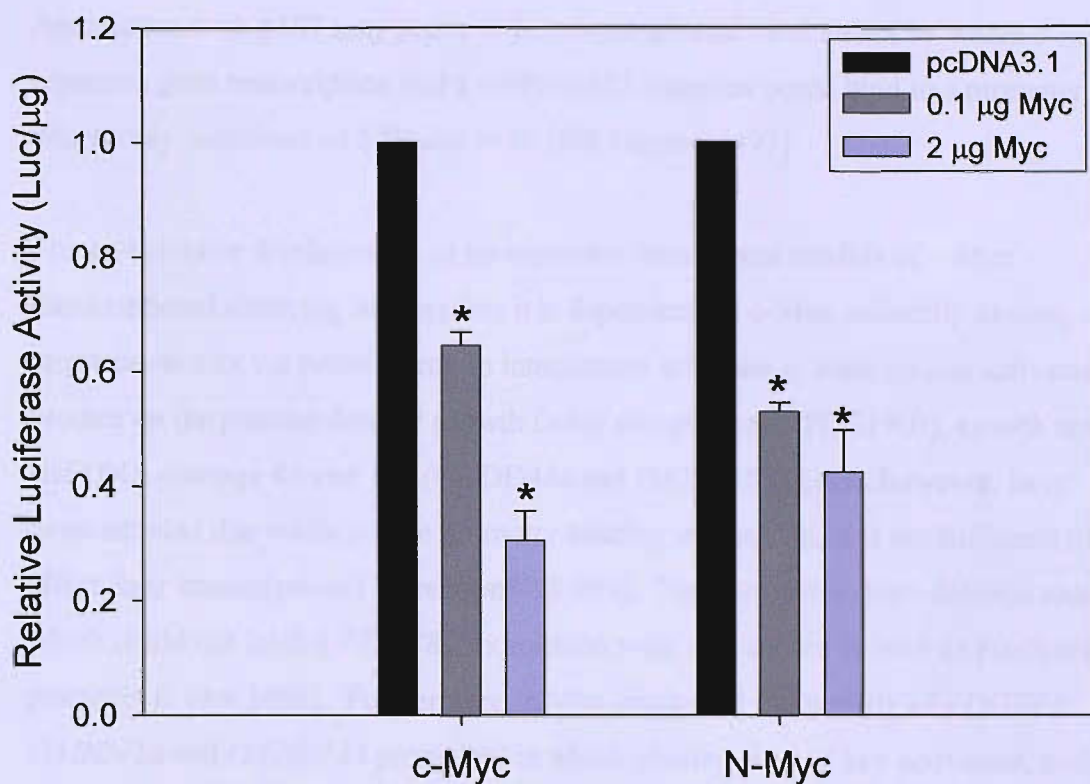


Fig. 5.4. The effect of Myc family members on human PPAR γ 1 promoter activity in SK-N-AS neuroblastoma cells. SK-N-AS cells were co-transfected with 2 μ g of a PPAR γ 1 promoter reporter (pGL3- γ 1p3000) and either 0.1 μ g (grey bar) or 2 μ g (purple bar) of c-Myc or N-myc expression plasmids. The total quantity of DNA for each transfection was normalised to 4 μ g (including reporter) with an empty expression vector (pcDNA3.1). Cells were harvested 24 hours post-transfection and luciferase activity measured. Data shows the relative mean luciferase activity (per μ g of protein) of the PPAR γ 1 promoter reporter co-transfected with the indicated amounts of c-Myc or N-Myc expression plasmids compared to promoter reporter activity in the presence of the empty expression vector control only (black bar), and represents two independent experiments \pm S.E. Statistics were calculated using a Student's *t*-test and showed that there was significant repression of the luciferase activity of the PPAR γ 1 promoter reporter in the presence 0.1 μ g and 2 μ g of both the c-Myc and N-Myc expression plasmids(*) ($p < 0.01$).

P2 promoter were mutated [497]. It is speculated that c-Myc and p107 are recruited to the P2 promoter via other protein partners bound to the E2F and INR sites. Association with p107 may prove to be a more general mechanism by which c-Myc represses gene transcription and a c-Myc/p107 complex could bind to a promoter which only contained an E2F site or an INR element [497].

The co-activator displacement or co-repressor recruitment models of c-Myc transcriptional silencing suggest that it is dependent on c-Myc indirectly binding to target promoters via protein-protein interactions with one of their critical activators. Studies on the platelet-derived growth factor receptor beta (*PDGFRB*), growth arrest and DNA damage 45 and 153 (*GADD45a* and *GADD153*) genes however, have demonstrated that while c-Myc promoter binding is essential, it is not sufficient to affect their transcriptional repression[498,499]. For example, c-Myc deletion mutants which could not inhibit *PDGFRB* expression were still shown to bind its proximal promoter *in vivo* [498]. Furthermore, c-Myc attenuated the activity of *PDGFRB*, *GADD45a* and *GADD153* promoters in which binding sites of key activators, such as Sp1 or NF-Y had either been mutated or deleted, suggesting that interactions with these factors was not essential for c-Myc repression as had previously been suggested[487,500]. It is still not clear how c-Myc is recruited to these promoters although it appears to require c-Myc dimerisation with Max[498,499]. In the case of the *PDGFRB* gene, c-Myc repression was abrogated by the HDAC inhibitor, Trichostatin A (TSA) although this was not associated with reduced histone acetylation at the *PDGFRB* proximal promoter[498]. c-Myc interaction with both the *PDGFRB* and *GADD* promoters did not affect binding of RNA Polymerase II suggesting that c-Myc initiates transcriptional repression after recruitment of the pre-initiation complex [498,499]. These findings suggested that c-Myc repression of the PPAR γ 1 promoter could involve multiple pathways. Therefore, next the mechanism or pathways critical for transcriptional inhibition of PPAR γ 1 by c-Myc in neuroblastoma cells were examined (**Fig. 5.5**).

5.7 The Miz-1 transcription factor stimulates PPAR γ 1 promoter activity

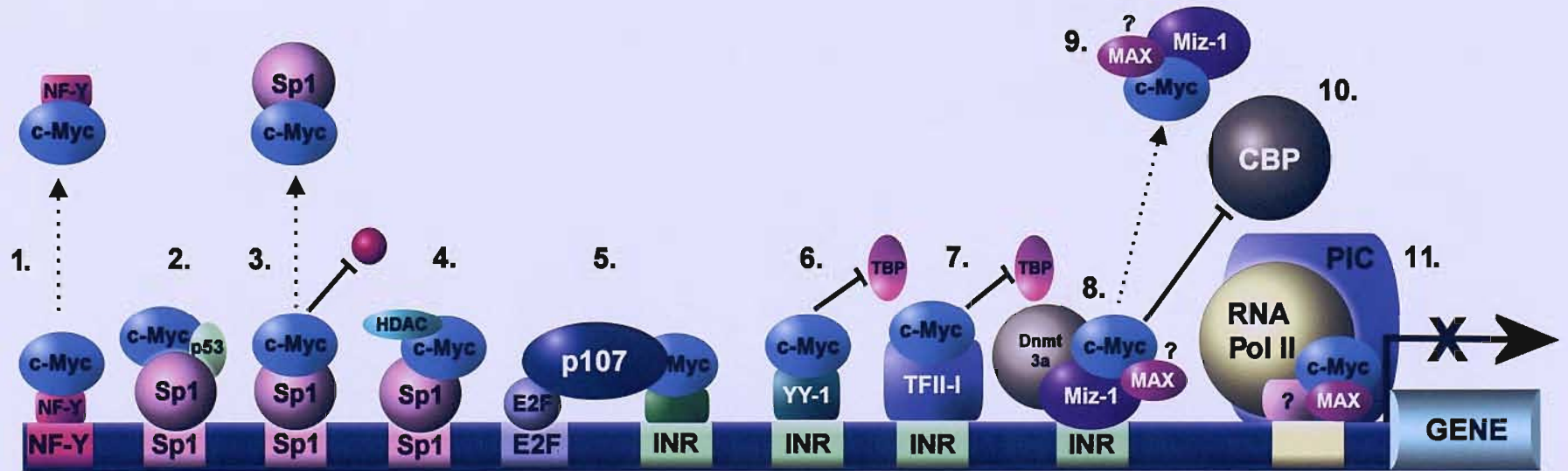
The structure of the human PPAR γ 1 proximal promoter is similar to those of other c-Myc repressed genes such as *p15^{INK4b}* and *Mad4* since it lacks a TATA box, is GC rich and contains at least one potential INR element [477,479]. Like PPAR γ 1, induction of *Mad4* transcription is associated with the differentiation of several cell types such as adipocytes [501]. c-Myc transcriptional repression of *Mad4* and other genes is mediated through its interaction with INR-bound Miz-1. Since both the proximal promoter structure and expression profile of *Mad4* and PPAR γ 1 transcripts were comparable, this suggested that attenuation of human PPAR γ 1 promoter activity by c-Myc also involved Miz-1. To test this hypothesis, the effect of Miz-1 on PPAR γ 1 promoter activity was studied by co-transfecting SK-N-AS neuroblastoma cells with a PPAR γ 1 promoter reporter (pGL3- γ 1p3000) and an expression plasmid encoding Miz-1 or an empty expression vector control. The cells were harvested 24 hours post transfection and luciferase activity measured. Miz-1 induced a 2-fold increase in reporter expression of the PPAR γ 1 promoter construct which was statistically significant at the 5% level (Fig. 5.6).

5.8 Repression of human PPAR γ 1 promoter activity by c-Myc is not dependent on its interaction with Miz-1

Two regions of Miz-1 that flank its central 12 zinc fingers are essential for interaction with c-Myc [464]. The second of these two regions (amino acids 637-718), located between zinc fingers 12 and 13, was predicted to form an amphipathic α -helix that was likely to interact with the HLH domain of c-Myc since they both had a similar structure [464]. c-Myc has subsequently been shown to associate with Miz-1 via a highly conserved region of the outer surface of its second helix, in the HLH motif [476]. This finding was made by Herold *et al* from a study to identify single point mutants of c-Myc that would disrupt its interaction with Miz-1 but retains its ability to dimerise with Max and activate gene transcription [476]. Initial deletion analysis had mapped the Miz-1 interaction site on c-Myc to the HLH domain.

Fig. 5.5. The potential mechanisms of c-Myc transcriptional repression. The promoter (blue bar) in this figure is hypothetical to illustrate the different pathways by which c-Myc could inhibit gene transcription (X), which include:

1. Attenuation of transcriptional activity of nuclear transcription factor-Y (NF-Y) mediated by c-Myc interaction with NF-Y. c-Myc may also act by sequestering NF-Y from DNA response element.
2. Inhibition of transactivation caused by co-operation between the tumour suppressor p53 and special factor 1 (Sp1).
3. Formation of a complex with Sp1 which blocks its recruitment of co-activators or sequesters Sp1 from DNA.
4. Recruitment of a histone acetylase (HDAC) or HDAC containing complex to the promoter of its target genes which causes transcriptional silencing by reduced histone acetylation.
5. Association between the retinoblastoma family member, p107. Interaction of a promoter with this p107/c-Myc inhibitory complex is likely to occur through other protein partners, for example, p107 binding to E2F and c-Myc via an initiator (INR) binding protein. This complex could also be recruited to a promoter which only contained an INR or E2F site.
6. Blocking interaction between TATA binding protein (TBP) and ying yang-1 (YY-1) at an INR element.
7. Preventing association of TBP and transcription factor II-I (TFII-I) at an INR element.
8. Formation of a ternary complex with myc interacting zinc finger protein 1 (MIZ-1) and the DNA methyltransferase co-repressor 3a (Dmmt3a).
9. Dimerisation with Miz-1 could sequester the transcription factor to discrete subnuclear foci which do not contain DNA.
10. Inhibiting Miz-1 transactivation by precluding recruitment of the co-activator creb interacting protein (CBP). There is still controversy over whether transcriptional repression by c-Myc is dependent on its dimerisation with Max.
11. Abrogation of gene transcription post-recruitment of RNA polymerase II (RNA Pol II).



Performing random mutagenesis on the carboxy terminus of c-Myc demonstrated that substitution of amino acids in the outer surface of its second helix, in particular replacement of valine by aspartic acid at position 394 (V394D) completely impaired c-Myc's ability to both bind Miz-1 and attenuate Miz-1 transactivation [476]. The V394D c-Myc mutant has been used to verify that c-Myc inhibition of *p15^{INK4B}*, *p21^{CIP1}* and *Nramp1* transcription is mediated by an interaction with Miz-1, since in contrast to wild-type c-Myc, it failed to repress the promoter activity of all three genes *in vitro* [476,481,502]. Therefore, to determine if c-Myc repression of PPAR γ 1 transcription also occurs through complex formation with Miz-1, increasing quantities of an expression plasmid encoding either wild-type c-Myc or a V394D c-Myc mutant were co-transfected with the PPAR γ 1 promoter reporter in SK-N-AS neuroblastoma cells and their effect on PPAR γ 1 promoter activity was observed. The amount of DNA for each transfection was normalised with a non-recombinant plasmid. **Fig. 5.7** shows the luciferase activity of the PPAR γ 1 promoter reporter in the presence of wild type c-Myc and the V394D c-Myc mutant was repressed to a similar extent relative to the luciferase activity of the PPAR γ 1 promoter construct in the presence of the non-recombinant plasmid. SK-N-AS cells transfected with 0.1 and 2 μ g of either Myc expression plasmid exhibited an approximately 30% and 65% reduction in PPAR γ 1 promoter reporter activity respectively. This dose-dependent inhibition of PPAR γ 1 promoter reporter activity in the presence of wild-type c-Myc and the V394D c-Myc mutant suggests that c-Myc represses PPAR γ 1 transcription via a Miz-1 independent mechanism. Therefore alternative models of c-Myc repression of the human PPAR γ 1 promoter activity in neuroblastoma cells were investigated.

5.9 The histone deacetylase inhibitor, Trichostatin A stimulates human PPAR γ 1 promoter activity

One mechanism of transcriptional repression involves recruitment of a histone deacetylase to a promoter. Deacetylation of histones is believed to block the disassembly of nucleosomes and thereby restricts the accessibility of DNA to components of the basal transcriptional machinery which inhibits gene activation [503]. c-Myc can interact with c-Myc modulator 1 (MM-1) and the retinoblastoma

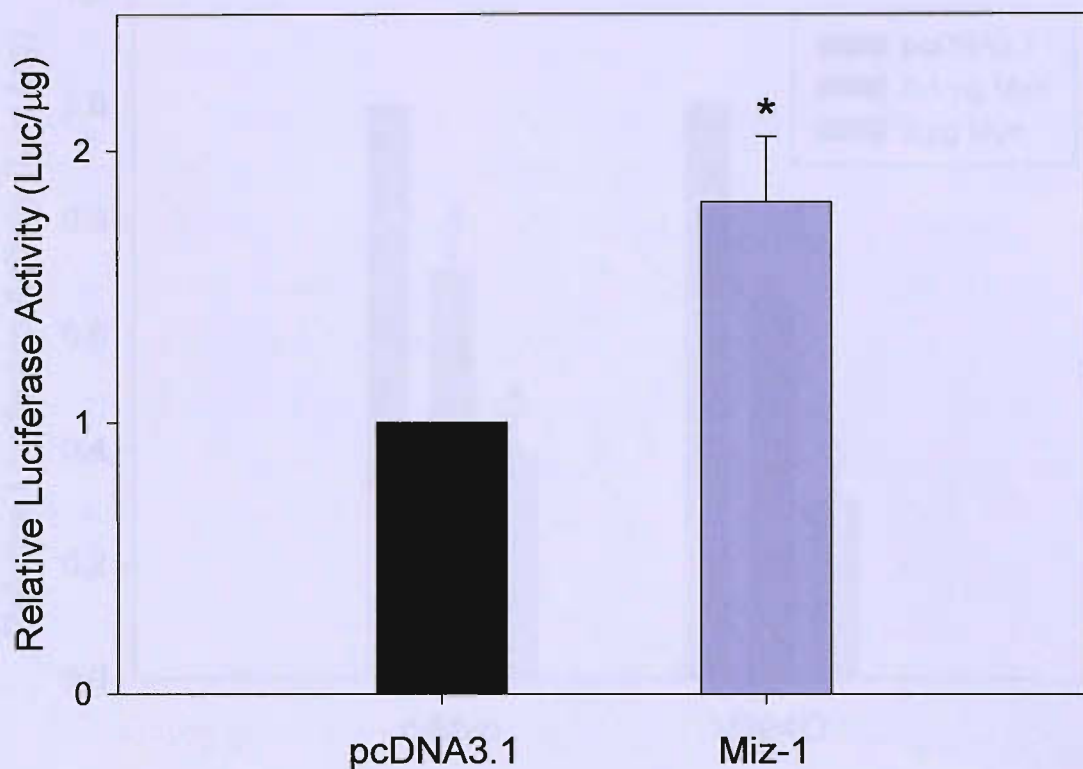


Fig. 5.6. The effect of Miz-1 on PPAR γ 1 promoter activity in SK-N-AS neuroblastoma cells. SK-N-AS cells were co-transfected with 2 μ g of a PPAR γ 1 promoter report (pGL3- γ 1p3000) and either an expression plasmid encoding Miz-1 or pcDNA3.1 as an empty expression vector control (2 μ g). Cells were harvested after 24 hours and luciferase activity measured. Data shows the relative mean luciferase activity (per μ g of protein) of the PPAR γ 1 promoter reporter co-transfected with Miz-1 (purple bar), compared with promoter reporter activity in the presence of the empty expression vector control (black bar), and represents three independent experiments \pm S.E. Statistics were calculated using a Student's *t*-test and showed that the luciferase activity of the PPAR γ 1 promoter reporter was significantly induced in the presence of 2 μ g of the Miz-1 expression plasmid(*) ($p < 0.05$).

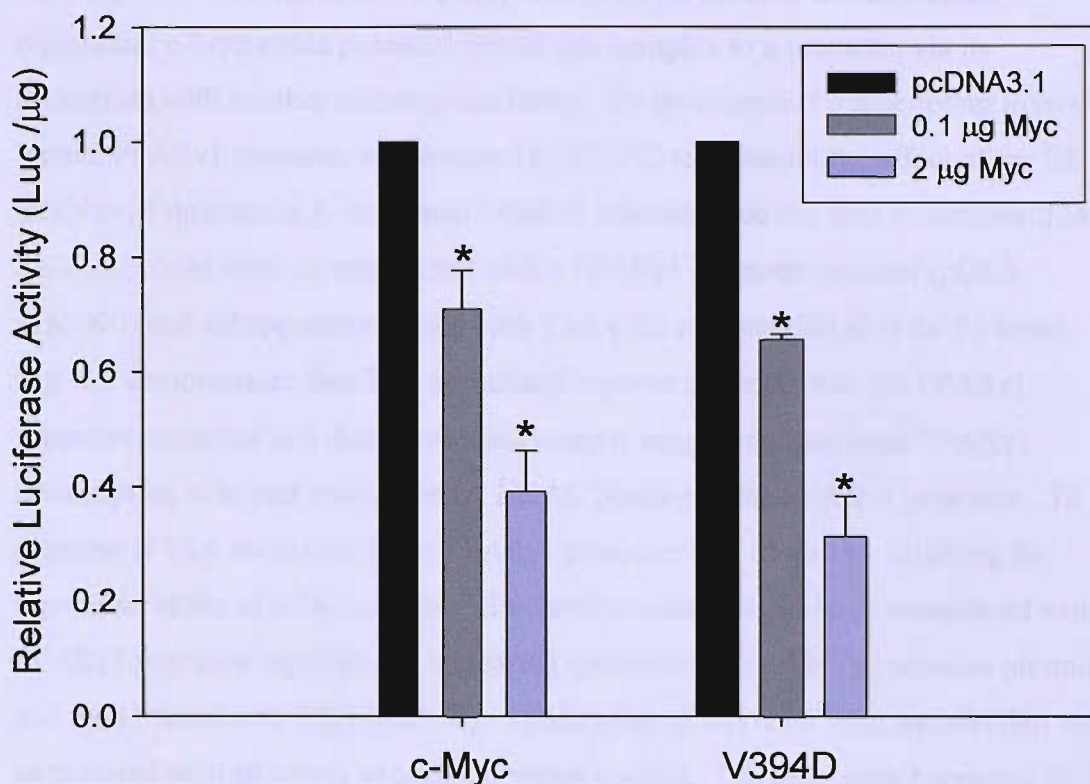


Fig. 5.7. The effect of the V394D c-Myc mutant on human PPAR γ 1 promoter activity in SK-N-AS neuroblastoma cells. SK-N-AS cells were co-transfected with 2 μ g of a PPAR γ 1 promoter reporter (pGL3- γ 1p3000) and either 0.1 μ g (grey bar) or 2 μ g (purple bar) of expression plasmids encoding either wild type c-Myc or the V394D c-Myc mutant. The total quantity of DNA for each transfection was normalised to 4 μ g (including reporter) with an empty expression vector (pcDNA3.1). Cells were harvested 24 hours post-transfection and luciferase activity measured. Data shows the relative mean luciferase activity (per μ g of protein) of the PPAR γ 1 promoter reporter co-transfected with the indicated amounts of c-Myc or V394D c-Myc mutant expression plasmids compared to promoter reporter activity in the presence of the empty expression vector control only (black bar), and represents two independent experiments \pm S.E. Statistics were calculated using a Student's *t*-test and showed that there was significant repression of the luciferase activity of the PPAR γ 1 promoter reporter in the presence of 0.1 μ g and 2 μ g c-Myc and V394D c-Myc mutant expression plasmids (*) ($p < 0.05$).

family member, p107 factors which both repress gene transcription by recruitment of a HDAC[493,497]. c-Myc via MM-1 forms a complex with the transcriptional co-repressors, TF1 β and mSin3A, and HDAC1 which inhibited the E-box dependent transcriptional activity of c-Myc[493]. However, to mediate transcriptional repression, c-Myc could potential recruit this complex to a promoter via its interaction with another transcription factor. To investigate if transcription from the human PPAR γ 1 promoter is attenuated by HDAC recruitment the affect of the HDAC inhibitor, Trichostatin A on human PPAR γ 1 promoter activity was investigated[363]. SK-N-AS cells were co-transfected with a PPAR γ 1 promoter reporter (pGL3- γ 1p3000) and subsequently treated with TSA (300 nM and 600 nM) for 24 hours. **Fig. 5.8** demonstrates that TSA stimulated reporter expression of the PPAR γ 1 promoter construct in a dose dependent manner suggesting that basal PPAR γ 1 transcription is in part modulated by HDAC binding to the PPAR γ 1 promoter. To examine if TSA induction of the PPAR γ 1 promoter was caused by relieving the repressive effect of c-Myc, SK-N-AS neuroblastoma cells were co-transfected with a PPAR γ 1 promoter reporter and increasing quantities of a c-Myc expression plasmid and then treated with TSA (600nM). The amount of DNA for each transfection was normalised with an empty expression vector control. The cells were harvested 24 hours post-transfection and luciferase activity measured. **Fig. 5.9** shows that PPAR γ 1 promoter reporter activity in the presence of 0.1 and 2 μ g of c-Myc expression plasmid was repressed to a similar level in both vehicle and TSA-treated SK-N-AS cells relative to the luciferase activity of the construct in vehicle and TSA-treated SK-N-AS cells transfected with the empty expression vector control (white and white striped bar respectively). Since TSA treatment did not significantly affect inhibition of PPAR γ 1 promoter reporter activity by c-Myc this indicates that HDAC activity is dispensable for c-Myc mediated repression of PPAR γ 1 transcription.

5.10 Determination of the region of c-Myc which mediates its repression of human PPAR γ 1 promoter activity

The *c-myc* gene comprises three exons, with the latter two exons (II and III) encoding a highly conserved nuclear phosphoprotein whose structural motifs are consistent with its function as a transcription factor [431,504].

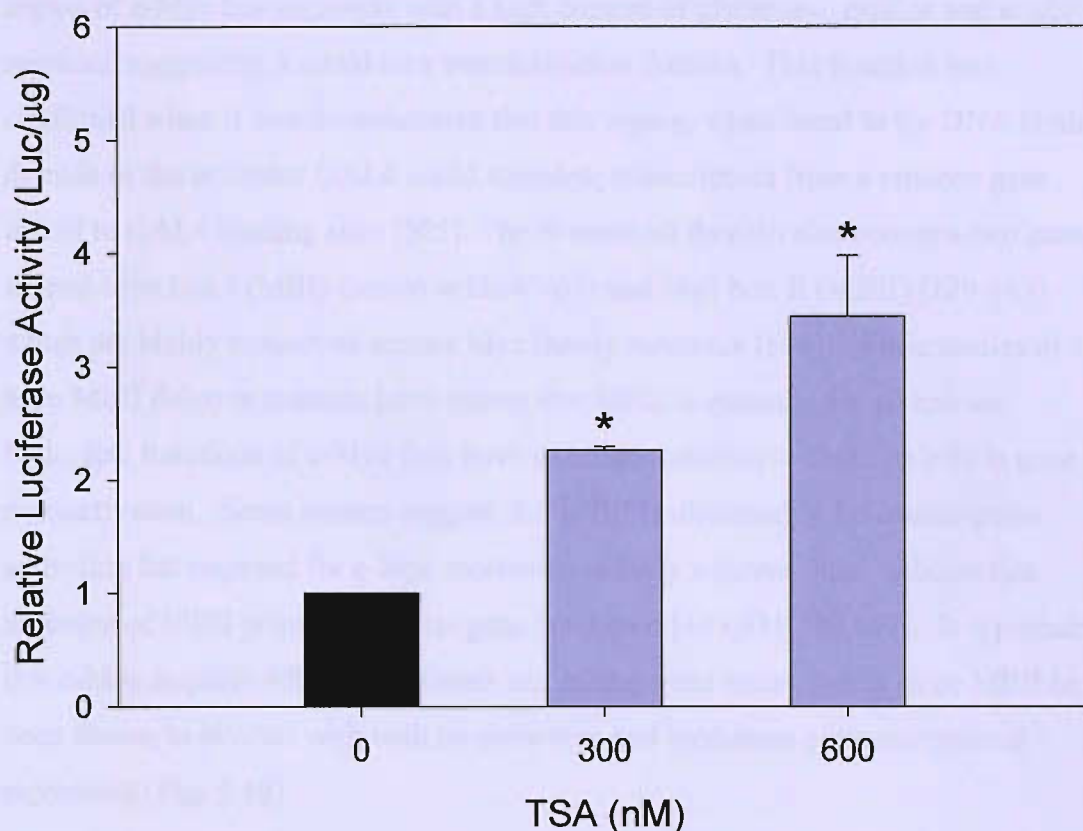


Fig. 5.8. The effect of the HDAC inhibitor, Trichostatin A (TSA) on human PPAR γ 1 promoter activity in SK-N-AS cells. SK-N-AS cells were transfected with the PPAR γ 1 promoter reporter (pGL3- γ 1p3000) and subsequently treated with TSA (300 nM and 600 nM) for 24 hours. The cells were then harvested and luciferase activity measured. Data shows the relative mean luciferase activity of the PPAR γ 1 promoter reporter (per μ g of protein) in the presence of TSA (purple bar) compared with vehicle (DMSO) treated cells (black bar) and represents two independent experiments \pm S.E. Statistics were calculated using a Student's *t*-test and showed that there was a significant induction of PPAR γ 1 promoter reporter activity in the presence of 300nM and 600 nM TSA (*) ($p < 0.05$).

Although the crystal structure of c-Myc has still not been resolved molecular modelling programs predict that c-Myc consists of a globular N-terminal region, a small unstructured middle section, from amino acids 204-237, and an α -helical C-terminal end [431]. The sequence between amino acids 1 and 143 of the N-terminal region of c-Myc has segments with a high content of glutamine, proline and acidic residues, suggesting it could be a transactivation domain. This function was confirmed when it was demonstrated that this region, when fused to the DNA binding domain of the activator GAL4 could stimulate transcription from a reporter gene linked to GAL4 binding sites [505]. The N-terminal domain also contains two motifs termed Myc box I (MBI) (amino acids 45-63) and Myc box II (MBII) (129-143) which are highly conserved among Myc family members [506]. While studies of c-Myc MBII deletion mutants have shown that MBII is essential for all known biological functions of c-Myc they have been less conclusive about its role in gene transactivation. Some reports suggest that MBII is dispensable for transcription activation but required for c-Myc repressive activity whereas other indicate that mutation of MBII primarily affects gene activation [429,431,506,507]. It is probable that c-Myc requires MBII to stimulate and inhibit gene transcription since MBII has been shown to interact with both co-activators and mediators of transcriptional repression (**Fig. 5.10**).

The central region of c-Myc (amino acids 143-320) includes Myc box III (MDIII), (amino acids 188-199) which may also have a function in attenuation of gene transactivation by c-Myc, and the primary nuclear localisation sequence (amino acids 320-328) [507-509]. The C-terminal domain (amino acids 355-439) comprises the basic-helix-loop-helix-leucine zipper motifs which were originally recognized as critical for dimerisation with Max and interaction with DNA [435]. Since the discovery of Max, an increasing number of c-Myc protein partners have been identified which appear to both promote and abrogate c-Myc biological activities [432,440]. As shown in **Fig. 5.5** c-Myc could potential repress gene transcription by several mechanisms and the regions of the c-Myc protein that interact with factors involved in these inhibitory pathways, including NF-Y, Sp1, p107, YY-1, TFII-I and Miz-1 have been mapped (**Fig. 5.10**, black bars) [431,432,440]. These findings illustrate that identifying the regions of the c-Myc protein that contribute to its repressive activity may help to elucidate which protein partners c-Myc interacts with

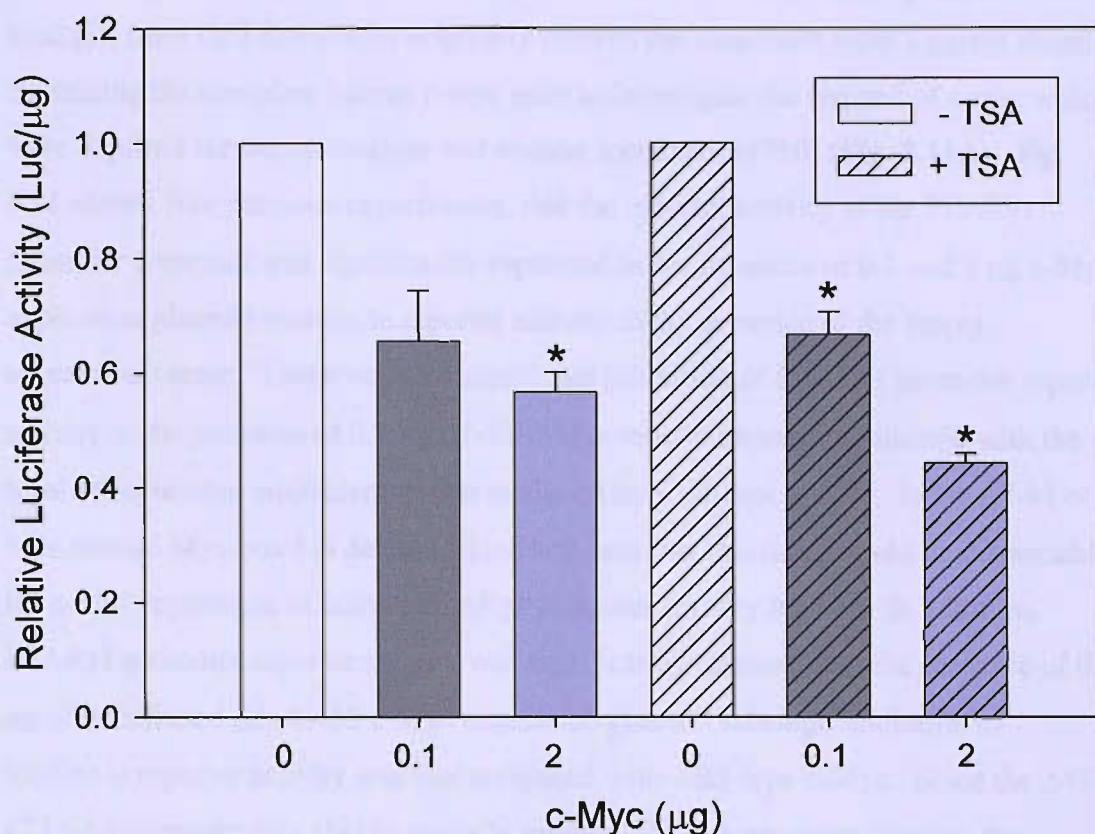


Fig. 5.9. The effect of the HDAC inhibitor, TSA on c-Myc repression of PPAR γ 1 promoter activity in SK-N-AS neuroblastoma cells. SK-N-AS cells were co-transfected with 2 μ g of the PPAR γ 1 promoter reporter (pGL3- γ 1p3000) and either 0.1 μ g (grey bar) or 2 μ g (purple bar) of a c-Myc expression plasmid. The total quantity of DNA for each transfection was normalised to 4 μ g (including reporter) with an empty expression vector (pcDNA3.1). The cells were subsequently treated with TSA (600 nM) (striped bars) or a vehicle control (DMSO). Cells were harvested 24 hours post transfection and luciferase activity measured. Data shows the relative mean luciferase activity of the PPAR γ 1 promoter reporter (per μ g of protein) co-transfected with the indicated amounts of c-Myc expression plasmid compared with promoter reporter activity in the presence of the empty expression vector control only (white bar) and represents two independent experiments \pm S.E. Statistics were calculated using a Student's *t*-test and showed there was significant repression of PPAR γ 1 promoter activity when co-transfected with 2 μ g of c-Myc expression plasmid in vehicle treated cells and with 0.1 μ g and 2 μ g of c-Myc expression plasmid, in the presence of 600 nM TSA (*) ($p < 0.01$).

to mediate inhibition of a target promoter (Fig. 5.10). Therefore, the effect of a series of c-Myc deletion mutants on human PPAR γ 1 promoter activity in SK-N-AS cells was investigated (Fig. 5.11). The c-Myc deletion mutant expression plasmids were a kind gift from Dr J Stone who originally derived the constructs from a parent plasmid containing the complete human c-myc gene to investigate the regions of c-myc which were required for transformation and nuclear localization[510] (Fig. 5.11A). Fig. 5.11 shows, like previous experiments, that the reporter activity of the PPAR γ 1 promoter construct was significantly repressed in the presence of 0.1 and 2 μ g c-Myc expression plasmid relative to reporter activity in the presence of the empty expression vector. There was also significant inhibition of PPAR γ 1 promoter reporter activity in the presence of 0.1 μ g Δ 7-91 c-Myc mutant expression plasmid with the level of repression equivalent to that mediated by wild-type c-Myc. In the Δ 7-91 c-Myc mutant Myc box I is deleted which suggests that this motif could be dispensable for c-Myc repression of human PPAR γ 1 promoter activity *in vitro*. In addition, PPAR γ 1 promoter reporter activity was significantly attenuated in the presence of 0.1 μ g of transfected Δ 414-433 c-Myc expression plasmid although inhibition of luciferase reporter activity was less compared with wild-type c-Myc. Since the Δ 414-433 c-Myc mutant was able to partially repress PPAR γ 1 promoter activity, this suggests that the leucine zipper domain may play a role in c-Myc repression of PPAR γ 1 transcription but is not essential for this function of c-Myc. Alternatively this result could reflect differences in the level of expression of the wild-type and c-Myc mutant protein.

In contrast, none of the other c-Myc deletion mutants analysed significantly attenuated the activity of the PPAR γ 1 promoter reporter. Overall this experiment indicates that Myc box III, the central region and basic-helix-loop-helix motifs of c-Myc may be essential for c-Myc inhibition of PPAR γ 1 promoter activity.

Fig. 5.10. The domain structure of the human c-Myc protein and its binding partners. The N-terminal domain (amino acids 1-143) contains the highly conserved Myc Box (MB) I and Myc Box (MB) II (blue boxes, position in protein shown by the amino acid number above). The central domain of c-Myc includes a third MB and the primary nuclear localization sequence (NLS) (black box, amino acids 320-328). The C-terminal region of c-Myc consists of a basic (BR, pink box), helix-loop-helix (HLH, grey box), leucine zipper (LZ, purple box) motif as well as the secondary nuclear localization sequence (amino acids 364-374). Below the c-Myc structure are listed some of the proteins which associate with the different domains of c-Myc. The black bars indicate the region of c-Myc which interacts with these proteins. The bHLHZ motif is necessary for c-Myc to heterodimerise with Max (c-Myc associated protein X) and bind directly to DNA activating gene transcription. The HLH is also required for interaction with Miz-1 (Myc-interacting zinc finger protein-1) and TFII-I (transcription factor II-I) which mediates transcriptional repression by c-Myc. In contrast, to Max, Miz-1 and TFII-I which promote c-Myc functions, AP-2 (activator protein-2) and BRCA-1 (breast cancer-1) which also associates with the C-terminal domain antagonize c-Myc transactivation by impairing DNA binding of the Myc-Max heterodimer or association of c-Myc with Max. c-Myc can also causes inhibition of transcription by interacting with YY-1 (ying-yang 1), Sp1 (special factor-1) and Smad transcription factors. The N-terminal of c-Myc can associate with protein factors which both activate and repress c-Myc transactivation. c-Myc forms a complex with TR-RAP (Transformation/transcription-domain-Associated protein) via MBII that promotes c-Myc transformation and may provide the link between c-Myc and a histone acetylase containing transcriptional complex. AMY-1 (Associate of c-Myc-1) another MBII interacting protein also stimulates E-box dependent transactivation. The adaptor protein Bin-1 and MM-1 (Myc modulator-1) inhibit c-Myc transactivation. Co-operation between the retinoblastoma protein family member, p107 and c-Myc appears to play an important role in its autorepression. The exact function of PAM (protein associated with Myc) remains unclear although it is speculated to have a function in chromatin modeling. c-Myc can associate with α -tubulin (α -TUB) and polymerized microtubules in vivo although the role of the interaction remained to be determined. This list of c-Myc protein partners described here is not exhaustive, however shows the main factors which have so far been reported on.

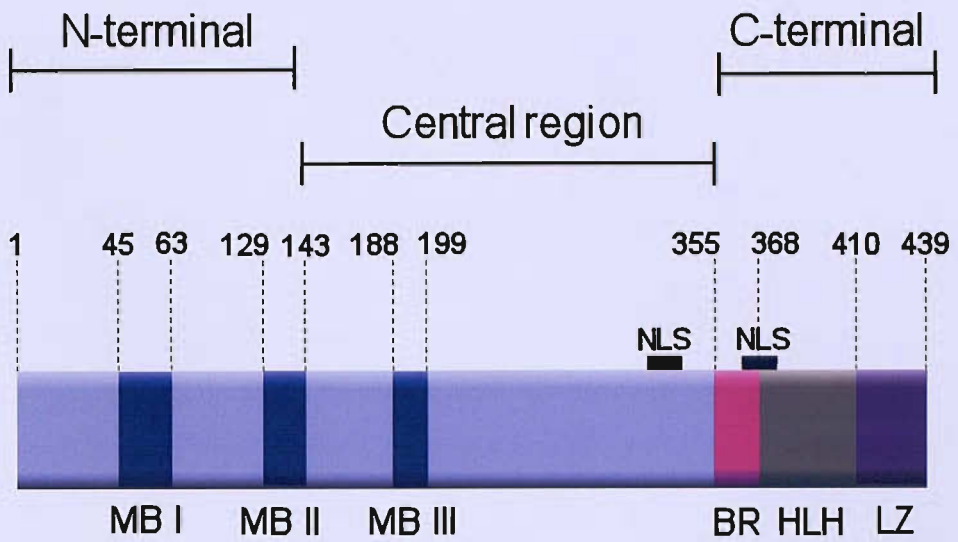
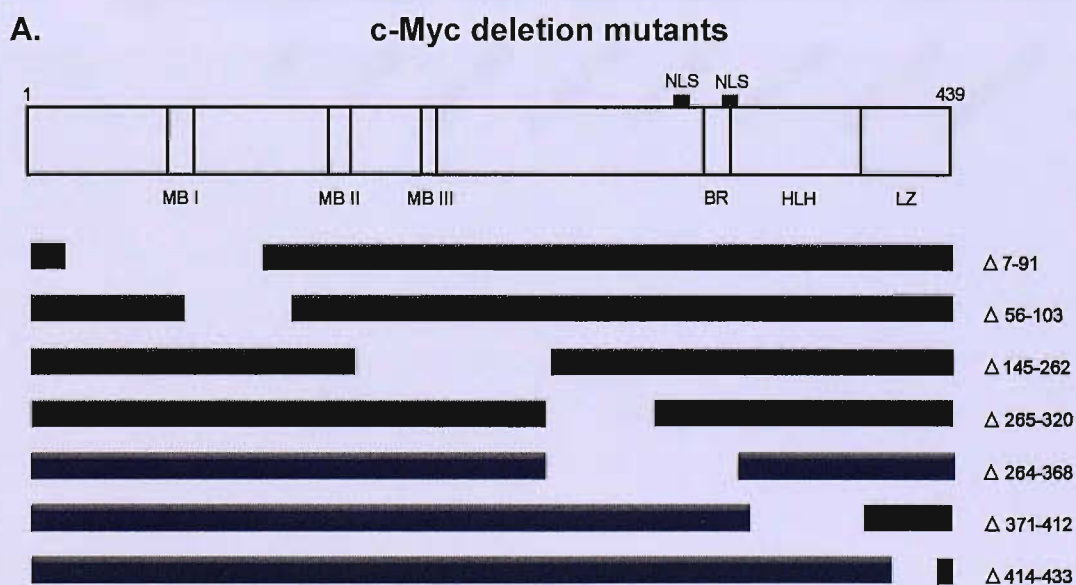


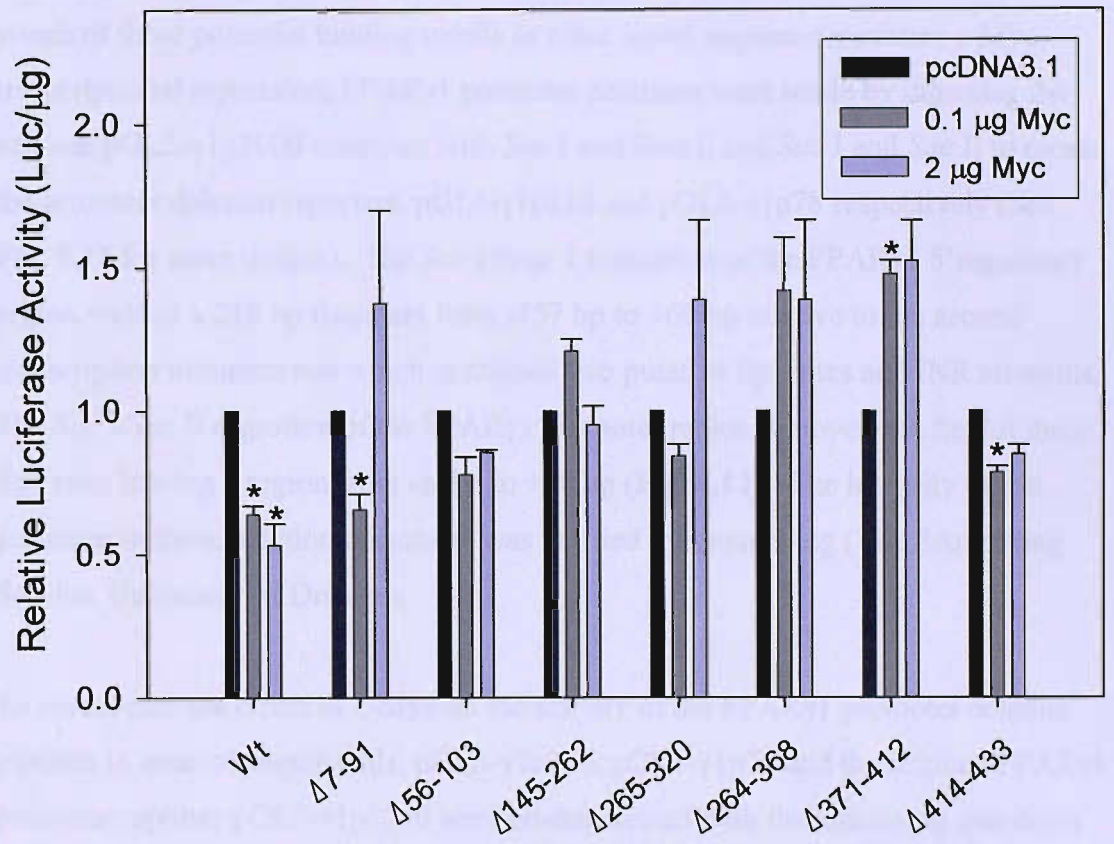
Fig. 5.11. The effect of c-Myc deletion mutants on human PPAR γ 1 promoter activity in SK-N-AS neuroblastoma cells. SK-N-AS cells were co-transfected with 2 μ g of a PPAR γ 1 promoter reporter (pGL3- γ 1p3000) and either 0.1 μ g (grey bar) or 2 μ g (purple bar) of an expression plasmid encoding either wild type c-Myc or one of seven c-Myc deletion mutants (A). The total quantity of DNA for each transfection was normalised to 4 μ g (including reporter) with an empty expression vector (pcDNA3.1). Cells were harvested 24 hours post-transfection and luciferase activity measured. Data shows the relative mean luciferase activity of the PPAR γ 1 promoter reporter (per μ g of protein) co-transfected with the indicated amounts of wild type c-Myc or c-Myc deletion mutant expression plasmid compared with promoter reporter activity in the presence of the empty expression vector control (black bar) and represent two independent experiments \pm S.E (B). Statistics were calculated using a Student's *t*-test and showed that there was significant repression of PPAR γ 1 promoter reporter activity in the presence of 0.1 μ g wild type c-Myc, Δ 9-71 c-Myc and Δ 414-433 c-Myc expression plasmids (*) ($p < 0.05$) whereas only co-transfection with 2 μ g of the wild type c-Myc expression plasmid significantly attenuated PPAR γ 1 promoter reporter activity (*) ($p < 0.05$). Significant stimulation of PPAR γ 1 promoter activity was observed in the presence of 0.1 μ g Δ 371-412 c-Myc expression plasmid (*) ($p < 0.05$).



B.11 Identification of the site of α -Myc transcriptional repression by the human PPA1Y promoter

The question of α -Myc growth inhibition requires that α -Myc transcriptional repression of the PPA1Y promoter is linked to the mechanism of α -Myc inhibition with respect to protein synthesis (Fig. 2). In order to identify the site of α -Myc transcriptional repression, we created a series of luciferase reporter constructs containing fragments of the PPA1Y promoter (Fig. 2B). The luciferase activity of these constructs was measured in the presence of pcDNA3.1, 0.1 μ g Myc, or 2 μ g Myc. The results are shown in Figure 2B. The luciferase activity of the PPA1Y promoter is repressed by 0.1 μ g Myc and 2 μ g Myc in a dose-dependent manner. The repression is most pronounced for the 0.1 μ g Myc treatment. The repression is also observed for the 2 μ g Myc treatment. The repression is observed for all constructs containing the PPA1Y promoter, but is most pronounced for the 0.1 μ g Myc treatment. The repression is also observed for the 2 μ g Myc treatment. The repression is observed for all constructs containing the PPA1Y promoter, but is most pronounced for the 0.1 μ g Myc treatment. The repression is also observed for the 2 μ g Myc treatment.

B.



5.11 Identification of the site of c-Myc transcriptional repression in the human PPAR γ 1 promoter

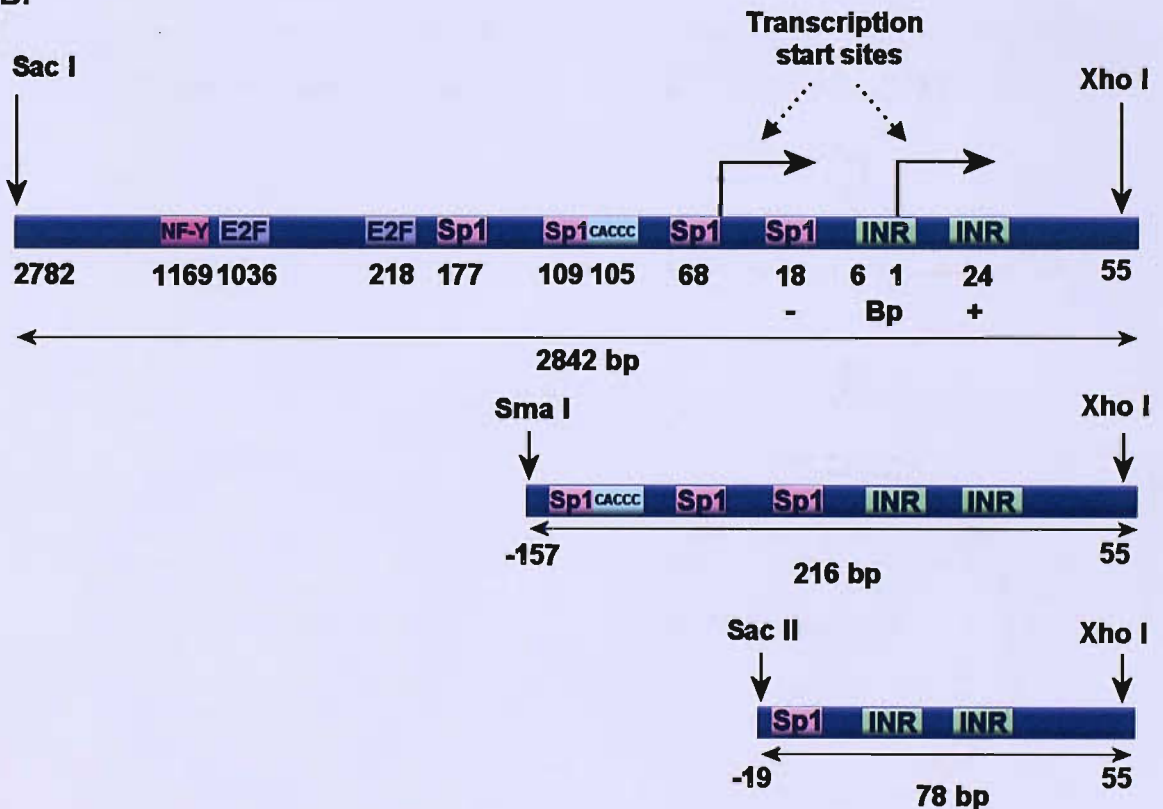
The regions of the c-Myc protein which appear to be required for c-Myc transcriptional repression of the PPAR γ 1 promoter indicates that the mechanism could involve interactions with several protein partners such as NF-Y, Sp1, TFII-I or YY-1 (See **Fig. 5.10**). Analysis of the human PPAR γ 1 promoter sequence revealed that it contains among others, a putative NF-Y site, and several Sp1 sites in addition to two INR elements to which TFII-I and YY-1 can bind (**Fig. 5.3**). To establish which of these potential binding motifs or other novel sequence mediates c-Myc transcriptional repression, PPAR γ 1 promoter deletions were made by digesting the original pGL3- γ 1p3000 construct with *Sac* I and *Sma* I, and *Sac* I and *Sac* II to create the promoter deletion reporters, pGL3- γ 1p216 and pGL3- γ 1p78 respectively (See **Fig. 5.12** for more details). The *Sac* I/*Sma* I truncation of the PPAR γ 1 5' regulatory region yielded a 218 bp fragment from -157 bp to +60 bp relative to the second transcription initiation site which contained two putative Sp1 sites and INR elements. The *Sac* I/*Sac* II digestion of the PPAR γ 1 promoter region removed the first of these Sp1 sites leaving a region from -18bp to +60 bp (**Fig. 5.12**). The integrity of the promoter in these deletion constructs was verified by sequencing (The Sequencing Service, University of Dundee).

To investigate the effect of c-Myc on the activity of the PPAR γ 1 promoter deletion mutants in neuroblastoma cells, pGL3- γ 1p216, pGL3- γ 1p78 and the original PPAR γ 1 promoter reporter pGL3- γ 1p3000 were co-transfected with the increasing quantities of c-Myc expression plasmid indicated in to SK-N-AS cells. Cells were harvested 24 hours post-transfection and luciferase activity measured. **Fig. 5.13** demonstrates that the reporter activity of all three PPAR γ 1 promoter constructs was significantly attenuated in the presence of 0.1 μ g and 2 μ g c-Myc expression plasmid compared with reporter activity in the presence of the empty expression vector. This suggests that the site of c-Myc repression in the PPAR γ 1 promoter is proximal to the second PPAR γ 1 transcription start site. This observation is consistent with studies of other c-Myc repressed genes such as *p21^{CIP1}*, *Mad4*, *PDGFRB* and *GADD45* which have also mapped the site of c-Myc transcriptional inhibition to the minimal promoter of these

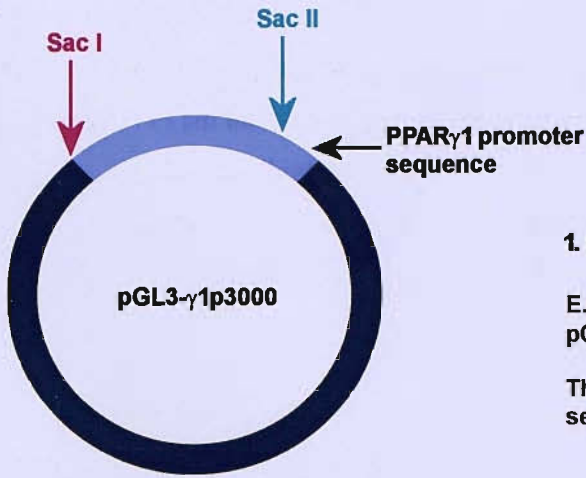
Fig. 5.12. Creation of human PPAR γ 1 promoter reporter deletion constructs.

Originally Fajas *et al* screened a PAC human genomic library to isolate the sequence which contained the entire human PPAR γ gene. A clone was identified which was shown to include the transcription initiation sites for both PPAR γ 1 and PPAR γ 2. To obtain the PPAR γ 1 5' regulatory region an 8-kb EcoRI fragment of this clone, which hybridized with the oligonucleotide specific for the PPAR γ 1 5'UTR was cloned in to pBluescript. A *Sac* I/*Xho* I digest of this clone generated a fragment of DNA, from approximately -2.8 kbp to +60 bp relative to the second transcription start site of PPAR γ 1, which was inserted in to the same sites in pGL3-Basic to create the PPAR γ 1 promoter reporter, pGL3- γ 1p3000[36]. We digested the pGL3- γ 1p3000 construct with *Sac* I and *Sma* I and *Sac* I and *Sac* II to create the promoter deletion reporters, pGL3- γ 1p216 and pGL3- γ 1p78 respectively since the promoter region contains a *Sma* I site which starts at position -159 and a *Sac* II site which starts at position -22 and because these endonucleases would not cut the vector backbone (B). In each case, following restriction digest the linearised plasmid was treated with T4 DNA polymerase to generate blunt ends which were subsequently ligated (See flow diagram opposite A). Fig. 5.12 B shows the promoter region found in each reporter construct and its potential sites of c-Myc transcriptional repression, including nuclear transcription factor-Y (NF-Y), elongation factor 2 (E2F) and special factor 1(Sp1) binding sites and two initiator (INR) elements.

B.



A.



1. Digest plasmid with restriction endonucleases.

E.g. To create pGL3-γ1p78 the original construct, pGL3-γ1p3000 is cut with Sac I and Sac II.

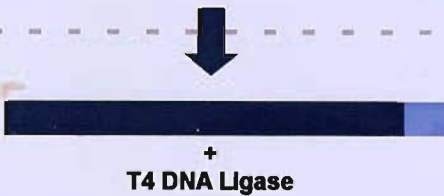
These endonucleases only have sites in promoter sequence.



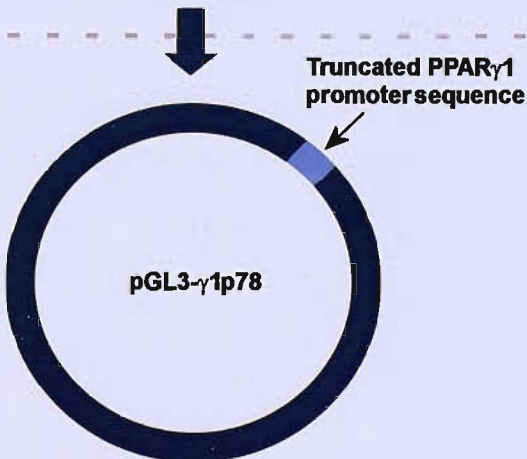
2. Gel purify linearised plasmid from released promoter fragment.



3. Incubate gel purified linearised plasmid with T4 DNA polymerase to remove Sac I and Sac II 3'overhangs generating blunt ends.

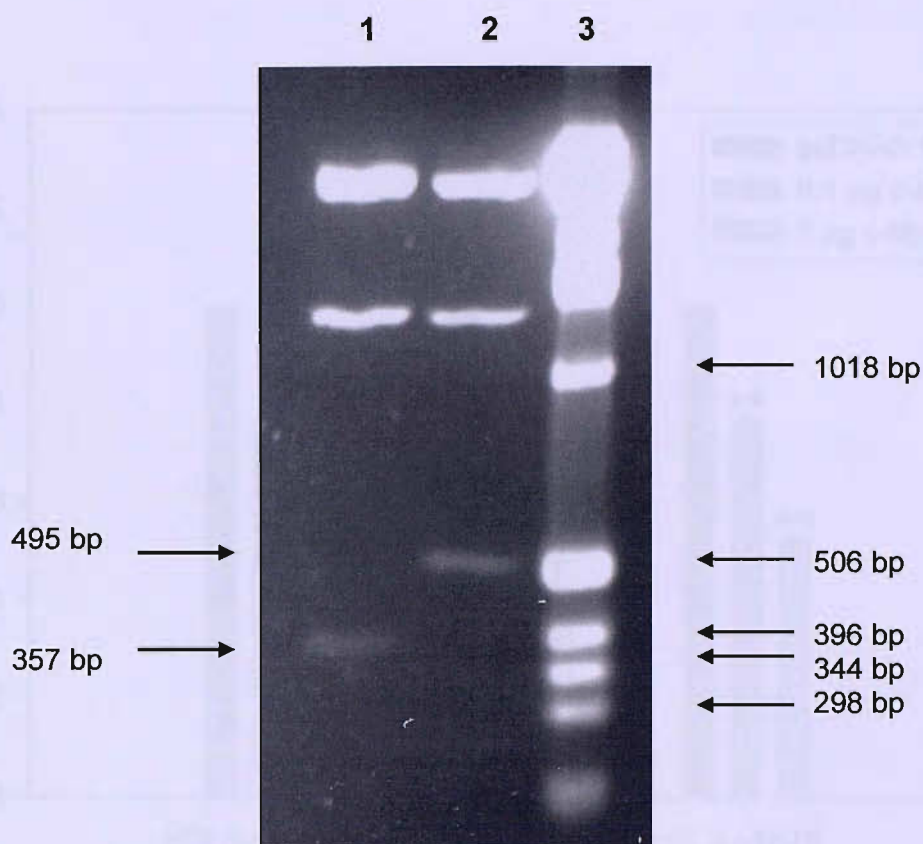


4. Plasmid is cleaned following T4 DNA Pol treatment and set up in ligation with T4 DNA ligase.



5. Ligation used to transform bacteria.

Transformants potentially containing PPAR γ 1 promoter deletion reporter screened by restriction digest and sequencing.



Lane
1. pGL3-γ1p78 <i>Bgl</i> I/ <i>Xho</i> I digest
2. pGL3-γ1p216 <i>Bgl</i> I/ <i>Xho</i> I digest
3. Invitrogen 1 Kb ladder

Fig. 5.12 C To confirm that the cloning was successful the potential pGL3-γ1p78 and pGL3-γ1p216 clones were digested with *Bgl* I and *Xho* I and run on 2% agarose gel. *Bgl* I cuts pGL3-Basic (4818 bp- 21 bp polylinker removed during cloning = 4797 bp) at positions 3273 and 4541 but not in the 300 bp region upstream from the second PPARγ1 transcription start site in pGL3-γ1p3000. Digesting the pGL3-γ1p3000 reporter with *Sac* I and *Sac* II, generates a 2759 bp fragment of the PPARγ1 5' regulatory region leaving a 78 bp proximal promoter upstream of the *Xho* I site. Therefore, digesting the pGL3-γ1p78 construct with *Bgl* I/*Xho* I should generate 3250 bp, 1268 bp and 357 bp fragments (357 bp fragment between second *Bgl* I site and *Xho* I site (*Xho* I site at +55 relative to start site of transcription)) (**Lane 1**). Digesting the pGL3-γ1p3000 bp reporter with *Sac* I and *Sma* I generates a 2621 bp fragment of the PPARγ1 5' regulatory region, leaving a 216 bp promoter upstream of the *Xho* I site. Therefore, digesting the pGL3-γ1p216 construct with *Bgl* I and *Xho* I should generate 3250 bp, 1268 bp and a 495 bp fragments (495 bp fragment between second *Bgl* I site and *Xho* I site) (**Lane 2**).

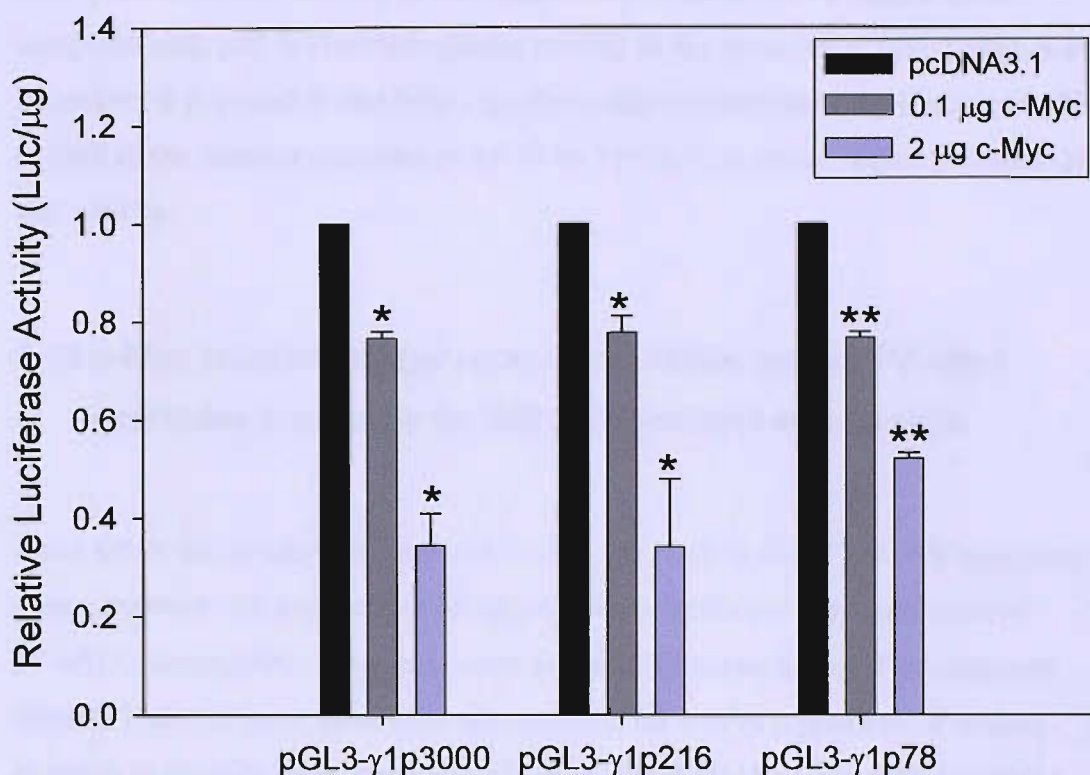


Fig. 5.13 The effect of c-Myc on the activity of PPAR γ 1 promoter deletion

constructs. SK-N-AS cells were co-transfected with 2 μ g of the PPAR γ 1 promoter reporter deletion constructs pGL3- γ 1p216 or pGL3- γ 1p78, or pGL3- γ 1p3000 and either 0.1 μ g (grey bar) or 2 μ g (purple bar) of an expression plasmid encoding c-Myc. The total quantity of DNA for each transfection was normalised to 4 μ g (including reporter) with an empty expression vector (pcDNA3.1). Cells were harvested 24 hours post-transfection and luciferase activity measured. Data shows the relative mean luciferase activity of the PPAR γ 1 promoter reporters (per μ g of protein) co-transfected with the indicated amounts of c-Myc expression plasmid compared with promoter reporter activity in the presence of the empty expression vector control (black bar) and represent two independent experiments \pm S.E. Statistics were calculated using a Student's *t*-test and showed that there was significant repression of both pGL3- γ 1p3000 promoter activity (*) ($p < 0.05$) and the promoter activity of the PPAR γ 1 promoter deletion mutants pGL3- γ 1p216 (*) ($p < 0.05$) and pGL3- γ 1p78 (**) ($p < 0.01$) in the presence of 0.1 μ g and 2 μ g c-Myc expression plasmid

genes [478,479,481,498,499]. In addition, when SK-N-AS cells were co-transfected with the PPAR γ 1 promoter deletion reporters and an expression plasmid encoding Miz-1, the luciferase activity of the constructs was induced to a similar level compared with pGL3- γ 1p3000 reporter activity in the presence of Miz-1 (**Fig. 5.14**). Therefore, it is probable that Miz-1 mediates this transactivation by binding to either or both of the initiator elements in the 78 bp PPAR γ 1 promoter region between -18 and + 60 bp.

5.12 c-Myc transcriptional repression of the human PPAR γ 1 promoter occurs by an INR-independent mechanism

Since either the putative GC box or two INR elements in the PPAR γ 1 5' regulatory region between -18 and + 60 bp could potentially mediate c-Myc inhibition of PPAR γ 1 transcription, it was necessary to create deletions of the 78 bp region to identify if one or more these sites was essential for c-Myc repression. Previous attempts to amplify short fragments of the proximal PPAR γ 1 5' regulatory region from human genomic DNA by PCR were unsuccessful possibly because of the core promoter's high GC content. In addition, the promoter region of interest was very short, therefore three pairs of oligonucleotides were designed and synthesized so that when annealed and ligated together they formed the -18 to + 60 bp sequence of the PPAR γ 1 5' regulatory region (**Fig. 5.15**). The insert of the complete 78 bp sequence was cloned in to pGL3-Basic to create the PPAR γ 1 promoter reporter, pGL3- γ 1p78oligo. The promoter region in the second construct termed pGL3- γ 1p58oligo lacks the Sp1 site and the first putative INR element is disrupted. The promoter sequence in the reporter called pGL3- γ 1p34oligo lacks both the Sp1 site and first INR and the second INR is partially deleted (**Fig. 5.15**). The promoters of all three constructs were verified by sequencing (The Sequencing Service, University of Dundee).

To investigate the effect of c-Myc on the activity of these synthetic PPAR γ 1 promoter reporters in neuroblastoma cells, pGL3- γ 1p78oligo, pGL3- γ 1p58oligo and pGL3- γ 1p34oligo constructs were co-transfected with increasing quantities of a c-Myc expression plasmid in to SK-N-AS cells (**Fig. 5.16**). The SK-N-AS cells were

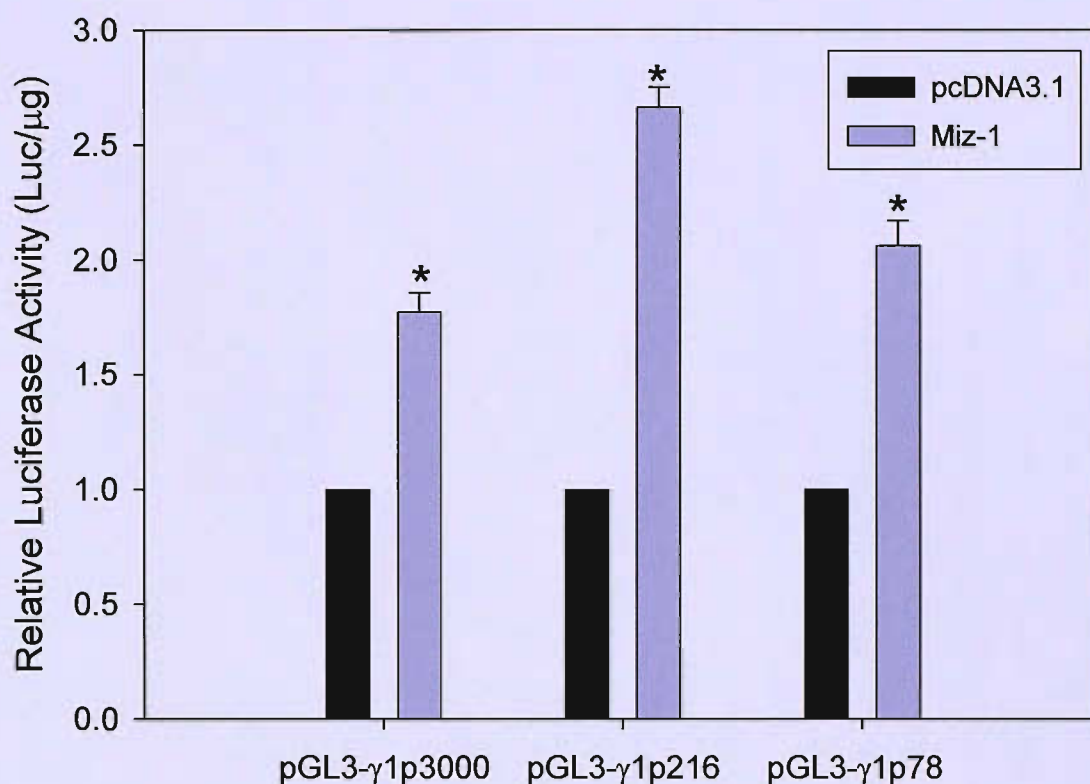
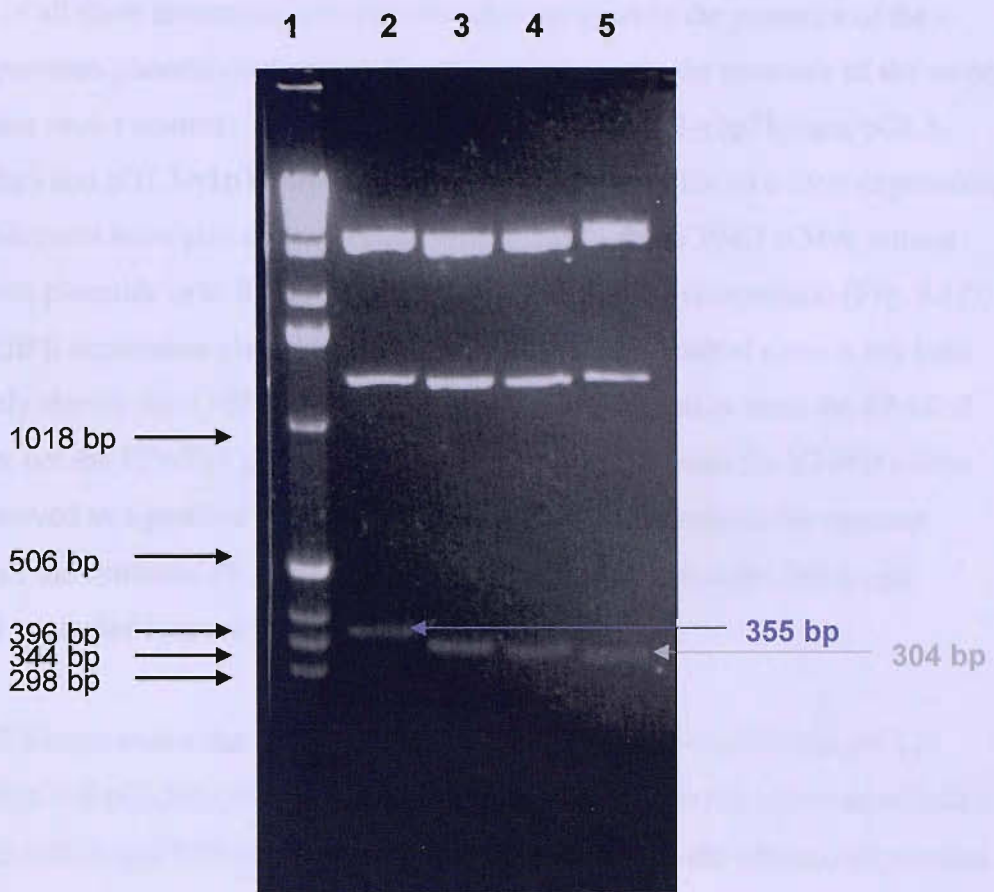


Fig. 5.14. The effect of Miz-1 on the activity of PPAR γ 1 promoter deletion constructs.

SK-N-AS cells were co-transfected with either 2 μ g of the PPAR γ 1 promoter reporter deletion constructs pGL3- γ 1p216 or pGL3- γ 1p78, or pGL3- γ 1p3000 and 2 μ g of an expression plasmid encoding Miz-1 or an empty expression vector (pcDNA3.1) (2 μ g). Cells were harvested 24 hours post-transfection and luciferase activity measured. Data shows the relative mean luciferase activity of the PPAR γ 1 promoter reporters (per μ g of protein) co-transfected with the Miz-1 expression plasmid (purple bar) compared with promoter reporter activity in the presence of the empty expression vector control (black bar) and represent two independent experiments \pm S.E. Statistics were calculated using a Student's *t*-test and showed that there was significant induction of pGL3- γ 1p3000 promoter activity (*) ($p < 0.05$) and the promoter activity of the PPAR γ 1 promoter deletion mutants pGL3- γ 1p216 (*) ($p < 0.05$) and pGL3- γ 1p78 (*) ($p < 0.05$) in the presence of 2 μ g Miz-1 expression plasmid.

Fig. 5.15. Creation of human PPAR γ 1 promoter reporter constructs using synthetic oligonucleotides. Three pairs of oligonucleotides were designed and synthesised (A) (1+2, 3+4, 5+6) so that when annealed and then ligated together they formed a continuous 78 bp sequence of the PPAR γ 1 5' regulatory region from -18 bp to +60 bp relative to the second PPAR γ 1 transcription start site.(B). These synthetic oligonucleotides were cloned in to pGL3-Basic via the indicated restriction sites to create the constructs pGL3- γ 1p78oligo, pGL3- γ 1p58oligo and pGL3- γ 1p34oligo which have the same 3' end at +60bp but have 5' termini at -18 bp, +3 bp and +27 bp respectively, relative to the transcription start site (Fig 5.15A below). The 78 bp promoter region contains a putative Sp1 site (starts at -18 bp, core sequence defined by MatInspector highlighted in red) and 2 potential INR elements (B). The INR at position -6 shown in blue overlaps the second PPAR γ 1 transcription start site (red G, +1), whereas the second INR highlighted in green is located downstream of this initiation site at position +24. The pGL3- γ 1p58oligo construct lacks the Sp1 site and the first potential INR element is disrupted whereas the pGL3- γ 1p34oligo reporter lacks both the Sp1 site and the first INR element and the second INR is disrupted. In Fig. 5.15C bases in the two potential INR elements in the PPAR γ 5' regulatory region which match the consensus INR sequence are shown in bold.



Lane

1. Invitrogen 1 Kb ladder
2. pGL3- γ 1p78oligo *Bgl* I/*Xho* I digest
3. pGL3- γ 1p58oligo *Bgl* I/*Xho* I digest
4. pGL3- γ 1p34oligo *Bgl* I/*Xho* I digest
5. pGL3-Basic *Bgl* I/*Xho* I digest

D. Potential pGL3- γ 1p78oligo, pGL3- γ 1p58oligo and pGL3- γ 1p34oligo clones were screened by digestion with *Bgl* I and *Xho* I and visualizing the digest result on a 2% agarose gel. *Bgl* I cuts pGL3-Basic (4818 bp) at position 3273 and 4541 but there is no *Bgl* I site in the 78 bp 5' PPAR γ 1 regulatory region. Since the PPAR γ 5' regulatory region does contain an *Xho* I site (+55 relative to transcription start site), digesting pGL3- γ 1p78oligo, pGL3- γ 1p58oligo and pGL3- γ 1p34oligo with *Bgl* I/*Xho* I should generate 355 bp (**Lane 2**), 335 bp (**Lane 3**), and 327 bp (**Lane 4**) fragments respectively, which corresponds to the region between the second *Bgl* I site and the *Xho* I site (at +55 relative to start site of transcription). As a control pGL3-Basic was also digested with *Bgl* I/*Xho* I and yielded a 304 bp fragment, which corresponds to the region after the second *Bgl* I site and the *Kpn* I-*Xho* I polylinker (**Lane 5**).

harvested after 24 hours and luciferase activity measured. Intriguingly, the reporter activity of all three constructs was significantly repressed in the presence of the c-Myc expression plasmid compared with reporter activity in the presence of the empty expression vector control. To verify that repression of pGL3- γ 1p78oligo, pGL3- γ 1p58oligo and pGL3- γ 1p34oligo reporter activity was specific to c-Myc expression, these constructs were also co-transfected with C/EBP β and V394D c-Myc mutant expression plasmids in to SK-N-AS neuroblastoma cells for comparison (**Fig. 5.17**). The C/EBP β expression plasmid was chosen as a negative control since it has been previously shown that C/EBP β specifically induces transcription from the PPAR γ 2 promoter not the PPAR γ 1 promoter [422]. Co-transfection with the V394D c-Myc mutant served as a positive control since it was predicted to repress the reporter activity of the synthetic PPAR γ 1 promoter to a similar extent as the full-length PPAR γ 1 promoter construct, pGL3- γ 1p3000.

Fig. 5.17 demonstrates that the reporter activity of the pGL3- γ 1p78oligo, pGL3- γ 1p58oligo and pGL3- γ 1p34oligo constructs was repressed in the presence of both 2 μ g of the c-Myc and V394D c-Myc mutant expression plasmids whereas expression of C/EBP β did not significantly alter the reporter activity of either of the constructs. Since the level of c-Myc inhibition of the reporter activity of both the full length and 34 bp PPAR γ 1 promoter constructs was comparable this suggests that repression of PPAR γ 1 transcription by c-Myc occurs by an INR-independent mechanism that is mediated by sequence located between + 27 and + 60 bp in the PPAR γ 1 5' regulatory region. Interestingly, when SK-N-AS cells were co-transfected with pGL3- γ 1p78oligo, pGL3- γ 1p58oligo or pGL3- γ 1p34oligo and a Miz-1 expression plasmid, the reporter activity of all three synthetic PPAR γ 1 promoter constructs was stimulated in the presence of the Miz-1 expression plasmid relative to reporter activity in the presence of the empty expression vector control (**Fig. 5.18**). Given that the promoter region of pGL3- γ 1p34oligo lacks an INR element, the Miz-1 effect on this construct, and potentially the other PPAR γ 1 promoter reporters, may be a consequence of its sequestration of c-Myc that is bound to a site within the 34 bp region of the PPAR γ 1 5' regulatory region thus relieving transcriptional repression by c-Myc.

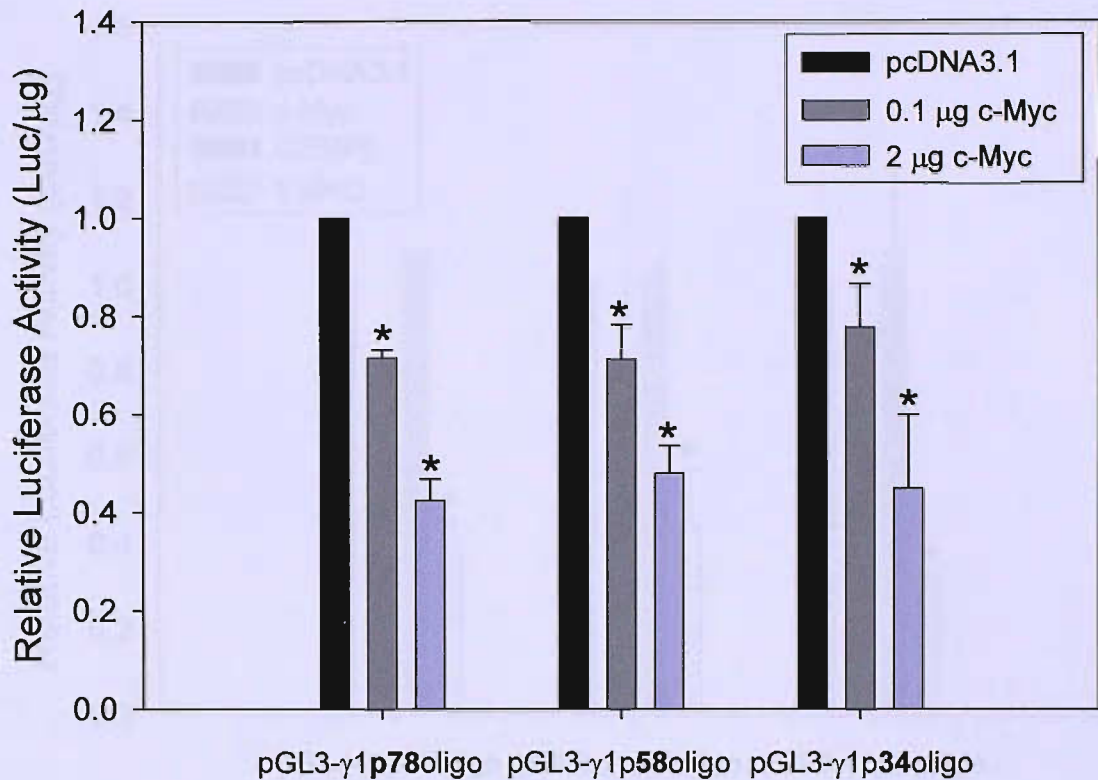


Fig. 5.16. The effect of c-Myc on the activity of synthetic oligonucleotide

PPAR γ 1 promoter reporters. SK-N-AS cells were co-transfected with 2 μ g of the synthetic oligonucleotide PPAR γ 1 promoter reporters, pGL3- γ 1p78oligo, pGL3- γ 1p58oligo or pGL3- γ 1p34oligo and either 0.1 μ g (grey bar) or 2 μ g (purple bar) of an expression plasmid encoding c-Myc. The total quantity of DNA for each transfection was normalised to 4 μ g (including reporter) with an empty expression vector (pcDNA3.1). Cells were harvested 24 hours post-transfection and luciferase activity measured. Data shows the relative mean luciferase activity of the PPAR γ 1 promoter reporters (per μ g of protein) co-transfected with the indicated amounts of c-Myc expression plasmid compared with promoter reporter activity in the presence of the empty expression vector control (black bar) and represent two independent experiments \pm S.E. Statistics were calculated using a Student's *t*-test and showed that there was significant repression of pGL3- γ 1p78oligo, pGL3- γ 1p58oligo and pGL3- γ 1p34oligo promoter activity in the presence of 0.1 μ g and 2 μ g c-Myc expression plasmid (*) ($p < 0.05$).

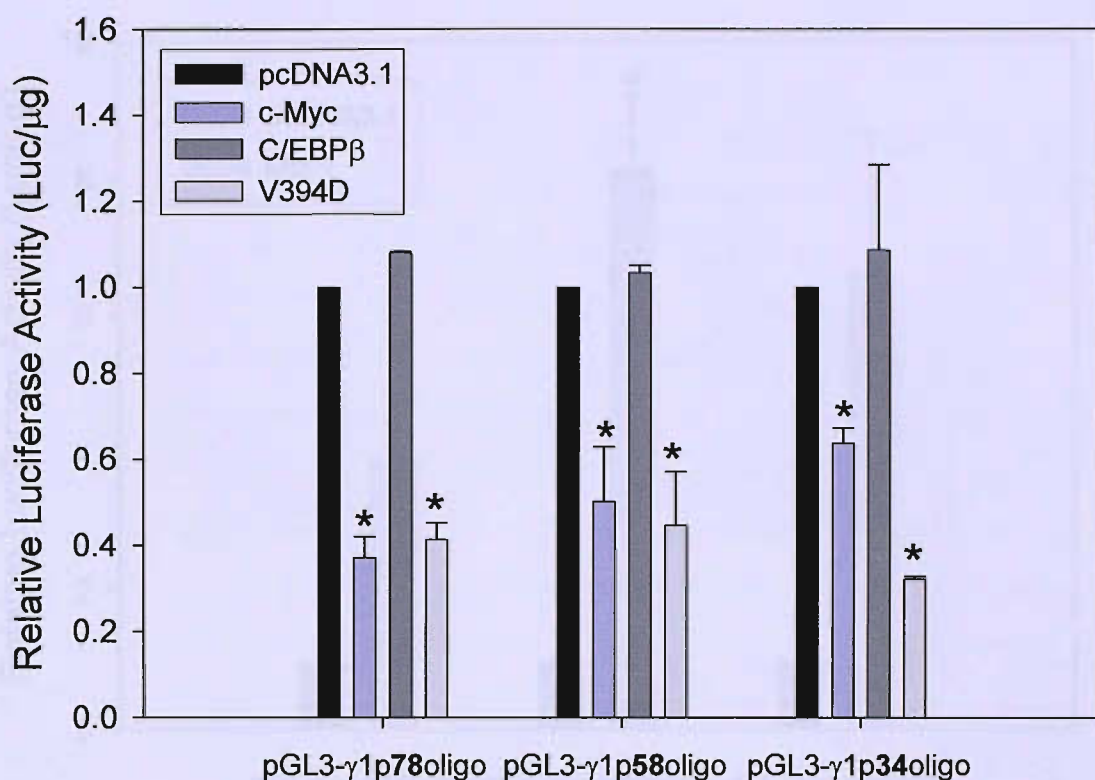


Fig. 5.17. The effect of c-Myc, C/EBPβ and the c-Myc V394D mutant on the activity of synthetic oligonucleotide PPARγ1 promoter reporters. SK-N-AS cells were co-transfected with 2 μg of the synthetic oligonucleotide PPARγ1 promoter reporters, pGL3-γ1p78oligo, pGL3-γ1p58oligo or pGL3-γ1p34oligo and 2 μg of an expression plasmid encoding either c-Myc (purple bar), C/EBPβ (dark grey bar) or the V394D c-Myc mutant (light grey bar) or an empty expression vector control (pcDNA 3.1) (black bar). Cells were harvested 24 hours post-transfection and luciferase activity measured. Data shows the relative mean luciferase activity of the PPARγ1 promoter reporters (per μg of protein) co-transfected with the indicated expression plasmid compared with promoter reporter activity in the presence of the empty expression vector control (black bar) and represent two independent experiments ± S.E. Statistics were calculated using a Student's *t*-test and showed that there was significant repression of pGL3-γ1p78oligo, pGL3-γ1p58oligo and pGL3-γ1p34oligo promoter activity in the presence c-Myc (*) ($p < 0.05$) and the V394D c-Myc mutant expression plasmid (*) ($p < 0.05$) but not the presence of C/EBPβ expression plasmid.

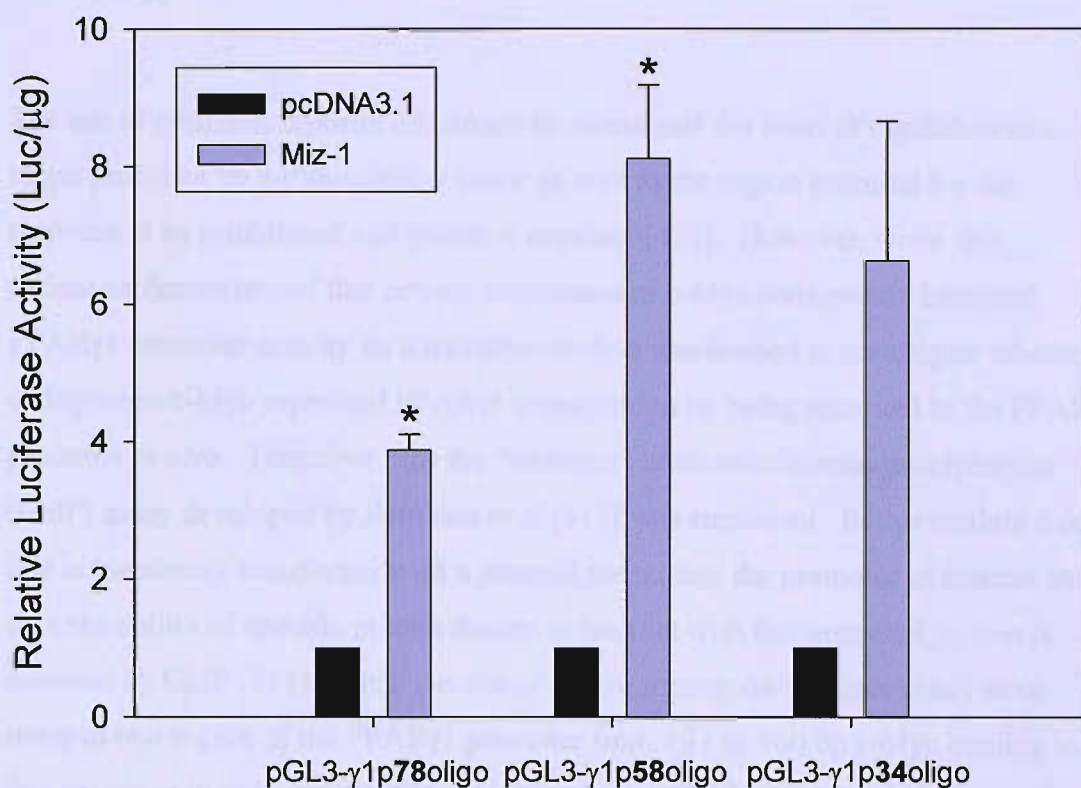


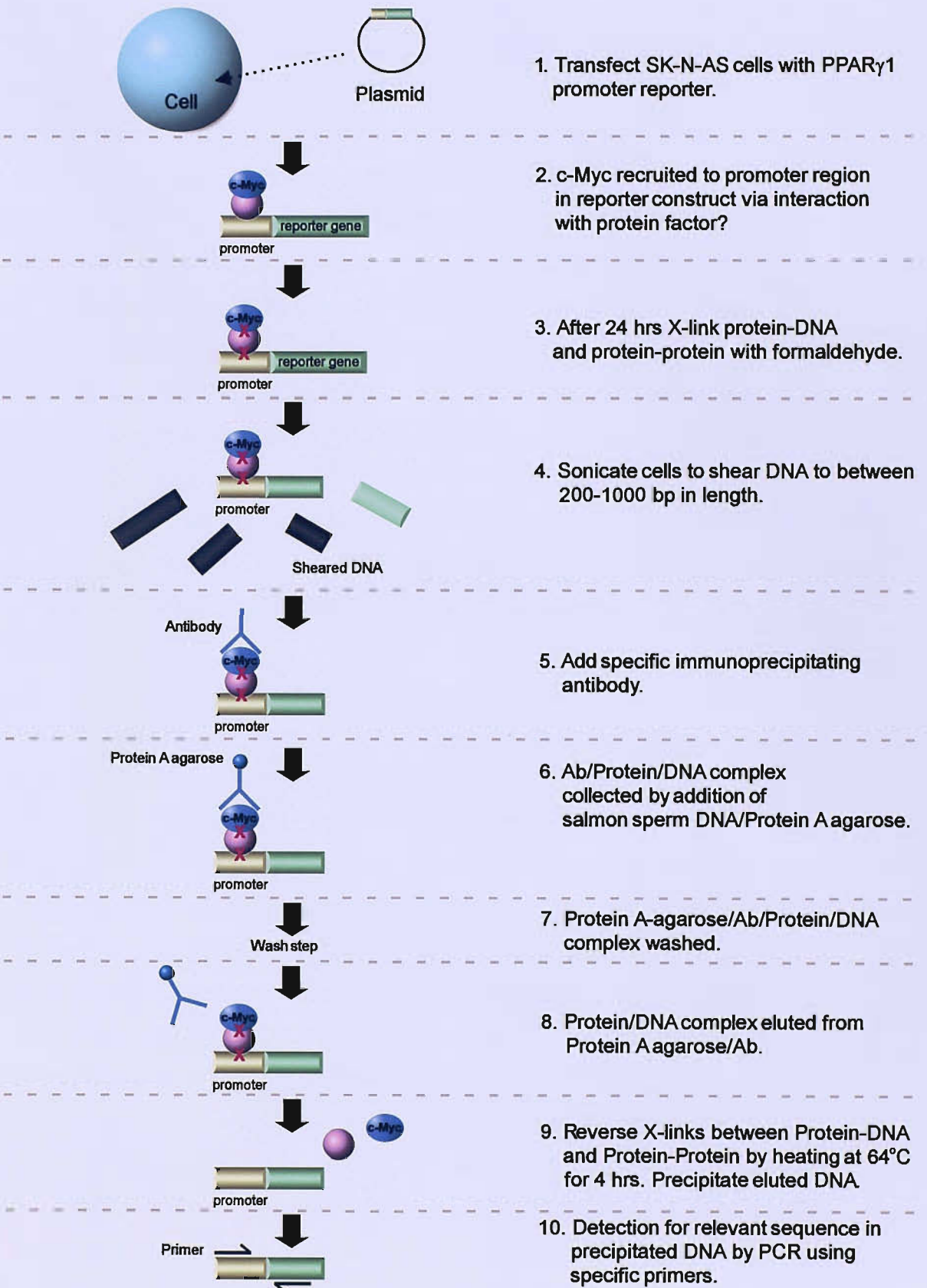
Fig. 5.18. The effect of Miz-1 on the activity of synthetic oligonucleotide PPAR γ 1 promoter reporters. SK-N-AS cells were co-transfected with either 2 μ g of the PPAR γ 1 promoter reporters, pGL3- γ 1p78oligo, pGL3- γ 1p58oligo, or pGL3- γ 1p34oligo and 2 μ g of an expression plasmid encoding Miz-1 or an empty expression vector (pcDNA3.1) (2 μ g). Cells were harvested 24 hours post-transfection and luciferase activity measured. Data shows the relative mean luciferase activity of the PPAR γ 1 promoter reporters (per μ g of protein) co-transfected with the Miz-1 expression plasmid (purple bar) compared with promoter reporter activity in the presence of the empty expression vector control (black bar) and represent two independent experiments \pm S.E. Statistics were calculated using a Student's *t*-test and showed that there was significant induction of the PPAR γ 1 promoter reporters, pGL3- γ 1p78oligo (*) ($p < 0.05$) and pGL3- γ 1p58oligo (**) in the presence of 2 μ g Miz-1 expression plasmid.

5.13 The use of a transient chromatin immunoprecipitation assay to evaluate c-Myc binding to the human PPAR γ 1 promoter *in vivo*.

The use of promoter reporter constructs to investigate the level of regulation of a target promoter by a transcription factor as well as the region essential for the response is an established and practical approach[432]. However, while this technique demonstrated that ectopic expression of c-Myc consistently inhibited PPAR γ 1 promoter activity an alternative method was needed to investigate whether endogenous c-Myc repressed PPAR γ 1 transcription by being recruited to the PPAR γ 1 promoter *in vivo*. Therefore next the “transient” chromatin immunoprecipitation (ChIP) assay developed by Farnham *et al* [511] was employed. In this method a cell line is transiently transfected with a plasmid containing the promoter of interest and then the ability of specific protein factors to interact with this sequence *in vivo* is assessed by ChIP [511]. Since the site of c-Myc repression had previously been mapped to a region of the PPAR γ 1 promoter from +27 to +60 bp c-Myc binding to this sequence *in vivo* was examined by transfecting SK-N-AS neuroblastoma cells with the synthetic PPAR γ 1 promoter reporter, pGL3- γ 1p34oligo.

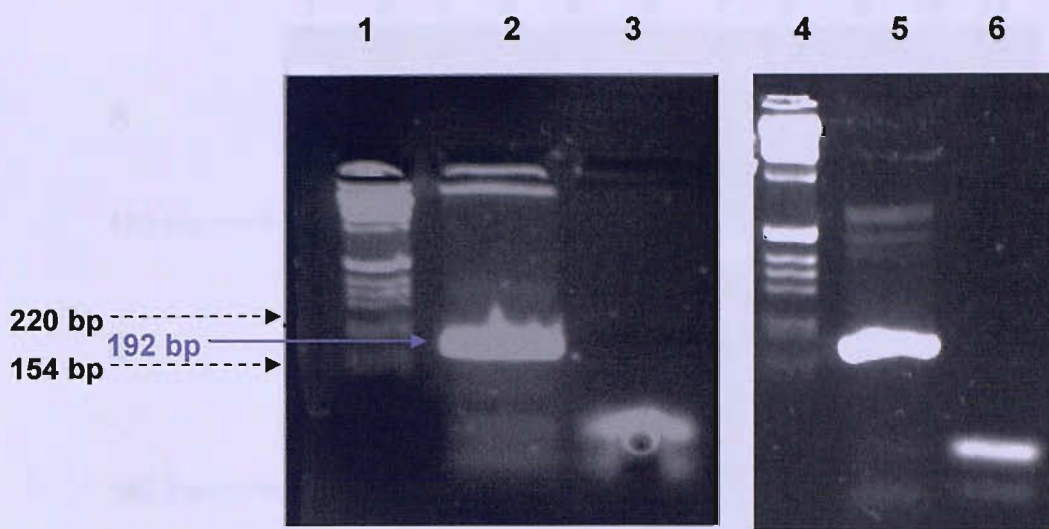
A detailed description of the ChIP protocol can be found in the methods chapter and a flow diagram of the procedure is depicted in **Fig. 5.19**. In summary, 24 hours post-transfection, protein-protein and protein-DNA complexes were cross-linked by incubating SK-N-AS cells with formaldehyde before lysing and sonicating the cells to shear the DNA. An antibody against c-Myc was then introduced in to the lysate to precipitate complexes containing the transcription factor. Finally the cross-links holding the complexes together were reversed and eluted DNA was precipitated and analysed by PCR. To detect binding by c-Myc to the PPAR γ 1 promoter sequence in pGL3- γ 1p34oligo, the forward primer used in the PCR was complementary to the 34 bp PPAR γ 1 regulatory region whereas the reverse primer recognized a sequence in the pGL3-Basic vector. The specificity of the primers was verified by performing a PCR using either the plasmid or input DNA from pGL3- γ 1p34oligo transfected SK-N-AS cells as a template (**Fig. 5.20**). Since the plasmid is present at a high copy number it was predicted that this would improve the efficiency of the immunoprecipitation and PCR. Importantly though, when this method was first used

Fig. 5.19. Summary of Transient chromatin immunoprecipitation (ChIP) assay.



to evaluate the *in vivo* interaction of the E2F1 transcription factor with a carboxylesterase promoter reporter, it was shown that in the presence of physiological normal levels of E2F1, the binding specificity that was originally detected at the endogenous carboxylesterase promoter was maintained on the transiently transfected plasmid [511]. Having confirmed the efficiency of the ChIP PCR primers, the binding of endogenous c-Myc to the 34 bp PPAR γ 1 regulatory region in SK-N-AS cells transfected with pGL3- γ 1p34oligo was studied (**Fig. 5.21**). A strong PCR signal was obtained when the input DNA sample of pGL3- γ 1p34oligo transfected SK-N-AS cells was used as the template (**Fig. 5.21 A, Lane 2**), although no PCR product was detected using the template DNA immunoprecipitated from these cells by the anti-c-Myc antibody (**Fig. 5.21 A, Lane 3**) even after additional PCR cycles (data not shown). To determine if this result was due to insufficient template, the PCR was repeated using increasing quantities of template DNA. While a PCR signal was now detected using both input and c-Myc antibody immunoprecipitated DNA samples from pGL3- γ 1p34oligo transfected SK-N-AS as the template (**Fig. 5.21 B, Lanes 2-3**), background PCR product was also observed in samples where the DNA template had been recovered from lysates of untransfected SK-N-AS cells or cells transfected with a control plasmid (pGL3-Basic) (**Fig. 5.21 B, Lanes 5-10**).

Therefore, to determine a new annealing temperature that would still allow amplification of the region in the PPAR γ promoter reporter, but reduce production of background or non-specific PCR signal, the effect of increasing the annealing temperature (originally 50°C) on product yield using pGL3- γ 1p34oligo as the template (**Fig. 5.22 A**) was evaluated. Preliminary experiments demonstrated that increasing the annealing temperature from 50°C to 60.9°C had no significant effect on the amount of amplified product obtained (data not shown). However, the PCR product yield did decrease when the annealing temperature was raised from 61.8 °C to 64.1°C, therefore the PCR reactions using the ChIP DNA samples were repeated with 64.1°C as the new annealing temperature (**Fig. 5.22 B**). Again at lower numbers of PCR cycles, a PCR product was detected using the input DNA sample of pGL3- γ 1p34oligo transfected SK-N-AS cells as template (**Fig. 5.22 B, top gel, Lane 2**) but no product was observed with the other DNA samples. After extra cycles of PCR, even at the higher annealing temperature, either a background or non-specific PCR product band was still also detected in samples with DNA templates from



Lane
1. Invitrogen 1 Kb ladder
2. pGL3- γ 1p34oligo template
3. Negative control - no template
4. Invitrogen 1 Kb ladder
5. Input DNA from transfected SK-N-AS cells
6. Negative control - no template

Fig. 5.20. Evaluation of the efficiency of transient ChIP primers using either plasmid or input DNA from SK-N-AS cells as the template. Two independent PCR reactions were set up using oligonucleotide 5, designed to create the synthetic PPAR γ 1 promoter reporters (see Fig 5.15), as the forward primer specific to the 34 bp promoter region in pGL3- γ 1p34oligo. The reverse primer used was complementary to part of the pGL3-Basic sequence 175 bp downstream from the start of oligonucleotide 5. To verify the specificity of these primers, they were used in a PCR reaction with the plasmid pGL3- γ 1p34oligo as the template (50 ng) and as shown in **lane 2** the correct size product (192 bp) was generated (See Materials and Methods for PCR conditions). To confirm that these primers would also work efficiently using DNA extracted from cells, SK-N-AS cells were transfected with 5 μ g of pGL3- γ 1p34oligo. After 24 hours the cells were cross-linked with formaldehyde, harvested, lysed and sonicated. Following reversal of protein-DNA and protein-protein cross-links the cell lysate was extracted with phenol-chloroform. 2 μ l of this extracted cell lysate was used as the template in a PCR reaction with the transient chip primers described above (**lane 5**). As shown in **lane 5** the same size product was generated using the extracted cell lysate with a yield comparable to that produced when the plasmid was used as the template.

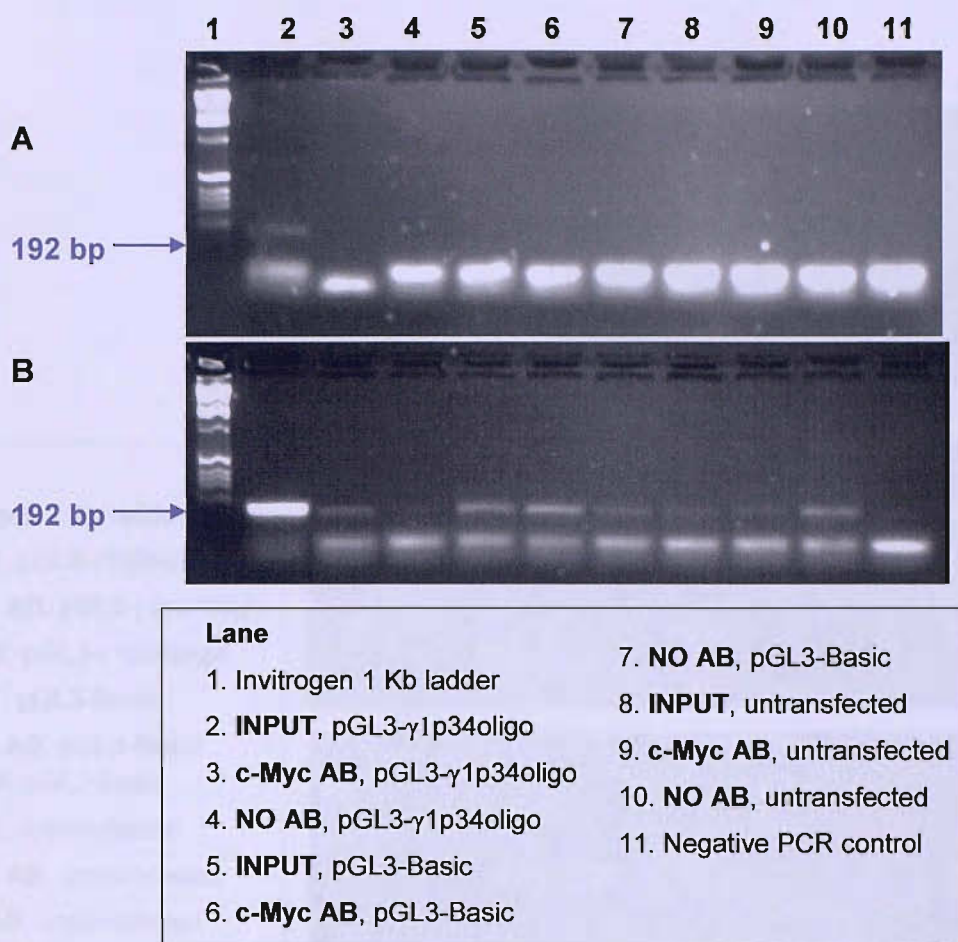


Fig. 5.21. Transient ChIP assay PCR results of SK-N-AS cells transfected with either pGL3- γ 1p34oligo or pGL3-Basic or untransfected cells. Immunoprecipitations were performed on prepared lysates from either untransfected SK-N-AS cells or SK-N-AS cells transfected with pGL3-Basic or pGL3- γ 1p34oligo using an antibody to c-Myc. DNA from, an input sample (**INPUT**), the immunoprecipitate (**c-Myc AB**), and a lysate sample with no added antibody (**NO AB**) was recovered and analysed by PCR, using specific transient ChIP primers (**Fig. 5.20**). **Fig. 5.21 A** shows the PCR products visualised on a 1.5 % DNA agarose gel obtained after 25 cycles with 2 μ l of template. A specific PCR product (192 bp) was obtained when the input DNA sample of pGL3- γ 1p34oligo transfected SK-N-AS cells was used as the template (**Lane 2**), although no product was observed in the other lanes even after additional PCR cycles (Data not shown). **Fig. 5.21 B** is representative gel of several independent PCR reactions which were performed using larger quantities of template and indicates that either a background or non-specific PCR product band was detected in samples where the DNA template had been recovered from lysates of untransfected SK-N-AS cells or cells transfected with pGL3-Basic (**Lanes 5-10**) but not in the negative control (**Lane 11**). In this example 3 μ l of template was used and the PCR products generated after 35 cycles are shown.

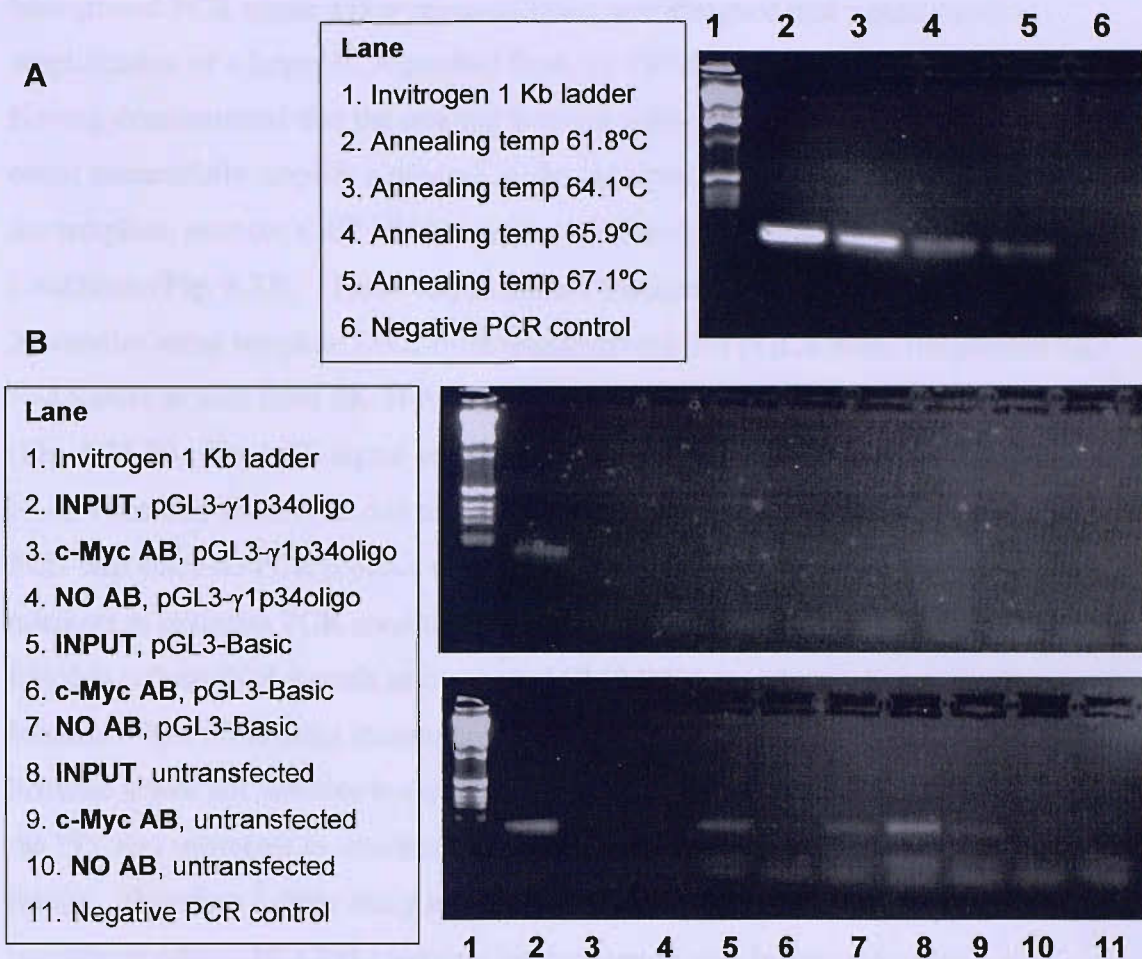


Fig. 5.22. Optimisation of PCR annealing temperature to reduce non-specific products in transient ChIP assay PCR reactions using DNA recovered from transfected or untransfected SK-N-AS cells. Fig. 5.22 A demonstrates the effect of increasing the annealing temperature of the PCR reaction between 61.8°C and 67.1°C on the product yield using the transient ChIP primers described in Fig. 5.20. Since a considerable reduction in product yield was achieved by increasing the annealing temperature from 61.8 °C to 64.1°C, a PCR reaction was performed using template DNA recovered from, input (INPUT), immunoprecipitated (c-Myc AB), and No antibody lysate (NO AB) samples with 64.1°C as the new annealing temperature (Fig. 5.22 B). After 30 cycles (top gel in Fig. 5.22B) of PCR, a specific product (192 bp) was obtained when the input DNA sample of pGL3- γ 1p34oligo transfected SK-N-AS cells was used as the template (Lane 2), although no product was observed in the other lanes. At 35 cycles (Bottom gel in Fig. 5.22.B) however, either a background or non-specific PCR product band was still also detected in samples where the DNA template had been recovered from lysates of untransfected SK-N-AS cells or cells transfected with pGL3-Basic (Lanes 5-10) but not in the negative control (Lane 11).

untransfected SK-N-AS cells or cells transfected with pGL3-Basic, but not in the negative control (**Fig. 5.22 B bottom gel**). As an alternative approach to reduce the background PCR signal a new reverse primer was designed that would result in amplification of a larger PCR product from the PPAR γ 1 promoter reporter template. Having demonstrated that the original forward primer and the new reverse primer could successfully amplify a product of the expected size using pGL3- γ 1p34oligo as the template, next the ChIP DNA samples were analysed using the same PCR conditions (**Fig. 5.23**). However, as before, the same size PCR product was detected in samples using template DNA from untransfected and pGL3-Basic transfected SK-N-AS cells as well from SK-N-AS cells containing the PPAR γ 1 promoter reporter (**Fig. 5.23 B**). The PCR signal seen in untransfected and pGL3-Basic transfected SK-N-AS cells may have been due to cross-contamination of the samples prior to the PCR step since no PCR product was observed in the PCR negative control. Further attempts to optimize PCR conditions and eliminate potential sources of contamination failed to reduce PCR signals using control ChIP DNA templates. In conclusion, because of the difficulties encountered in developing a transient chip assay in this instance it was not possible to develop this technique to investigate c-Myc binding to the PPAR γ 1 promoter *in vivo* because of the potential risk of generating false positive results. Therefore further study is warranted to identify an alternative approach to investigate c-Myc-PPAR γ 1 promoter interactions *in vivo* in neuroblastoma cells.

5.14 The Sp1 transcription factor stimulates human PPAR γ 1 promoter activity

Further examination of the sequence between + 27 and + 60 bp of the PPAR γ 1 5' regulatory region reveals the presence of a GC-box-like element (or Sp1-like binding site) starting at position +39 (GGGCGC) that was not identified by the MatInspector analysis. There is however, variation in published consensus sequences for GC boxes/Sp1 binding sites and the parameters used by MatInspector to define a GC box/Sp1 site could have meant that it did not reveal this putative Sp1-like site (See Appendix). For instance, some reports suggest a GC-box/Sp1 site has 4 guanine bases both up and downstream of the central cytosine (GGGGCGGGG) whereas other studies describe a GC-box/Sp1 site as a sequence of just four nucleotides with

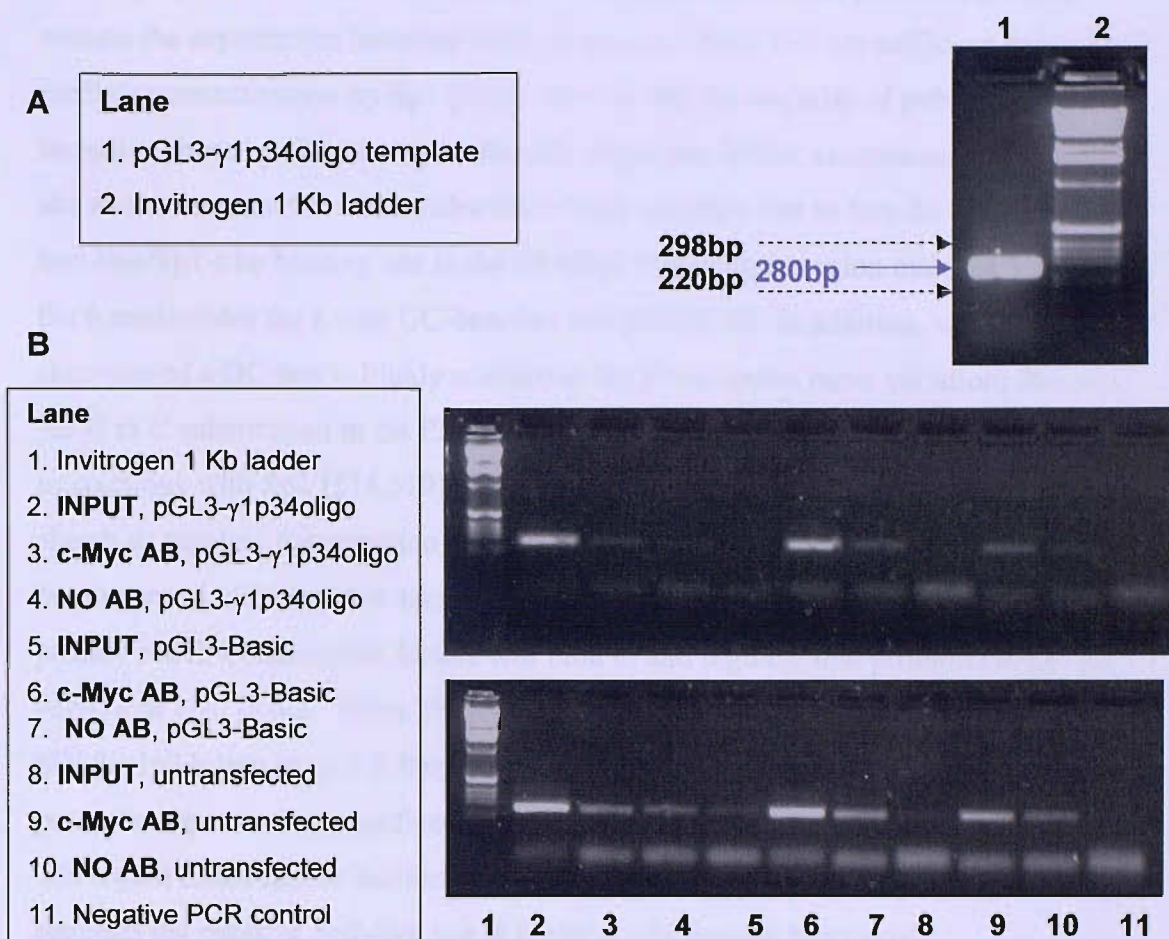


Fig. 5.23. Transient ChIP assay PCR results of SK-N-AS cells transfected with either pGL3- γ 1p34oligo or pGL3-Basic or untransfected cells using new reverse primer. The specificity of the new reverse ChIP primer was verified by performing a PCR with the original forward primer and the pGL3- γ 1p34oligo plasmid as template. **Fig. 5.23 A** shows that the correct size product of 280 bp was generated. **Fig. 5.23 B:** Immunoprecipitations were performed on prepared lysates from either untransfected SK-N-AS cells or SK-N-AS cells transfected with pGL3-Basic or pGL3- γ 1p34oligo using an antibody to c-Myc. DNA from, an input sample (**INPUT**), the immunoprecipitate (**c-Myc AB**), and a lysate sample with no added antibody (**NO AB**) was recovered and analysed by PCR using the new reverse primer. **Fig. 5.23 B** shows the PCR products obtained after 30 cycles (top gel) and 35 cycles (bottom gel) with 4 μ l of template. After 30 cycles the correct size PCR product was obtained when the input and c-Myc AB immunoprecipitated DNA sample of pGL3- γ 1p34oligo transfected SK-N-AS cells was used as the template (**Lanes 2-3**) although a background band was also observed in samples where the DNA template had been recovered from lysates of untransfected SK-N-AS cells or cells transfected with pGL3-Basic (**Lanes 5-10**).

the consensus of GCGG [512,513]. Analysis of sequence-specific recognition of DNA by Sp1 however, has shown that DNA sequences within promoters, which contain the asymmetric hexanucleotide sequence GGGCGG are sufficient to bind and mediate transactivation by Sp1 [514]. This is why the majority of publications, including those by Gartel *et al* on the p21 promoter, define a consensus GC-Box/Sp1 site as this asymmetric hexanucleotide, which suggests that in fact the putative GC-box-like/Sp1-like binding site in the PPAR γ 1 5' regulatory region matches 5 out of the 6 nucleotides for a core GC-box/Sp1 site [515-518]. In addition, while the 5' end sequence of a GC box is highly conserved the 3' end shows more variation; therefore the G to C substitution in the PPAR γ 1 promoter putative GC-box may not impair interactions with Sp1 [514,519]. Indeed Sp1 and other transcription factors have been shown to regulate transcription via non-consensus binding sites in the promoters of target genes indicating that analysis of a promoter sequence alone is insufficient to predict which transcription factors will bind to and regulate that promoter either *in vitro* or *in vivo* [520]. When SK-N-AS cells were transfected with equal quantities of pGL3- γ 1p34oligo or pGL3-Basic, the luciferase activity of the 34 bp PPAR γ 1 promoter reporter was significantly higher relative to pGL3-Basic (**Fig. 5.24**). Since this region could induce luciferase expression above the promoter-less vector, this suggests the putative Sp1-like site at position +39 may be functional.

Sp1 was the first cloned and characterized member of an ever growing family of transcription factors which all contain a highly conserved DNA binding domain close to their C-termini which consists of three tandem Cys₂His₂ zinc finger motifs [512,521-524]. The amino-terminal of Sp1 contains glutamine-rich and serine/threonine-rich transactivation domains and Sp1 has been implicated in the activation of numerous genes with housekeeping, tissue-specific and cell-cycle regulatory functions [525-529]. The embryos of Sp1 null mice show retarded growth, severe morphological defects and die after day 10 of development demonstrating a key role for Sp1 early mouse embryogenesis and maintenance of differentiated cells [512,522,524]. Studies by Gartel *et al* suggest that transcriptional attenuation of the cyclin dependent kinase inhibitor, p21^{CIP1} by c-Myc may be mediated by an interaction between its central domain and Sp1, a previously identified key activator of the p21 promoter [485,492,515,530]. c-Myc may abrogate transcription by sequestering Sp1 from DNA or by forming an inhibitory complex at the promoter

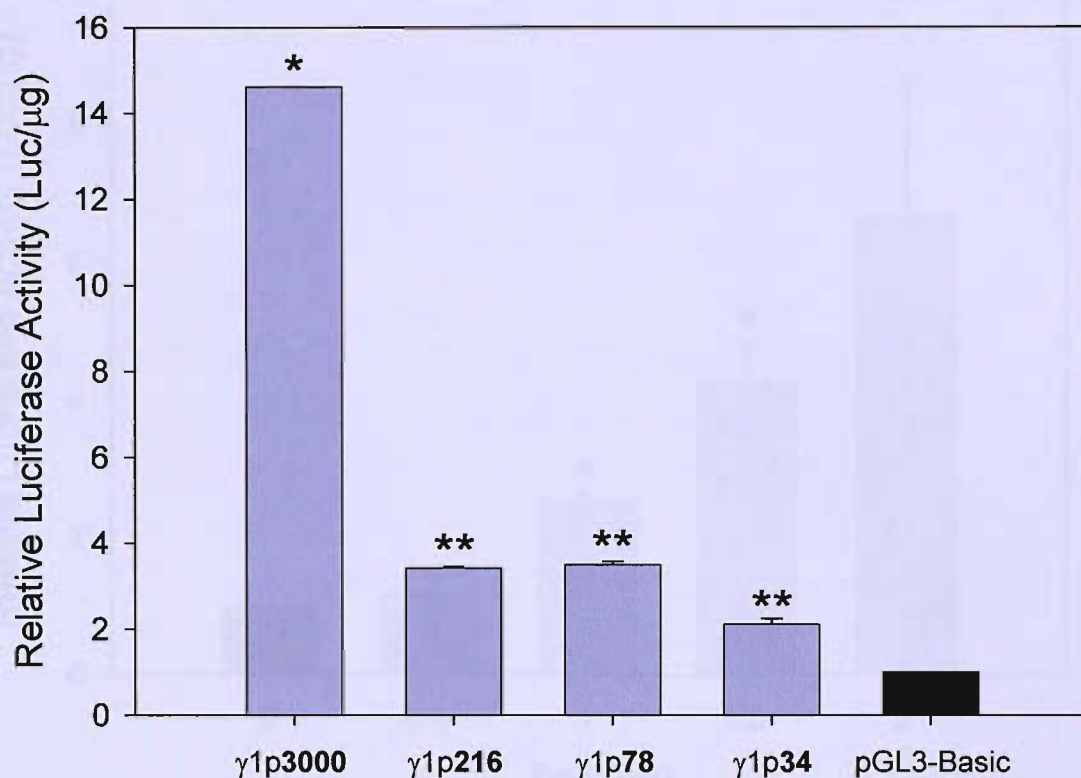


Fig. 5.24. Shows the activity of human PPAR γ 1 promoter constructs relative to pGL3-Basic which lacks a eukaryotic promoter. SK-N-AS cells were transfected with one of the following PPAR γ 1 promoter reporters; pGL3- γ 1p3000, pGL3- γ 1p216, pGL3- γ 1p78oligo, pGL3- γ 1p34oligo or pGL3-Basic (2 μ g). Cells were harvested 24 hours post-transfection and luciferase activity measured. Data shows the relative mean luciferase activity of the PPAR γ 1 promoter reporters (per μ g of protein) (purple bars) relative to pGL3-Basic of two independent experiments \pm S.E. Statistics were calculated using a Student's *t*-test and showed that level of luciferase reporter activity of pGL3- γ 1p3000 (*) ($p < 0.001$), pGL3- γ 1p216, pGL3- γ 1p78oligo and pGL3- γ 1p34oligo (**) ($p < 0.01$) was significantly higher compared to pGL3-Basic luciferase activity.

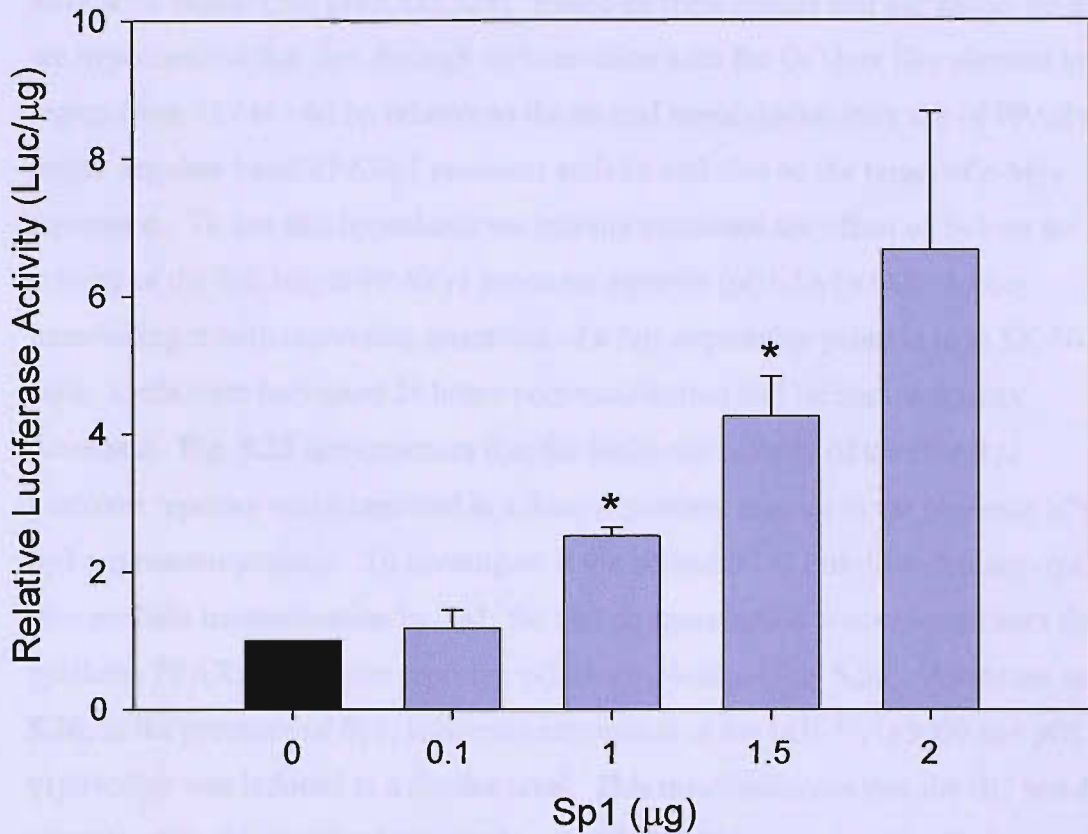


Fig. 5.25. The effect of Sp1 on human PPAR γ 1 promoter activity in SK-N-AS neuroblastoma cells. SK-N-AS cells were co-transfected with 2 μ g of a PPAR γ 1 promoter reporter (pGL3- γ 1p3000) and the indicated quantities of Sp1 expression plasmid. The total quantity of DNA for each transfection was normalised to 4 μ g (including reporter) with an empty expression vector (pcDNA3.1). Cells were harvested 24 hours post-transfection and luciferase activity measured. Data shows the relative mean luciferase activity of the PPAR γ 1 promoter reporter (per μ g of protein) co-transfected with the indicated amounts of Sp1 expression plasmid (purple bars) compared with promoter reporter activity in the presence of the empty expression vector control (black bar) and represent two independent experiments \pm S.E. Statistics were calculated using a Student's *t*-test and showed that there was significant activation of the pGL3- γ 1p3000 promoter reporter in the presence of 1 and 1.5 μ g of the Sp1 expression plasmid (*) ($p < 0.05$).

which prevents Sp1 making contact with components of the basal transcriptional machinery such as TATA-binding protein and TAF130 (TATA-binding protein associated factor-130) [485,522,524]. Based on these results and our earlier findings we hypothesized that Sp1 through its interaction with the GC-box like element in the region from +27 to +60 bp relative to the second transcription start site of PPAR γ 1 might regulate basal PPAR γ 1 promoter activity and also be the target of c-Myc repression. To test this hypothesis we initially examined the effect of Sp1 on the activity of the full length PPAR γ 1 promoter reporter (pGL3- γ 1p3000) by co-transfecting it with increasing quantities of a Sp1 expression plasmid in to SK-N-AS cells. Cells were harvested 24 hours post-transfection and luciferase activity measured. **Fig. 5.25** demonstrates that the luciferase activity of the PPAR γ 1 promoter reporter was stimulated in a dose-dependent manner in the presence of the Sp1 expression plasmid. To investigate if the potential GC box-like element could also mediate transactivation by Sp1, the Sp1 co-transfection was repeated with the synthetic PPAR γ 1 promoter reporter, pGL3- γ 1p34oligo (**Fig. 5.26**). As shown in **Fig. 5.26**, in the presence of Sp1, luciferase expression of the pGL3- γ 1p3000 and pGL3- γ 1p34oligo was induced to a similar level. This result indicates that the GC box-like element, at position +39 relative to the second PPAR γ 1 start site, is sufficient to stimulate transcription by Sp1.

5.15 The effect of p53 on human PPAR γ 1 promoter activity in neuroblastoma cells

The tumour suppressor p53 sometimes described as “the guardian of the genome” is a critical regulator of cellular stress responses [531,532]. In normal proliferating cells the p53 protein has a short half live and p53 levels are low or undetectable [533]. In response to a variety of intracellular and extracellular stresses including DNA damage, hypoxia, nucleotide imbalance, oxidative stress, spindle damage or oncogenic activation p53 protein is rapidly stabilized and is proposed to determine the fate of the cell based on the degree of damage [531,532]. p53 can induce growth arrest and direct DNA repair, however in cases of severe irreversible damage p53 stimulates apoptosis to prevent propagation of cells with a malignant phenotype [218,534-538]. p53 mainly regulates these and other cellular processes by

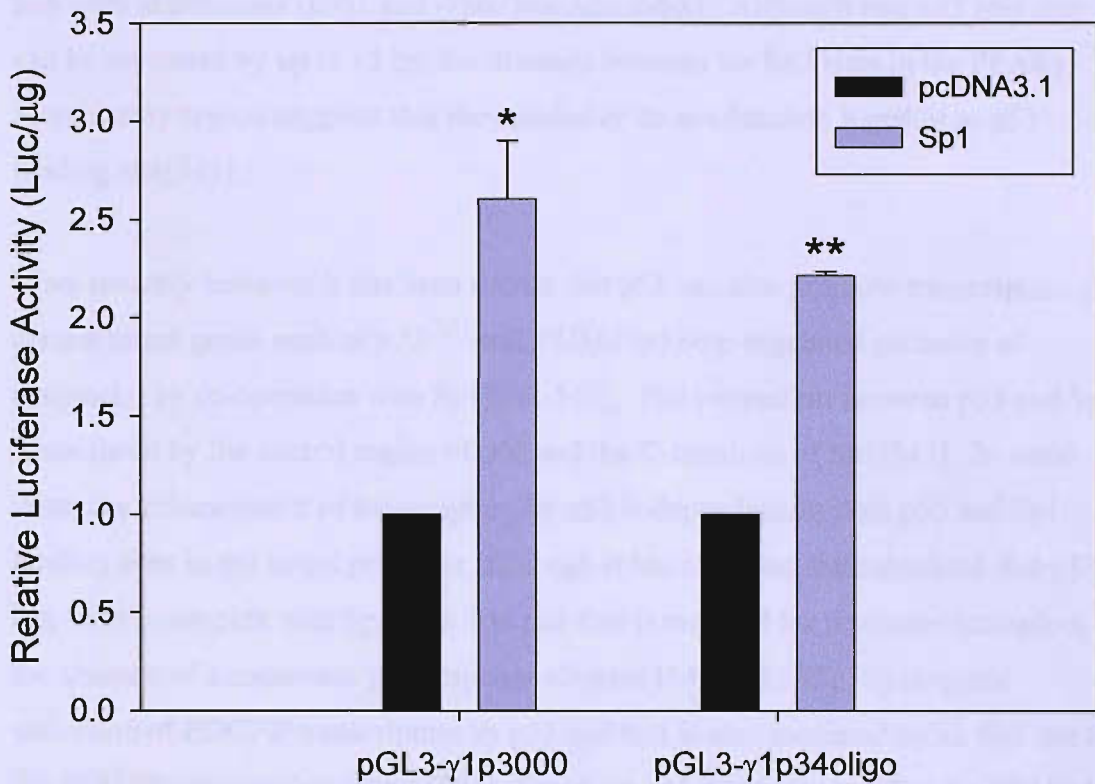


Fig. 5.26. The effect of Sp1 on the synthetic oligonucleotide PPAR γ 1 promoter reporter pGL3- γ 1p34oligo. SK-N-AS cells were co-transfected with 2 μ g of the PPAR γ 1 promoter reporters, pGL3- γ 1p3000 or pGL3- γ 1p34oligo and 2 μ g of a Sp1 expression plasmid or an empty expression vector control (pcDNA3.1) (2 μ g). Cells were harvested 24 hours post-transfection and luciferase activity measured. Data shows the relative mean luciferase activity of the PPAR γ 1 promoter reporters (per μ g of protein) co-transfected with the Sp1 expression plasmid (purple bars) compared with reporter activity in the presence of the empty expression vector control (black bar) and represent two independent experiments \pm S.E. Statistics were calculated using a Student's *t*-test and showed that there was a significant increase in the level of luciferase reporter activity of pGL3- γ 1p3000 (*) ($p < 0.05$) and pGL3- γ 1p34oligo constructs (**) ($p < 0.01$) in the presence of the Sp1 expression plasmid.

functioning as activator of transcription of numerous genes[539]. The stabilized p53 protein forms a tetramer of two p53 dimers which recognizes a p53 response element that consists of two consecutive half sites[540,541]. The MatInspector analysis of the human PPAR γ 1 promoter region from -2842 to + 60bp identified two putative p53 half sites at positions -1001 and -786 (See Appendix). Although two p53 half sites can be separated by up to 13 bp, the distance between the half sites in the PPAR γ 1 5' regulatory region suggests that they probably do not function together as p53 binding site[541].

More recently however it has been shown that p53 can also promote transcription of certain target genes such as *p21^{CIP1}* and *PUMA* (p53-up-regulated mediator of apoptosis) by co-operation with Sp1[542-545]. The interaction between p53 and Sp1 is mediated by the central region of p53 and the C-terminus of Sp1[542]. In some instances enhancement of transcription by p53 is dependent on both p53 and Sp1 binding sites in the target promoter, although it has also been demonstrated that p53 can form a complex with Sp1 at an Sp1 site that is required for promoter activation, in the absence of a consensus p53 response element [542,543,545]. Synergistic activation of *PDGFB* transcription by p53 and Sp1 is also mediated by an Sp1 site in the *PDGFB* proximal promoter [491]. Since we had demonstrated that the PPAR γ 1 promoter might be regulated by Sp1, we decided to investigate the possibility that Sp1 stimulated PPAR γ 1 promoter activity through co-operation with p53, by initially examining the effect of p53 on PPAR γ 1 promoter activity. SK-N-AS cells were co-transfected with a PPAR γ 1 promoter reporter (pGL3- γ 1p3000) and a p53 expression plasmid and harvested after 24 hours and luciferase activity measured. **Fig. 5.27** demonstrates that reporter expression of the PPAR γ 1 promoter construct was significantly induced in the presence of the p53 expression vector compared with reporter activity in the presence of the non-recombinant vector.

To evaluate which region of the PPAR γ 1 promoter mediates this p53 transactivation, the PPAR γ 1 promoter deletion reporters, pGL3- γ 1p216 and pGL3- γ 1p78 were also co-transfected with the p53 expression vector in to SK-N-AS cells. As shown in **Fig. 5.28** the luciferase reporter activity of the two PPAR γ 1 promoter deletion constructs was induced to a similar level, in the presence of the p53 expression vector, compared with the full length PPAR γ 1 promoter reporter. It is therefore probable that p53

activation of the PPAR γ 1 promoter involves an interaction between p53 and Sp1 bound to a site in the region from -18 to + 60 bp relative to the PPAR γ 1 start site. To verify that the effect on the activity of the PPAR γ 1 promoter reporter was due to exogenous expression of p53 the co-transfection experiment with the PPAR γ 1 promoter reporter (pGL3- γ 1p3000) was repeated in H1299 non-small lung carcinoma cells which are p53 null [546]. As in SK-N-AS cells, the luciferase activity of the PPAR γ 1 promoter reporter was also stimulated in the presence of the p53 expression vector in H1299 cells compared with luciferase activity of the construct in the presence of the empty expression vector control although the fold induction was less than in the neuroblastoma cell line (**Fig. 5.29**). This may reflect differences in the transfection efficiency of the two cell types or the relative expression of the p53 protein.

As a positive control H1299 cells were co-transfected with the reporter Hdm2luc03, which is under the control of the proximal region of the Hdm2 promoter that contains two p53 binding sites, and the p53 expression plasmid. Hdm2 (Human double minute 2) is the major ubiquitin E3 ligase which induces p53 degradation, therefore activation of Hdm2 transcription by p53 creates an autoregulatory feedback loop which maintains p53 levels in the cell[532]. **Fig. 5.30** demonstrates that there was a large, dose-dependent increase in the reporter activity of Hdm2luc03 in the presence of the p53 expression plasmid compared with reporter activity in the presence of the empty vector control. The induction of reporter expression of the Hdm2luc03 construct in the presence of the p53 plasmid was considerably greater compared with p53 stimulation of reporter activity of the PPAR γ 1 promoter construct.

Transactivation of the proximal promoter in the Hdm2luc03 construct is mediated by direct binding to a p53 response element which may result in greater induction of reporter activity compared with that achieved by co-operation between p53 and Sp1.

These experiments confirm that induction of luciferase activity of the PPAR γ 1 promoter reporter in the presence of the transfected p53 plasmid is a consequence of ectopic p53 expression. Unlike numerous other cancers, neuroblastomas are wild type for p53 although there is still controversy over whether p53 is functional in neuroblastoma. Some reports suggest p53 protein is restricted to the cytoplasm while other studies show p53 expression in the nucleus and up-regulation of p53 target

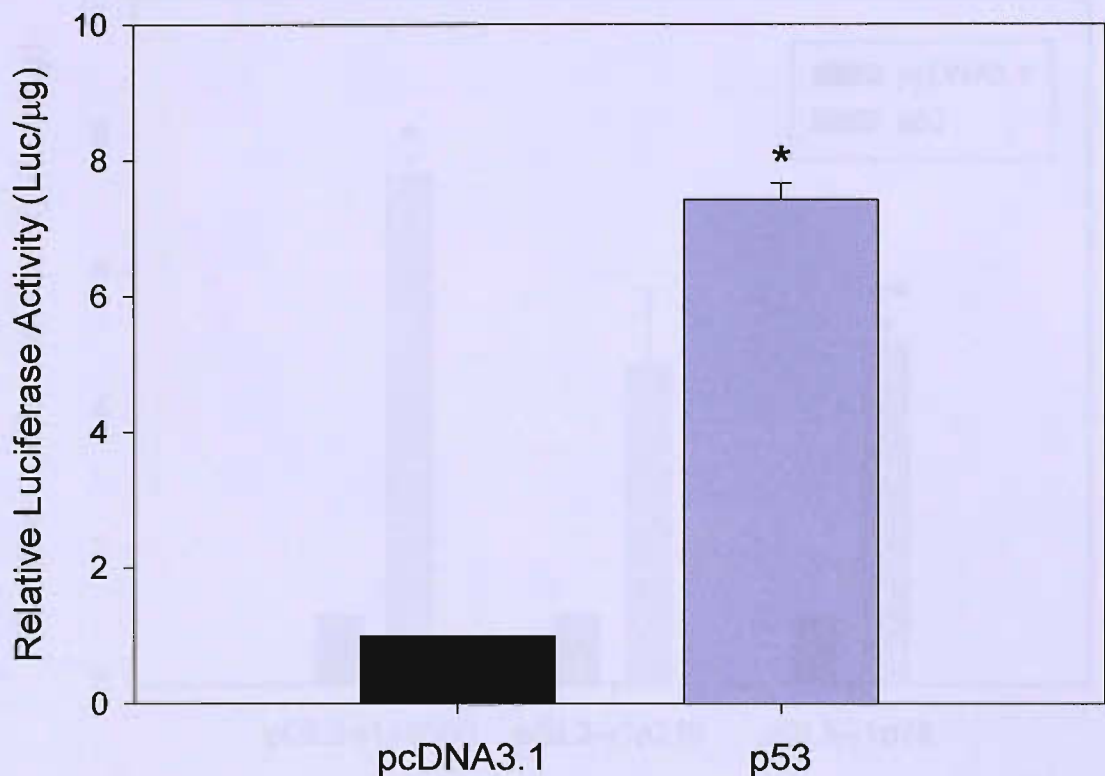


Fig. 5.27. The effect of p53 on human PPAR γ 1 promoter activity in SK-N-AS neuroblastoma cells. SK-N-AS cells were co-transfected with 2 μ g of a PPAR γ 1 promoter reporter (pGL3- γ 1p3000) and either 100 ng of a p53 expression plasmid or an empty expression vector (pcDNA3.1) (100ng). Cells were harvested 24 hours post-transfection and luciferase activity measured. Data shows the relative mean luciferase activity of the PPAR γ 1 promoter reporter (per μ g of protein) co-transfected with the p53 expression plasmid (purple bars) compared with promoter reporter activity in the presence of the empty expression vector control (black bar) and represent two independent experiments \pm S.E. Statistics were calculated using a Student's *t*-test and showed that there was significant induction of the pGL3- γ 1p3000 promoter reporter in the presence of 100 ng of p53 expression plasmid (*) ($p < 0.01$).

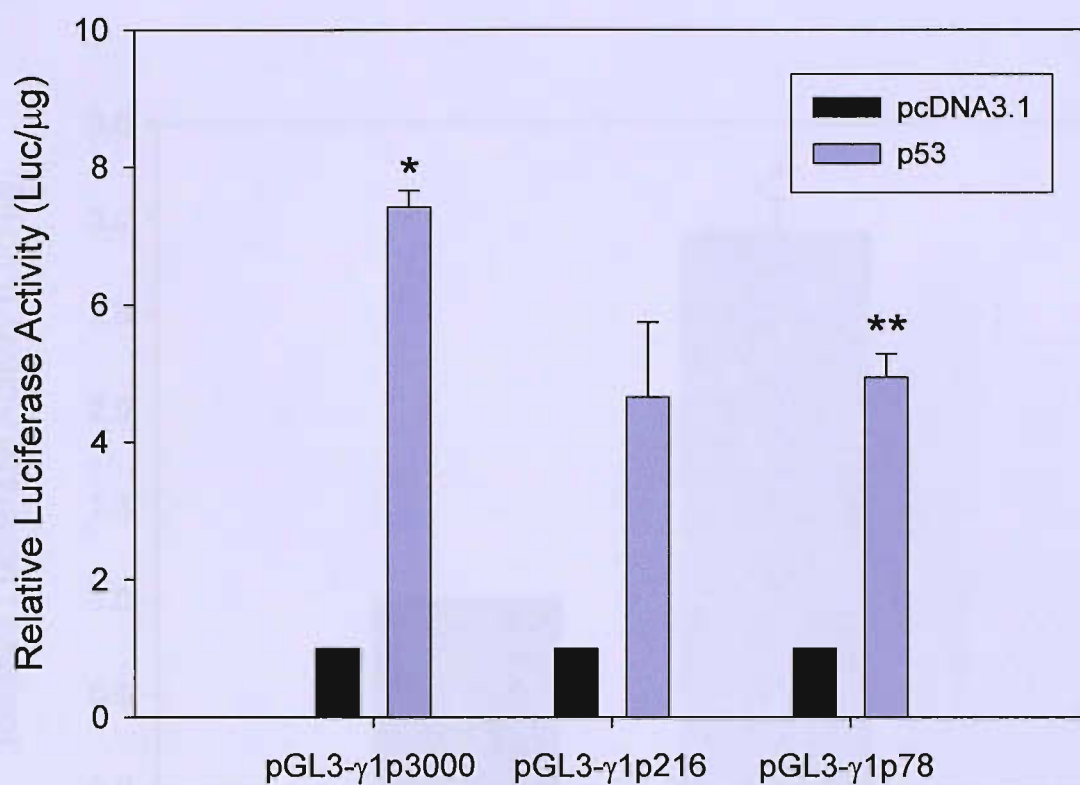


Fig. 5.28. The effect of p53 on the activity of PPAR γ 1 promoter deletion

constructs. SK-N-AS cells were co-transfected with either 2 μ g of the PPAR γ 1 promoter reporter deletion constructs pGL3- γ 1p216 or pGL3- γ 1p78, or pGL3- γ 1p3000 and 100 ng of an expression plasmid encoding p53 or an empty expression vector (pcDNA3.1) (100ng). Cells were harvested 24 hours post-transfection and luciferase activity measured. Data shows the relative mean luciferase activity of the PPAR γ 1 promoter reporters (per μ g of protein) co-transfected with the p53 expression plasmid (purple bar) compared with promoter reporter activity in the presence of the empty expression vector control (black bar) and represent two independent experiments \pm S.E. Statistics were calculated using a Student's *t*-test and showed that there was significant induction of pGL3- γ 1p3000 promoter activity (*) ($p < 0.01$) and the promoter activity of the PPAR γ 1 promoter deletion mutant pGL3- γ 1p78 (**) ($p < 0.05$) in the presence of 100 ng of p53 expression plasmid.

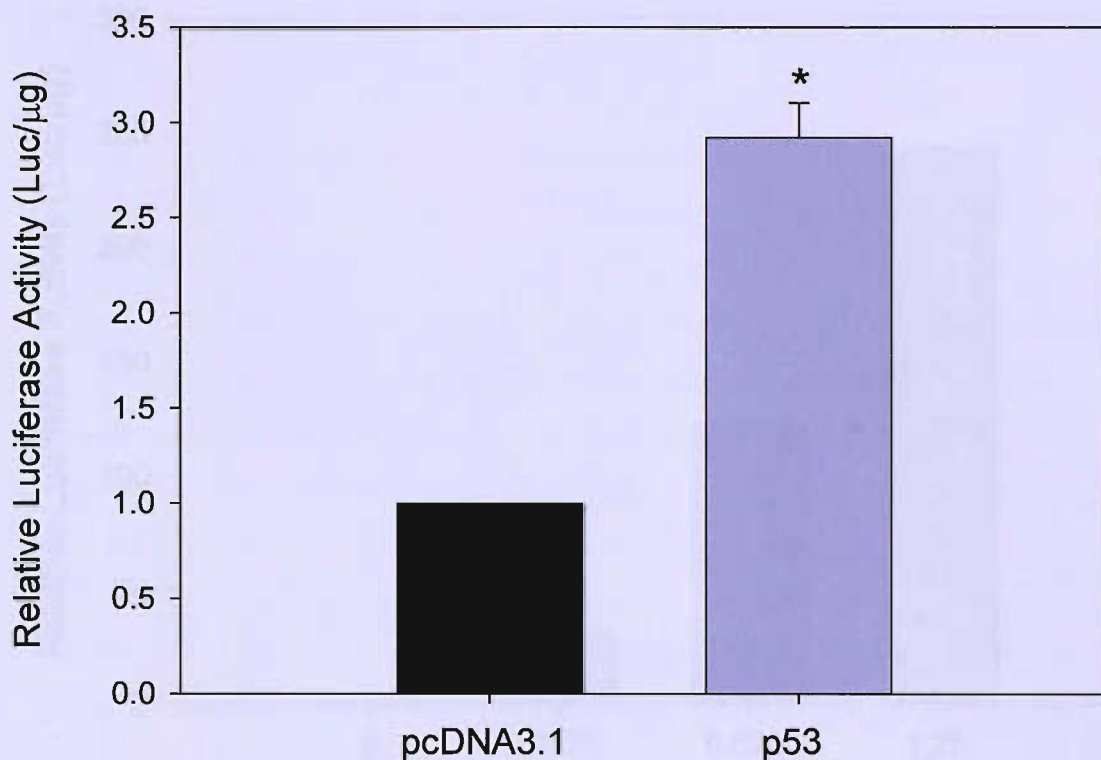


Fig. 5.29. The effect of p53 on human PPAR γ 1 promoter activity in the p53 null H1299 lung cancer cell line. H1299 cells were co-transfected with 2 μ g of a PPAR γ 1 promoter reporter (pGL3- γ 1p3000) and either 100 ng of a p53 expression plasmid or an empty expression vector (pcDNA3.1) (100ng). Cells were harvested 24 hours post-transfection and luciferase activity measured. Data shows the relative mean luciferase activity of the PPAR γ 1 promoter reporter (per μ g of protein) co-transfected with the p53 expression plasmid (purple bar) compared with promoter reporter activity in the presence of the empty expression vector control (black bar) and represent two independent experiments \pm S.E. Statistics were calculated using a Student's *t*-test and showed that there was significant induction of the pGL3- γ 1p3000 promoter reporter in H1299 cells the presence of 100 ng of p53 expression plasmid (*) ($p < 0.05$).

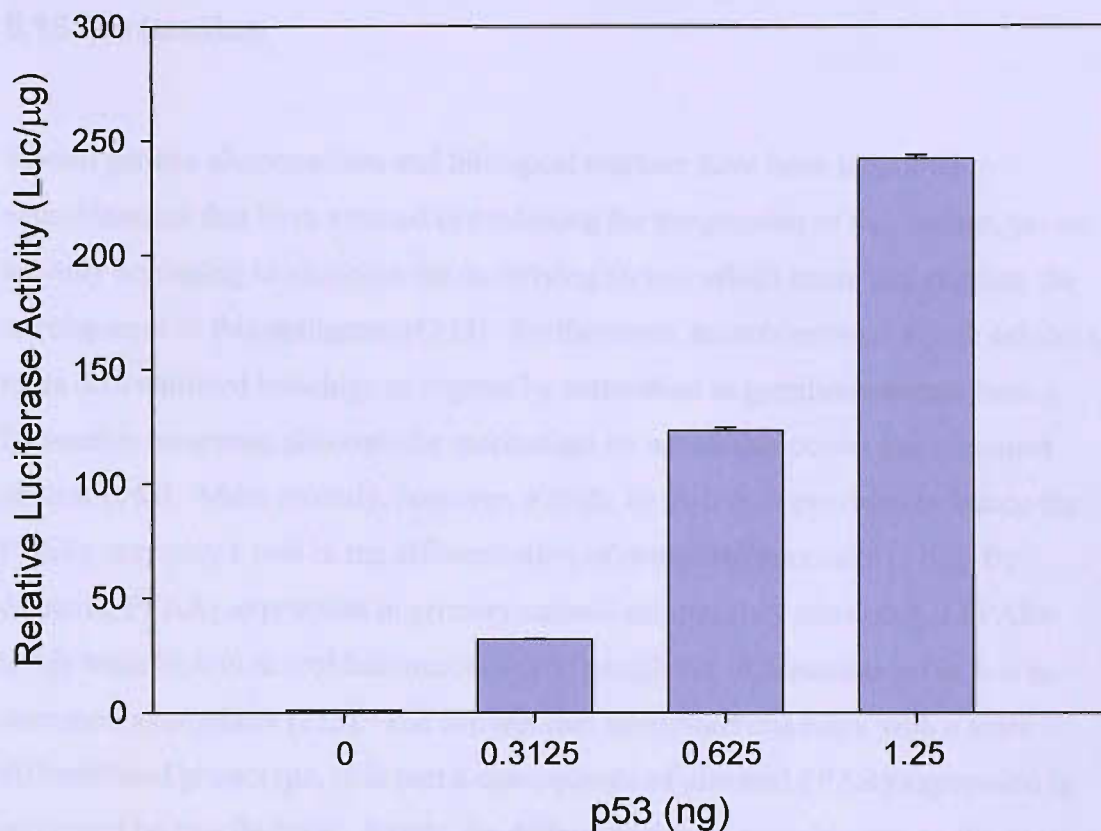


Fig. 5.30. The effect of p53 on Hdm2 promoter reporter activity in the p53 null H1299 lung cancer cell line. H1299 cells were co-transfected with 2 μg of an hdm2 promoter reporter (hdm2luc03) and the indicated amounts of a p53 expression plasmid. The total quantity of DNA for each transfection was normalised to 2.00125 μg (including reporter) with an empty expression vector (pcDNA3.1). Cells were harvested 24 hours post-transfection and luciferase activity measured. Data shows the relative luciferase activity of the PPAR γ 1 promoter reporter (per μg of protein) co-transfected with the p53 expression plasmid (purple bars) compared with promoter reporter activity in the presence of the empty expression vector control (black bar) and represents the mean of three independent luminescence readings \pm S.E.

genes following irradiation of neuroblastoma cells *in vitro* [547]. If p53 can localize to the nucleus these results suggest that p53 could interact with Sp1 to stimulate PPAR γ 1 promoter activity in neuroblastoma cells.

5.16 Discussion

Several genetic abnormalities and biological markers have been identified in neuroblastoma that have assisted in predicting the progression of the disease, yet we are only beginning to elucidate the underlying factors which cause and regulate the development of this malignancy[253]. Furthermore, neuroblastomas which exhibit a more differentiated histology or regress by maturation to ganglioneuromas have a favourable prognosis although the mechanism by which this occurs has remained unclear [548]. More recently, however, a study by Han *et al* provided evidence that PPAR γ may play a role in the differentiation of neuroblastoma cells [213]. By detecting PPAR γ expression in primary neuroblastomas they showed that PPAR γ levels were high in neuroblastoma cells with ganglionic differentiation but low in immature neuroblasts [213]. The concept that neuroblastoma cells, with a more differentiated phenotype, is in part a consequence of elevated PPAR γ expression is supported by two findings. Firstly, the differentiation of neuroblastoma cells *in vitro*, by agents such as retinoic acid, caused increased PPAR γ expression and secondly that levels of PPAR γ also correlate with the maturational status of cells from other tissues such as the colon [213,418]. While the mechanism of PPAR γ transactivation has been extensively studied little is known about the regulation of PPAR γ gene expression[39]. Therefore, this prompted an investigation of how PPAR γ expression is modulated in neuroblastoma cells since this might provide further insight in to its function in this cancer.

Experiments using a PPAR γ 1 promoter reporter construct demonstrated that PPAR γ mRNA expression in neuroblastoma cells *in vitro* is controlled by the level of promoter activation. The transiently transfected PPAR γ 1 promoter reporter was differentially stimulated in SK-N-AS and IMR-32 neuroblastoma cell lines and the degree of reporter induction correlated with the levels of endogenous PPAR γ mRNA detected in these two cell types. To explore how PPAR γ 1 promoter activity in

neuroblastoma cells is modulated, the PPAR γ 1 promoter sequence contained in the reporter construct was examined using MatInspector to identify putative regulatory elements. The analysis revealed that this PPAR γ 1 5' regulatory region included two potential E-boxes, which directly interact with members of the Myc family of transcription factors, and mediate gene transactivation as well as several sites that indirectly recruit c-Myc and are implicated in c-Myc mediated transcriptional repression [549]. c-Myc is a critical regulator of cell proliferation and deregulated c-Myc, N-Myc and L-Myc expression is involved in the genesis of a diverse range of human cancers. Furthermore, c-Myc and N-Myc expression is down-regulated following induction of differentiation of neuroblastoma and other cell types [213,458]. c-Myc is capable of transforming both primary and established cell lines *in vitro*, a function which is dependent on its ability to both activate and repress gene transcription[429,504]. Indeed, c-Myc attenuates the expression of genes that promote growth arrest and differentiation such as *p21^{CIP1/WAF}*, *p15^{INK4b}*, *Mad4* and *C/EBP- α* which indicates why c-Myc functioning as transcriptional repressor influences its oncogenic capacity [461,474,479,481].

As Myc and PPAR γ have reverse expression profiles and potentially opposing functions in neuroblastoma cells, it was speculated that Myc family members might also abrogate PPAR γ expression. However, the presence of two E-boxes in the PPAR γ 1 promoter also suggested that there was the potential for Myc to positively regulate the expression of PPAR γ . Nevertheless, the activity of a PPAR γ 1 promoter reporter was significantly attenuated when co-transfected in to SK-N-AS neuroblastoma cells with expression plasmids encoding either c- or N-Myc. This suggested that recruitment of c-Myc or N-Myc to sites in the PPAR γ 1 promoter which could mediate transcriptional repression may overcome any activation caused by their direct binding to the upstream E-boxes. Alternatively the putative E-boxes in the PPAR γ 1 promoter sequence could be non-functional.

Several different models of c-Myc transcriptional repression have been proposed; therefore next each of these mechanisms was investigated to determine which were involved in inhibition of PPAR γ 1 promoter activation by c-Myc in neuroblastoma cells (**Fig. 5.5**). Firstly while Miz-1 can stimulate PPAR γ 1 promoter reporter activity *in vitro*, c-Myc repressed PPAR γ 1 transcription by a Miz-1 independent mechanism,

since a c-Myc V394D mutant, deficient in Miz-1 binding, was equally effective at attenuating PPAR γ 1 promoter driven luciferase activity compared with wild-type c-Myc. However, if Miz-1 can directly interact with the PPAR γ 1 promoter this raises the question of why c-Myc does not repress PPAR γ 1 transcription through complex formation with Miz-1. Interestingly, the reporter activity of a PPAR γ 1 promoter construct (pGL3- γ 1p34oligo) in which both of the potential INR elements were disrupted was still significantly induced in the presence of Miz-1 and attenuated by c-Myc. As Miz-1 is known to be an INR-binding protein, this suggests that activation of the PPAR γ 1 promoter reporter by Miz-1 may in fact be due its sequestration of c-Myc bound to the PPAR γ 1 5' regulatory region.

An alternative hypothesis is that Miz-1 only stimulates INR-dependent transcription under certain physiological conditions such as in response to DNA damage [482,550]. For instance, association between Miz-1 and topoisomerase II binding protein (TopBP1) attenuates Miz-1 activity, but following UV irradiation TopBP1 expression is down-regulated which releases Miz-1 allowing it to stimulate expression of genes including *p21^{CIP1/WAF}* [476]. In these circumstances c-Myc may attenuate gene transcription via Miz-1, while in unstressed conditions when Miz-1 is inactive wild-type c-Myc or a V394D c-Myc mutant could mediate transcriptional repression via an alternative mechanism. These findings are corroborated by the work of Adhikary *et al* who showed that deletion of the Miz-1 gene in mice impaired early embryonic development but did not alter the expression of *p21^{CIP1/WAF}* [482]. Furthermore, gene expression microarray analysis of HepG2 cells in which siRNAs were used to knockdown Miz-1 expression failed to identify *p21^{CIP1/WAF}* as a direct target gene of Miz-1 [551]. In another study Rat1a fibroblasts expressing the V394D c-Myc mutant or wild-type c-Myc exhibited equivalent colon formation suggesting that Miz-1 inactivation could also be dispensable for c-Myc mediated transformation [552].

However, as c-Myc mutants have been identified which had impaired transactivation function but retained the ability to repress gene transcription and transform cells, this indicates that transcriptional inhibition by c-Myc is still critical for transformation [497,553,554]. In contrast, c-Myc-Miz-1 complexes have been detected at promoters *in vivo* under normal cell culture conditions and ectopic expression of Miz-1 in some cell types promotes growth arrest which was antagonized

by c-Myc expression[464,474,479,481]. This suggests that the contribution that repression of Miz-1 by c-Myc makes to its biological functions could be dependent on the cell type.

In addition, c-Myc repression of PPAR γ 1 promoter reporter activity in SK-N-AS neuroblastoma cells does not appear to require recruitment of a HDAC or HDAC-containing complex. Incubation of SK-N-AS cells with the HDAC inhibitor trichostatin A (TSA) stimulated basal PPAR γ 1 promoter reporter activity in a dose-dependent manner; although the level of c-Myc mediated repression of the reporter in the presence of TSA was comparable to that achieved by c-Myc in vehicle treated cells. This result is supported by a Claassen *et al* publication which also demonstrated that TSA treatment induced transcription from the p21^{CIP1/WAF} promoter but failed to block inhibition by c-Myc [503]. The structure of the p21^{CIP1/WAF} and PPAR γ 1 promoters are similar and contain several Sp1 sites. HDAC inhibitors consistently stimulate p21^{CIP1/WAF} expression through increased acetylation of the chromatin at the Sp1 sites in the p21^{CIP1/WAF} promoter [555]. It is possible that TSA induction of the PPAR γ 1 promoter activity involves similar mechanism although precisely how HDACs are recruited to these promoters and HDAC inhibitors induce expression remains elusive. Further study is warranted to investigate TSA regulation of PPAR γ 1 transcription since this might also provide insight in to the mechanism by which HDAC recruitment modulates the activity of promoters of other genes including p21^{CIP1/WAF}.

Recently considerable progress has been made in identifying and analysing protein partners of c-Myc [431,440]. Several of these factors including NF-Y, Sp1, p107, YY-1, TFII-I and Miz-1 have been implicated in distinct pathways of c-Myc transcriptional repression [431,440,504]. Since the regions of c-Myc which interact with its protein partners have been determined, a number of c-Myc deletion mutants were used to investigate which c-Myc domains, and therefore potential protein factors, were involved in c-Myc inhibition of PPAR γ 1 promoter reporter activity in neuroblastoma cells (See **Fig. 5.10**). It was demonstrated that the level of repression of PPAR γ 1 promoter reporter activity by a c-Myc mutant lacking MBI (Δ 7-91) was comparable to wild-type c-Myc when the SK-N-AS cell line was transfected with 0.1 μ g of the expression plasmids. The pRb family member, p107 which is required for

c-Myc autorepression, interacts with c-Myc via a region that encompasses MBI and MBII, therefore the MBI motif and association with p107 may be dispensable for c-Myc repression of transcription from the PPAR γ 1 promoter in neuroblastoma cells [497]. However, it is plausible that p107 could interact with the c-Myc mutant through MBII only, so further investigation is needed to show whether a c-Myc-p107 complex plays a role in modulating PPAR γ 1 promoter activity.

PPAR γ 1 promoter reporter activity was also significantly inhibited by a c-Myc mutant with a deletion in the leucine zipper domain (Δ 414-433) however the level of repression was less compared with wild-type c-Myc. The leucine zipper together with the basic and HLH region of c-Myc is essential for heterodimerisation with Max. c-Myc/Max heterodimers through their interaction with E-boxes promote gene transcription, although c-Myc/Max complexes have also been detected at the promoters of c-Myc repressed genes *in vivo* suggesting they are also required for c-Myc mediated transcriptional repression [443]. Conversely, Gartel *et al* showed that deletion of the entire C-terminal domain of c-Myc did not impair its ability to attenuate the p21^{CIP1/WAF} promoter *in vitro* [485]. These findings suggest that the leucine zipper, possibly by promoting cMyc/Max heterodimerisation, contributes to, but is it not essential for, c-Myc transcriptional inhibition of PPAR γ 1 transcription.

However, it is necessary to be cautious when interpreting these results because the differences in the level of repression mediated by the Δ 414-433 c-Myc mutant and the other c-Myc mutants compared with wild-type c-Myc could have been a result of variation in the amount of protein expressed from the c-Myc mutant and wild-type expression plasmids in the SK-N-AS cell line. Stone *et al* however, demonstrated that when the plasmids encoding the normal and mutant c-myc genes were transfected in to COS-7 cells they produced comparable amounts of protein [510]. Nevertheless, to verify that the effect of the c-Myc mutants on PPAR γ 1 promoter reporter activity was due to the introduced deletion rather than major differences in their protein expression, the level of protein produced from the expression plasmids in SK-N-AS cells should be assessed by western blot. In contrast, to the Δ 7-91 and Δ 414-433 c-Myc mutants, none of the other c-Myc mutants examined significantly abrogated the activity of the PPAR γ 1 promoter reporter which indicates that Myc box III, the central region and basic-helix-loop-helix motifs of c-Myc may play a role in c-Myc

repression of the PPAR γ 1 promoter. MBII was not deleted in any of the c-Myc mutants examined; therefore it would be interesting to investigate the role of this motif in c-Myc repression of the PPAR γ 1 promoter since it has been shown to be essential for all known biological functions of c-Myc.

The domains of c-Myc implicated in mediating inhibition of PPAR γ 1 transcription, suggested it could still involve several distinct mechanisms. Therefore, to further resolve the c-Myc repression pathway experiments were devised to identify binding sites in the PPAR γ 1 promoter involved in this process. The PPAR γ 1 promoter sequence in the pGL3- γ 1p3000 reporter was initially truncated by digesting it with specific restriction endonucleases to create the PPAR γ 1 promoter deletion reporters called pGL3- γ 1p216 and pGL3- γ 1p78 (Fig. 5.12). The reporter activity of the PPAR γ 1 promoter deletion constructs was significantly repressed in the presence of co-transfected c-Myc. Furthermore, the level of inhibition of the PPAR γ 1 promoter deletions by c-Myc was comparable to its effect on the full length PPAR γ 1 promoter construct, which suggested that the site of c-Myc repression was located in a region close to the second PPAR γ 1 transcription start site. This result was consistent with those from studies on c-Myc regulation of *p21^{CIP1/WAF}*, *p15^{INK4b}*, *Nramp1* and *Mad4* expression, since they also showed that the site of c-Myc repression occurred in the genes' core promoter [474,475,479,481].

The PPAR γ 1 5' regulatory sequence in the pGL3- γ 1p78 construct contained a putative Sp1 site and two INR elements. As either of these sites could mediate c-Myc transcriptional inhibition of PPAR γ 1 transcription further deletions of the PPAR γ 1 5' regulatory region from -18 to +60 bp were made to establish which of its binding motifs were involved in the mechanism of c-Myc repression. This was achieved by generating three PPAR γ 1 promoter reporter constructs, termed pGL3- γ 1p78oligo, pGL3- γ 1p58oligo and pGL3- γ 1p34oligo containing promoter inserts created by annealing and ligating pairs of synthetic oligonucleotides. The pGL3- γ 1p78oligo construct contained the entire PPAR γ 1 5' regulatory sequence from -18 to +60 bp. In the pGL3- γ 1p58oligo reporter the first 20 bp of this sequence were deleted so it lacked the Sp1 site and the first of the two INR elements was interrupted. The final construct, pGL3- γ 1p34oligo lacked the PPAR γ 1 5' regulatory sequence from -18 to +26 bp, therefore the second INR element was also partially deleted. Interestingly, in

SK-N-AS neuroblastoma cells, c-Myc repressed the reporter activity of all three constructs to a similar extent. This effect was specific to c-Myc expression, since co-transfecting the synthetic PPAR γ 1 promoter constructs with a control plasmid encoding C/EBP β did not significantly affect their reporter activity. Moreover, the luciferase expression of pGL3- γ 1p78oligo, pGL3- γ 1p58oligo and pGL3- γ 1p34oligo was significantly attenuated in the presence of the V394D c-Myc mutant. This result corroborates the earlier finding that c-Myc repression of the full-length PPAR γ 1 promoter reporter occurred by a Miz-1-independent mechanism. This hypothesis is also supported by the observation that c-Myc was able to inhibit the reporter expression of a PPAR γ 1 promoter construct (pGL3- γ 1p34oligo) in which both of the putative INR elements, the binding sites of Miz-1, were disrupted.

Therefore, next c-Myc recruitment to the PPAR γ 1 promoter *in vivo* was examined using a “transient” ChIP assay which involved transfecting SK-N-AS neuroblastoma cells with the PPAR γ 1 promoter reporter, pGL3- γ 1p34oligo and then assessing the ability of c-Myc to interact with the PPAR γ 1 5’regulatory sequence in the construct by ChIP assay. The initial PCR reaction, using input DNA from pGL3- γ 1p34oligo transfected SK-N-AS cells, yielded a product, representing the PPAR γ 1 5’regulatory region, although no PCR product was detected using template DNA from these cells obtained by immunoprecipitation with an anti-c-Myc antibody, even after more PCR cycles. This indicated that either c-Myc was not recruited to this sequence *in vivo* or that the quantity of template DNA used in the PCR was inadequate to observe a signal. However, when the amount of template was increased, while PCR product was detected with c-Myc antibody- immunoprecipitated DNA from SK-N-AS cells transfected with the PPAR γ 1 promoter reporter, PCR signal was also observed when using template DNA from untransfected SK-N-AS cells or cells transfected with the control plasmid pGL3-Basic. Optimisation of the PCR annealing temperature or use of an alternative reverse primer failed to reduce amplification of the background or non-specific PCR signal. After trying several approaches to prevent contamination of control samples, it appeared that it would not possible to conclude from these experiments, whether endogenous c-Myc binds to the PPAR γ 1 5’regulatory sequence in the reporter pGL3- γ 1p34oligo *in vivo*, since the PCR signal detected using a larger quantity of c-Myc antibody-immunoprecipitated DNA as template, may have been a false positive result.

Further examination of the PPAR γ 1 5' regulatory sequence from +27 to +60 bp for potential transcription factor binding sites revealed a GC-box-like element/Sp1-like site at position +39, which matched the consensus sequence of the core region of an Sp1 binding site (GGGCGG) except for substitution of guanine for cytosine at the sixth nucleotide. Gartel *et al* demonstrated that c-Myc inhibition of the p21^{CIP1/WAF} promoter was dependent on an interaction between c-Myc and one of its critical activators, Sp1, therefore experiments were performed to determine if Sp1 was also a regulator of PPAR γ 1 transcription and therefore a potential target of c-Myc mediated repression [485,492]. When either the full length (pGL3- γ 1p3000) or deletion (pGL3- γ 1p34oligo) PPAR γ 1 promoter constructs were co-transfected in to SK-N-AS cells with an expression plasmid encoding Sp1, their reporter activity was significantly stimulated. Furthermore, the fold-induction of the two reporter constructs was similar, inferring that Sp1 could be a modulator of PPAR γ 1 promoter activity and potentially mediates transactivation from a GC-box like element at position +39 in the PPAR γ 1 5' regulatory sequence. This region of the PPAR γ 1 promoter may regulate PPAR γ 1 transcription since the reporter activity of pGL3- γ 1p34oligo was significantly greater than a control plasmid, pGL3-Basic which lacks a promoter.

Moreover, Sp1 transactivation of PPAR γ 1 transcription may be modulated by the tumour suppressor p53. p53 can function as an activator of gene transcription by directly binding to its cognate response element as a tetramer composed of two p53 dimers [540,541]. More recently, however, it was shown that p53 also stimulates gene transcription through its interaction with Sp1 [542-545]. Co-transfection of the PPAR γ 1 promoter construct pGL3- γ 1p3000 with a p53 expression plasmid in SK-N-AS neuroblastoma cells significantly induced its reporter activity. Similar results were obtained when the co-transfection experiment was repeated in p53 null H1299 lung cancer cells. Expression of exogenous p53 in H1299 cells stimulated a positive control reporter, confirming that the effect of co-transfecting the p53 expression plasmid on PPAR γ 1 promoter reporter activity was specifically mediated by increased p53 expression. The site of p53 transactivation was mapped to a region of the PPAR γ 1 promoter from -18 to + 60 bp. As this sequence lacks a p53 consensus site but contains a putative Sp1 site and a GC-box-like element it is speculated that

p53 induces transcription from the PPAR γ 1 promoter by complex formation with Sp1 bound to one or more of these sites.

c-Myc repression of PPAR γ 1 transcription is mediated by the same promoter region which suggests that the mechanism of inhibition involves disrupting the Sp1-p53 interaction. However, to prove this hypothesis it will be necessary to confirm that Sp1 and p53 form a complex in SK-N-AS neuroblastoma cells. This could be demonstrated by performing an immunoprecipitation of SK-N-AS cell extracts using an anti-Sp1 and then analyse the immunoprecipitated proteins by western blot to detect for the presence of p53. As further verification of the model the Sp1-p53 complex must also be shown to bind to the PPAR γ 1 promoter *in vivo* by CHIP assay. Two mechanisms have been proposed to explain how c-Myc abrogates Sp1 transcriptional activity. Firstly, c-Myc could form an inhibitory complex with Sp1 at the promoter which prevents its association with co-activators or p53 [492]. Alternatively, c-Myc through its interaction with the C-terminal DNA-binding zinc finger domain of Sp1 may titrate Sp1 proteins from the target promoter. Gartel *et al* postulate that promoters with multiple Sp1 sites may be sensitive to subtle changes in Sp1 levels such that sequestration of Sp1 by c-Myc would lead to transcriptional repression [485].

In the future it would be beneficial to investigate if c-Myc and Sp1 interact with the endogenous PPAR γ 1 promoter sequence *in vivo*. Furthermore, it would be interesting to establish whether over-expression of c-Myc either reduces Sp1 binding at the promoter or promotes formation of a c-Myc-Sp1 complex *in vivo*. Several alternative methods could also be used to elucidate the mechanism of c-Myc repression of PPAR γ 1 transcription. c-Myc and Sp1 binding to the PPAR γ 1 promoter *in vitro* might be demonstrated using a DNA pulldown assay with double-stranded oligonucleotides representing bases from +27 to +60 of the PPAR γ 1 5' regulatory region. The effect of co-transfected c-Myc on Sp1's interaction with the PPAR γ 1 promoter could also be studied using this approach. In addition, it would be possible to show association between c-Myc and Sp1 by performing immunoprecipitations of SK-N-AS neuroblastoma cell extracts using antibodies against Sp1 followed by immunoblotting with an anti-c-Myc anti-body. Further study is warranted to identify the region of Sp1 that is responsible for the interaction with c-Myc. This question

could be addressed by assessing the ability of GST-fusion proteins encoding different domains of Sp1 to bind to c-Myc in SK-N-AS cell extracts. Ultimately, using these various approaches, will establish if c-Myc transcriptional inhibition of PPAR γ 1 transcription is dependent on either, sequestration of one of the PPAR γ 1 promoter's activators, Sp1, or on formation of a repressive complex with Sp1 at the PPAR γ 1 core promoter that attenuates co-activator or p53 recruitment.

6 DISCUSSION

Since the discovery of the first PPAR isoform over a decade ago, the PPAR biology field has rapidly expanded and demonstrated that PPARs are expressed in a wide range of human tissues and have important roles in normal cell functions and in the regulation of the pathogenesis of certain diseases [17]. In particular, the PPAR γ isoform has been detected in several different primary human tumour tissues [188]. Administration of PPAR γ ligands to cancer cells *in vitro* and *in vivo* can attenuate their growth. Furthermore, use of the synthetic PPAR γ ligand troglitzone in small scale clinical trials of patients with liposarcoma and prostate cancer caused morphological differentiation, disease stabilization or regression of tumours [209,239]. Collectively, these findings indicate that PPAR γ might function as a tumour suppressor in human malignancies and PPAR γ ligands have potential as a novel therapy for cancers that currently have limited treatment options such as aggressive neuroblastomas.

Neuroblastoma is a childhood neoplasm originating from cells of the neural crest [245]. The clinical hallmark of neuroblastoma is its diversity. Low risk patients who present with localised disease or tumours with favourable biology have an excellent prognosis and can often be treated with surgery alone. Conversely, other neuroblastoma patients are diagnosed with highly aggressive disseminated tumours. The mortality rate of patients with these advanced stage neuroblastomas is still high and there has been little improvement in survival rates over the past 20 years despite the use of intensive multi-modal therapies. The concept that poor prognosis neuroblastomas could be treated by inducing them to complete terminal differentiation or undergo programmed cell death is supported by the well-documented evidence that some neuroblastoma tumours spontaneously regress by these mechanisms without therapy [213].

The natural PPAR γ 15dPGJ₂ inhibits the growth of neuroblastoma cell lines *in vitro*. In addition, the growth arrest induced by 15dPGJ₂ is accompanied by differentiation or programmed cell death depending on the neuroblastoma cell type and the ligand

concentration administered. Conversely, in some neuroblastoma cell lines low 15dPGJ₂ concentrations stimulated cell proliferation. Therefore, the use of 15dPGJ₂ or other PPAR γ ligands as a treatment for neuroblastoma was dependent on understanding how they regulate such diverse biological responses.

Transient transfection experiments using a PPAR responsive reporter showed that 15dPGJ₂ induces PPAR γ transcriptional activity in neuroblastoma cell lines and that the level of PPRE-mediated transcription correlated with degree of growth inhibition. Higher levels of PPAR γ transactivation were associated with more pronounced inhibition of neuroblastoma cell growth. Furthermore, at the same concentration of ligand, neuroblastoma cell lines that were less responsive to 15dPGJ₂ exhibited lower PPAR γ transactivation compared with more sensitive neuroblastoma cell lines. Comparable levels of PPRE-mediated transcription also induced differentiation or programmed cell death, suggesting that the cellular response mediated by PPAR γ ligands is dependent on the genotype of the neuroblastoma cell. Indeed, growth inhibition by 15dPGJ₂ is dependent on PPAR γ transcriptional activity, since constitutive expression of a PPAR γ dominant negative receptor in IMR-32 neuroblastoma cells blocked the anti-proliferative effect mediated by 15dPGJ₂. Therefore, further study is warranted to identify the direct *in vivo* targets of PPAR γ that mediate its biological responses in neuroblastoma cells.

In neuroblastoma, the retinoblastoma family members' pRb, p107 and p130 may modulate the level of induction of PPAR γ transcriptional activity by PPAR γ ligands such as 15dPGJ₂, since ectopic expression of pRb, p107 or p130 attenuated stimulation of PPRE-transcription by 15dPGJ₂ in neuroblastoma cells *in vitro*. The mechanism of transcriptional repression of PPAR γ by pRb appears to be dependent on its pocket domain and recruitment of a histone deacetylase. Furthermore, the growth inhibitory effect of 15dPGJ₂ in SK-N-AS neuroblastoma cells was enhanced by co-treatment with the HDAC inhibitor trichostatin A. This observation suggests that using PPAR γ ligands in combination with agents that enhance their ability to stimulate PPAR γ transactivation might prove more effective in the treatment of neuroblastoma. HDAC recruitment may well be one example of several pathways that modulate PPAR γ transactivation in neuroblastoma cells. For instance, PPAR γ transcriptional activity could also be regulated by post-translational modifications,

expression of an endogenous PPAR γ dominant negative mutant or by the levels of RXR, co-activator and PPAR β/δ in the neuroblastoma cell [67,74,233,234] [33,232,314,315]. Therefore, it would be interesting to investigate if these factors also impact on the biological responses induced by PPAR γ ligands in neuroblastoma cells.

Conversely, some PPAR γ ligands may mediate growth inhibition of neuroblastoma cells through PPAR γ -independent pathways. We showed that the synthetic PPAR γ ligand ciglitazone had an anti-proliferative effect on neuroblastoma cell lines; however was a less potent inhibitor of neuroblastoma cell growth compared with 15dPGJ₂. In addition, ciglitazone did not stimulate a PPAR responsive reporter in IMR-32 and SK-N-AS neuroblastoma cells at concentrations which had been demonstrated to induce growth arrest. In contrast, to 15dPGJ₂, stable expression of an artificial PPAR γ dominant negative receptor failed to attenuate the growth inhibitory effect of ciglitazone on IMR-32 neuroblastoma cells which indicates that ciglitazone can mediate this response independently from its ability to stimulate PPAR γ transcriptional activity. Recent publications have suggested that TZDs can also inhibit proliferation of other cancer cell types by PPAR γ -independent mechanisms [382]. Identifying the PPAR γ independent pathway of PPAR γ ligands in neuroblastoma cells may also assist in the development of novel anti-cancer therapies. However, this mechanism may be specific to TZDs, thus in the future the effect of other types of synthetic PPAR γ ligand on neuroblastoma cell growth should be investigated.

In addition, to PPAR γ ligands stimulating the differentiation of neuroblastoma cell lines, it has also been demonstrated that the level of PPAR γ protein expression in primary neuroblastoma tissues correlates with the maturational status of the tumour cell. For instance, PPAR γ protein expression was low in undifferentiated neuroblasts but high in neuroblasts exhibiting morphological features of the mature phenotype such as ganglionic differentiation [213]. Although these observations indicated a role for PPAR γ in neuroblastoma, the function of the receptor in this neoplasm remains unclear. To address the cellular role of PPAR γ the factors that are important in regulating PPAR γ expression in neuroblastoma cells were examined. The finding that PPAR γ protein levels relate to the differentiation status of primary

neuroblastomas is supported by the observation that neuroblastoma cell lines express very different level of PPAR γ mRNA. PPAR γ mRNA expression in neuroblastoma cell lines appears to be modulated by the level of PPAR γ 1 promoter activity. A PPAR γ 1 promoter reporter was differentially stimulated in IMR-32 and SK-N-AS neuroblastoma cells and the degree of activation mirrored levels of endogenous mRNA expression detected in the cell lines. Next the PPAR γ 1 promoter sequence was examined for potential regulatory motifs to identify transcription factors which might modulate PPAR γ 1 transcription in neuroblastoma cells. The analysis revealed a large number of putative transcription factor binding motifs, including sites that could mediate regulation by the Myc family of transcription factors. Co-transfection of a PPAR γ 1 promoter construct with expression plasmids encoding c-Myc or N-Myc in to SK-N-AS neuroblastoma cells significantly attenuated its reporter activity. The discovery that c-Myc and N-Myc, which are both oncogenic, can negatively regulate PPAR γ 1 promoter activity *in vitro* lends support to the hypothesis that PPAR γ functions as a tumour suppressor. Repression of PPAR γ expression by Myc family members is also supported by the observation that the expression of c-Myc and N-Myc is opposite to PPAR γ levels in primary neuroblastoma cells, since PPAR γ expression is high in neuroblasts with ganglionic differentiation where Myc levels are low or undetectable.

c-Myc inhibition of PPAR γ 1 promoter activity in neuroblastoma cells occurs by a Miz-1 and HDAC independent mechanism. Furthermore, the site of c-Myc transcriptional repression, in the PPAR γ 1 promoter was mapped to a region close to the start site of PPAR γ 1 transcription. This same region also mediates activation of the PPAR γ 1 promoter by the Sp1 transcription factor. Therefore, c-Myc may attenuate PPAR γ 1 transcription by forming an inhibitory complex with Sp1 or by sequestering it from its response element. However, to resolve this mechanism it will be necessary to show whether c-Myc can interact with Sp1 and if it can bind to the PPAR γ 1 promoter *in vivo*. Although Myc repression and Sp1 stimulation of PPAR γ 1 promoter activity are potentially two mechanisms by which PPAR γ 1 transcription is regulated in neuroblastoma cells, analysis of the PPAR γ 1 promoter sequence revealed potential binding sites for many other transcription factors. Therefore, the next stage in understanding the cellular role of PPAR γ will be to identify other pathways that modulate PPAR γ 1 expression in neuroblastoma cells.

Appendix

This appendix shows the MatInspector analysis of the human PPAR γ 1 promoter sequence. The key included below is a guide to understanding the information it provides.

1. **Further information** – This indicates the type of potential transcription factor binding site.

2. **Position** – This shows where the site is in the sequence (please note this position is relative to the Xho I site at the end of the sequence not the start site of transcription).

3. **Strand** – This indicates whether the site is on the positive or negative strand of the DNA.

4. **Core and Matrix similarity** – MatInspector defines the consensus sequence of a transcription factor binding site as the matrix.

- Each position in the matrix has a C_i vector. This represents the conservation of the individual nucleotide positions in the matrix as numerical values and is used in the MatInspector program.
- The maximum C_i value of 100 is reached by a position with total conservation of one nucleotide, whereas the minimum value of 0 is reached by a position with equal distribution of all 4 nucleotides.
- The program MatId also defines a core region within the matrix which is represented by the four consecutive nucleotides with the highest C_i sum.
- On the MatInspector output base pairs marked in red have a high information content- e.g the nucleotide is highly conserved at that position.
- Bases in capitals denote the core sequence.
- The maximum core similarity of 1 is only reached when the highest conserved bases of a matrix match exactly in the sequence.
- A good match to the matrix similarity usually has a value of greater than 0.8
- The MatInspector analysis identified a total of 481 matches (potential binding sites) in the PPAR γ 1 promoter sequence. The sites included below were initially considered because of their known tissue distribution and function.

Further Information	Opt.	Position	Str.	Core sim.	Matrix sim.	Sequence
MYC-MAX binding sites	0.92	3 - 17	(+)	1	0.944	gctcCACGcggtggc
NF-kappaB (p50)	0.83	31 - 45	(-)	1	0.86	cgGGGGatccactag
Activator protein 2	0.89	38 - 50	(+)	0.976	0.92	atCCCCcgggcctg
MyT1 zinc finger transcription factor involved in primary neurogenesis	0.75	67 - 79	(-)	0.75	0.757	tcaTAGTtactg
c-Rel	0.91	290 - 304	(+)	1	0.915	actggcagTTCCtca
Signal transducers and activators of transcription	0.87	293 - 311	(-)	1	0.882	gtgttttgaGGAActgcc
Cdx-2 mammalian caudal related intestinal transcr. factor	0.84	357 - 375	(-)	1	0.888	atatattTTTAittctct
MyT1 zinc finger transcription factor involved in primary neurogenesis	0.75	382 - 394	(-)	0.75	0.843	tacAAGGttactt
Octamer-binding factor 1, POU-specific domain	0.86	411 - 423	(+)	0.98	0.886	agcattATTCata
Octamer-binding factor 1, POU-specific domain	0.86	448 - 460	(+)	0.98	0.963	ctaaatATTCatc
Transcriptional repressor CDP	0.81	452 - 468	(+)	0.846	0.888	atattcATCAattcatg
Octamer-binding factor 1, POU-specific domain	0.86	502 - 514	(-)	0.98	0.904	gtcaatATTCcat
Transcriptional repressor CDP	0.81	546 - 562	(-)	0.795	0.876	aggctcATCCatgttat
Octamer-binding factor 1	0.8	571 - 585	(+)	0.75	0.869	actatgctAAGTgaa
Myogenic MADS factor MEF-2	0.89	616 - 638	(-)	1	0.895	acaattcatataAATAgaatcat
Octamer-binding factor 1	0.8	625 - 639	(+)	1	0.835	tttatatgAATTgtc
Clox	0.81	646 - 662	(+)	0.806	0.834	aggtaaATCTalagaga
Barx2, homeobox transcription factor that preferentially binds to paired TAAT motifs	0.95	693 - 709	(+)	1	0.98	gactgtTAATggagagg
c-Rel	0.91	705 - 719	(+)	1	0.922	agagggggTTCCttt
Octamer-binding factor 1	0.84	725 - 739	(+)	0.771	0.87	gtgATGAaaatgttc
Drosophila hairy and enhancer of split homologue 1 (HES-1)	0.87	934 - 948	(-)	1	0.991	gtggCACGtgccctgt
Drosophila hairy and enhancer of split homologue	0.87	935 - 949	(+)	1	0.987	caggCACGtgccacc

1 (HES-1)						
AhR nuclear translocator homodimers	0.89	935 - 949	(-)	1	0.989	ggggcaCGTGcctg
Basic helix-loop-helix protein known as Dec1, Stra13 or Sharp2	0.85	1024 - 1038	(+)	0.75	0.853	ggcdCAAGgatcc
Octamer-binding factor 1	0.8	1114 - 1128	(+)	0.75	0.876	tctatggATTTaca
Octamer-binding factor 1	0.8	1118 - 1132	(-)	0.846	0.875	aaAATGtaaatacca
Octamer-binding factor 1	0.8	1135 - 1149	(+)	1	0.885	atatattAATTatt
Barx2, homeobox transcription factor that preferentially binds to paired TAAT motifs	0.95	1136 - 1152	(+)	1	0.971	ttatatTAATtattcct
Neuron-restrictive silencer factor	0.69	1208 - 1228	(+)	1	0.752	cccAGCActtggaaagctga
Tumor suppressor p53 (3' half site)	0.92	1272 - 1292	(-)	1	0.947	gactgtgtctgaCATGtgc
Barx2, homeobox transcription factor that preferentially binds to paired TAAT motifs	0.95	1297 - 1313	(-)	1	0.971	taattTAATtgtag
Homeodomain proteins MSX-1 and MSX-2	0.97	1300 - 1312	(-)	1	0.995	aattTAATtgtt
Octamer-binding factor 1	0.8	1300 - 1314	(-)	1	0.825	ttaatttAATTggt
AT-binding transcription factor 1	0.79	1306 - 1322	(-)	1	0.8	tttttttAATTta
BTB/POZ-bZIP transcription factor BACH1 forms heterodimers with the small Maf protein family	0.82	1458 - 1482	(-)	1	0.821	ttctccaTGAGacaggggtgtgc
Distal-less 3 homeodomain transcription factor	0.91	1530 - 1542	(-)	1	0.916	cttgTAATcca
Elk-1	0.92	1556 - 1572	(-)	1	0.954	tcaggcGGAAgtgctcc
Nuclear factor Y (Y-box binding factor)	0.9	1614 - 1628	(+)	1	0.927	caggCCAAtaatgg
Cut-like homeodomain protein	0.75	1618 - 1634	(+)	1	0.829	ccAATAaatggctttc
NF-kappaB	0.82	1635 - 1649	(-)	1	0.869	caGGGActgaccact
GATA-binding factor 3	0.91	1648 - 1660	(-)	0.812	0.918	cacGGATcttaca
Tumor suppressor p53 (5' half site)	0.91	1695 - 1715	(-)	1	0.922	aaatcaacataatCATGtctt
Octamer-binding factor 1	0.8	1703 - 1717	(+)	0.75	0.864	atfatgtGATTtaa

Octamer-binding factor 1, POU-specific domain	0.86	1720 - 1732	(-)	0.98	0.961	gaaaaATT C agc
E2F, involved in cell cycle regulation, interacts with Rb p107 protein	0.84	1747 - 1761	(+)	0.857	0.843	tcc tcg cAAA ctt
MyT1 zinc finger transcription factor involved in primary neurogenesis	0.88	1751 - 1763	(-)	1	0.994	gca AAGT ttg cg
MyT1 zinc finger transcription factor involved in primary neurogenesis	0.75	1753 - 1765	(+)	0.75	0.798	caa AACT ttg ctt
Runt-related transcription factor 2 / CBFA1 (core-binding factor, runt domain, alpha subunit 1)	0.84	1762 - 1776	(-)	1	0.881	gtt GTGGT gaagc
Monomers of the nur subfamily of nuclear receptors (nur77, nurr1, nor-1)	0.89	1772 - 1790	(-)	1	0.947	tacag AAGG ctc ctg ttg
Tumor suppressor p53 (3' half site)	0.92	2002 - 2022	(+)	0.828	0.926	aacc ca ctt gga CAGG tcac
MyT1 zinc finger transcription factor involved in primary neurogenesis	0.75	2045 - 2057	(+)	0.75	0.756	gaa AAGG t ca ctg
c-Myc/Max heterodimer	0.92	2063 - 2077	(+)	0.895	0.927	ccaa CAC Atgagaaa
Myeloid zinc finger protein MZF1	0.98	2097 - 2103	(-)	1	1	gt GGGG a
MYC-associated zinc finger protein related transcription factor	0.88	2106 - 2118	(-)	1	0.895	atg ggt GGGG acg
Myeloid zinc finger protein MZF1	0.98	2108 - 2114	(-)	1	1	gt GGGG a
Yin and Yang 1	0.84	2110 - 2128	(+)	1	0.841	cccc CCAT gtt g ctgag
Barx2, homeobox transcription factor that preferentially binds to paired TAAT motifs	0.95	2168 - 2184	(+)	1	0.971	ttctg TAAT gag tt a
Barx2, homeobox transcription factor that preferentially binds to paired TAAT motifs	0.95	2190 - 2206	(+)	1	0.959	tg ttt TAAT gattaaa
Octamer-binding factor 1	0.8	2219 - 2233	(-)	0.75	0.8	tacatg gt TATT cac
Octamer-binding factor 1, POU-specific domain	0.86	2300 - 2312	(+)	1	0.907	cgaaa ATG C tt
Phox2a (ARIX) and Phox2b	0.87	2306 - 2322	(+)	1	0.927	atg ctt TAAT taa att
MyT1 zinc finger transcription factor involved in primary	0.75	2313 - 2325	(-)	0.75	0.799	aga AAAT ta aatt

neurogenesis						
Meis1b and Hoxa9 form heterodimeric binding complexes on target DNA	0.78	2323 - 2337	(-)	1	0.901	TGACatttaaaga
Tumor suppressor p53 (5' half site)	0.91	2384 - 2404	(-)	0.885	0.912	tcgccagagtgCTTGccct
Ras-responsive element binding protein 1	0.79	2428 - 2442	(+)	1	0.825	cCCAGaccggcct
Sp2, member of the Sp/XKLF transcription factors with three C2H2 zinc fingers in a conserved carboxyl-terminal domain	0.8	2431 - 2445	(-)	0.772	0.803	gccagggccGGTCtg
NF-kappaB	0.88	2446 - 2460	(+)	0.904	0.912	cgGGGcatccccct
NF-kappaB (p50)	0.83	2446 - 2460	(-)	1	0.969	agGGGgatgccccg
MyT1 zinc finger transcription factor involved in primary neurogenesis	0.88	2457 - 2469	(-)	1	0.889	ccgAAGTtaggg
EGR1, early growth response 1	0.86	2510 - 2526	(+)	0.789	0.884	agcgttgTGGCgagga
Myc associated zinc finger protein (MAZ)	0.9	2518 - 2530	(+)	1	0.909	tggcGAGGagcaa
E2F, involved in cell cycle regulation, interacts with Rb p107 protein	0.84	2565 - 2579	(+)	1	0.927	gacgaggGAAgccc
Zinc finger / POZ domain transcription factor	0.95	2602 - 2612	(+)	1	0.963	ctgGCGggg
Zinc finger / POZ domain transcription factor	0.95	2604 - 2614	(+)	0.875	0.952	gtgcGCGGgcg
Stimulating protein 1 SP1, ubiquitous zinc finger transcription factor	0.89	2606 - 2620	(+)	1	0.894	gcgagGGCGggcgcc
Core promoter-binding protein (CPBP) with 3 Krueppel-type zinc fingers	0.87	2623 - 2645	(+)	1	0.895	gcccgggCCGCtccctcccagt
Transcriptional repressor, binds to elements found predominantly in genes that participate in lipid metabolism	0.73	2672 - 2694	(+)	1	0.991	cctgccCCCAccccacccccac
MYC-associated zinc finger protein related transcription factor	0.88	2674 - 2686	(-)	1	0.92	gggggtGGGGgca
Stimulating protein 1 SP1, ubiquitous zinc finger transcription factor	0.89	2674 - 2688	(-)	0.819	0.913	gtgggGGTGggggca
Ras-responsive element binding protein 1	0.79	2677 - 2691	(+)	1	0.853	cCCCAccccaccccc

MYC-associated zinc finger protein related transcription factor	0.88	2680 - 2692	(-)	1	0.898	gggggtGGGGgtg
GC box elements	0.88	2680 - 2694	(-)	0.872	0.922	gtgggGGTggggtg
Ras-responsive element binding protein 1	0.79	2683 - 2697	(+)	1	0.853	cCCCAccccacccc
MYC-associated zinc finger protein related transcription factor	0.88	2686 - 2698	(-)	1	0.898	gggggtGGGGgtg
GC box elements	0.88	2686 - 2700	(-)	0.872	0.922	gtgggGGTggggtg
Ras-responsive element binding protein 1	0.79	2689 - 2703	(+)	1	0.853	cCCCAccccacccc
Zinc finger transcription factor ZBP-89	0.93	2690 - 2712	(+)	1	0.968	cccccccCaCCCCcagccggcg
MYC-associated zinc finger protein related transcription factor	0.88	2692 - 2704	(-)	1	0.898	gggggtGGGGgtg
GC box elements	0.88	2692 - 2706	(-)	0.872	0.922	ctgggGGTggggtg
Activator protein 2	0.89	2698 - 2710	(+)	0.976	0.914	caCCCCcagccgg
Core promoter-binding protein (CPBP) with 3 Krueppel-type zinc fingers	0.87	2707 - 2729	(+)	1	0.909	ccggcgcCCGCgccccccccgc
Zinc finger / POZ domain transcription factor	0.95	2707 - 2717	(-)	1	0.954	gcggGGGCcgg
Core promoter-binding protein (CPBP) with 3 Krueppel-type zinc fingers	0.87	2713 - 2735	(+)	1	0.957	ccccgcCCGCccccgcgccggg
Zinc finger / POZ domain transcription factor	0.95	2713 - 2723	(-)	1	0.957	gcggGGGCggg
Stimulating protein 1 SP1, ubiquitous zinc finger transcription factor	0.89	2715 - 2729	(-)	1	0.938	gcgggGGCgggcgcg
EGR1, early growth response 1	0.86	2717 - 2733	(-)	1	0.934	cggcgcggGGGCgggcg
Drosophila hairy and enhancer of split homologue 1 (HES-1)	0.92	2758 - 2772	(+)	0.833	0.943	ccgccgcGGCaggc
Stimulating protein 1 SP1, ubiquitous zinc finger transcription factor	0.89	2765 - 2779	(+)	1	0.89	gggcaGGCgggccc
MYC-associated zinc finger protein related transcription factor	0.88	2767 - 2779	(+)	1	0.884	gcaggcGGGGccc
Ras-responsive element binding protein 1	0.79	2818 - 2832	(-)	1	0.82	aCCCAagcggccag

List of References

1. Glass C.K. (2006). Going nuclear in metabolic and cardiovascular disease. *Journal of Clinical Investigation* *116*: 556-560.
2. Germain P., Altucci L., Bourguet W., Rochette-Egly C., and Gronemeyer H. (2003). Nuclear receptor superfamily: Principles of signaling. *Pure and Applied Chemistry* *75*: 1619-1664.
3. Moras D. and Gronemeyer H. (1998). The nuclear receptor ligand-binding domain: structure and function. *Current Opinion in Cell Biology* *10*: 384-391.
4. Aranda A. and Pascual A. (2001). Nuclear hormone receptors and gene expression. *Physiological Reviews* *81*: 1269-1304.
5. Szanto A., Narkar V., Shen Q., Uray I.P., Davies P.J.A., and Nagy L. (2004). Retinoid X receptors: X-ploring their (patho)physiological functions. *Cell Death and Differentiation* *11*: S126-S143.
6. Auwerx J., Baulieu E., Beato M., Becker-Andre M., Burbach P.H., Camerino G., Chambon P., Cooney A., Dejean A., Dreyer C. *et al.* (1999). A unified nomenclature system for the nuclear receptor superfamily. *Cell* *97*: 161-163.
7. Yen P.M., Ando S., Feng X., Liu Y., Maruvada P., and Xia X.M. (2006). Thyroid hormone action at the cellular, genomic and target gene levels. *Molecular and Cellular Endocrinology* *246*: 121-127.
8. Mangelsdorf D.J. and Evans R.M. (1995). The RXR heterodimers and orphan receptors. *Cell* *83*: 841-850.
9. Kliewer S.A., Lehmann J.M., and Willson T.M. (1999). Orphan nuclear receptors: Shifting endocrinology into reverse. *Science* *284*: 757-760.
10. Ingraham H.A. and Redinbo M.R. (2005). Orphan nuclear receptors adopted by crystallography. *Current Opinion in Structural Biology* *15*: 708-715.
11. Lazar M.A. (2002). Mechanism of Action of Hormones That Act on Nuclear Receptors. In *Williams Textbook of Endocrinology*, (Larsen PR, Kronenberg HM, Melmed S, Polonsky K.S., eds. Elsevier), pp. 35-44.
12. Leblanc B.P. and Stunnenberg H.G. (1995). 9-*cis* retinoic acid signaling - changing partners causes some excitement. *Genes & Development* *9*: 1811-1816.
13. Leid M., Kastner P., and Chambon P. (1992). Multiplicity generates diversity in the retinoic acid signaling pathways. *Trends in Biochemical Sciences* *17*: 427-433.
14. Lin R.J., Nagy L., Inoue S., Shao W.L., Miller W.H., and Evans R.M. (1998). Role of the histone deacetylase complex in acute promyelocytic leukaemia. *Nature* *391*: 811-814.
15. Grignani F., De Matteis S., Nervi C., Tomassoni L., Gelmetti V., Ciocce M., Fanelli M., Ruthardt M., Ferrara F.F., Zamir I. *et al.* (1998). Fusion proteins of the retinoic acid receptor- α recruit histone deacetylase in promyelocytic leukaemia. *Nature* *391*: 815-818.

16. Issemann I. and Green S. (1990). Activation of a member of the steroid-hormone receptor superfamily by peroxisome proliferators. *Nature* 347: 645-650.
17. Desvergne B. and Wahli W. (1999). Peroxisome proliferator-activated receptors: Nuclear control of metabolism. *Endocrine Reviews* 20: 649-688.
18. Sher T., Yi H.F., McBride O.W., and Gonzalez F.J. (1993). cDNA Cloning, Chromosomal Mapping, and Functional-Characterization of the Human Peroxisome Proliferator Activated Receptor. *Biochemistry* 32: 5598-5604.
19. Hihi A.K., Michalik L., and Wahli W. (2002). PPARs: transcriptional effectors of fatty acids and their derivatives. *Cellular and Molecular Life Sciences* 59: 790-798.
20. Willson T.M., Brown P.J., Sternbach D.D., and Henke B.R. (2000). The PPARs: From orphan receptors to drug discovery. *Journal of Medicinal Chemistry* 43: 527-550.
21. Kliewer S.A., Forman B.M., Blumberg B., Ong E.S., Borgmeyer U., Mangelsdorf D.J., Umehara K., and Evans R.M. (1994). Differential Expression and Activation of A Family of Murine Peroxisome Proliferator-Activated Receptors. *Proceedings of the National Academy of Sciences of the United States of America* 91: 7355-7359.
22. Vohl M.C., Lepage P., Gaudet D., Brewer C.G., Betard C., Perron P., Houde G., Cellier C., Faith J.M., Despres J.P. *et al.* (2000). Molecular scanning of the human PPAR α gene: association of the L162V mutation with hyperapobetalipoproteinemia. *Journal of Lipid Research* 41: 945-952.
23. Chew C.H., Samian M.R., Najimudin N., and Tengku-Muhammad T.S. (2003). Molecular characterisation of six alternatively spliced variants and a novel promoter in human PPAR α . *Biochemical and Biophysical Research Communications* 305: 235-243.
24. Torra I.P., Jamshidi Y., Flavell D.M., Fruchart J.C., and Staels B. (2002). Characterization of the human PPAR α promoter: Identification of a functional nuclear receptor response element. *Molecular Endocrinology* 16: 1013-1028.
25. Meijer H.A. and Thomas A.A.M. (2002). Control of eukaryotic protein synthesis by upstream open reading frames in the 5'-untranslated region of an mRNA. *Biochemical Journal* 367: 1-11.
26. Mandard S., Muller M., and Kersten S. (2004). Peroxisome proliferator-activated receptor alpha target genes. *Cellular and Molecular Life Sciences* 61: 393-416.
27. Schoonjans K., Staels B., and Auwerx J. (1996). Role of the peroxisome proliferator-activated receptor (PPAR) in mediating the effects of fibrates and fatty acids on gene expression. *Journal of Lipid Research* 37: 907-925.
28. Auboeuf D., Rieusset J., Fajas L., Vallier P., Frering V., Riou J.P., Staels P., Auwerx J., Laville M., and Vidal H. (1997). Tissue distribution and quantification of the expression of mRNAs of peroxisome proliferator-activated receptors and liver X receptor-alpha in humans - No alteration in adipose tissue of obese and NIDDM patients. *Diabetes* 46: 1319-1327.
29. Escher P. and Wahli W. (2000). Peroxisome proliferator-activated receptors: insight into multiple cellular functions. *Mutation Research-Fundamental and Molecular Mechanisms of Mutagenesis* 448: 121-138.

30. Skogsberg J., Kannisto K., Roshani L., Gagne E., Hamsten A., Larsson C., and Ehrenborg E. (2000). Characterization of the human peroxisome proliferator activated receptor delta gene and its expression. *International Journal of Molecular Medicine* 6: 73-81.
31. Yoshikawa T., Brkanac Z., Dupont B.R., Xing G.Q., Leach R.J., and DeteraWadleigh S.D. (1996). Assignment of the human nuclear hormone receptor, NUC1 (PPAR β/δ), to chromosome 6p21.1-p21.2. *Genomics* 35: 637-638.
32. Larsen L.K., Amri E.Z., Mandrup S., Pacot C., and Kristiansen K. (2002). Genomic organization of the mouse peroxisome proliferator-activated receptor beta/delta gene: alternative promoter usage and splicing yield transcripts exhibiting differential translational efficiency. *Biochemical Journal* 366: 767-775.
33. Shi Y.H., Hon M., and Evans R.M. (2002). The peroxisome proliferator-activated receptor delta, an integrator of transcriptional repression and nuclear receptor signaling. *Proceedings of the National Academy of Sciences of the United States of America* 99: 2613-2618.
34. Holst D., Luquet S., Nogueira V., Kristiansen K., Leverve X., and Grimaldi P.A. (2003). Nutritional regulation and role of peroxisome proliferator- activated receptor delta in fatty acid catabolism in skeletal muscle. *Biochimica et Biophysica Acta-Molecular and Cell Biology of Lipids* 1633: 43-50.
35. Peters J.M., Lee S.S.T., Li W., Ward J.M., Gavrilova O., Everett C., Reitman M.L., Hudson L.D., and Gonzalez F.J. (2000). Growth, adipose, brain, and skin alterations resulting from targeted disruption of the mouse peroxisome proliferator- activated receptor beta(delta). *Molecular and Cellular Biology* 20: 5119-5128.
36. Fajas L., Auboeuf D., Raspe E., Schoonjans K., Lefebvre A.M., Saladin R., Najib J., Laville M., Fruchart J.C., Deeb S. *et al.* (1997). The organization, promoter analysis, and expression of the human PPAR γ gene. *Journal of Biological Chemistry* 272: 18779-18789.
37. Beamer B.A., Negri C., Yen C.J., Gavrilova O., Rumberger J.M., Durcan M.J., Yarnall D.P., Hawkins A.L., Griffin C.A., Burns D.K. *et al.* (1997). Chromosomal localization and partial genomic structure of the human peroxisome proliferator activated receptor- γ (hPPAR γ) gene. *Biochemical and Biophysical Research Communications* 233: 756-759.
38. Fajas L., Fruchart J.C., and Auwerx J. (1998). PPAR γ 3 mRNA: a distinct PPAR gamma mRNA subtype transcribed from an independent promoter. *Febs Letters* 438: 55-60.
39. Sundvold H. and Lien S. (2001). Identification of a novel peroxisome proliferator-activated receptor PPAR γ promoter in man and transactivation by the nuclear receptor ROR alpha 1. *Biochemical and Biophysical Research Communications* 287: 383-390.
40. Elbrecht A., Chen Y.L., Cullinan C.A., Hayes N., Leibowitz M.D., Moller D.E., and Berger J. (1996). Molecular cloning, expression and characterization of human peroxisome proliferator activated receptors γ 1 and γ 2. *Biochemical and Biophysical Research Communications* 224: 431-437.
41. Zhu Y.J., Korenberg J.R., Chen X.N., Noya D., Rao M.S., and Reddy J.K. (1995). Structural Organization of Mouse Peroxisome Proliferator Activated Receptor-Gamma (mPPAR γ) Gene - Alternative Promoter Use and Different Splicing Yield 2

mPPAR γ Isoforms. Proceedings of the National Academy of Sciences of the United States of America 92: 7921-7925.

42. Ricote M., Huang J., Fajas L., Li A., Welch J., Najib J., Witztum J.L., Auwerx J., Palinski W., and Glass C.K. (1998). Expression of the peroxisome proliferator-activated receptor γ (PPAR γ) in human atherosclerosis and regulation in macrophages by colony stimulating factors and oxidized low density lipoprotein. Proceedings of the National Academy of Sciences of the United States of America 95: 7614-7619.
43. Mukherjee R., Jow L., Croston G.E., and Paterniti J.R. (1997). Identification characterization, and tissue distribution of human peroxisome proliferator-activated receptor (PPAR) isoforms PPAR γ 2 versus PPAR γ 1 and activation with retinoid X receptor agonists and antagonists. Journal of Biological Chemistry 272: 8071-8076.
44. VidalPuig A.J., Considine R.V., JimenezLinan M., Werman A., Pories W.J., Caro J.F., and Flier J.S. (1997). Peroxisome proliferator-activated receptor gene expression in human tissues - Effects of obesity, weight loss, and regulation by insulin and glucocorticoids. Journal of Clinical Investigation 99: 2416-2422.
45. VidalPuig A., JimenezLinan M., Lowell B.B., Hamann A., Hu E., Spiegelman B., Flier J.S., and Moller D.E. (1996). Regulation of PPAR γ gene expression by nutrition and obesity in rodents. Journal of Clinical Investigation 97: 2553-2561.
46. Werman A., Hollenberg A., Solanes G., Bjorbaek C., VidalPuig A.J., and Flier J.S. (1997). Ligand-independent activation domain in the N terminus of peroxisome proliferator-activated receptor PPAR γ (PPAR γ) - Differential activity of PPAR γ 1 and γ -2 isoforms and influence of insulin. Journal of Biological Chemistry 272: 20230-20235.
47. Hi R., Osada S., Yumoto N., and Osumi T. (1999). Characterization of the amino-terminal activation domain of peroxisome proliferator-activated receptor α - Importance of alpha-helical structure in the transactivating function. Journal of Biological Chemistry 274: 35152-35158.
48. Warnmark A., Treuter E., Wright A.P.H., and Gustafsson J.A. (2003). Activation functions 1 and 2 of nuclear receptors: Molecular strategies for transcriptional activation. Molecular Endocrinology 17: 1901-1909.
49. Lee M.S., Kliewer S.A., Provencal J., Wright P.E., and Evans R.M. (1993). Structure of the Retinoid-X Receptor-Alpha Dna-Binding Domain - A Helix Required for Homodimeric Dna-Binding. Science 260: 1117-1121.
50. Hard T., Kellenbach E., Boelens R., Kaptein R., Dahlman K., Carlstedtduke J., Freedman L.P., Maler B.A., Hyde E.I., Gustafsson J.A. et al. (1990). H-1-Nmr Studies of the Glucocorticoid Receptor DNA-Binding Domain - Sequential Assignments and Identification of Secondary Structure Elements. Biochemistry 29: 9015-9023.
51. Hard T., Kellenbach E., Boelens R., Maler B.A., Dahlman K., Freedman L.P., Carlstedtduke J., Yamamoto K.R., Gustafsson J.A., and Kaptein R. (1990). Solution Structure of the Glucocorticoid Receptor DNA-Binding Domain. Science 249: 157-160.
52. Schwabe J.W.R., Neuhaus D., and Rhodes D. (1990). Solution Structure of the DNA-Binding Domain of the Estrogen-Receptor. Nature 348: 458-461.

53. Hsu M.H., Palmer C.N.A., Song W., Griffin K.J., and Johnson E.F. (1998). A carboxyl-terminal extension of the zinc finger domain contributes to the specificity and polarity of peroxisome proliferator-activated receptor DNA binding. *Journal of Biological Chemistry* 273: 27988-27997.
54. Akiyama T.E., Baumann C.T., Sakai S., Hager G.L., and Gonzalez F.J. (2002). Selective intranuclear redistribution of PPAR isoforms by RXR α . *Molecular Endocrinology* 16: 707-721.
55. Gervois P., Torra I.P., Chinetti G., Grotzinger T., Dubois G., Fruchart J.C., Fruchart-Najib J., Leitersdorf E., and Staels B. (1999). A truncated human peroxisome proliferator-activated receptor PPAR α splice variant with dominant negative activity. *Molecular Endocrinology* 13: 1535-1549.
56. Holt J.A., Consiler T.G., Williams S.P., Ayscue A.H., Leesnitzer L.M., Wisely G.B., and Billin A.N. (2003). Helix 1/8 interactions influence the activity of nuclear receptor ligand-binding domains. *Molecular Endocrinology* 17: 1704-1714.
57. Nolte R.T., Wisely G.B., Westin S., Cobb J.E., Lambert M.H., Kurokawa R., Rosenfeld M.G., Willson T.M., Glass C.K., and Milburn M.V. (1998). Ligand binding and co-activator assembly of the peroxisome proliferator-activated receptor- γ . *Nature* 395: 137-143.
58. Uppenberg J., Svensson C., Jaki M., Bertilsson G., Jendeberg L., and Berkenstam A. (1998). Crystal structure of the ligand binding domain of the human nuclear receptor PPAR γ . *Journal of Biological Chemistry* 273: 31108-31112.
59. Xu H.E., Lambert M.H., Montana V.G., Parks D.J., Blanchard S.G., Brown P.J., Sternbach D.D., Lehmann J.M., Wisely G.B., Willson T.M. et al. (1999). Molecular recognition of fatty acids by peroxisome proliferator-activated receptors. *Molecular Cell* 3: 397-403.
60. Cronet P., Petersen J.F.W., Folmer R., Blomberg N., Sjoblom K., Karlsson U., Lindstedt E.L., and Bamberg K. (2001). Structure of the PPAR α and PPAR γ ligand binding domain in complex with AZ 242; Ligand selectivity and agonist activation in the PPAR family. *Structure* 9: 699-706.
61. Gampe R.T., Montana V.G., Lambert M.H., Miller A.B., Bledsoe R.K., Milburn M.V., Kliewer S.A., Willson T.M., and Xu H.E. (2000). Asymmetry in the PPAR γ /RXR α crystal structure reveals the molecular basis of heterodimerization among nuclear receptors. *Molecular Cell* 5: 545-555.
62. Xu H.E., Lambert M.H., Montana V.G., Plunket K.D., Moore L.B., Collins J.B., Oplinger J.A., Kliewer S.A., Gampe R.T., McKee D.D. et al. (2001). Structural determinants of ligand binding selectivity between the peroxisome proliferator-activated receptors. *Proceedings of the National Academy of Sciences of the United States of America* 98: 13919-13924.
63. Blanquart C., Barbier O., Fruchart J.C., Staels B., and Glineur C. (2003). Peroxisome proliferator-activated receptors: regulation of transcriptional activities and roles in inflammation. *Journal of Steroid Biochemistry and Molecular Biology* 85: 267-273.
64. Ohshima T., Koga H., and Shimotohno K. (2004). Transcriptional activity of peroxisome proliferator-activated receptor γ is modulated by SUMO-1 modification. *Journal of Biological Chemistry* 279: 29551-29557.

65. Gelman L., Michalik L., Desvergne A., and Wahli W. (2005). Kinase signaling cascades that modulate peroxisome proliferator-activated receptors. *Current Opinion in Cell Biology* 17: 216-222.
66. Diradourian C., Girard J., and Pegorier J.P. (2005). Phosphorylation of PPARs: from molecular characterization to physiological relevance. *Biochimie* 87: 33-38.
67. Adams M., Reginato M.J., Shao D.L., Lazar M.A., and Chatterjee V.K. (1997). Transcriptional activation by peroxisome proliferator-activated receptor- γ is inhibited by phosphorylation at a consensus mitogen-activated protein kinase site. *Journal of Biological Chemistry* 272: 5128-5132.
68. Hardy K. and Chaudhri G. (1997). Activation and signal transduction via mitogen-activated protein (MAP) kinases in T lymphocytes. *Immunology and Cell Biology* 75: 528-545.
69. Juge-Aubry C.E., Hammar E., Siegrist-Kaiser C., Pernin A., Takeshita A., Chin W.W., Burger A.G., and Meier C.A. (1999). Regulation of the transcriptional activity of the peroxisome proliferator-activated receptor- α by phosphorylation of a dependent trans-activating domain. *Journal of Biological Chemistry* 274: 10505-10510.
70. Barger P.M., Browning A.C., Garner A.N., and Kelly D.P. (2001). p38 mitogen-activated protein kinase activates peroxisome proliferator-activated receptor- α . A potential role in the cardiac metabolic stress response. *Journal of Biological Chemistry* 276: 44495-44501.
71. Gray J.P., Burns K.A., Leas T.L., Perdew G.H., and Heuvel J.P.V. (2005). Regulation of peroxisome proliferator-activated receptor- α by protein kinase C. *Biochemistry* 44: 10313-10321.
72. Lazennec G., Canaple L., Saugy D., and Wahli W. (2000). Activation of peroxisome proliferator-activated receptors (PPARs) by their ligands and protein kinase A activators. *Molecular Endocrinology* 14: 1962-1975.
73. Blanquart C., Mansouri R., Paumelle R., Fruchart J.C., Staels B., and Glineur C. (2004). The protein kinase C signaling pathway regulates a molecular switch between transactivation and transrepression activity of the peroxisome proliferator-activated receptor α . *Molecular Endocrinology* 18: 1906-1918.
74. Camp H.S., Tafuri S.R., and Leff T. (1999). c-Jun N-terminal kinase phosphorylates peroxisome proliferator-activated receptor- γ 1 and negatively regulates its transcriptional activity. *Endocrinology* 140: 392-397.
75. Hu E.D., Kim J.B., Sarraf P., and Spiegelman B.M. (1996). Inhibition of adipogenesis through MAP kinase-mediated phosphorylation of PPAR γ . *Science* 274: 2100-2103.
76. Shao D.L., Rangwala S.M., Bailey S.T., Krakow S.L., Reginato M.J., and Lazar M.A. (1998). Interdomain communication regulating ligand binding by PPAR γ . *Nature* 396: 377-380.
77. Zhang B., Berger J., Zhou G.C., Elbrecht A., Biswas S., White-Carrington S., Szalkowski D., and Moller D.E. (1996). Insulin- and mitogen-activated protein kinase-mediated phosphorylation and activation of peroxisome proliferator-activated receptor- γ . *Journal of Biological Chemistry* 271: 31771-31774.

78. Floyd Z.E. and Stephens J.M. (2002). Interferon- γ -mediated activation and ubiquitin-proteasome-dependent degradation of PPAR γ in adipocytes. *Journal of Biological Chemistry* 277: 4062-4068.
79. Blanquart C., Barbier O., Fruchart J.C., Staels B., and Glineur C. (2002). Peroxisome proliferator-activated receptor- α (PPAR γ) turnover by the ubiquitin-proteasome system controls the ligand-induced expression level of its target genes. *Journal of Biological Chemistry* 277: 37254-37259.
80. Nandi D., Tahiliani P., Kumar A., and Chandu D. (2006). The ubiquitin-proteasome system. *Journal of Biosciences* 31: 137-155.
81. Hodges M., Tissot C., and Freemont P.S. (1998). Protein regulation: Tag wrestling with relatives of ubiquitin. *Current Biology* 8: R749-R752.
82. Hauser S., Adelmant G., Sarraf P., Wright H.M., Mueller E., and Spiegelman B.M. (2000). Degradation of the peroxisome proliferator-activated receptor- γ is linked to ligand-dependent activation. *Journal of Biological Chemistry* 275: 18527-18533.
83. Yamashita D., Yamaguchi T., Shimizu M., Nakata N., Hirose F., and Osumi T. (2004). The transactivating function of peroxisome proliferator-activated receptor- γ is negatively regulated by SUMO conjugation in the amino-terminal domain. *Genes to Cells* 9: 1017-1029.
84. Floyd Z.E. and Stephens J.M. (2004). Control of peroxisome proliferator-activated receptor γ 2 stability and activity by SUMOylation. *Obesity Research* 12: 921-928.
85. Pascual G., Fong A.L., Ogawa S., Gamliel A., Li A.C., Perissi V., Rose D.W., Willson T.M., Rosenfeld M.G., and Glass C.K. (2005). A SUMOylation-dependent pathway mediates transrepression of inflammatory response genes by PPAR γ . *Nature* 437: 759-763.
86. Forman B.M., Chen J., and Evans R.M. (1997). Hypolipidemic drugs, polyunsaturated fatty acids, and eicosanoids are ligands for peroxisome proliferator-activated receptors α and γ . *Proceedings of the National Academy of Sciences of the United States of America* 94: 4312-4317.
87. Krey G., Braissant O., L'Horsset F., Kalkhoven E., Perroud M., Parker M.G., and Wahli W. (1997). Fatty acids, eicosanoids, and hypolipidemic agents identified as ligands of peroxisome proliferator-activated receptors by coactivator-dependent receptor ligand assay. *Molecular Endocrinology* 11: 779-791.
88. Keller H., Dreyer C., Medin J., Mahfoudi A., Ozato K., and Wahli W. (1993). Fatty acids and retinoids control lipid-metabolism through activation of peroxisome proliferator-activated receptor retinoid-x receptor heterodimers. *Proceedings of the National Academy of Sciences of the United States of America* 90: 2160-2164.
89. Lin Q.O., Ruuska S.E., Shaw N.S., Dong D., and Noy N. (1999). Ligand selectivity of the peroxisome proliferator-activated receptor- α . *Biochemistry* 38: 185-190.
90. Duval C., Fruchart J.C., and Staels B. (2004). PPAR α , fibrates, lipid metabolism and inflammation. *Archives des Maladies du Coeur et des Vaisseaux* 97: 665-672.
91. Brown P.J., Winegar D.A., Plunket K.D., Moore L.B., Lewis M.C., Wilson J.G., Sundseth S.S., Koble C.S., Wu Z.D., Chapman J.M. *et al.* (1999). A ureido-thioisobutyric acid (GW9578) is a subtype-selective PPAR γ agonist with potent lipid-lowering activity. *Journal of Medicinal Chemistry* 42: 3785-3788.

92. Rang H.P., Dale M.M., and Ritter J.M. (1999). Local hormones, inflammation and allergy. In *Pharmacology*, pp. 198-228.
93. Bishop-Bailey D. and Wray J. (2003). Peroxisome proliferator-activated receptors: a critical review on endogenous pathways for ligand generation. *Prostaglandins & Other Lipid Mediators* 71: 1-22.
94. Yu K., Bayona W., Kallen C.B., Harding H.P., Ravera C.P., McMahon G., Brown M., and Lazar M.A. (1995). Differential Activation of Peroxisome Proliferator-Activated Receptors by Eicosanoids. *Journal of Biological Chemistry* 270: 23975-23983.
95. Johnson T.E., Holloway M.K., Vogel R., Rutledge S.J., Perkins J.J., Rodan G.A., and Schmidt A. (1997). Structural requirements and cell-type specificity for ligand activation of peroxisome proliferator-activated receptors. *Journal of Steroid Biochemistry and Molecular Biology* 63: 1-8.
96. Wei Z.L. and Kozikowski A.P. (2003). A short and efficient synthesis of the pharmacological research tool GW501516 for the peroxisome proliferator-activated receptor- β/δ . *Journal of Organic Chemistry* 68: 9116-9118.
97. Oliver W.R., Shenk J.L., Snaith M.R., Russell C.S., Plunket K.D., Bodkin N.L., Lewis M.C., Winegar D.A., Sznajdman M.L., Lambert M.H. *et al.* (2001). A selective peroxisome proliferator-activated receptor- β/δ agonist promotes reverse cholesterol transport. *Proceedings of the National Academy of Sciences of the United States of America* 98: 5306-5311.
98. Kliewer S.A., Sundseth S.S., Jones S.A., Brown P.J., Wisely G.B., Koble C.S., Devchand P., Wahli W., Willson T.M., Lenhard J.M. *et al.* (1997). Fatty acids and eicosanoids regulate gene expression through direct interactions with peroxisome proliferator-activated receptors- α and γ . *Proceedings of the National Academy of Sciences of the United States of America* 94: 4318-4323.
99. Kliewer S.A., Lenhard J.M., Willson T.M., Patel I., Morris D.C., and Lehmann J.M. (1995). A prostaglandin J(2) metabolite binds peroxisome proliferator-activated receptor- γ and promotes adipocyte differentiation. *Cell* 83: 813-819.
100. Forman B.M., Tontonoz P., Chen J., Brun R.P., Spiegelman B.M., and Evans R.M. (1995). 15-deoxy- $\Delta^{12,14}$ -prostaglandin J₂ is a ligand for the adipocyte determination factor PPAR γ . *Cell* 83: 803-812.
101. Maxey K.M., Hessler E., MacDonald J., and Hitchingham L. (2000). The nature and composition of 15-deoxy- $\Delta^{12,14}$ -prostaglandin J₂. *Prostaglandins & Other Lipid Mediators* 62: 15-21.
102. Powell W.S. (2003). 15-deoxy- $\Delta^{12,14}$ -prostaglandin J₂ : endogenous PPAR γ ligand or minor eicosanoid degradation product? *Journal of Clinical Investigation* 112: 828-830.
103. Davies S.S., Pontsler A.V., Marathe G.K., Harrison K.A., Murphy R.C., Hinshaw J.C., Prestwich G.D., St Hilaire A., Prescott S.M., Zimmerman G.A. *et al.* (2001). Oxidized alkyl phospholipids are specific, high affinity peroxisome proliferator-activated receptor- γ ligands and agonists. *Journal of Biological Chemistry* 276: 16015-16023.
104. Spiegelman B.M. (1998). PPAR γ : Adipogenic regulator and thiazolidinedione receptor. *Diabetes* 47: 507-514.

105. Liu K.G., Lambert M.H., Ayscue A.H., Henke B.R., Leesnitzer L.M., Oliver W.R., Plunket K.D., Xu H.E., Sternbach D.D., and Willson T.M. (2001). Synthesis and biological activity of L-tyrosine-based PPAR γ agonists with reduced molecular weight. *Bioorganic & Medicinal Chemistry Letters* 11: 3111-3113.
106. Willson T.M., Cobb J.E., Cowan D.J., Wiethe R.W., Correa I.D., Prakash S.R., Beck K.D., Moore L.B., Klierer S.A., and Lehmann J.M. (1996). The structure-activity relationship between peroxisome proliferator-activated receptor- γ agonism and the antihyperglycemic activity of thiazolidinediones. *Journal of Medicinal Chemistry* 39: 665-668.
107. Henke B.R., Blanchard S.G., Brackeen M.F., Brown K.K., Cobb J.E., Collins J.L., Harrington W.W., Hashim M.A., Hull-Ryde E.A., Kaldor I. *et al.* (1998). N-(2-benzoylphenyl)-L-tyrosine PPAR γ agonists. 1. Discovery of a novel series of potent antihyperglycemic and antihyperlipidemic agents. *Journal of Medicinal Chemistry* 41: 5020-5036.
108. Agostini M., Gurnell M., Savage D.B., Wood E.M., Smith A.G., Rajanayagam O., Garnes K.T., Levinson S.H., Xu H.E., Schwabe J.W.R. *et al.* (2004). Tyrosine Agonists reverse the molecular defects associated with dominant-negative mutations in human peroxisome proliferator- activated receptor- γ . *Endocrinology* 145: 1527-1538.
109. Tugwood J.D., Issemann I., Anderson R.G., Bundell K.R., Mcpheat W.L., and Green S. (1992). The Mouse Peroxisome Proliferator Activated Receptor Recognizes A Response Element in the 5' Flanking Sequence of the Rat Acyl Coa Oxidase Gene. *Embo Journal* 11: 433-439.
110. Palmer C.N.A., Hsu M.H., Griffin K.J., and Johnson E.F. (1995). Novel Sequence Determinants in Peroxisome Proliferator Signaling. *Journal of Biological Chemistry* 270: 16114-16121.
111. JugeAubry C., Pernin A., Favez T., Burger A.G., Wahli W., Meier C.A., and Desvergne B. (1997). DNA binding properties of peroxisome proliferator-activated receptor subtypes on various natural peroxisome proliferator response elements - Importance of the 5'-flanking region. *Journal of Biological Chemistry* 272: 25252-25259.
112. Zhao Q., Chasse S.A., Devarakonda S., Sierk M.L., Ahvazi B., and Rastinejad F. (2000). Structural basis of RXR-DNA interactions. *Journal of Molecular Biology* 296: 509-520.
113. Kumar S., Saradhi M., Chaturvedi N.K., and Tyagi R.K. (2006). Intracellular localization and nucleocytoplasmic trafficking of steroid receptors: An overview. *Molecular and Cellular Endocrinology* 246: 147-156.
114. Sumanasekera W.K., Tien E.S., Turpey R., Vanden Heuvel J.P., and Perdew G.H. (2003). Evidence that peroxisome proliferator-activated receptor- α is complexed with the 90-kDa heat shock protein and the hepatitis virus B X-associated protein 2. *Journal of Biological Chemistry* 278: 4467-4473.
115. Sumanasekera W.K., Tien E.S., Davis J.W., Turpey R., Perdew G.H., and Vanden Heuvel J.P. (2003). Heat shock protein-90 (Hsp90) acts as a repressor of peroxisome proliferator-activated receptor- α (PPAR α) and PPAR β/δ activity. *Biochemistry* 42: 10726-10735.

116. Bishop-Bailey D., Hla T., and Warner T.D. (2000). Bisphenol A diglycidyl ether (BADGE) is a PPAR γ agonist in an ECV304 cell line. *British Journal of Pharmacology* *131*: 651-654.
117. Tsubouchi Y., Sano H., Kawahito Y., Mukai S., Yamada R., Kohno M., Inoue K., Hla T., and Kondo M. (2000). Inhibition of human lung cancer cell growth by the peroxisome proliferator-activated receptor- γ agonists through induction of apoptosis. *Biochemical and Biophysical Research Communications* *270*: 400-405.
118. Berger J., Patel H.V., Woods J., Hayes N.S., Parent S.A., Clemas J., Leibowitz M.D., Elbrecht A., Rachubinski R.A., Capone J.P. *et al.* (2000). A PPAR γ mutant serves as a dominant negative inhibitor of PPAR signaling and is localized in the nucleus. *Molecular and Cellular Endocrinology* *162*: 57-67.
119. Yu C., Markan K., Temple K.A., Deplewski D., Brady M.J., and Cohen R.N. (2005). The nuclear receptor corepressors NCoR and SMRT decrease peroxisome proliferator-activated receptor γ transcriptional activity and repress 3T3-L1 adipogenesis. *Journal of Biological Chemistry* *280*: 13600-13605.
120. Stanley T.B., Leesnitzer L.M., Montana V.G., Galardi C.M., Lambert M.H., Holt J.A., Xu K.E., Moore L.B., Blanchard S.G., and Stimmel J.B. (2003). Subtype specific effects of peroxisome proliferator-activated receptor ligands corepressor affinity. *Biochemistry* *42*: 9278-9287.
121. Krogsdam A.M., Nielsen C.A.F., Neve S., Holst D., Helledie T., Thomsen B., Bendixen C., Mandrup S., and Kristiansen K. (2002). Nuclear receptor corepressor-dependent repression of peroxisome-proliferator-activated receptor- β/δ -mediated transactivation. *Biochemical Journal* *363*: 157-165.
122. Ishizuka T. and Lazar M.A. (2003). The N-CoR/histone deacetylase 3 complex is required for repression by thyroid hormone receptor. *Molecular and Cellular Biology* *23*: 5122-5131.
123. Holbert M.A. and Marmorstein R. (2005). Structure and activity of enzymes that remove histone modifications. *Current Opinion in Structural Biology* *15*: 673-680.
124. Luger K. (2006). Dynamic nucleosomes. *Chromosome Research* *14*: 5-16.
125. Craig J.M. (2005). Heterochromatin-many flavours, common themes. *Bioessays* *27*: 17-28.
126. Santos-Rosa H. and Caldas C. (2005). Chromatin modifier enzymes, the histone code and cancer. *European Journal of Cancer* *41*: 2381-2402.
127. Peterson C.L. and Laniel M.A. (2004). Histones and histone modifications. *Current Biology* *14*: R546-R551.
128. Ehrenhofer-Murray A.E. (2004). Chromatin dynamics at DNA replication, transcription and repair. *European Journal of Biochemistry* *271*: 2335-2349.
129. Goll M.G. and Bestor T.H. (2002). Histone modification and replacement in chromatin activation. *Genes & Development* *16*: 1739-1742.
130. Codina A., Love J.D., Li Y., Lazar M.A., Neuhaus D., and Schwabe J.W.R. (2005). Structural insights into the interaction and activation of histone deacetylase 3 by nuclear receptor corepressors. *Proceedings of the National Academy of Sciences of the United States of America* *102*: 6009-6014.

131. Tan N.S., Shaw N.S., Vinckenbosch N., Liu P., Yasmin R., Desvergne B., Wahli W., and Noy N. (2002). Selective cooperation between fatty acid binding proteins and peroxisome proliferator-activated receptors in regulating transcription. *Molecular and Cellular Biology* 22: 5114-5127.
132. Egea P.F., Mitschler A., Rochel N., Ruff M., Chambon P., and Moras D. (2000). Crystal structure of the human RXR α ligand-binding domain bound to its natural ligand: 9-cis retinoic acid. *Embo Journal* 19: 2592-2601.
133. Johnson B.A., Wilson E.M., Li Y., Moller D.E., Smith R.G., and Zhou G.C. (2000). Ligand-induced stabilization of PPAR γ monitored by NMR spectroscopy: Implications for nuclear receptor activation. *Journal of Molecular Biology* 298: 187-194.
134. Durand B., Saunders M., Gaudon C., Roy B., Losson R., and Chambon P. (1994). Activation Function-2 (AF-2) of Retinoic Acid Receptor and 9-Cis Retinoic Acid Receptor - Presence of A Conserved Autonomous Constitutive Activating Domain and Influence of the Nature of the Response Element on Af-2 Activity. *Embo Journal* 13: 5370-5382.
135. Gurnell M., Wentworth J.M., Agostini M., Adams M., Collingwood T.N., Provenzano C., Browne P.O., Rajanayagam O., Burris T.P., Schwabe J.W. *et al.* (2000). A dominant-negative peroxisome proliferator-activated receptor- γ (PPAR γ) mutant is a constitutive repressor and inhibits PPAR gamma-mediated adipogenesis. *Journal of Biological Chemistry* 275: 5754-5759.
136. Babb R. and Bowen B.R. (2003). SDP1 is a peroxisome-proliferator-activated receptor γ 2 co-activator that binds through its SCAN domain. *Biochemical Journal* 370: 719-727.
137. Kodera Y., Takeyama K., Murayama A., Suzawa M., Masuhiro Y., and Kato S. (2000). Ligand type-specific interactions of peroxisome proliferator-activated receptor- γ with transcriptional coactivators. *Journal of Biological Chemistry* 275: 33201-33204.
138. Chen S.Y., Johnson B.A., Li Y., Aster S., McKeever B., Mosley R., Moller D.E., and Zhou G.C. (2000). Both coactivator LXXLL motif-dependent and -independent interactions are required for peroxisome proliferator-activated receptor gamma (PPAR γ) function. *Journal of Biological Chemistry* 275: 3733-3736.
139. Collingwood T.N., Urnov F.D., and Wolffe A.P. (1999). Nuclear receptors: coactivators, corepressors and chromatin remodeling in the control of transcription. *Journal of Molecular Endocrinology* 23: 255-275.
140. Heinlein C.A., Ting H.J., Yeh S.Y., and Chang C.S. (1999). Identification of ARA70 as a ligand-enhanced coactivator for the peroxisome proliferator-activated receptor- γ . *Journal of Biological Chemistry* 274: 16147-16152.
141. Rosenfeld M.G. and Glass C.K. (2001). Coregulator codes of transcriptional regulation by nuclear receptors. *Journal of Biological Chemistry* 276: 36865-36868.
142. Puigserver P. and Spiegelman B.M. (2003). Peroxisome proliferator-activated receptor- γ coactivator 1 α (PGC-1 α): Transcriptional coactivator and metabolic regulator. *Endocrine Reviews* 24: 78-90.

143. Debril M.B., Gelman L., Fayard E., Annicotte J.S., Rocchi S., and Auwerx J. (2004). Transcription factors and nuclear receptors interact with the SWI/SNF complex through the BAF60c subunit. *Journal of Biological Chemistry* 279: 16677-16686.
144. Yang W., Rachez C., and Freedman L.P. (2000). Discrete roles for peroxisome proliferator-activated receptor gamma and retinoid X receptor in recruiting nuclear receptor coactivators. *Molecular and Cellular Biology* 20: 8008-8017.
145. Metivier R., Reid G., and Gannon F. (2006). Transcription in four dimensions: nuclear receptor-directed initiation of gene expression. *Embo Reports* 7: 161-167.
146. Lefebvre P., Chinetti G., Fruchart J.C., and Staels B. (2006). Sorting out the roles of PPAR α in energy metabolism and vascular homeostasis. *Journal of Clinical Investigation* 116: 571-580.
147. Goikoetxea M.J., Beaumont J., and Diez J. (2004). Peroxisome proliferator-activated receptor- α and hypertensive heart disease. *Drugs* 64: 9-18.
148. Barbier O., Fontaine C., Fruchart J.C., and Staels B. (2004). Genomic and non-genomic interactions of PPAR α with xenobiotic-metabolizing enzymes. *Trends in Endocrinology and Metabolism* 15: 324-330.
149. Tan N.S., Michalik L., Noy N., Yasmin R., Pacot C., Heim M., Fluhmann B., Desvergne B., and Wahli W. (2001). Critical roles of PPAR β/δ in keratinocyte response to inflammation. *Genes & Development* 15: 3263-3277.
150. Xue L.Z., Fletcher G.C., and Tolkovsky A.M. (1999). Autophagy is activated by apoptotic signalling in sympathetic neurons: An alternative mechanism of death execution. *Molecular and Cellular Neuroscience* 14: 180-198.
151. Barak Y., Liao D., He W.M., Ong E.S., Nelson M.C., Olefsky J.M., Boland R., and Evans R.M. (2002). Effects of peroxisome proliferator-activated receptor PPAR β/δ on placentation, adiposity, and colorectal cancer. *Proceedings of the National Academy of Sciences of the United States of America* 99: 303-308.
152. Vosper H., Patel L., Graham T.L., Khoudoli G.A., Hill A., Macphee C.H., Pinto I., Smith S.A., Suckling K.E., Wolf C.R. *et al.* (2001). The peroxisome proliferator-activated receptor- β/δ promotes lipid accumulation in human macrophages. *Journal of Biological Chemistry* 276: 44258-44265.
153. Michalik L., Desvergne B., Tan N.S., Basu-Modak S., Escher P., Rieusset J., Peters J.M., Kaya G., Gonzalez F.J., Zakany J. *et al.* (2001). Impaired skin wound healing in peroxisome proliferator-activated receptor PPAR α and PPAR β/δ mutant mice. *Journal of Cell Biology* 154: 799-814.
154. Tan N.S., Michalik L., Di-Poi N., Desvergne B., and Wahli W. (2004). Critical roles of the nuclear receptor PPAR β/δ (peroxisome-proliferator-activated receptor- β/δ) in skin wound healing. *Biochemical Society Transactions* 32: 97-102.
155. Park B.H., Vogelstein B., and Kinzler K.W. (2001). Genetic disruption of PPAR β/δ decreases the tumorigenicity of human colon cancer cells. *Proceedings of the National Academy of Sciences of the United States of America* 98: 2598-2603.
156. Glinghammar B., Skogsberg J., Hamsten A., and Ehrenborg E. (2003). PPAR β/δ activation induces COX-2 gene expression and cell proliferation in human hepatocellular carcinoma cells. *Biochemical and Biophysical Research Communications* 308: 361-368.

157. Gupta R.A., Wang D.Z., Katkuri S., Wang H.B., Dey S.K., and DuBois R.N. (2004). Activation of nuclear hormone receptor peroxisome proliferator- activated receptor- β/δ accelerates intestinal adenoma growth. *Nature Medicine* 10: 245-247.
158. Stephen R.L., Gustafsson M.C.U., Jarvis M., Tatoud R., Marshall B.R., Knight D., Ehrenborg E., Harris A.L., Wolf C.R., and Palmer C.N.A. (2004). Activation of PPAR β/δ stimulates the proliferation of human breast and prostate cancer cell lines. *Toxicology* 202: 52-53.
159. Barak Y., Nelson M.C., Ong E.S., Jones Y.Z., Ruiz-Lozano P., Chien K.R., Koder A., and Evans R.M. (1999). PPAR γ is required for placental, cardiac, and adipose tissue development. *Molecular Cell* 4: 585-595.
160. Marin H.E., Peraza M.A., Billin A.N., Willson T.M., Ward J.M., Kennett M.J., Gonzalez F.J., and Peters J.M. (2006). Ligand activation of peroxisome proliferator-activated receptor- γ inhibits colon carcinogenesis. *Cancer Res* 66: 4394-4401.
161. Fajas L., Fruchart J.C., and Auwerx J. (1998). Transcriptional control of adipogenesis. *Current Opinion in Cell Biology* 10: 165-173.
162. Rosen E.D., Sarraf P., Troy A.E., Bradwin G., Moore K., Milstone D.S., Spiegelman B.M., and Mortensen R.M. (1999). PPAR γ is required for the differentiation of adipose tissue *in vivo* and *in vitro*. *Molecular Cell* 4: 611-617.
163. Okuno M., Arimoto E., Nishizuka M., Nishihara T., and Imagawa M. (2002). Isolation of up- or down-regulated genes in PPAR γ - expressing NIH-3T3 cells during differentiation into adipocytes. *Febs Letters* 519: 108-112.
164. Chawla A., Schwarz E.J., Dimaculangan D.D., and Lazar M.A. (1994). Peroxisome Proliferator-Activated Receptor PPAR γ - Adipose-Predominant Expression and Induction Early in Adipocyte Differentiation. *Endocrinology* 135: 798-800.
165. Morrison R.F. and Farmer S.R. (1999). Role of PPAR γ in regulating a cascade expression of cyclin-dependent kinase inhibitors, p18(INK4c) and p21(Waf1/Cip1), during adipogenesis. *Journal of Biological Chemistry* 274: 17088-17097.
166. Watanabe M., Inukai K., Katagiri H., Awata T., Oka Y., and Katayama S. (2003). Regulation of PPAR γ transcriptional activity in 3T3-L1 adipocytes. *Biochemical and Biophysical Research Communications* 300: 429-436.
167. Hu E.D., Tontonoz P., and Spiegelman B.M. (1995). Transdifferentiation of Myoblasts by the Adipogenic Transcription Factors PPAR γ and C/EBP α . *Proceedings of the National Academy of Sciences of the United States of America* 92: 9856-9860.
168. Wright H.M., Clish C.B., Mikami T., Hauser S., Yanagi K., Hiramatsu R., Serhan C.N., and Spiegelman B.M. (2000). A synthetic antagonist for the peroxisome proliferator- activated receptor- γ inhibits adipocyte differentiation. *Journal of Biological Chemistry* 275: 1873-1877.
169. Park Y., Freedman B.D., Lee E.J., Park S., and Jameson J.L. (2003). A dominant negative PPAR γ mutant shows altered cofactor recruitment and inhibits adipogenesis in 3T3-L1 cells. *Diabetologia* 46: 365-377.
170. Gerhold D.L., Liu F., Jiang G., Li Z., Xu J., Lu M., Sachs J.R., Bagchi A., Fridman A., Holder D.J. et al. (2002). Gene expression profile of adipocyte differentiation and

- its regulation by peroxisome proliferator-activated receptor- γ agonists. *Endocrinology* 143: 2106-2118.
171. Yeh W.C., Cao Z.D., Classon M., and Mcknight S.L. (1995). Cascade Regulation of Terminal Adipocyte Differentiation by 3 Members of the C/EBP Family of Leucine-Zipper Proteins. *Genes & Development* 9: 168-181.
 172. Malecki M.T. (2005). Genetics of type 2 diabetes mellitus. *Diabetes Research and Clinical Practice* 68: S10-S21.
 173. Edelman S.V. (2003). The Role of the Thiazolidinediones in the Practical Management of Patients with Type 2 Diabetes and Cardiovascular Risk Factors. *Reviews in Cardiovascular Medicine* 4: s29-s37.
 174. Gurnell M., Savage D.B., Chatterjee V.K.K., and O'Rahilly S. (2003). The metabolic syndrome: Peroxisome proliferator-activated receptor- γ and its therapeutic modulation. *Journal of Clinical Endocrinology and Metabolism* 88: 2412-2421.
 175. Semple R.K., Chatterjee V.K.K., and O'Rahilly S. (2006). PPAR γ and human metabolic disease. *Journal of Clinical Investigation* 116: 581-589.
 176. Barroso I., Gurnell M., Crowley V.E.F., Agostini M., Schwabe J.W., Soos M.A., Maslen G.L., Williams T.D.M., Lewis H., Schafer A.J. *et al.* (1999). Dominant negative mutations in human PPAR γ associated with severe insulin resistance, diabetes mellitus and hypertension. *Nature* 402: 880-883.
 177. Hegele R.A., Cao H.N., Frankowski C., Mathews S.T., and Leff T. (2002). PPAR γ F388L, a transactivation-deficient mutant, in familial partial lipodystrophy. *Diabetes* 51: 3586-3590.
 178. Agarwal A.K. and Garg A. (2002). A novel heterozygous mutation in peroxisome proliferator-activated receptor- γ gene in a patient with familial partial lipodystrophy. *Journal of Clinical Endocrinology and Metabolism* 87: 408-411.
 179. Savage D.B., Tan G.D., Acerini C.L., Jebb S.A., Agostini M., Gurnell M., Williams R.L., Umpleby A.M., Thomas E.L., Bell J.D. *et al.* (2003). Human metabolic syndrome resulting from dominant-negative mutations in the nuclear receptor peroxisome proliferator-activated receptor- γ . *Diabetes* 52: 910-917.
 180. Hauner H. (2002). The mode of action of thiazolidinediones. *Diabetes-Metabolism Research and Reviews* 18: S10-S15.
 181. Komers R. and Vrana A. (1998). Thiazolidinediones - Tools for the research of metabolic syndrome X. *Physiological Research* 47: 215-225.
 182. Sewter C. and Vidal-Puig A. (2002). PPAR γ and the thiazolidinediones: molecular basis for a treatment of 'Syndrome X'? *Diabetes Obesity & Metabolism* 4: 239-248.
 183. Lebovitz H.E. (2002). Rationale for and role of thiazolidinediones in type 2 diabetes mellitus. *American Journal of Cardiology* 90: 34G-41G.
 184. Ricote M., Huang J.T., Welch J.S., and Glass C.K. (1999). The peroxisome proliferator-activated receptor- γ (PPAR γ) as a regulator of monocyte/macrophage function. *Journal of Leukocyte Biology* 66: 733-739.

185. Gelman L., Fruchart J.C., and Auwerx J. (1999). An update on the mechanisms of action of the peroxisome proliferator-activated receptors (PPARs) and their roles in inflammation and cancer. *Cellular and Molecular Life Sciences* 55: 932-943.
186. Na H.K. and Surh Y.J. (2003). Peroxisome proliferator-activated receptor- γ (PPAR γ) ligands as bifunctional regulators of cell proliferation. *Biochemical Pharmacology* 66: 1381-1391.
187. Tontonoz P., Nagy L., Alvarez J.G.A., Thomazy V.A., and Evans R.M. (1998). PPAR γ promotes monocyte/macrophage differentiation and uptake of oxidized LDL. *Cell* 93: 241-252.
188. Wang T., Xu J., Yu X., Yang R., and Han Z.C. (2005). Peroxisome proliferator-activated receptor- γ in malignant diseases. - *Crit Rev Oncol Hematol*. 2005 Dec 30;.
189. Clay C.E., Namen A.M., Fonteh A.N., Atsumi G., High K.P., and Chilton F.H. (2000). 15-deoxy- $\Delta^{12,14}$ -prostaglandin J₂ induces diverse biological responses via PPAR γ activation in cancer cells. *Prostaglandins & Other Lipid Mediators* 62: 23-32.
190. Mueller E., Sarraf P., Tontonoz P., Evans R.M., Martin K.J., Zhang M., Fletcher C., Singer S., and Spiegelman B.M. (1998). Terminal differentiation of human breast cancer through PPAR γ . *Molecular Cell* 1: 465-470.
191. Takahashi N., Okumura T., Motomura L., Fujimoto Y., Kawabata I., and Kohgo Y. (1999). Activation of PPAR γ inhibits cell growth and induces apoptosis in human gastric cancer cells. *Febs Letters* 455: 135-139.
192. Butler R., Mitchell S.H., Tindall D.J., and Young C.Y.F. (2000). Nonapoptotic cell death associated with S-phase arrest of prostate cancer cells via the peroxisome proliferator-activated receptor gamma ligand, 15-deoxy- $\Delta^{12,14}$ -prostaglandin J₂. *Cell Growth & Differentiation* 11: 49-61.
193. Eibl G., Wente M.N., Reber H.A., and Hines O.J. (2001). Peroxisome proliferator-activated receptor- γ induces pancreatic cancer cell apoptosis. *Biochemical and Biophysical Research Communications* 287: 522-529.
194. Nakashiro K., Begum N.M., Uchida D., Kawamata H., Shintani S., Sato M., and Hamakawa H. (2003). Thiazolidinediones inhibit cell growth of human oral squamous cell carcinoma *in vitro* independent of peroxisome proliferator- activated receptor- γ . *Oral Oncology* 39: 855-861.
195. Badawi A.F., Eldeen M.B., Liu Y.Y., Ross E.A., and Badr M.Z. (2004). Inhibition of rat mammary gland carcinogenesis by simultaneous targeting of cyclooxygenase-2 and peroxisome proliferator-activated receptor- γ (Retracted article. See vol. 65, pg. 8057, 2005). *Cancer Res* 64: 1181-1189.
196. Yoshimura R., Matsuyama M., Segawa Y., Hase T., Mitsuhashi M., Tsuchida K., Wada S., Kawahito Y., Sano H., and Nakatani T. (2003). Expression of peroxisome proliferator-activated receptors (PPARs) in human urinary bladder carcinoma and growth inhibition by its agonists. *International Journal of Cancer* 104: 597-602.
197. Yu J., Qiao L., Zimmermann L., Ebert M.P.A., Zhang H.X., Lin W., Rocken C., Malferteiner P., and Farrell G.C. (2006). Troglitazone inhibits tumor growth in hepatocellular carcinoma *in vitro* and *in vivo*. *Hepatology* 43: 134-143.
198. Subbarayan V., Sabichi A.L., Kim J., Llansa N., Logothetis C.J., Lippman S.M., and Menter D.G. (2004). Differential peroxisome proliferator-activated receptor- γ

isoform expression and agonist effects in normal and malignant prostate cells. *Cancer Epidemiology Biomarkers & Prevention* 13: 1710-1716.

199. Yoshizawa K., Cioca D.P., Kawa S., Tanaka E., and Kiyosawa K. (2002). Peroxisome proliferator-activated receptor gamma ligand troglitazone induces cell cycle arrest and apoptosis of hepatocellular carcinoma cell lines. *Cancer* 95: 2243-2251.
200. Yang F.G., Zhang Z.W., Xin D.Q., Shi C.J., Wu J.P., Guo Y.L., and Guan Y.F. (2005). Peroxisome proliferator-activated receptor- γ ligands induce cell cycle arrest and apoptosis in human renal carcinoma cell lines. *Acta Pharmacologica Sinica* 26: 753-761.
201. Yoshizumi T., Ohta T., Ninomiya I., Terada I., Fushida S., Fujimura T., Nishimura G., Shimizu K., Yi S.G., and Miwa K. (2004). Thiazolidinedione, a peroxisome proliferator-activated receptor- γ ligand, inhibits growth and metastasis of HT-29 human colon cancer cells through differentiation-promoting effects. *International Journal of Oncology* 25: 631-639.
202. Lapillonne H., Konopleva M., Tsao T., Gold D., McQueen T., Sutherland R.L., Madden T., and Andreeff M. (2003). Activation of peroxisome proliferator-activated receptor- γ by a novel synthetic triterpenoid 2-cyano-3,12-dioxooleana-1,9-dien-28-oic acid induces growth arrest and apoptosis in breast cancer cells. *Cancer Res* 63: 5926-5939.
203. Chang T.H. and Szabo E. (2000). Induction of differentiation and apoptosis by ligands of peroxisome proliferator-activated receptor- γ in non-small cell lung cancer. *Cancer Res* 60: 1129-1138.
204. Han S.W., Sidell N., Fisher P.B., and Roman J. (2004). Up-regulation of p21 gene expression by peroxisome proliferator-activated receptor- γ in human lung carcinoma cells. *Clinical Cancer Research* 10: 1911-1919.
205. Sato H., Ishihara S., Kawashima K., Moriyama N., Suetsugu H., Kazumori H., Okuyama T., Rumi M.A.K., Fukuda R., Nagasue N. *et al.* (2000). Expression of peroxisome proliferator-activated receptor PPAR γ in gastric cancer and inhibitory effects of PPAR gamma agonists. *British Journal of Cancer* 83: 1394-1400.
206. Yin F., Wakino S., Liu Z.W., Kim S., Hsueh W.A., Collins A.R., Van Herle A.J., and Law R.E. (2001). Troglitazone inhibits growth of MCF-7 breast carcinoma cells by targeting G1 cell cycle regulators. *Biochemical and Biophysical Research Communications* 286: 916-922.
207. Wang C.G., Fu M.F., D'Amico M., Albanese C., Zhou J.N., Brownlee M., Lisanti M.P., Chatterjee V.K.K., Lazar M.A., and Pestell R.G. (2001). Inhibition of cellular proliferation through IKB kinase- independent and peroxisome proliferator-activated receptor- γ dependent repression of cyclin D1. *Molecular and Cellular Biology* 21: 3057-3070.
208. Zander T., Kraus J.A., Grommes C., Schlegel U., Feinstein D., Klockgether T., Landreth G., Koenigsknecht J., and Heneka M.T. (2002). Induction of apoptosis in human and rat glioma by agonists of the nuclear receptor PPAR γ . *Journal of Neurochemistry* 81: 1052-1060.
209. Demetri G.D., Fletcher C.D.M., Mueller E., Sarraf P., Naujoks R., Campbell N., Spiegelman B.M., and Singer S. (1999). Induction of solid tumor differentiation by the peroxisome proliferator-activated receptor- γ ligand troglitazone in patients with

liposarcoma. *Proceedings of the National Academy of Sciences of the United States of America* 96: 3951-3956.

210. Hirase N., Yanase T., Mu Y.M., Muta K., Umemura T., Takayanagi R., and Nawata H. (1999). Thiazolidinedione induces apoptosis and monocytic differentiation in the promyelocytic leukemia cell line HL60. *Oncology* 57: 17-25.
211. Haydon R.C., Zhou L., Feng T., Breyer B., Cheng H.W., Jiang W., Ishikawa A., Peabody T., Montag A., Simon M.A. *et al.* (2002). Nuclear receptor agonists as potential differentiation therapy agents for human osteosarcoma. *Clinical Cancer Research* 8: 1288-1294.
212. Sarraf P., Mueller E., Jones D., King F.J., DeAngelo D.J., Partridge J.B., Holden S.A., Chen L.B., Singer S., Fletcher C. *et al.* (1998). Differentiation and reversal of malignant changes in colon cancer through PPAR γ . *Nature Medicine* 4: 1046-1052.
213. Han S.W., Greene M.E., Pitts J., Wada R.K., and Sidell N. (2001). Novel expression and function of peroxisome proliferator- activated receptor-PPAR γ (PPAR γ) in human neuroblastoma cells. *Clinical Cancer Research* 7: 98-104.
214. Kroemer G., Petit P., Zamzami N., Vayssiere J.L., and Mignotte B. (1995). The Biochemistry of Programmed Cell-Death. *Faseb Journal* 9: 1277-1287.
215. Marino G. and Lopez-Otin C. (2004). Autophagy: molecular mechanisms, physiological functions and relevance in human pathology. *Cellular and Molecular Life Sciences* 61: 1439-1454.
216. Hughes D. and Mehmet H. (2003). Introduction to Cell Proliferation and Cell Death. In *Cell Proliferation and Apoptosis*, (Hughes D, Mehmet H, eds.), pp. 1-11.
217. King J.B. (2000). Growth: A Balance of Cell Proliferation, Death and Differentiation. King JB, ed.), pp. 146-173.
218. Fridman J.S. and Lowe S.W. (2003). Control of apoptosis by p53. *Oncogene* 22: 9030-9040.
219. Elstner E., Muller C., Koshizuka K., Williamson E.A., Park D., Asou H., Shintaku P., Said J.W., Heber D., and Koeffler H.P. (1998). Ligands for peroxisome proliferator-activated receptor- γ and retinoic acid receptor inhibit growth and induce apoptosis of human breast cancer cells in vitro and in BNX mice. *Proceedings of the National Academy of Sciences of the United States of America* 95: 8806-8811.
220. Leung W.K., Bai A.H.C., Chan V.Y.W., Yu J., Chan M.W.Y., To K.F., Wu J.R., Chan K.K., Fu Y.G., Chan F.K.L. *et al.* (2004). Effect of peroxisome proliferator activated receptor- γ ligands on growth and gene expression profiles of gastric cancer cells. *Gut* 53: 331-338.
221. Reggiori F. and Klionsky D.J. (2002). Autophagy in the eukaryotic cell. *Eukaryotic Cell* 1: 11-21.
222. Yang Y.P., Liang Z.Q., Gu Z.L., and Qin Z.H. (2005). Molecular mechanism and regulation of autophagy. *Acta Pharmacologica Sinica* 26: 1421-1434.
223. Petiot A., Pattingre S., Arico S., Meley D., and Codogno P. (2002). Diversity of signaling controls of macroautophagy in mammalian cells. *Cell Structure and Function* 27: 431-441.

224. Arico S., Petiot A., Bauvy C., Dubbelhuis P.F., Meijer A.J., Codogno P., and Ogier-Denis E. (2001). The tumor suppressor PTEN positively regulates macroautophagy by inhibiting the phosphatidylinositol 3-kinase/protein kinase B pathway. *Journal of Biological Chemistry* 276: 35243-35246.
225. Downes C.P., Bennett D., McConnachie G., Leslie N.R., Pass I., MacPhee C., Patel L., and Gray A. (2001). Antagonism of PI 3-kinase-dependent signalling pathways by the tumour suppressor protein, PTEN. *Biochemical Society Transactions* 29: 846-851.
226. Leslie N.R., Gray A., Pass I., Orchiston E.A., and Downes C.P. (2000). Analysis of the cellular functions of PTEN using catalytic domain and C-terminal mutations: differential effects of C-terminal deletion on signalling pathways downstream of phosphoinositide 3-kinase. *Biochemical Journal* 346: 827-833.
227. Kubota T., Koshizuka K., Williamson E.A., Asou H., Said J.W., Holden S., Miyoshi I., and Koeffler H.P. (1998). Ligand for peroxisome proliferator-activated receptor- γ (troglitazone) has potent antitumor effect against human prostate cancer both *in vitro* and *in vivo*. *Cancer Res* 58: 3344-3352.
228. Rodway H.A., Hunt A.N., Kohler J.A., Postle A.D., and Lillycrop K.A. (2004). Lysophosphatidic acid attenuates the cytotoxic effects and degree of peroxisome proliferator-activated receptor- γ activation induced by 15-deoxy- $\Delta^{12,14}$ -prostaglandin J₂ in neuroblastoma cells. *Biochemical Journal* 382: 83-91.
229. Girnun G.D., Smith W.M., Drori S., Sarraf P., Mueller E., Eng C., Nambiar P., Rosenberg D.W., Bronson R.T., Edelman W. *et al.* (2002). APIC-dependent suppression of colon carcinogenesis by PPAR γ . *Proceedings of the National Academy of Sciences of the United States of America* 99: 13771-13776.
230. Lefebvre A.M., Chen I.H., Desreumaux P., Najib J., Fruchart J.C., Geboes K., Briggs M., Heyman R., and Auwerx J. (1998). Activation of the peroxisome proliferator-activated receptor- γ promotes the development of colon tumors in C57BL/6J-APC(Min)/+ mice. *Nature Medicine* 4: 1053-1057.
231. Pino M.V., Kelley M.F., and Jayyosi Z. (2004). Promotion of colon tumors in C57BL/6J-APC(min)/+ mice by thiazolidinedione PPAR γ agonists and a structurally unrelated PPAR gamma agonist. *Toxicologic Pathology* 32: 58-63.
232. Sarraf P., Mueller E., Smith W.M., Wright H.M., Kum J.B., Aaltonen L.A., de la Chapelle A., Spiegelman B.M., and Eng C. (1999). Loss-of-function mutations in PPAR γ associated with human colon cancer. *Molecular Cell* 3: 799-804.
233. Sabatino L., Casamassimi A., Peluso G., Barone M.V., Capaccio D., Migliore C., Bonelli P., Pedicini A., Febraro A., Ciccodicola A. *et al.* (2005). A novel peroxisome proliferator-activated receptor- γ isoform with dominant negative activity generated by alternative splicing. *Journal of Biological Chemistry* 280: 26517-26525.
234. Kim H.J., Woo I.S., Kang E.S., Eun S.Y., Kim H.J., Lee J.H., Chang K.C., Kim J.H., and Seo H.G. (2006). Identification of a truncated alternative splicing variant of human PPAR γ 1 that exhibits dominant negative activity. *Biochemical and Biophysical Research Communications*.
235. Yin Y.Z., Yuan H.Y., Wang C.G., Pattabiraman N., Rao M., Pestell R.G., and Glazer R.I. (2006). 3-Phosphoinositide-dependent protein kinase-1 activates the peroxisome proliferator-activated receptor- γ and promotes adipocyte differentiation. *Molecular Endocrinology* 20: 268-278.

236. Lacroix L., Lazar V., Michiels S., Ripoche H., Dessen P., Talbot M., Caillou B., Levillain J.P., Schlumberger M., and Bidart J.M. (2005). Follicular thyroid tumors with the PAX8-PPAR γ 1 rearrangement display characteristic genetic alterations. *American Journal of Pathology* 167: 223-231.
237. Lacroix L., Mian C., Barrier T., Talbot M., Caillou B., Schlumberger M., and Bidart J.M. (2004). PAX8 and peroxisome proliferator-activated receptor PPAR γ 1 gene expression status in benign and malignant thyroid tissues. *European Journal of Endocrinology* 151: 367-374.
238. Kroll T.G., Sarraf P., Pecciarini L., Chen C.J., Mueller E., Spiegelman B.M., and Fletcher J.A. (2000). PAX8-PPAR γ 1 fusion in oncogene human thyroid carcinoma. *Science* 289: 1357-1360.
239. Mueller E., Smith M., Sarraf P., Kroll T., Aiyer A., Kaufman D.S., Oh W., Demetri G., Figg W.D., Zhou X.P. *et al.* (2000). Effects of ligand activation of peroxisome proliferator-activated receptor- γ in human prostate cancer. *Proceedings of the National Academy of Sciences of the United States of America* 97: 10990-10995.
240. Debrock G., Vanhentenrijk V., Sciort R., Debiec-Rychter M., Oyen R., and Van Oosterom A. (2003). A phase II trial with rosiglitazone in liposarcoma patients. *British Journal of Cancer* 89: 1409-1412.
241. Smith M.R., Manola J., Kaufman D.S., George D., Oh W.K., Mueller E., Slovin S., Spiegelman B., Small E., and Kantoff P.W. (2004). Rosiglitazone versus placebo for men with prostate carcinoma and a rising serum prostate-specific antigen level after radical prostatectomy and/or radiation therapy. *Cancer* 101: 1569-1574.
242. Kulke M.H., Demetri G.D., Sharpless N.E., Ryan D.P., Shivdasani R., Clark J.S., Spiegelman B.M., Kim H., Mayer R.J., and Fuchs C.S. (2002). A phase II study of troglitazone, an activator of the PPAR γ receptor, in patients with chemotherapy-resistant metastatic colorectal cancer. *Cancer Journal* 8: 395-399.
243. Hisatake J., Ikezoe T., Carey M., Holden S., Tomoyasu S., and Koeffler H.P. (2000). Down-regulation of prostate-specific antigen expression by ligands for peroxisome proliferator-activated receptor-PPAR γ in human prostate cancer. *Cancer Res* 60: 5494-5498.
244. Bown N. (2001). Neuroblastoma tumour genetics: clinical and biological aspects. *Journal of Clinical Pathology* 54: 897-910.
245. Weinstein J.L., Katzenstein H.M., and Cohn S.L. (2003). Advances in the diagnosis and treatment of neuroblastoma. *Oncologist* 8: 278-292.
246. Castleberry R.P. (1997). Neuroblastoma. *European Journal of Cancer* 33: 1430-1437.
247. Haase G.M., Perez C., and Atkinson J.B. (1999). Current Aspects of Biology, Risk Assessment, and Treatment of Neuroblastoma. *Seminars in Surgical Oncology* 16: 91-104.
248. Maris J.M. and Matthay K.K. (1999). Molecular Biology of Neuroblastoma. *Journal of Clinical Oncology* 17: 2264-2279.
249. Schell M. and Bergeron C. (2003). Neuroblastoma. *Oprhanet Encyclopedia* 1-5.
250. Shimada H., Ambros I.M., Dehner L.P., Hata J., Joshi V.V., and Roald B. (1999). Terminology and Morphologic Criteria of Neuroblastic Tumors. *Cancer* 86: 349-363.

251. Lau L. (2002). Neuroblastoma: A single institution's experience with 128 children and an evaluation of clinical and biological prognostic factors. *Pediatric Hematology and Oncology 19*: 79-89.
252. Tonini G.P. and Pistoia V. (2006). Molecularly Guided Therapy of Neuroblastoma: A Review of Different Approaches. *Current Pharmaceutical Design 12*: 2303-2317.
253. Simpson J.K. and Gaze M.N. (1998). Current Management of Neuroblastoma. *The Oncologist 3*: 253-262.
254. Brodeur G.M., Pritchard J., Berthold F., Carlsen N.L.T., Castel V., Castleberry R.P., Debernardi B., Evans A.E., Favrot M., Hedborg F. *et al.* (1993). Revisions of the International Criteria for Neuroblastoma Diagnosis, Staging, and Response to Treatment. *Journal of Clinical Oncology 11*: 1466-1477.
255. Brodeur G.M., Seeger R.C., Barrett A., Berthold F., Castleberry R.P., Dangio G., Debernardi B., Evans A.E., Favrot M., Freeman A.I. *et al.* (1988). International Criteria for Diagnosis, Staging, and Response to Treatment in Patients with Neuroblastoma. *Journal of Clinical Oncology 6*: 1874-1881.
256. Castel V., Garcia-Miguel P., Canete A., Melero C., Navajas A., Ruiz-Jimenez J.I., Navarro S., and Badal M.D. (1999). Prospective evaluation of the International Neuroblastoma Staging System (INSS) and the International Neuroblastoma Response Criteria (INRC) in a multicentre setting. *European Journal of Cancer 35*: 606-611.
257. Nickerson H.J., Matthay K.K., Seeger R.C., Brodeur G.M., Shimada H., Perez C., Atkinson J.B., Selch M., Gerbing R.B., Stram D.O. *et al.* (2000). Favorable biology and outcome of stage IV-S neuroblastoma with supportive care or minimal therapy: A Children's Cancer Group study. *Journal of Clinical Oncology 18*: 477-486.
258. Cotterill S.J., Pearson A.D.J., Pritchard J., Foot A.B.M., Roald B., Kohler J.A., and Imeson J. (2000). Clinical prognostic factors in 1277 patients with neuroblastoma: results of The European Neuroblastoma Study Group 'Survey' 1982-1992. *European Journal of Cancer 36*: 901-908.
259. Saito T., Tsunematsu Y., Saeki M., Honna T., Masaki E., Kojima Y., and Miyauchi J. (1997). Trends of survival in neuroblastoma and independent risk factors for survival at a single institution. *Medical and Pediatric Oncology 29*: 197-205.
260. Ladenstein R., Urban C., Gadner H., Fink F.M., Zoubek A., Emminger W., Grienberger H., Schmitt K., Ambros P.F., Ambros I.M. *et al.* (1995). First Experience with Prognostic Factors in Unselected Neuroblastoma Patients - the Austrian Neuroblastoma-87 Study. *European Journal of Cancer 31A*: 637-641.
261. Monsaingeon M., Perel Y., Simonnet G., and Corcuff J.B. (2003). Comparative values of catecholamines and metabolites for the diagnosis of neuroblastoma. *European Journal of Pediatrics 162*: 397-402.
262. Simon T., Hero B., Hunneman D.H., and Berthold F. (2003). Tumour markers are poor predictors for relapse or progression in neuroblastoma. *European Journal of Cancer 39*: 1899-1903.
263. Sato Y., Sasaki H., Kobayashi Y., Haruki N., Toyama T., Kondo S., and Fujii Y. (2003). Expression of PPAR γ is correlated with the clinical course of neuroblastoma. *Journal of Pediatric Surgery 38*: 205-210.

264. Strenger V., Kerbl R., Dornbusch H., Ladenstein R., Ambros P.F., Ambros I.M., and Urban C. (2006). Diagnostic and Prognostic Impact of Urinary Catecholamines in Neuroblastoma Patients. *Pediatric Blood & Cancer* 1-7.
265. Massaron S., Seregini E., Luksch R., Casanova M., Botti C., Ferrari L., Martinetti A., Molteni S.N., Bellani F.F., and Bombardieri E. (1998). Neuron-specific enolase evaluation in patients with neuroblastoma. *Tumor Biology* 19: 261-268.
266. Zeltzer P.M., Marangos P.J., Evans A.E., and Schneider S.L. (1986). Serum Neuron-Specific Enolase in Children with Neuroblastoma - Relationship to Stage and Disease Course. *Cancer* 57: 1230-1234.
267. Hann H.W.L., Stahlhut M.W., and Evans A.E. (1986). Source of Increased Ferritin in Neuroblastoma - Studies with Concanavalin A-Sepharose Binding. *Journal of the National Cancer Institute* 76: 1031-1033.
268. Hann H.W.L., Levy H.M., and Evans A.E. (1980). Serum Ferritin As A Guide to Therapy in Neuroblastoma. *Cancer Res* 40: 1411-1413.
269. Nakagawara A. and Brodeur G.M. (1997). Role of neurotrophins and their receptors in human neuroblastomas: a primary culture study. *European Journal of Cancer* 33: 2050-2053.
270. Schramm A., Schulte J.H., Astrahantseff K., Apostolov O., van Limpt V., Sieverts H., Kuhfittig-Kulle S., Pfeiffer P., Versteeg R., and Eggert A. (2005). Biological effects of TrkA and TrkB receptor signaling in neuroblastoma. *Cancer Letters* 228: 143-153.
271. Matsushima H. and Bogenmann E. (1993). Expression of TrkA Cdna in Neuroblastomas Mediates Differentiation *in vitro* and *in vivo*. *Molecular and Cellular Biology* 13: 7447-7456.
272. Nakagawara A., Arimanakagawara M., Scavarda N.J., Azar C.G., Cantor A.B., and Brodeur G.M. (1993). Association Between High-Levels of Expression of the Trk Gene and Favorable Outcome in Human Neuroblastoma. *New England Journal of Medicine* 328: 847-854.
273. Gross N., Beck D., Beretta C., Jackson D., and Perruisseau G. (1995). Cd44 Expression and Modulation on Human Neuroblastoma Tumors and Cell-Lines. *European Journal of Cancer* 31A: 471-475.
274. Combaret V., Lasset C., Frappaz D., Bouvier R., Thiesse P., Rebillard A.C., Philip T., and Favrot M.C. (1995). Evaluation of CD44 Prognostic Value in Neuroblastoma - Comparison with the Other Prognostic Factors. *European Journal of Cancer* 31A: 545-549.
275. Terpe H.J., Christiansen H., Gonzalez M., Berthold F., and Lampert F. (1995). Differentiation and Prognosis of Neuroblastoma in Correlation to the Expression of Cd44S. *European Journal of Cancer* 31A: 549-552.
276. Norris M.D., Bordow S.B., Marshall G.M., Haber P.S., Cohn S.L., and Haber M. (1996). Expression of the gene for multidrug-resistance-associated protein and outcome in patients with neuroblastoma. *New England Journal of Medicine* 334: 231-238.

277. Streutker C.J., Thorner P., Fabricius N., Weitzman S., and Zielenska M. (2001). Telomerase activity as a prognostic factor in neuroblastomas. *Pediatric and Developmental Pathology* 4: 62-67.
278. Ohali A., Avigad S., Ash S., Goshen Y., Luria D., Feinmesser M., Zaizov R., and Yaniv I. (2006). Telomere Length Is a Prognostic Factor in Neuroblastoma. *Cancer* 107: 1391-1399.
279. Kohl N.E., Kanda N., Schreck R.R., Bruns G., Latt S.A., Gilbert F., and Alt F.W. (1983). Transposition and Amplification of Oncogene-Related Sequences in Human Neuroblastomas. *Cell* 35: 359-367.
280. Schwab M., Alitalo K., Klempnauer K.H., VARMUS H.E., BISHOP J.M., Gilbert F., Brodeur G., Goldstein M., and Trent J. (1983). Amplified DNA with Limited Homology to Myc Cellular Oncogene Is Shared by Human Neuroblastoma Cell-Lines and A Neuro-Blastoma Tumor. *Nature* 305: 245-248.
281. Shimizu N., Itoh N., Utiyama H., and Wahl G.M. (1998). Selective entrapment of extrachromosomally amplified DNA by nuclear budding and micronucleation during S phase. *Journal of Cell Biology* 140: 1307-1320.
282. Storlazzi C.T., Fioretos T., Surace C., Lonoce A., Mastroilli A., Strombeck B., D'Addabbo P., Iacovelli F., Minervini C., Aventin A. *et al.* (2006). MYC-containing double minutes in hematologic malignancies: evidence in favor of the episome model and exclusion of MYC as the target gene. *Human Molecular Genetics* 15: 933-942.
283. Brodeur G.M., Seeger R.C., Schwab M., Varmus H.E., and Bishop J.M. (1984). Amplification of N-Myc in Untreated Human Neuroblastomas Correlates with Advanced Disease Stage. *Science* 224: 1121-1124.
284. Berthold F., Sahin K., Hero B., Christiansen H., Gehring M., Harms D., Horz S., Lampert F., Schwab M., and Terpe J. (1997). The current contribution of molecular factors to risk estimation in neuroblastoma patients. *European Journal of Cancer* 33: 2092-2097.
285. Nesbit C.E., Tersak J.M., and Prochownik E.V. (1999). MYC oncogenes and human neoplastic disease. *Oncogene* 18: 3004-3016.
286. Parise I.Z.S., Haddad B.R., Cavalli L.R., Pianovski M.A.D., Maggio E.M., Parise G.A., Watanabe F.M., Ioshii S.O., Rone J.D., Caleffe L.G. *et al.* (2006). Neuroblastoma in Southern Brazil - An 11-year study. *Journal of Pediatric Hematology Oncology* 28: 82-87.
287. Melegh Z., Balint I., Toth E., Csernak E., and Nagy K. (2003). Detection of n-myc gene amplification in neuroblastoma by comparative, in situ, and real-time polymerase chain reaction. *Pediatric Pathology & Molecular Medicine* 22: 213-222.
288. Matthay K.K. (2000). MYCN expression in neuroblastoma: A mixed message? *Journal of Clinical Oncology* 18: 3591-3594.
289. Bordow S.B., Norris M.D., Haber P.S., Marshall G.M., and Haber M. (1998). Prognostic significance of MYCN oncogene expression in childhood neuroblastoma. *Journal of Clinical Oncology* 16: 3286-3294.
290. Chan H.S.L., Gallie B.L., DeBoer G., Haddad G., Ikegaki N., Dimitroulakos J., Yeger H., and Ling V. (1997). MYCN protein expression as a predictor of neuroblastoma prognosis. *Clinical Cancer Research* 3: 1699-1706.

291. Kaneko Y. and Knudson A.G. (2000). Mechanism and relevance of ploidy in neuroblastoma. *Genes Chromosomes & Cancer* 29: 89-95.
292. Bown N., Cotterill S., Lastowska M., O'Neill S., Pearson A.D.J., Plantaz D., Meddeb M., Danglot G., Brinkschmidt C., Christiansen H. *et al.* (1999). Gain of chromosome arm 17q and adverse outcome in patients with neuroblastoma. *New England Journal of Medicine* 340: 1954-1961.
293. Bown N., Lastowska M., Cotterill S., O'Neill S., Ellershaw C., Roberts P., Lewis L., and PEARSON A.D.J. (2001). 17q gain in neuroblastoma predicts adverse clinical outcome. *Medical and Pediatric Oncology* 36: 14-19.
294. Maris J.M., Weiss M.J., Guo C., Gerbing R.B., Stram D.O., White P.S., Hogarty M.D., Sulman E.P., Thompson P.M., Lukens J.N. *et al.* (2000). Loss of heterozygosity at 1p36 independently predicts for disease progression but not decreased overall survival probability in neuroblastoma patients: A Children's Cancer Group study. *Journal of Clinical Oncology* 18: 1888-1899.
295. Matthay K.K., Villablanca J.G., Seeger R.C., Stram D.O., Harris R.E., Ramsay N.K., Swift P., Shimada H., Black C.T., Brodeur G.M. *et al.* (1999). Treatment of high-risk neuroblastoma with intensive chemotherapy, radiotherapy, autologous bone marrow transplantation, and 13-cis-retinoic acid. *New England Journal of Medicine* 341: 1165-1173.
296. Barbui T., Finazzi G., and Falanga A. (1998). The impact of all-trans-retinoic acid on the coagulopathy of acute promyelocytic leukemia. *Blood* 91: 3093-3102.
297. Shimada H., Ambros I.M., Dehner L.P., Hata J., Joshi V.V., Roald B., Stram D.O., Gerbing R.B., Lukens J.N., Matthay K.K. *et al.* (1999). The International Neuroblastoma Pathology classification (the Shimada system). *Cancer* 86: 364-372.
298. Gaetano C., Matsumoto K., and Thiele C.J. (1991). Retinoic Acid Negatively Regulates P34Cdc2 Expression During Human Neuroblastoma-Differentiation. *Cell Growth & Differentiation* 2: 487-493.
299. Tumilowi J.J., Nichols W.W., Cholon J.J., and Greene A.E. (1970). Definition of A Continuous Human Cell Line Derived from Neuroblastoma. *Cancer Res* 30: 2110-&.
300. Wood J.N., Bevan S.J., Coote P.R., Dunn P.M., Harmar A., Hogan P., Latchman D.S., Morrison C., Rougon G., Theveniau M. *et al.* (1990). Novel Cell-Lines Display Properties of Nociceptive Sensory Neurons. *Proceedings of the Royal Society of London Series B-Biological Sciences* 241: 187-194.
301. Clay C.E., Namen A.M., Atsumi G., Willingham M.C., High K.P., Kute T.E., Trimboli A.J., Fonteh A.N., Dawson P.A., and Chilton F.H. (1999). Influence of J series prostaglandins on apoptosis and tumorigenesis of breast cancer cells. *Carcinogenesis* 20: 1905-1911.
302. Clay C.E., Atsumi G., High K.P., and Chilton F.H. (2001). Early de novo gene expression is required for 15-deoxy- $\Delta^{12,14}$ -prostaglandin J₂-induced apoptosis in breast cancer cells. *Journal of Biological Chemistry* 276: 47131-47135.
303. Chen Y.X., Zhong X.Y., Qin Y.F., Bing W., and He L.Z. (2003). 15-deoxy- $\Delta^{12,14}$ -prostaglandin J₂ inhibits cell growth and induces apoptosis of MCG- 803 human gastric cancer cell line. *World Journal of Gastroenterology* 9: 2149-2153.

304. Begum N.M., Nakashiro K.I., Kawamata H., Uchida D., Shintani S., Ikawa Y., Sato M., and Hamakawa H. (2002). Expression of peroxisome proliferator-activated receptor γ and the growth inhibitory effect of its synthetic ligands in human salivary gland cancer cell lines. *International Journal of Oncology* 20: 599-605.
305. Emmans V.C., Rodway H.A., Hunt A., and Lillycrop K.A. (2004). Regulation of cellular processes by PPAR γ ligands in neuroblastoma cells is modulated by the level of retinoblastoma protein expression. *Biochemical Society Transactions* 32: 840-842.
306. Piva R., Gianferretti P., Ciucci A., Taulli R., Belardo G., and Santoro M.G. (2005). 15-deoxy- $\Delta^{12,14}$ -prostaglandin J₂ induces apoptosis in human malignant B cells: an effect associated with inhibition of NF-kappa B activity and down-regulation of antiapoptotic proteins. *Blood* 105: 1750-1758.
307. Li L.Y., Tao J.C., Davaille J., Feral C., Mallat A., Rieusset J., Vidal H., and Lotersztajn S. (2001). 15-deoxy- $\Delta^{12,14}$ -prostaglandin J₂ induces apoptosis of human hepatic myofibroblasts - A pathway involving oxidative stress independently of peroxisome-proliferator-activated receptors. *Journal of Biological Chemistry* 276: 38152-38158.
308. Kondo M., Oya-Ito T., Kumagai T., Osawa T., and Uchida K. (2001). Cyclopentenone prostaglandins as potential inducers of intracellular oxidative stress. *Journal of Biological Chemistry* 276: 12076-12083.
309. Straus D.S., Pascual G., Li M., Welch J.S., Ricote M., Hsiang C.H., Sengchanthalangsy L.L., Ghosh G., and Glass C.K. (2000). 15-deoxy- $\Delta^{12,14}$ -prostaglandin J₂ inhibits multiple steps in the NF-kappa B signaling pathway. *Proceedings of the National Academy of Sciences of the United States of America* 97: 4844-4849.
310. Castrillo A., az-Guerra M.J.M., Hortelano S., Martin-Sanz P., and Bosca L. (2000). Inhibition of I kappa B kinase and I kappa B phosphorylation by 15-deoxy- $\Delta^{12,14}$ -prostaglandin J₂ in activated murine macrophages. *Molecular and Cellular Biology* 20: 1692-1698.
311. Rossi A., Kapahi P., Natoli G., Takahashi T., Chen Y., Karin M., and Santoro M.G. (2000). Anti-inflammatory cyclopentenone prostaglandins are direct inhibitors of I kappa B kinase. *Nature* 403: 103-108.
312. Kim E.J., Park K.S., Chung S.Y., Sheen Y.Y., Moon D.C., Song Y.S., Kim K.S., Song S., Yun Y.P., Lee M.K. et al. (2003). Peroxisome proliferator-activated receptor- γ activator 15-deoxy- $\Delta^{12,14}$ -prostaglandin J₂ inhibits neuroblastoma cell growth through induction of apoptosis: Association with extracellular signal-regulated kinase signal pathway. *Journal of Pharmacology and Experimental Therapeutics* 307: 505-517.
313. Chinery R., Coffey R.J., Graves-Deal R., Kirkland S.C., Sanchez S.C., Zackert W.E., Oates J.A., and Morrow J.D. (1999). Prostaglandin J₂ and 15-deoxy- $\Delta^{12,14}$ -prostaglandin J₂ induce proliferation of cyclooxygenase-depleted colorectal cancer cells. *Cancer Res* 59: 2739-2746.
314. Feilchenfeldt J., Brundler M.A., Soravia C., Totsch M., and Meier C.A. (2004). Peroxisome proliferator-activated receptors (PPARs) and associated transcription factors in colon cancer: reduced expression of PPAR γ -coactivator 1 (PGC-1). *Cancer Letters* 203: 25-33.

315. Jiang W.G., Douglas-Jones A., and Mansel R.E. (2003). Expression of peroxisome-proliferator activated receptor- γ (PPAR γ) and the PPAR γ co-activator, PGC-1, in human breast cancer correlates with clinical outcomes. *International Journal of Cancer* 106: 752-757.
316. Laurora S., Pizzimenti S., Briatore F., Fraioli A., Maggio M., Reffo P., Ferretti C., Dianzani M.U., and Barrera G. (2003). Peroxisome proliferator-activated receptor ligands affect growth-related gene expression in human leukemic cells. *Journal of Pharmacology and Experimental Therapeutics* 305: 932-942.
317. Patel L., Pass I., Coxon P., Downes C.P., Smith S.A., and Macphee C.H. (2001). Tumor suppressor and anti-inflammatory actions of PPAR γ agonists are mediated via upregulation of PTEN. *Current Biology* 11: 764-768.
318. Fajas L., Egler V., Reiter R., Miard S., Lefebvre A.M., and Auwerx J. (2003). PPAR γ controls cell proliferation and apoptosis in an RB- dependent manner. *Oncogene* 22: 4186-4193.
319. Fajas L., Egler V., Reiter R., Hansen J., Kristiansen K., Debril M.B., Miard S., and Auwerx J. (2002). The retinoblastoma-histone deacetylase 3 complex inhibits PPAR γ and adipocyte differentiation. *Developmental Cell* 3: 903-910.
320. DiCiommo D., Gallie B.L., and Bremner R. (2000). Retinoblastoma: the disease, gene and protein provide critical leads to understand cancer. *Seminars in Cancer Biology* 10: 255-269.
321. Zhu L.A. (2005). Tumour suppressor retinoblastoma protein Rb: A transcriptional regulator. *European Journal of Cancer* 41: 2415-2427.
322. Friend S.H., Horowitz J.M., Gerber M.R., Wang X.F., Bogenmann E., Li F.P., and Weinberg R.A. (1987). Deletions of A DNA-Sequence in Retinoblastomas and Mesenchymal Tumors - Organization of the Sequence and Its Encoded Protein. *Proceedings of the National Academy of Sciences of the United States of America* 84: 9059-9063.
323. Harbour J.W. and Dean D.C. (2000). Rb function in cell-cycle regulation and apoptosis. *Nature Cell Biology* 2: E65-E67.
324. Lundberg A.S. and Weinberg R.A. (1999). Control of the cell cycle and apoptosis (Reprinted from *Eur J Cancer*, vol 35, pg 531-539, 1999). *European Journal of Cancer* 35: 1886-1894.
325. PlanasSilva M.D. and Weinberg R.A. (1997). The restriction point and control of cell proliferation. *Current Opinion in Cell Biology* 9: 768-772.
326. Weinberg R.A. (1995). The Retinoblastoma Protein and Cell-Cycle Control. *Cell* 81: 323-330.
327. Classon M., Salama S., Gorka C., Mulloy R., Braun P., and Harlow E. (2000). Combinatorial roles for pRB, p107, and p130 in E2F-mediated cell cycle control. *Proceedings of the National Academy of Sciences of the United States of America* 97: 10820-10825.
328. Wikenheiser-Brokamp K.A. (2006). Retinoblastoma family proteins: insights gained through genetic manipulation of mice. *Cellular and Molecular Life Sciences* 63: 767-780.

329. Cobrinik D. (2005). Pocket proteins and cell cycle control. *Oncogene* 24: 2796-2809.
330. Classon M. and Dyson N. (2001). p107 and p130: Versatile proteins with interesting pockets. *Experimental Cell Research* 264: 135-147.
331. Paggi M.G. and Giordano A. (2001). Who is the boss in the Retinoblastoma family? The point of view of Rb2/p130, the little brother. *Cancer Res* 61: 4651-4654.
332. Tonini T., Hillson C., and Claudio P.P. (2002). Interview with the retinoblastoma family members: Do they help each other? *Journal of Cellular Physiology* 192: 138-150.
333. Kaelin W.G. (1999). Functions of the retinoblastoma protein. *Bioessays* 21: 950-958.
334. Lee J.O., Russo A.A., and Pavletich N.P. (1998). Structure of the retinoblastoma tumour-suppressor pocket domain bound to a peptide from HPV E7. *Nature* 391: 859-865.
335. Lee C. and Cho Y. (2002). Interactions of SV40 large T antigen and other viral proteins with retinoblastoma tumour suppressor. *Reviews in Medical Virology* 12: 81-92.
336. Frolov M.V. and Dyson N.J. (2004). Molecular mechanisms of E2F-dependent activation and pRB-mediated repression. *Journal of Cell Science* 117: 2173-2181.
337. Morrison A.J., Sardet C., and Herrera R.E. (2002). Retinoblastoma protein transcriptional repression through histone deacetylation of a single nucleosome. *Molecular and Cellular Biology* 22: 856-865.
338. Brehm A., Miska E.A., McCance D.J., Reid J.L., Bannister A.J., and Kouzarides T. (1998). Retinoblastoma protein recruits histone deacetylase to repress transcription. *Nature* 391: 597-601.
339. Magnaghi-Jaulin L., Groisman R., Naguibneva I., Robin P., Lorain S., Le Villain J.P., Troalen F., Trouche D., and Harel-Bellan A. (1998). Retinoblastoma protein represses transcription by recruiting a histone deacetylase. *Nature* 391: 601-605.
340. Omura-Minamisawa M., Diccianni M.B., Chang R.C., Batova A., Bridgeman L.J., Schiff J., Cohn S.L., London W.B., and Yu A.L. (2001). p16/p14(ARF) cell cycle regulatory pathways in primary neuroblastoma: p16 expression is associated with advanced stage disease. *Clinical Cancer Research* 7: 3481-3490.
341. Molenaar J.J., van Sluis P., Boon K., Versteeg R., and Caron H.N. (2003). Rearrangements and increased expression of cyclin DI (CCND1) in neuroblastoma. *Genes Chromosomes & Cancer* 36: 242-249.
342. Drummond D.C., Noble C.O., Kirpotin D.B., Guo Z.X., Scott G.K., and Benz C.C. (2005). Clinical development of histone deacetylase inhibitors as anticancer agents. *Annual Review of Pharmacology and Toxicology* 45: 495-528.
343. Liu T., Kuljaca S., Tee A., and Marshall G.M. (2006). Histone deacetylase inhibitors: Multifunctional anticancer agents. *Cancer Treatment Reviews* 1-9.
344. Fang J.Y. (2005). Histone deacetylase inhibitors, anticancerous mechanism and therapy for gastrointestinal cancers. *Journal of Gastroenterology and Hepatology* 20: 988-994.

345. Mei S.P., Ho A.D., and Mahlknecht U. (2004). Role of histone deacetylase inhibitors in the treatment of cancer (Review). *International Journal of Oncology* 25: 1509-1519.
346. De Ruijter A.J.M., Van Gennip A.H., Caron H.N., Kemp S., and Van Kuilenburg A.B.P. (2003). Histone deacetylases (HDACs): characterization of the classical HDAC family. *Biochemical Journal* 370: 737-749.
347. Finnin M.S., Donigian J.R., Cohen A., Richon V.M., Rifkind R.A., Marks P.A., Breslow R., and Pavletich N.P. (1999). Structures of a histone deacetylase homologue bound to the TSA and SAHA inhibitors. *Nature* 401: 188-193.
348. O'Connor O.A., Heaney M.L., Schwartz L., Richardson S., Willim R., Gregor-Cortelli B., Curly T., Moskowitz C., Portlock C., Horwitz S. et al. (2006). Clinical experience with intravenous and oral formulations of the novel histone deacetylase inhibitor suberoylanilide hydroxamic acid in patients with advanced hematologic malignancies. *Journal of Clinical Oncology* 24: 166-173.
349. Kelly W.K., O'Connor O.A., Krug L.M., Chiao J.H., Heaney M., Curley T., Gregor-Cortelli B., Tong W., Secrist J.P., Schwartz L. et al. (2005). Phase I study of an oral histone deacetylase inhibitor, suberoylanilide hydroxamic acid, in patients with advanced cancer. *Journal of Clinical Oncology* 23: 3923-3931.
350. Kelly W.K., Richon V.M., O'Connor O., Curley T., Gregor-Cortelli B., Tong W., Klang M., Schwartz L., Richardson S., Rosa E. et al. (2003). Phase I clinical trial of histone deacetylase inhibitor: Suberoylanilide hydroxamic acid administered intravenously. *Clinical Cancer Research* 9: 3578-3588.
351. Monneret C. (2005). Histone deacetylase inhibitors. *European Journal of Medicinal Chemistry* 40: 1-13.
352. Atadja P., Gao L., Kwon P., Trogani N., Walker H., Hsu M., Yeleswarapu L., Chandramouli N., Perez L., Versace R. et al. (2004). Selective growth inhibition of tumor cells by a novel histone deacetylase inhibitor, NVP-LAQ824. *Cancer Res* 64: 689-695.
353. Chang T.H. and Szabo E. (2002). Enhanced growth inhibition by combination differentiation therapy with ligands of peroxisome proliferator-activated PPAR γ and inhibitors of histone deacetylase in adenocarcinoma of the lung. *Clinical Cancer Research* 8: 1206-1212.
354. Coffey D.C., Kutko M.C., Glick R.D., Swendeman S.L., Butler L., Rifkind R., Marks P.A., Richon V.M., and LaQuaglia M.P. (2000). Histone deacetylase inhibitors and retinoic acids inhibit growth of human neuroblastoma *in vitro*. *Medical and Pediatric Oncology* 35: 577-581.
355. Subramanian C., Opipari A.W., Bian X., Castle V.P., and Kwok R.P.S. (2005). Ku70 acetylation mediates neuroblastoma cell death induced by histone deacetylase inhibitors. *Proceedings of the National Academy of Sciences of the United States of America* 102: 4842-4847.
356. Jaboin J., Wild J., Hamidi H., Khanna C., Kim C.J., Robey R., Bates S.E., and Thiele C.J. (2002). MS-27-275, an inhibitor of histone deacetylase, has marked *in vitro* and *in vivo* antitumor activity against pediatric solid tumors. *Cancer Res* 62: 6108-6115.
357. Ouwehand K., De Ruijter A.J.M., van Bree C., Caron H.N., and Van Kuilenburg A.B.P. (2005). Histone deacetylase inhibitor BL1521 induces a G1-phase arrest in

- neuroblastoma cells through altered expression of cell cycle proteins. *Febs Letters* 579: 1523-1528.
358. De Ruijter A.J.M., Kemp S., Kramer G., Meinsma R.J., Kaufmann J.O., Caron H.N., and Van Kuilenburg A.B.P. (2004). The novel histone deacetylase inhibitor BL1521 inhibits proliferation and induces apoptosis in neuroblastoma cells. *Biochemical Pharmacology* 68: 1279-1288.
359. De Ruijter A.J.M., Meinsma R.J., Bosma P., Kemp S., Caron H.N., and Van Kuilenburg A.B.P. (2005). Gene expression profiling in response to the histone deacetylase inhibitor BL1521 in neuroblastoma. *Experimental Cell Research* 309: 451-467.
360. Goldsmith K.C. and Hogarty M.D. (2005). Targeting programmed cell death pathways with experimental therapeutics: opportunities in high-risk neuroblastoma. *Cancer Letters* 228: 133-141.
361. Tang X.X., Robinson M.E., Riceberg J.S., Kim D.Y., Kung B., Titus T.B., Hayashi S., Flake A.W., Carpentieri D., and Ikegaki N. (2004). Favorable neuroblastoma genes and molecular therapeutics of neuroblastoma. *Clinical Cancer Research* 10: 5837-5844.
362. Coffey D.C., Kutko M.C., Glick R.D., Butler L.M., Heller G., Rifkind R.A., Marks P.A., Richon V.M., and La Quaglia M.P. (2001). The histone deacetylase inhibitor, CBHA, inhibits growth of human neuroblastoma xenografts *in vivo*, alone and synergistically with all-trans retinoic acid. *Cancer Res* 61: 3591-3594.
363. Yoshida M., Kijima M., Akita M., and Beppu T. (1990). Potent and Specific-Inhibition of Mammalian Histone Deacetylase both *in vivo* and *in vitro* by Trichostatin-A. *Journal of Biological Chemistry* 265: 17174-17179.
364. Rashid S.F., Moore J.S., Walker E., Driver P.M., Engel J., Edwards C.E., Brown G., Uskokovic M.R., and Campbell M.J. (2001). Synergistic growth inhibition of prostate cancer cells by 1 alpha,25 Dihydroxyvitamin D-3 and its 19-nor-hexafluoride analogs in combination with either sodium butyrate or trichostatin A. *Oncogene* 20: 1860-1872.
365. Padilla J., Kaur K., Cao H.J., Smith T.J., and Phipps R.P. (2000). Peroxisome proliferator activator receptor-gamma agonists and 15-deoxy- $\Delta^{12,14}$ -prostaglandin J₂ induce apoptosis in normal and malignant B-lineage cells. *Journal of Immunology* 165: 6941-6948.
366. Bogazzi F., Ultimieri F., Raggi F., Russo D., Vanacore R., Guida C., Viacava P., Cecchetti D., Acerbi G., Brogioni S. *et al.* (2004). PPAR γ inhibits GH synthesis and secretion and increases apoptosis of pituitary GH-secreting adenomas. *European Journal of Endocrinology* 150: 863-875.
367. Zhang W., Zhang H, and Xing L. (2006). Influence of ciglitazone on A549 cells growth *in vitro* and *in vivo* and mechanism. *Journal of Huazhong University of Science and Technology, Medical Sciences* 26: 36-39.
368. Bottoni P., Giardina B., Martorana G.E., Zuppi C., De Sole P., Rossi C., and Scatena R. (2005). A two-dimensional electrophoresis preliminary approach to human hepatocarcinoma differentiation induced by PPAR-agonists. *Journal of Cellular and Molecular Medicine* 9: 462-467.

369. Hoehner J.C. and Prabhakaran K. (2003). Induced differentiation affords neuroblastoma cells protection from hypoxic injury. *Journal of Pediatric Surgery* 38: 1069-1074.
370. Lombet A., Zujovic V., Kandouz M., Billardon C., Carvajal-Gonzalez S., Gompel A., and Rostene W. (2001). Resistance to induced apoptosis in the human neuroblastoma cell line SK-N-SH in relation to neuronal differentiation - Role of Bcl-2 protein family. *European Journal of Biochemistry* 268: 1352-1362.
371. Pahlman S., Hoehner J.C., Nanberg E., Hedborg F., Fagerstrom S., Gestblom C., Johansson I., Larsson U., Lavenius E., Ortoft E. et al. (1995). Differentiation and Survival Influences of Growth-Factors in Human Neuroblastoma. *European Journal of Cancer* 31A: 453-458.
372. Monard D., Rentsch M., Schuerchthgeb Y., and Lindsay R.M. (1977). Morphological-Differentiation of Neuroblastoma-Cells in Medium Supplemented with Delipidated Serum - (Neurobiology Glial-Neuronal Interactions Fatty Acids Cellular Morphology). *Proceedings of the National Academy of Sciences of the United States of America* 74: 3893-3897.
373. Shim K.S., Rosner M., Freilinger A., Lubec G., and Hengstschlager M. (2006). Bach2 is involved in neuronal differentiation of N1E-115 neuroblastoma cells. *Experimental Cell Research* 1-15.
374. Placha W., Gil D., mbinska-Kiec A., and Laidler P. (2003). The effect of PPAR γ ligands on the proliferation and apoptosis of human melanoma cells. *Melanoma Research* 13: 447-456.
375. Gain P., Thuret G., Chiquet C., Dumollard J.M., Mosnier J.F., Burillon C., Delbosc B., Herve P., and Campos L. (2001). Value of two mortality assessment techniques for organ cultured corneal endothelium: trypan blue versus TUNEL technique. *British Journal of Ophthalmology* 86: 306-310.
376. Mower D.A., Peckham D.W., Illera V.A., Fishbaugh J.K., Stunz L.L., and Ashman R.F. (1994). Decreased Membrane Phospholipid Packing and Decreased Cell-Size Precede Dna Cleavage in Mature Mouse B-Cell Apoptosis. *Journal of Immunology* 152: 4832-4842.
377. O'Brien M.C., Healy S.F., Raney S.R., Hurst J.M., Avner B., Hanly A., Mies C., Freeman J.W., Snow C., Koester S.K. et al. (1997). Discrimination of late apoptotic/necrotic cells (type III) by flow cytometry in solid tumors. *Cytometry* 28: 81-89.
378. Familian A., Zwart B., Huisman H.G., Rensink I., Roem D., Hordijk P.L., Aarden L.A., and Hack C.E. (2001). Chromatin-independent binding of serum amyloid P component to apoptotic cells. *Journal of Immunology* 167: 647-654.
379. Lin J., Yang J., Lee J., Hsieh W., and Chung J. (2006). Berberine induces cell cycle arrest and apoptosis in human gastric carcinoma SNU-5 cell line. *World Journal of Gastroenterology* 12: 21-28.
380. Kumi-Diaka J., Hassanhi M., Brown J., Merchant K., Garcia C., and Jimenez W. (2006). CytoregR inhibits growth and proliferation of human adenocarcinoma cells via induction of apoptosis. *Journal of Carcinogenesis* 5: 1-8.
381. Allred C.D. and Kilgore M.W. (2005). Selective activation of PPAR γ in breast, colon, and lung cancer cell lines. *Molecular and Cellular Endocrinology* 235: 21-29.

382. Palakurthi S.S., Aktas H., Grubissich L.M., Mortensen R.M., and Halperin J.A. (2001). Anticancer effects of thiazolidinediones are independent of peroxisome proliferator-activated receptor- γ and mediated by inhibition of translation initiation. *Cancer Res* 61: 6213-6218.
383. Shiau C.W., Yang C.C., Kulp S.K., Chen K.F., Chen C.S., Huang J.W., and Chen C.S. (2005). Thiazolidinediones mediate apoptosis in prostate cancer cells in part through inhibition of Bcl-xL/Bcl-2 functions independently of PPAR γ . *Cancer Res* 65: 1561-1569.
384. Lennon A.M., Ramage M., Dessouroux A., and Pierre M. (2002). MAP kinase cascades are activated in astrocytes and preadipocytes by 15-deoxy- $\Delta^{12,14}$ -prostaglandin J₂ and the thiazolidinedione ciglitazone through peroxisome proliferator activator receptor gamma-independent mechanisms involving reactive oxygenated species. *Journal of Biological Chemistry* 277: 29681-29685.
385. Perez-Ortiz J.M., Tranque P., Vaquero C.F., Domingo B., Molina F., Calvo S., Jordan J., Cena V., and Llopis J. (2004). Glitazones differentially regulate primary astrocyte and glioma cell survival - Involvement of reactive oxygen species and peroxisome proliferator-activated receptor- γ . *Journal of Biological Chemistry* 279: 8976-8985.
386. Mayo L.D. and Donner D.B. (2002). The PTEN, Mdm2, p53 tumor suppressor-oncoprotein network. *Trends in Biochemical Sciences* 27: 462-467.
387. Mayo L.D., Dixon J.E., Durden D.L., Tonks N.K., and Donner D.B. (2002). PTEN protects p53 from Mdm2 and sensitizes cancer cells to chemotherapy. *Journal of Biological Chemistry* 277: 5484-5489.
388. Stambolic V., MacPherson D., Sas D., Lin Y., Snow B., Jang Y., Benchimol S., and Mak T.W. (2001). Regulation of PTEN transcription by p53. *Molecular Cell* 8: 317-325.
389. Sivaraman V.S., Wang H.Y., Nuovo G.J., and Malbon C.C. (1997). Hyperexpression of mitogen-activated protein kinase in human breast cancer. *Journal of Clinical Investigation* 99: 1478-1483.
390. Zhang X.D., Gillespie S.K., Borrow J.M., and Hersey P. (2004). The histone deacetylase inhibitor suberic bishydroxamate regulates the expression of multiple apoptotic mediators and induces mitochondria-dependent apoptosis of melanoma cells. *Molecular Cancer Therapeutics* 3: 425-435.
391. Mirakian R., Nye K., Palazzo F.F., Goode A.W., and Hammond L.J. (2002). Methods for detecting apoptosis in thyroid diseases. *Journal of Immunological Methods* 265: 161-175.
392. Rodriguez-Hernandez A., Brea-Calvo G., Fernandez-Ayala D.J.M., Cordero M., Navas P., and Sanchez-Alcazar J.A. (2006). Nuclear caspase-3 and capase-7 activation, and poly(ADP-ribose) polymerase cleavage are early events in camptothecin-induced apoptosis. *Apoptosis* 11: 131-139.
393. Duriez P.J. and Shah G.M. (1997). Cleavage of poly(ADP-ribose) polymerase: a sensitive parameter to study cell death. *Biochemistry and Cell Biology-Biochimie et Biologie Cellulaire* 75: 337-349.
394. Rumi M.A.K., Ishihara S., Kadowaki Y., Ortega-Cava C.F., Kazumori H., Kawashima K., Yoshino N., Yuki T., Ishimura N., and Kinoshita Y. (2004).

Peroxisome proliferator-activated receptor- γ -dependent and -independent growth inhibition of gastrointestinal tumour cells. *Genes to Cells* 9: 1113-1123.

395. Chen F., Wang M.C., O'Connor J.P., He M., Tripathi T., and Harrison L.E. (2003). Phosphorylation of PPAR γ via active ERK1/2 leads to its physical association with p65 and inhibition of NF-kappa beta. *Journal of Cellular Biochemistry* 90: 732-744.
396. Valentiner U., Carlsson M., Erttmann R., Hildebrandt H., and Schumacher U. (2005). Ligands for the peroxisome proliferator-activated receptor- γ have inhibitory effects on growth of human neuroblastoma cells *in vitro*. *Toxicology* 213: 157-168.
397. Fehlberg S., Trautwein S., Goke A., and Goke R. (2002). Bisphenol A diglycidyl ether induces apoptosis in tumour cells independently of peroxisome proliferator-activated receptor- γ , in caspase-dependent and -independent manners. *Biochemical Journal* 362: 573-578.
398. Seargent J.M., Yates E.A., and Gill J.H. (2004). GW9662, a potent antagonist of PPAR gamma, inhibits growth of breast tumour cells and promotes the anticancer effects of the PPAR γ agonist rosiglitazone, independently of PPAR γ activation. *British Journal of Pharmacology* 143: 933-937.
399. Safer J.D., Cohen R.N., Hollenberg A.N., and Wondisford F.E. (1998). Defective release of corepressor by hinge mutants of the thyroid hormone receptor found in patients with resistance to thyroid hormone. *Journal of Biological Chemistry* 273: 30175-30182.
400. Clifton-Bligh R.J., de Zegher F., Wagner R.L., Collingwood T.N., Francois I., Van Helvoirt M., Fletterick R.J., and Chatterjee V.K.K. (1998). A novel TR beta mutation (R383H) in resistance to thyroid hormone syndrome predominantly impairs corepressor release and negative transcriptional regulation. *Molecular Endocrinology* 12: 609-621.
401. Yoh S.M., Chatterjee V.K.K., and Privalsky M.L. (1997). Thyroid hormone resistance syndrome manifests as an aberrant interaction between mutant T-3 receptors and transcriptional corepressors. *Molecular Endocrinology* 11: 470-480.
402. Collingwood T.N., Rajanayagam O., Adams M., Wagner R., Cavailles V., Kalkhoven E., Matthews C., Nystrom E., Stenlof K., Lindstedt G. *et al.* (1997). A natural transactivation mutation in the thyroid hormone beta receptor: Impaired interaction with putative transcriptional mediators. *Proceedings of the National Academy of Sciences of the United States of America* 94: 248-253.
403. Semple R.K., Meirhaeghe A., Vidal-Puig A.J., Schwabe J.W.R., Wiggins D., Gibbons G.F., Gurnell M., Chatterjee V.K.K., and O'Rahilly S. (2005). A dominant negative human peroxisome proliferator-activated receptor PPAR α is a constitutive transcriptional corepressor and inhibits signaling through all PPAR isoforms. *Endocrinology* 146: 1871-1882.
404. Teresi R.E., Shaiu C.W., Chen C.S., Chatterjee V.K., Waite K.A., and Eng C. (2006). Increased PTEN expression due to transcriptional activation of PPAR γ by Lovastatin and Rosiglitazone. *International Journal of Cancer* 118: 2390-2398.
405. Crosby M.B., Svenson J.L., Zhang J., Nicol C.J., Gonzalez F.J., and Gilkeson G.S. (2005). Peroxisome proliferation-activated receptor PPAR γ is not necessary for synthetic PPAR gamma agonist inhibition of inducible nitric-oxide synthase and nitric oxide. *Journal of Pharmacology and Experimental Therapeutics* 312: 69-76.

406. Lim S., Jin C.J., Kim M., Chung S.S., Park H.S., Lee I.K., Lee C.T., Cho Y.M., Lee H.K., and Park K.S. (2006). PPAR γ gene transfer sustains apoptosis, inhibits vascular smooth muscle cell proliferation, and reduces neointima formation after balloon injury in rats. *Arteriosclerosis Thrombosis and Vascular Biology* 26: 808-813.
407. Hawcroft G., Gardner S.H., and Hull M.A. (2003). Activation of peroxisome proliferator-activated receptor- γ does not explain the antiproliferative activity of the nonsteroidal anti-inflammatory drug indomethacin on human colorectal cancer cells. *Journal of Pharmacology and Experimental Therapeutics* 305: 632-637.
408. Bren-Mattison Y., Van Putten V., Chan D., Winn R., Geraci M.W., and Nemenoff R.A. (2005). Peroxisome proliferator-activated receptor- γ (PPAR γ) inhibits tumorigenesis by reversing the undifferentiated phenotype of metastatic non-small-cell lung cancer cells (NSCLC). *Oncogene* 24: 1412-1422.
409. Wick M., Hurteau G., Dessev C., Chan D., Geraci M.W., Winn R.A., Heasley L.E., and Nemenoff R.A. (2002). Peroxisome proliferator-activated receptor- γ is a target of nonsteroidal anti-inflammatory drugs mediating cyclooxygenase-independent inhibition of lung cancer cell growth. *Molecular Pharmacology* 62: 1207-1214.
410. Itami A., Watanabe G., Shimada Y., Hashimoto Y., Kawamura J., Kato M., Hosotani R., and Imamura M. (2001). Ligands for peroxisome proliferator-activated receptor gamma inhibit growth of pancreatic cancers both in vitro and in vivo. *International Journal of Cancer* 94: 370-376.
411. Lu M.L., Kwan T., Yu C.J., Chen F., Freedman B., Schafer J.M., Lee E.J., Jameson J.L., Jordan V.C., and Cryns V.L. (2005). Peroxisome proliferator-activated receptor- γ agonists promote TRAIL-induced apoptosis by reducing survivin levels via cyclin D3 repression and cell cycle arrest. *Journal of Biological Chemistry* 280: 6742-6751.
412. Shimizu K., Shiratori K., Kobayashi M., and Kawamata H. (2004). Troglitazone inhibits the progression of chronic pancreatitis and the profibrogenic activity of pancreatic stellate cells via a PPAR γ -independent mechanism. *Pancreas* 29: 67-74.
413. Tzamelis I., Fang H., Ollero M., Shi H., Hamm J.K., Kievit P., Hollenberg A.N., and Flier J.S. (2004). Regulated production of a peroxisome proliferator-activated receptor- γ ligand during an early phase of adipocyte differentiation in 3T3-L1 adipocytes. *Journal of Biological Chemistry* 279: 36093-36102.
414. Yang F., Zhang Y., Cao Y.L., Wang S.H., and Liu L. (2005). Establishment and utilization of a tetracycline-controlled inducible RNA interfering system to repress gene expression in chronic myelogenous leukemia cells. *Acta Biochimica et Biophysica Sinica* 37: 851-856.
415. Nikitakis N.G., Hebert C., Lopes M.A., Reynolds M.A., and Sauk J.J. (2002). PPAR γ -mediated antineoplastic effect of NSAID sulindac on human oral squamous carcinoma cells. *International Journal of Cancer* 98: 817-823.
416. Galli A., Ceni E., Crabb D.W., Mello T., Salzano R., Grappone C., Milani S., Surrenti E., Surrenti C., and Casini A. (2004). Antidiabetic thiazolidinediones inhibit invasiveness of pancreatic cancer cells via PPAR γ independent mechanisms. *Gut* 53: 1688-1697.
417. Irshad S., Pedley R.B., Anderson J., Latchman D.S., and Budhram-Mahadeo V. (2004). The Brn-3b transcription factor regulates the growth, behavior, and

- invasiveness of human neuroblastoma cells *in vitro* and *in vivo*. *Journal of Biological Chemistry* 279: 21617-21627.
418. Lefebvre A.M., Paulweber B., Fajas L., Woods J., McCrary C., Colombel J.F., Najib J., Fruchart J.C., Datz C., Vidal H. *et al.* (1999). Peroxisome proliferator-activated receptor- γ is induced during differentiation of colon epithelium cells. *Journal of Endocrinology* 162: 331-340.
 419. Schild R.L., Sonnenberg-Hirche C.M., Schaiff W.T., Bildirici I., Nelson D.M., and Sadovsky Y. (2006). The kinase p38 Regulates Peroxisome Proliferator Activated Receptor- γ in Human Trophoblasts. *Placenta* 27: 191-199.
 420. Schaiff W.T., Carlson M.G., Smith S.D., Levy R., Nelson D.M., and Sadovsky Y. (2000). Peroxisome proliferator-activated receptor- γ modulates differentiation of human trophoblast in a ligand-specific manner. *Journal of Clinical Endocrinology and Metabolism* 85: 3874-3881.
 421. Al-Shali K., Cao H.N., Knoers N., Hermus A.R., Tack C.J., and Hegele R.A. (2004). A single-base mutation in the peroxisome proliferator-activated receptor- γ 4 promoter associated with altered *in vitro* expression and partial lipodystrophy. *Journal of Clinical Endocrinology and Metabolism* 89: 5655-5660.
 422. Saladin R., Fajas L., Dana S., Halvorsen Y.D., Auwerx J., and Briggs M. (1999). Differential regulation of peroxisome proliferator activated receptor- γ 1 (PPAR γ 1) and PPAR γ messenger RNA expression in the early stages of adipogenesis. *Cell Growth & Differentiation* 10: 43-48.
 423. Cho Y.C. and Jefcoate C.R. (2004). PPAR γ 1 synthesis and adipogenesis in C3H10T1/2 cells depends on S-phase progression, but does not require mitotic clonal expansion. *Journal of Cellular Biochemistry* 91: 336-353.
 424. Yajima Y., Sato M., Sumida M., and Kawashima S. (2003). Mechanism of adult primitive mesenchymal ST-13 preadipocyte differentiation. *Endocrinology* 144: 2559-2565.
 425. Rieusset J., Andreelli F., Auboeuf D., Rogues M., Vallier P., Riou J.P., Auwerx J., Laville M., and Vidal H. (1999). Insulin acutely regulates the expression of the peroxisome proliferator-activated receptor- γ in human adipocytes. *Diabetes* 48: 699-705.
 426. Wang X., Southard R.C., and Kilgore M.W. (2004). The increased expression of peroxisome proliferator-activated receptor- γ 1 in human breast cancer is mediated by selective promoter usage. *Cancer Res* 64: 5592-5596.
 427. Cartharius K., Frech K., Grote K., Klocke B., Haltmeier M., Klingenhoff A., Frisch M., Bayerlein M., and Werner T. (2005). MatInspector and beyond: promoter analysis based on transcription factor binding sites. *Bioinformatics* 21: 2933-2942.
 428. Quandt K., Frech K., Karas H., Wingender E., and Werner T. (1995). MatInd and MatInspector: New fast and versatile tools for detection of consensus matches in nucleotide sequence data. *Nucleic Acids Research* 23: 4878-4884.
 429. Eisenman R.N. (2001). Deconstructing Myc. *Genes & Development* 15: 2023-2030.
 430. Packham G., Porter C.W., and Cleveland J.L. (1996). c-Myc induces apoptosis and cell cycle progression by separable, yet overlapping, pathways. *Oncogene* 13: 461-469.

431. Facchini L.M. and Penn L.Z. (1998). The molecular role of Myc in growth and transformation: recent discoveries lead to new insights. *Faseb Journal* 12: 633-651.
432. Oster S.K., Ho C.S.W., Soucie E.L., and Penn L.Z. (2002). The myc oncogene: (M)under-bar-arvelousl(Y)under-bar (C)under-bar-omplex. (San Diego: Academic Press Inc).
433. Dang C.V. (1999). *c-myc* target genes involved in cell growth, apoptosis, and metabolism. *Molecular and Cellular Biology* 19: 1-11.
434. Schmidt E.V. (1999). The role of *c-myc* in cellular growth control. *Oncogene* 18: 2988-2996.
435. Luscher B. and Larsson L.G. (1999). The basic region/helix-loop-helix/leucine zipper domain of Myc proto-oncoproteins: Function and regulation. *Oncogene* 18: 2955-2966.
436. Chang D.H., ngelin-Duclos C., and Calame K. (2000). BLIMP-1: trigger for differentiation of myeloid lineage. *Nature Immunology* 1: 169-176.
437. Slungaard A., Confer D.L., and Schubach W.H. (1987). Rapid Transcriptional Down-Regulation of c-Myc Expression During Cyclic Adenosine Monophosphate-Promoted Differentiation of Leukemic-Cells. *Journal of Clinical Investigation* 79: 1542-1547.
438. Heath V.J., Gillespie D.A.F., and Crouch D.H. (2000). Inhibition of the terminal stages of adipocyte differentiation by c-Myc. *Experimental Cell Research* 254: 91-98.
439. Dang C.V., Resar L.M.S., Emison E., Kim S., Li Q., Prescott J.E., Wonsey D., and Zeller K. (1999). Function of the c-Myc oncogenic transcription factor. *Experimental Cell Research* 253: 63-77.
440. Sakamuro D. and Prendergast G.C. (1999). New Myc-interacting proteins: a second Myc network emerges. *Oncogene* 18: 2942-2954.
441. Blackwood E.M. and Eisenman R.N. (1991). Max - A Helix-Loop-Helix Zipper Protein That Forms A Sequence-Specific Dna-Binding Complex with Myc. *Science* 251: 1211-1217.
442. Grandori C., Cowley S.M., James L.P., and Eisenman R.N. (2000). The Myc/Max/Mad network and the transcriptional control of cell behavior. *Annual Review of Cell and Developmental Biology* 16: 653-699.
443. Mao D.Y.L., Watson J.D., Yan P.S., Barsyte-Lovejoy D., Khosravi F., Wong W.W.L., Farnham P.J., Huang T.H.M., and Penn L.Z. (2003). Analysis of Myc bound loci identified by CpG island arrays shows that Max is essential for Myc-dependent repression. *Current Biology* 13: 882-886.
444. Amati B., Frank S.R., Donjerkovic D., and Taubert S. (2001). Function of the c-Myc oncoprotein in chromatin remodeling and transcription. *Biochimica et Biophysica Acta-Reviews on Cancer* 1471: M135-M145.
445. McMahon S.B., Wood M.A., and Cole M.D. (2000). The essential cofactor TRRAP recruits the histone acetyltransferase hGCN5 to c-Myc. *Molecular and Cellular Biology* 20: 556-562.

446. McMahon S.B., Van Buskirk H.A., Dugan K.A., Copeland T.D., and Cole M.D. (1998). The novel ATM-related protein TRRAP is an essential cofactor for the c-Myc and E2F oncoproteins. *Cell* 94: 363-374.
447. Liu X.H., Tesfai J., Evrard Y.A., Dent S.Y.R., and Martinez E. (2003). c-Myc transformation domain recruits the human STAGA complex and requires TRRAP and GCN5 acetylase activity for transcription activation. *Journal of Biological Chemistry* 278: 20405-20412.
448. Bouchard C., Dittrich O., Kiermaier A., Dohmann K., Menkel A., Eilers M., and Luscher B. (2001). Regulation of cyclin D2 gene expression by the Myc/Max/Mad network: Myc-dependent TRRAP recruitment and histone acetylation at the cyclin D2 promoter. *Genes & Development* 15: 2042-2047.
449. Frank S.R., Schroeder M., Fernandez P., Taubert S., and Amati B. (2001). Binding of c-Myc to chromatin mediates mitogen-induced acetylation of histone H4 and gene activation. *Genes & Development* 15: 2069-2082.
450. Cheng S.W.G., Davies K.P., Yung E., Beltran R.J., Yu J., and Kalpana G.V. (1999). c-Myc interacts with INI1/hSNF5 and requires the SWI/SNF complex for transactivation function. *Nature Genetics* 22: 102-105.
451. Coller H.A., Grandori C., Tamayo P., Colbert T., Lander E.S., Eisenman R.N., and Golub T.R. (2000). Expression analysis with oligonucleotide microarrays reveals that MYC regulates genes involved in growth, cell cycle, signaling, and adhesion. *Proceedings of the National Academy of Sciences of the United States of America* 97: 3260-3265.
452. Menssen A. and Hermeking H. (2002). Characterization of the c-MYC-regulated transcriptome by SAGE: Identification and analysis of c-MYC target genes. *Proceedings of the National Academy of Sciences of the United States of America* 99: 6274-6279.
453. Watson J.D., Oster S.K., Shago M., Khosravi F., and Penn L.Z. (2002). Identifying genes regulated in a Myc-dependent manner. *Journal of Biological Chemistry* 277: 36921-36930.
454. Wanzel M., Herold S., and Eilers M. (2003). Transcriptional repression by Myc. *Trends in Cell Biology* 13: 146-150.
455. Gardner L., Lee L., and Dang C. (2002). The c-Myc Oncogenic Transcription Factor. In *The Encyclopedia of Cancer*, Academic Press), pp. 1-13.
456. Nilsson J.A. and Cleveland J.L. (2003). Myc pathways provoking cell suicide and cancer. *Oncogene* 22: 9007-9021.
457. Slave I., Ellenbogen R., Jung W.H., Vawter G.F., Kretschmar C., Grier H., and Korf B.R. (1990). Myc Gene Amplification and Expression in Primary Human Neuroblastoma. *Cancer Res* 50: 1459-1463.
458. Hammerling U., Bjelfman C., and Pahlman S. (1987). Different Regulation of N-Myc and c-Myc Expression During Phorbol Ester-Induced Maturation of Human Sh-Sy5y Neuro-Blastoma Cells. *Oncogene* 2: 73-77.
459. Kabilova T.O., Chernolovskaya E.L., Vladimirova A.V., and Vlassov V.V. (2006). Inhibition of human carcinoma and neuroblastoma cell proliferation by anti-c-Myc siRNA. *Oligonucleotides* 16: 15-25.

460. Zhe X., CHEN J., Liu T., Zhang L., Li P., and Wang D. (2006). The relationship between expressions of N-Myc and c-Myc oncogenes in neuroblastoma: an *in situ* hybridization and immunocytochemical study. *Chinese Medical Sciences Journal* 14: 102-106.
461. Li L.H., Nerlov C., Prendergast G., Macgregor D., and Ziff E.B. (1994). c-Myc represses transcription *in-vivo* by a novel mechanism dependent on the initiator element and MBII. *Embo Journal* 13: 4070-4079.
462. Park D.S., Razani B., Lasorella A., Schreiber-Agus N., Pestell R.G., Iavarone A., and Lisanti M.P. (2001). Evidence that Myc isoforms transcriptionally repress caveolin-1 gene expression via an INR-dependent mechanism. *Biochemistry* 40: 3354-3362.
463. Philipp A., Schneider A., Vasrik I., Finke K., Xiong Y., Beach D., Alitalo K., and Eilers M. (1994). Repression of Cyclin D1 - A Novel Function of Myc. *Molecular and Cellular Biology* 14: 4032-4043.
464. Peukert K., Staller P., Schneider A., Carmichael G., Hanel F., and Eilers M. (1997). An alternative pathway for gene regulation by Myc. *Embo Journal* 16: 5672-5686.
465. Smale S.T. and Baltimore D. (1989). The Initiator As A Transcription Control Element. *Cell* 57: 103-113.
466. Roy A.L., Carruthers C., Gutjahr T., and Roeder R.G. (1993). Direct Role for Myc in Transcription Initiation Mediated by Interactions with TFII-I. *Nature* 365: 359-361.
467. Shrivastava A., Saleque S., Kalpana G.V., Artandi S., Goff S.P., and Calame K. (1993). Inhibition of Transcriptional Regulator Yin-Yang-1 by Association with c-Myc. *Science* 262: 1889-1892.
468. Maheswaran S., Lee H.Y., and Sonenshein G.E. (1994). Intracellular Association of the Protein Product of the Oncogene with the Tata-Binding Protein. *Molecular and Cellular Biology* 14: 1147-1152.
469. Numoto M., Niwa O., Kaplan J., Wong K.K., Merrell K., Kamiya K., Yanagihara K., and Calame K. (1993). Transcriptional Repressor Zf5 Identifies A New Conserved Domain in Zinc-Finger Proteins. *Nucleic Acids Research* 21: 3767-3775.
470. Bardwell V.J. and Treisman R. (1994). The POZ Domain - A Conserved Protein-Protein Interaction Motif. *Genes & Development* 8: 1664-1677.
471. Huynh K.D. and Bardwell V.J. (1998). The BCL-6 POZ domain and other POZ domains interact with the co-repressors N-CoR and SMRT. *Oncogene* 17: 2473-2484.
472. Li X.M., Peng H.Z., Schultz D.C., Lopez-Guisa J.M., Rauscher F.J., and Marmorstein R. (1999). Structure-function studies of the BTB/POZ transcriptional repression domain from the promyelocytic leukemia zinc finger oncoprotein. *Cancer Res* 59: 5275-5282.
473. Phan R.T., Saito M., Basso K., Niu H.F., and la-Favera R. (2005). BCL6 interacts with the transcription factor Miz-1 to suppress the cyclin-dependent kinase inhibitor p21 and cell cycle arrest in germinal center B cells. *Nature Immunology* 6: 1054-1060.

474. Staller P., Peukert K., Kiermaier A., Seoane J., Lukas J., Karsunky H., Moroy T., Bartek J., Massague J., Hanel F. *et al.* (2001). Repression of p15(INK4b) expression by Myc through association with Miz-1. *Nature Cell Biology* 3: 392-399.
475. Bowen H., Biggs T.E., Phillips E., Baker S.T., Perry V.H., Mann D.A., and Barton C.H. (2002). c-Myc represses and Miz-1 activates the murine Natural resistance-associated protein 1 promoter. *Journal of Biological Chemistry* 277: 34997-35006.
476. Herold S., Wanzel M., Beuger V., Frohme C., Beul D., Hillukkala T., Syvaoja J., Saluz H.P., Haenel F., and Eilers M. (2002). Negative regulation of the mammalian UV response by Myc through association with Miz-1. *Molecular Cell* 10: 509-521.
477. Seoane J., Pouppnot C., Staller P., Schader M., Eilers M., and Massague J. (2001). TGF beta influences Myc, Miz-1 and Smad to control the CDK inhibitor p15(INK4b). *Nature Cell Biology* 3: 400-408.
478. Marcotte R., Chen J.M., Huard S., and Wang E. (2005). c-Myc creates an activation loop by transcriptionally repressing its own functional inhibitor, hMad4, in young fibroblasts, a loop lost in replicatively senescent fibroblasts. *Journal of Cellular Biochemistry* 96: 1071-1085.
479. Kime L. and Wright S.C. (2003). Mad4 is regulated by a transcriptional repressor complex that contains Miz-1 and c-Myc. *Biochemical Journal* 370: 291-298.
480. Seoane J., Le H.V., and Massague J. (2002). Myc suppression of the p21(Cip1) Cdk inhibitor influences the outcome of the p53 response to DNA damage. *Nature* 419: 729-734.
481. Wu S.Q., Cetinkaya C., Munoz-Alonso M.J., der Lehr N., Bahram F., Beuger V., Eilers M., Leon J., and Larsson L.G. (2003). Myc represses differentiation-induced p21CIP1 expression via Miz-1-dependent interaction with the p21 core promoter. *Oncogene* 22: 351-360.
482. Adhikary S., Peukert K., Karsunky H., Beuger V., Lutz W., Elsasser H.P., Moroy T., and Eilers M. (2003). Miz1 is required for early embryonic development during gastrulation. *Molecular and Cellular Biology* 23: 7648-7657.
483. Bowen H., Lapham A., Phillips E., Yeung I., ter-Koltunoff M., Levi B.Z., Perry V.H., Mann D.A., and Barton C.H. (2003). Characterization of the murine Nramp1 promoter - Requirements for transactivation by Miz-1. *Journal of Biological Chemistry* 278: 36017-36026.
484. Brenner C., Deplus R., Didelot C., Lorient A., Vire E., De Smet C., Gutierrez A., Danovi D., Bernard D., Boon T. *et al.* (2005). Myc represses transcription through recruitment of DNA methyltransferase corepressor. *Embo Journal* 24: 336-346.
485. Gartel A.L., Ye X., Goufman E., Shianov P., Hay N., Najmabadi F., and Tyner A.L. (2001). Myc represses the p21((WAF1/CIP1)) promoter and interacts with Sp1/Sp3. *Proceedings of the National Academy of Sciences of the United States of America* 98: 4510-4515.
486. Feng X.H., Liang Y.Y., Liang M., Zhai W.G., and Lin X. (2002). Direct interaction of c-Myc with Smad2 and Smad3 to inhibit TGF-beta-mediated induction of the CDK inhibitor p15(Ink4B). *Molecular Cell* 9: 133-143.
487. Oster S.K., Marhin W.W., Asker C., Facchini L.M., Dion P.A., Funa K., Post M., Sedivy J.M., and Penn L.Z. (2000). Myc is an essential negative regulator of platelet-

- derived growth factor beta receptor expression. *Molecular and Cellular Biology* 20: 6768-6778.
488. Izumi H., Molander C., Penn L.Z., Ishisaki A., Kohno K., and Funa K. (2001). Mechanism for the transcriptional repression by c-Myc on PDGF beta-receptor. *Journal of Cell Science* 114: 1533-1544.
 489. Gartel A.L. and Radhakrishnan S.K. (2005). Lost in transcription: p21 repression, mechanisms, and consequences. *Cancer Res* 65: 3980-3985.
 490. Kim M.K.H. and Carroll W.L. (2004). Autoregulation of the N-myc gene is operative in neuroblastoma and involves histone deacetylase 2. *Cancer* 101: 2106-2115.
 491. Uramoto H., Hackzell A., Wetterskog D., Ballagi A., Izumi H., and Funa K. (2004). pRb, Myc and p53 are critically involved in SV40 large T antigen repression of PDGF beta-receptor transcription. *Journal of Cell Science* 117: 3855-3865.
 492. Gartel A.L. and Shchors K. (2003). Mechanisms of c-myc-mediated transcriptional repression of growth arrest genes. *Experimental Cell Research* 283: 17-21.
 493. Satou A., Taira T., Iguchi-Arigo S.M.M., and Ariga H. (2001). A novel transrepression pathway of c-Myc. Recruitment of a transcriptional corepressor complex to c-Myc by MM-1, a c-Myc-binding protein. *Journal of Biological Chemistry* 276: 46562-46567.
 494. Penn L.J.Z., Brooks M.W., Laufer E.M., and Land H. (1990). Negative Autoregulation of C-Myc Transcription. *Embo Journal* 9: 1113-1121.
 495. Penn L.J.Z., Brooks M.W., Laufer E.M., Littlewood T.D., Morgenstern J.P., Evan G.I., Lee W.M.F., and Land H. (1990). Domains of Human c-Myc Protein Required for Autosuppression and Cooperation with Ras Oncogenes Are Overlapping. *Molecular and Cellular Biology* 10: 4961-4966.
 496. Facchini L.M., Chen S.J., Marhin W.W., Lear J.N., and Penn L.Z. (1997). The Myc negative autoregulation mechanism requires Myc-Max association and involves the c-myc P2 minimal promoter. *Molecular and Cellular Biology* 17: 100-114.
 497. Luo Q., Li J., Cenkci B., and Kretzner L. (2004). Autorepression of c-Myc requires both initiator and E2F-binding site elements and cooperation with the p107 gene product. *Oncogene* 23: 1088-1097.
 498. Mao D.Y.L., Baryte-Lovejoy D., Ho C.S.W., Watson J.D., Stojanova A., and Penn L.Z. (2004). Promoter-binding and repression of PDGFRB by c-Myc are separable activities. *Nucleic Acids Research* 32: 3462-3468.
 499. Baryte-Lovejoy D., Mao D.Y.L., and Penn L.Z. (2004). c-Myc represses the proximal promoters of GADD45a and GADD153 by a post-RNA polymerase II recruitment mechanism. *Oncogene* 23: 3481-3486.
 500. Amundson S.A., Zhan Q., Penn L.Z., and Fornace A.J. (1998). Myc suppresses induction of the growth arrest genes gadd34, gadd45, and gadd153 by DNA-damaging agents. *Oncogene* 17: 2149-2154.
 501. Pulverer B., Sommer A., McArthur G.A., Eisenman R.N., and Luscher B. (2000). Analysis of Myc/Max/Mad network members in adipogenesis: Inhibition of the proliferative burst and differentiation by ectopically expressed mad1. *Journal of Cellular Physiology* 183: 399-410.

502. Lapham A.S., Phillips E.S., and Barton C.H. (2004). Transcriptional control of Nramp 1: a paradigm for the repressive action of c-Myc. *Biochemical Society Transactions* 32: 1084-1086.
503. Claassen G.F. and Hann S.R. (2000). A role for transcriptional repression of p21(CIP1) by c-Myc in overcoming transforming growth factor beta-induced cell-cycle arrest. *Proceedings of the National Academy of Sciences of the United States of America* 97: 9498-9503.
504. Claassen G.F. and Hann S.R. (1999). Myc-mediated transformation: the repression connection. *Oncogene* 18: 2925-2933.
505. Kato G.J., Barrett J., Villagarcia M., and Dang C.V. (1990). An Amino-Terminal c-Myc Domain Required for Neoplastic Transformation Activates Transcription. *Molecular and Cellular Biology* 10: 5914-5920.
506. Oster S.K., Mao D.Y.L., Kennedy J., and Penn L.Z. (2003). Functional analysis of the N-terminal domain of the Myc oncoprotein. *Oncogene* 22: 1998-2010.
507. Herbst A., Hemann M.T., Tworowski K.A., Salghetti S.E., Lowe S.W., and Tansey W.P. (2005). A conserved element in Myc that negatively regulates its proapoptotic activity. *Embo Reports* 6: 177-183.
508. Herbst A., Salghetti S.E., Kim S.Y., and Tansey W.P. (2004). Multiple cell-type-specific elements regulate Myc protein stability. *Oncogene* 23: 3863-3871.
509. Dang C.V. and Lee W.M.F. (1988). Identification of the Human C-Myc Protein Nuclear Translocation Signal. *Molecular and Cellular Biology* 8: 4048-4054.
510. Stone J., Delange T., Ramsay G., Jakobovits E., Bishop J.M., Varmus H., and Lee W. (1987). Definition of Regions in Human c-Myc That Are Involved in Transformation and Nuclear-Localization. *Molecular and Cellular Biology* 7: 1697-1709.
511. Lavrarr J.L. and Farnham P.J. (2004). The use of transient chromatin Immunoprecipitation assays to test models for E2F1-specific transcriptional activation. *Journal of Biological Chemistry* 279: 46343-46349.
512. Philipsen S. and Suske G. (1999). A tale of three fingers: the family of mammalian Sp/XKLF transcription factors. *Nucleic Acids Research* 27: 2991-3000.
513. Perez-Gomez C., Mates J.M., Gomez-Fabre P.M., Del Castillo-Olivares A., Alonso F.J., and Marquez J. (2003). Genomic organization and transcriptional analysis of the human L-glutaminase gene. *Biochemical Journal* 370: 771-784.
514. Kriwacki R.W., Schultz S.C., Steitz T.A., and Caradonna J.P. (1992). Sequence-Specific Recognition of Dna by Zinc-Finger Peptides Derived from the Transcription Factor Sp1. *Proceedings of the National Academy of Sciences of the United States of America* 89: 9759-9763.
515. Tyner A.L., Goufman E., and Gartel A.L. (1999). Sp1 and Sp3 transactivate basal p21(WAF1/CIP1) transcription in the Caco-2 colon adenocarcinoma cell line. *Gastroenterology* 116: G2287.
516. Segal J.A., Barnett J.L., and Crawford D.L. (1999). Functional analyses of natural variation in Sp1 binding sites of a TATA-less promoter. *Journal of Molecular Evolution* 49: 736-749.

517. Ji C.H., Casinighino S., McCarthy T.L., and Centrella M. (1997). Multiple and essential Sp1 binding sites in the promoter for transforming growth factor-beta type I receptor. *Journal of Biological Chemistry* 272: 21260-21267.
518. Baker D.L., Dave V., Reed T., and Periasamy M. (1996). Multiple Sp1 binding sites in the cardiac slow twitch muscle sarcoplasmic reticulum Ca^{2+} -ATPase gene promoter are required for expression in Sol8 muscle cells. *Journal of Biological Chemistry* 271: 5921-5928.
519. Park G.H., Plummer H.K., and Krystal G.W. (1998). Selective Sp1 binding is critical for maximal activity of the human c-kit promoter. *Blood* 92: 4138-4149.
520. Brightbill H.D., Plevy S.E., Modlin R.L., and Smale S.T. (2000). A prominent role for Sp1 during lipopolysaccharide-mediated induction of the IL-10 promoter in macrophages. *Journal of Immunology* 164: 1940-1951.
521. Bouwman P. and Philipsen S. (2002). Regulation of the activity of Sp1-related transcription factors. *Molecular and Cellular Endocrinology* 195: 27-38.
522. Suske G. (1999). The Sp-family of transcription factors. *Gene* 238: 291-300.
523. Lania L., Majello B., and De Luca P. (1997). Transcriptional regulation by the Sp family proteins. *International Journal of Biochemistry & Cell Biology* 29: 1313-1323.
524. Kaczynski J., Cook T., and Urrutia R. (2003). Sp1-and Kruppel-like transcription factors. *Genome Biology* 4.
525. Suico M.A., Koga T., Shuto T., Hisatsune A., Lu Z., Basbaum C., Okiyoneda T., and Kai H. (2004). Sp1 is involved in the transcriptional activation of lysozyme in epithelial cells. *Biochemical and Biophysical Research Communications* 324: 1302-1308.
526. Black A.R., Black J.D., and Azizkhan-Clifford J. (2001). Sp1 and kruppel-like factor family of transcription factors in cell growth regulation and cancer. *Journal of Cellular Physiology* 188: 143-160.
527. Samson S.L. and Wong N.C. (2002). Role of Sp1 in insulin regulation of gene expression. - *J Mol Endocrinol.* 2002 Dec;29(3):265-79.
528. Heegaard A.M., Xie Z.J., Young M.F., and Nielsen K.L. (2004). Transforming growth factor beta stimulation of biglycan gene expression is potentially mediated by Sp1 binding factors. *Journal of Cellular Biochemistry* 93: 463-475.
529. Nichols A.F., Itoh T., Zolezzi F., Hutsell S., and Linn S. (2003). Basal transcriptional regulation of human damage-specific DNA-binding protein genes DDB1 and DDB2 by Sp1, E2F, N-myc and NF1 elements. *Nucleic Acids Research* 31: 562-569.
530. Nakagawa T., Takahashi M., Ozaki T., Watanabe K., Hayashi S., Hosoda M., Todo S., and Nakagawara A. (2003). Negative autoregulation of p73 and p53 by Delta Np73 in regulating differentiation and survival of human neuroblastoma cells. *Cancer Letters* 197: 105-109.
531. Liu G. and Chen X.B. (2006). Regulation of the p53 transcriptional activity. *Journal of Cellular Biochemistry* 97: 448-458.

532. Latonen L. and Laiho M. (2005). Cellular UV damage responses - Functions of tumor suppressor p53. *Biochimica et Biophysica Acta-Reviews on Cancer* 1755: 71-89.
533. Vousden K.H. (2002). Activation of the p53 tumor suppressor protein. *Biochimica et Biophysica Acta-Reviews on Cancer* 1602: 47-59.
534. Meek D.W. (2004). The p53 response to DNA damage. *DNA Repair* 3: 1049-1056.
535. Vogelstein B., Lane D., and Levine A.J. (2000). Surfing the p53 network. *Nature* 408: 307-310.
536. Bates S. and Vousden K.H. (1999). Mechanisms of p53-mediated apoptosis. *Cellular and Molecular Life Sciences* 55: 28-37.
537. Levine A.J. (1997). p53, the cellular gatekeeper for growth and division. *Cell* 88: 323-331.
538. Oren M. and Rotter V. (1999). Introduction: p53 - the first twenty years. *Cellular and Molecular Life Sciences* 55: 9-11.
539. Harms K., Nozell S., and Chen X. (2004). The common and distinct target genes of the p53 family transcription factors. *Cellular and Molecular Life Sciences* 61: 822-842.
540. Mclure K.G. and Lee P.W.K. (1998). How p53 binds DNA as a tetramer. *Embo Journal* 17: 3342-3350.
541. Wang Y., Schwedes J.F., Parks D., Mann K., and Tegtmeyer P. (1995). Interaction of P53 with Its Consensus DNA-Binding Site. *Molecular and Cellular Biology* 15: 2157-2165.
542. Lagger G., Doetzelhofer A., Schuettengruber B., Haidweger E., Simboeck E., Tischler J., Chiocca S., Suske G., Rotheneder H., Wintersberger E. *et al.* (2003). The tumor suppressor p53 and histone deacetylase 1 are antagonistic regulators of the cyclin-dependent kinase inhibitor p21/WAF1/CIP1 gene. *Molecular and Cellular Biology* 23: 2669-2679.
543. Koutsodontis G., Tentis I., Papakosta P., Moustakas A., and Kardassis D. (2001). Sp1 plays a critical role in the transcriptional activation of the human cyclin-dependent kinase inhibitor p21(WAF1/Cip1) gene by the p53 tumor suppressor protein. *Journal of Biological Chemistry* 276: 29116-29125.
544. Koutsodontis G., Vasilaki E., Chou W.C., Papakosta P., and Kardassis D. (2005). Physical and functional interactions between members of the tumour suppressor p53 and the Sp families of transcription factors: importance for the regulation of genes involved in cell-cycle arrest and apoptosis. *Biochemical Journal* 389: 443-455.
545. Schavinsky-Khrapunsky Y., Huleihel M., Aboud M., and Torgeman A. (2003). Role of protein kinase C and the Sp1-p53 complex in activation of p21(WAF-1) expression by 12-O-tetradecanoylphorbol-13-acetate in human T cells. *Oncogene* 22: 5315-5324.
546. Wang Y.C., Blandino G., and Givol D. (1999). Induced p21(waf) expression in H1299 cell line promotes cell senescence and protects against cytotoxic effect of radiation and doxorubicin. *Oncogene* 18: 2643-2649.

547. Tweddle D.A., Malcolm A.J., Cole M., Pearson A.D.J., and Lunec J. (2001). p53 Cellular localization and function in neuroblastoma - Evidence for defective G(1) arrest despite WAF1 induction in MYCN-amplified cells. *American Journal of Pathology* 158: 2067-2077.
548. Evans A., Gerson J., and Schnauffer L. (1976). Spontaneous regression of neuroblastoma. *National Cancer Institute Monograph* 44: 49-54.
549. Adhikary S., Marinoni F., Hock A., Hulleman E., Popov N., Beier R., Bernard S., Quarto M., Capra M., Goettig S. et al. (2005). The ubiquitin ligase HectH9 regulates transcriptional activation by myc and is essential for tumor cell proliferation. *Cell* 123: 409-421.
550. Wanzel M., Kleine-Kohlbrecher D., Herold S., Hock A., Berns K., Park J., Hemmings B., and Eilers M. (2005). Akt and 14-3-3 eta regulate Miz1 to control cell-cycle arrest after DNA damage. *Nature Cell Biology* 7: 30-+.
551. Ziegelbauer J., Shan B., Yager D., Larabell C., Hoffmann B., and Tjian R. (2001). Transcription factor MIZ-1 is regulated via microtubule association. *Molecular Cell* 8: 339-349.
552. Patel J.H. and McMahon S.B. (2006). Targeting of MIZ-1 is essential for MYC mediated apoptosis. - *J Biol Chem.* 2005 Dec 13;.
553. Xiao Q.R., Claassen G., Shi J.Y., Adachi S., Sedivy J., and Hann S.R. (1998). Transactivation-defective c-MycS retains the ability to regulate proliferation and apoptosis. *Genes & Development* 12: 3803-3808.
554. Lee L.A., Dolde C., Barrett J., Wu C.S., and Dang C.V. (1996). A link between c-myc-mediated transcriptional repression and neoplastic transformation. *Journal of Clinical Investigation* 97: 1687-1695.
555. Li H. and Wu X.X. (2004). Histone deacetylase inhibitor, Trichostatin A, activates p21(WAF1/CIP1) expression through downregulation of c-myc and release of the repression of c-myc from the promoter in human cervical cancer cells. *Biochemical and Biophysical Research Communications* 324: 860-867.